UNIVERSITY OF DERBY

STABILITY OF PROTEIN-BASED DRUGS:

HERCEPTIN® A CASE STUDY

Ian Michael Shropshire

Doctor of Philosophy 2015

CONTENTS

Page

List of figures and tables

Statement of contribution

Abstract

Acknowledgements

Chapter 1

1.	**General Introduction**	
1.1	Rationale for study	1
1.2	General Stability issues and existing guidelines	2
1.2.1	Hospital Pharmacy Practice and In Use Drug Stability	3
1.2.2	Guidelines for stability assessment	5
1.3	Trastuzumab Case Study	7
1.3.1	Trastuzumab and Cancer	7
1.3.1.1	HER2 and Cell Signalling	8
1.3.1.2	Mechanisms of Trastuzumab Action	10
1.3.1.2.1	Inhibition of tumour cell proliferation	11
1.3.1.2.2	Antibody-dependant cell-mediated cytotoxicity (ADCC)	14
1.3.1.3	Formulation and practice aspects of drug compounding	14
1.4	Structure of Trastuzumab	15
1.4.1	General Protein Structure	15
1.4.1.1	Primary	15
1.4.1.2	Secondary	15
1.4.1.3	Tertiary	16
1.4.1.4	Quaternary	16
1.4.2	IgG Antibody Structure	18
1.4.2.1	Antibody fragments	18
1.4.2.2	Chain Structure Heavy and light chains	18
1.4.2.3	Glycosylation	20

1.4.3	Trastuzumab structure	20
1.5	Protein stability	22
1.5.1	Physical Stability	23
1.5.1.1	Adsorption	23
1.5.1.2	Conformational stability	23
1.5.1.3	Aggregation	24
1.5.1.3.1	Low Order Aggregation (Dimers, trimers and other low order oligomers)	24
1.5.1.4	Denaturation	25
1.5.1.4.1	High Order Aggregation (Precipitation)	25
1.5.2	Chemical stability	26
1.5.2.1	Chemical Degradation	26
1.5.2.1.1	Deamination to succinimide	26
1.5.2.1.2	Hydrolysis of succinimide and isomerism of aspartic acid product	29
1.5.2.1.3	Proteolysis	30
1.5.2.1.4	Disulphide exchange	32
1.5.2.1.5	Oxidation	33
1.5.2.1.6	Maillard Reaction	35
1.5.2.1.7	Para-glutamate formation	35
1.6	Generic Techniques for determining Stability	36
1.6.1	Physical techniques	36
1.6.1.1	Size Exclusion Liquid Chromatography	36
1.6.1.2	Ion Exchange chromatography (IEX)	37
1.6.1.3	Sodium Dodecyl Sulphate-Polyacrylamide Gel Electrophoresis (SDS-PAGE)	37
1.6.1.4	Attenuated Total Reflectance Fourier Transform Infra-Red Spectroscopy (ATR-FTIR)	38
1.6.1.5	Dynamic Light Scattering	39
1.6.1.6	Electrospray Mass Spectroscopy	40
1.6.2	Biological Techniques	41
1.6.2.1	ELISA	41
1.6.2.2	Cellular Assay	42
1.7	Method Rationale	45
1.7.1	Selection of Physical Techniques	45

1.7.2	Selection of Biological Assay	46
1.8	Quality Assurance and Quality Control	47
1.9	Aims and objectives	48
1.10	Hypothesis	49

Chapter 2

2.	**Method Development of Physicochemical Core techniques for Stability assessments**	
2.1	Introduction	50
2.2	Methods and materials	51
2.2.1	Preparation of Trastuzumab (Herceptin® Roche)	51
2.2.2	Size exclusion liquid chromatography (SEC-LC)	51
2.2.2.1	Instrumentation	51
2.2.2.2	Conditions for chromatographic separation	52
2.2.2.3	Chromatogram processing and analysis	52
2.2.3	Development of Attenuated Total Reflectance Fourier Transform Infra-red (ATR-FT-IR) Spectroscopy for the analysis of Trastuzumab	52
2.2.3.1	Instrumentation	52
2.2.3.2	ATR plate installation, set-up and optimisation of throughput signal	53
2.2.3.3	Spectra acquisition	53
2.2.3.4	Spectra processing and analysis	53
2.3	Quality Control and Quality Assurance	54
2.3.1	Trastuzumab	54
2.3.2	Size exclusion chromatography	54
2.3.3	Attenuated Total Reflectance Fourier Transform Infra-red (ATR-FT-IR) Spectroscopy	55
2.4	Results and Discussion	56
2.4.1	Size exclusion chromatography	56
2.4.2	ATR-FT-IR	64
2.5	Conclusions	71

Chapter 3

3.	**Use of physicochemical techniques to determine Trastuzumab stability**	
3.1	Introduction	73
3.2	Materials and Methods	79
3.2.1	Materials	79
3.2.2	Methods	81
3.2.2.1	pH	81
3.2.2.2	Visual Appearance	81
3.2.2.3	Sub-visible Particle Analysis and Trastuzumab Assay	82
3.2.2.3.1	Size Exclusion Chromatography (SE-LC) method 1	82
3.2.2.4	Size Exclusion Chromatography (SE-LC) method 2	82
3.2.2.4.1	Instrumentation	82
3.2.2.4.2	Conditions for chromatographic separation	83
3.2.2.4.3	Chromatogram processing and analysis	83
3.2.2.5	Attenuated Total Reflectance Fourier Transform Infra-red (ATR-FT-IR) Spectroscopy	83
3.1.1.1	Electrophoresis: SDS-Page (Sodium Dodecyl Sulphate Poly Acrylamide Gel Electrophoresis)	83
3.2	Results and Discussion	84
3.3	Results for clinically relevant infusions	84
3.3.1	pH	84
3.3.2	Appearance	86
3.3.3	Sub-visible particle analysis	88
3.3.4	Attenuated Total Reflectance Infra-Red Spectroscopy (ATR-FT-IR): Assessment of changes in Trastuzumab secondary structure	94
3.3.5	Electrophoresis SDS-PAGE: Trastuzumab degradation (fragmentation and aggregation)	98
3.4	Stability of sub-clinically relevant infusion (0.1 mg/mL) and original vial concentrate (21 mg/mL)	100
3.4.1	Stability of sub clinically relevant infusion (0.1 mg/mL)	100
3.4.2	Percentage dimer content of original vial concentrate (21 mg/mL)	106
3.5	Stability of clinically relevant infusions at room temperature	106
3.6	Conclusions	109

Chapter 4

4.	**Development of Cellular Assay**	
4.1	Introduction	111
4.2	Materials and Methods	114
4.2.1	Preparation of Trastuzumab (Herceptin®)	114
4.2.2	Cell lines	115
4.2.2.1	Reviving cells from cryogenic storage	116
4.2.2.2	Maintenance of BT474 Cells	116
4.2.2.3	Maintenance of MCF7 Cells	116
4.2.2.4	Cell Passage and Seeding of BT474 cells	116
4.2.2.5	Fixing and staining colonies of BT474 cells	117
4.2.2.6	Method of stain release of crystal violet from BT474 cells and absorbance measurements of crystal violet at 540 nm as a measure of cell number/viability to calibrate instrument response for comparison to CCK8 reporter chemistry data	118
4.2.2.7	BT474 cell line colony formation assay	118
4.2.2.8	MCF7 cell line Colony formation assay	119
4.2.2.9	Method for assessing potency of an inhibitor of the MCF7 cell line for the development of colony formation assay protocols	119
4.2.3	Method of cell counting using a commercial cell counting kit (Sigma Aldrich, CCK8) assay	119
4.2.4	Optimisation of a commercial cell counting kit (Sigma Aldrich, CCK8) assay method	120
4.2.5	Stability indicating capability of using a commercial cell counting kit (Sigma Aldrich, CCK8) to distinguish between differences in viability induced by changes in active Trastuzumab concentrations by thermal degradation	121
4.3	Quality Assurance and Quality Control	122
4.4	Study Limitations	123
4.5	Results and discussion	123
4.5.1	MCF7 and BT474 propagation and proliferation assessment	123
4.5.1.1	MCF7 seeding and colony growth characteristics	123
4.5.1.2	BT474 seeding and colony growth characteristics	124
4.5.2	Development of MCF7 and BT474 colony formation assays	126

4.5.2.1	MCF7 cell-line colony counting with and without methanol inhibitor	126
4.5.2.2	BT474 cell-line colony counting following exposure to Trastuzumab and placebo respectively	127
4.5.3	BT474 viability assessment using colorimetric methods	129
4.5.3.1	Comparison of Crystal violet (CV) stain release method and CCK8 assay	130
4.5.3.2	Development of CCK8 assay	136
4.5.3.3	Optimised CCK8 assay	139
4.5.3.4	The stability indicating capability of CCK8 assay	143
4.6	Conclusions	144

Chapter 5

5.	**Forced degradation studies of Trastuzumab**	
5.1	Introduction	145
5.2	Materials and Methods	149
5.2.1	Size exclusion liquid chromatography (SE-LC)	150
5.2.2	Attenuated Total Reflectance Fourier Transform Infra-red (ATR-FT-IR) Spectroscopy and protein secondary structure determination	150
5.3	Results and Discussion	151
5.4	Conclusions	160

Chapter 6

6.	**Use of cellular assay to determine Trastuzumab stability**	
6.1	Introduction	162
6.2	Materials and methods	164
6.2.1	Test materials	164
6.2.1.1	Reference Trastuzumab (Herceptin® Roche)	164
6.2.1.2	Infusion bag samples	164
6.2.2	Drug storage conditions and sampling protocol	164
6.2.3	Biological testing with the BT474 cell-line	165
6.2.3.1	Maintenance of cells	165
6.2.3.2	Seeding BT474 cells for biological testing	165

6.2.3.3	Determination of BT474 Cell viability after addition of Trastuzumab using Cell Counting Kit CCK8	166
6.2.4	Colony Formation Assay	167
6.3	Quality Assurance and Quality Control	167
6.4	Study limitations	168
6.5	Results and discussion	168
6.5.1.1	Determination of cell viability as an indicator of potency of stored Trastuzumab	168
6.5.1.2	Assessment of biological activity day 0, 7, 14 and 28	168
6.5.1.3	Assessment of biological activity day 35, 43 and 119	170
6.5.1.4	Day 35	172
6.5.1.5	Day 43	174
6.5.1.6	Day 119	176
6.5.1.7	Summary of biological activity results	178
6.5.1.8	Percentage viability of BT474 cell count (normalised to base cell viability without drug)	181
6.5.1.9	Stability of 0.1 mg/ml infusion bags and 21 mg/ml vial concentrate	186
6.5.1.10	Summary of normalised biological activity results for day 119	191
6.6	Conclusions 194	

Chapter 7

7.	**General Discussion and conclusion**	
7.1	Introduction	195
7.2	Future work	198
7.3	Conclusion	201

References	202
Appendix	218

List of figures, tables and schemes

Figures **Page**

Chapter 1

Figure 1 Schematic representation of the HER2:HER3 heterodimer 10
Figure 2 X-ray crystal structure of (A) Trastuzumab Fab fragment bound with (B) extra-cellular domain of HER2 12
Figure 3 Bound Trastuzumab prevents the formation of the dimer with HER3 13
Figure 4 Schematic of the four levels of protein structure 17
Figure 5 Schematic representation of the IgG molecule 19
Figure 6 Amide regions of the FTIR spectrum 39
Figure 7 Schematic of the Trastuzumab-ELISA 42
Figure 8 Mechanism of a WST-8 formazan dye assay 44

Chapter 2

Figure 1 Representative size exclusion liquid chromatography (SE-LC) of Trastuzumab UV detection at 220 nm 57
Figure 2 Representative size exclusion chromatogram of Trastuzumab UV detection at 280 nm 58
Figure 3 SE-LC calibration of instrument response (UV detection at 280 nm) to Trastuzumab for a range of concentrations 60
Figure 4 SE-LC chromatogram with UV detection at 220 nm (peaks for monomer on scale) of Trastuzumab (0.1 mg/mL) after heating in a water bath at 75 ^{o}C for 5 minutes 62
Figure 5 SE-LC chromatogram with UV detection at 220 nm (showing peaks for monomer off scale) of Trastuzumab (0.1 mg/mL) after heating in a water bath at 75 ^{o}C for 5 minutes 63
Figure 6 Infra-red spectrum from 2,000 cm^{-1} to 1,000 cm^{-1} of germanium crystal ATR in air 64
Figure 7 Infra-red spectrum of reconstituted Trastuzumab 21 mg/mL from two vials 4,000 cm^{-1} to 1000 cm^{-1} wave numbers 66
Figure 8 Infra-red spectra of reconstituted Trastuzumab 21 mg/mL from two vials

Amide I region (1,800 cm^{-1} to 1500 cm^{-1} wave numbers) 67
Figure 9 Infra-red difference spectrum of reconstituted Trastuzumab (heat-stressed and not heat-stressed) at 0.1 mg/mL concentration. Showing region 2,000 cm^{-1} to 1,000 cm^{-1} wave numbers 69
Figure 10 Infra-red spectra of reconstituted Trastuzumab at 0.1 mg/mL, 0.5 mg/mL, 15 mg/mL and 21 mg/mL showing Amide I region (1800 cm^{-1} to 1500 cm^{-1} wave numbers) 71

Chapter 3

Figure 1 Percentage dimer at each time point for 0.5 mg/mL and 6 mg/mL infusions. Standard error is shown with inferential error bars 91
Figure 2 Correlation graph of dimer content with monomer content for the 0.5 mg/mL infusion. Standard error bars shown 91
Figure 3 Correlation graph of dimer content with monomer content for the 6 mg/mL infusion with standard error bars 92
Figure 4 ATR-FT-IR difference spectra of 0.1 mg/mL infusion. 96
Figure 5 ATR-FT-IR difference spectra of 6.0 mg/mL infusion sample 97
Figure 6 Difference spectra of A 0.1 and B 0.5 mg/mL infusions 103
Figure 7 Difference Spectra for 0.1 mg/mL infusion (bag 1) 104
Figure 8 Difference spectra for 0.1 mg/mL infusion (bag 2) 105
Figure 9 Difference spectra for 0.1 mg/mL infusion (bag 4) 105

Chapter 4

Figure 1 Micrograph of fixed and stained BT474 colonies at x100 magnification after a 14 day incubation or growth period within a 6-well micro-plate 113
Figure 2 Photograph of MCF7 colonies resulting from an initial seeding density of 300 cells per well 124
Figure 3 Photograph of BT474 colonies resulting from an initial seeding density of 14,000 cells per well 125
Figure 4 Photograph of MCF7 colonies in 6-well plate resulting from an initial seeding density of 300 cells per well 126
Figure 5 Colony formation assay bar chart showing action of Trastuzumab on colony count as a function of well drug concentrations in a 6 well-plate format 128
Figure 6 Cell seeding calibration in 96 well-plate format for re-solubilised

CV stain and CCK8 formazan dye absorbance at 540 nm and 450 nm respectively as a function of cell number 131
Figure 7 Plot of vertical deviation ($y_{observed} - y_{calculated}$) of observed y data point values from calculated y values of the least-squares line $y = m x + c$ 135
Figure 8 Graph showing absorbance as a function of read time seeding density 10,000 cells per well 137
Figure 9 Graph showing absorbance as a function of read time seeding density 10,000 cells per well after 4 days growth 138
Figure 10 Representative biological assay calibration plot showing the relationship between projected BT474 cell number after a 4 day uninhibited growth period and absorbance at 450 nm 139
Figure 11 Plot of vertical deviation ($y_{observed} - y_{calculated}$) of observed y data point values from calculated values of y of the least-squares line $y = m x + c$ 142

Chapter 5

Figure 1 Forced degradation conditions used to test drug product and drug substance 146
Figure 2 Micrographs of BT474 colony formation: with (A) Trastuzumab that was thermally stressed at 75^{o}C and (B) Trastuzumab that was not stressed as a control. Micrograph of crystal violet stained BT474 colonies 152
Figure 3 Calibration plot showing absorbance measured at 450 nm versus initial cell count for BT474 at low passage number 153
Figure 4 Plot showing the effect of thermally stressed Trastuzumab (0.1 mg/mL) on cellular viability as measured by CCK 8 absorbance at 450 nm after 2 hours incubation with CCK8 reagent 154
Figure 5 Plot showing the effect of thermally stressed Trastuzumab on cellular viability as measured by CCK 8 absorbance at 450 nm after 4 hours incubation 155
Figure 6 Size exclusion chromatogram of Trastuzumab at 0.1 mg/ml concentration thermally stressed at 75 ^{o}C for 20 minutes compared to fresh Trastuzumab at 0.1 mg/ml 156
Figure 7 Size exclusion chromatogram of Trastuzumab at 0.1 mg/ml concentration thermally stressed at 75 ^{o}C for 10 minutes and analysed immediately 157

Figure 8. Size exclusion chromatogram of Trastuzumab standard at 0.1mg/ml concentration (blue trace) and Trastuzumab at 0.1 mg/ml concentration thermally stressed at 75^{o}C for 15 minutes and analysed after 4 days 158
Figure 9 Size exclusion chromatogram for ambient storage of 0.1 mg/mL infusion sample compared to fresh Trastuzumab standard 159
Figure 10. Attenuated Total Reflectance (ATR) Fourier Transform Infra-red spectrum of fresh standard of Trastuzumab at 0.1mg/ml and Trastuzumab at 0.1 mg/ml concentration stressed 75 ^{o}C for 20 minutes 160

Chapter 6

Figure 1 Schematic showing typical dose-response curve of BT474 cells over a 0 to 100 nM range 170
Figure 2 A plot of absorbance as a function of drug dose is shown for combined data for stored (day 35) infusion bags (replicates = 16) at
a concentration of 0.5 mg/mL 173
Figure 3 A plot of absorbance as a function of drug dose is shown for combined data for stored (day 35) infusion bags (replicates = 16)
at a concentration of 6 mg/mL 174
Figure 4 A plot of absorbance as a function of drug dose is shown for combined data for stored (day 43) infusion bags (replicates = 16)
at a concentration of 0.5 mg/mL 175
Figure 5 A plot of absorbance as a function of drug dose is shown for combined data for stored (day 43) infusion bags 1 and 2 for plate A and B (replicates = 16) at a concentration of 6 mg/mL 176
Figure 6 A plot of absorbance as a function of drug dose is shown for combined data for stored (day 119) infusion bags (replicates = 16)
at a concentration of 0.5 mg/mL 177
Figure 7 A plot of absorbance as a function of drug dose is shown for combined data for stored (day 119) infusion bags (replicates = 16)
at a concentration of 6 mg/mL 178
Figure 8 Plot showing normalised dose-response. 0.5 mg/mL infusion test sample and reference Trastuzumab expressed as percentage viability of maximum uninhibited cell viability (no drug) set to 100% 182

Figure 9 Plot showing normalised dose-response with reduced scale (0 – 10 nM). 0.5 mg/mL infusion test sample and reference Trastuzumab expressed as percentage viability of maximum uninhibited cell viability (no drug) set to 100% 183
Figure 10 Plot showing normalised dose-response with reduced scale (0 – 10 nM). 6mg/mL infusion test sample and reference Trastuzumab expressed as percentage viability of maximum uninhibited cell viability (no drug) set to 100% 184
Figure 11 Plot showing normalised dose-response with reduced scale (0 – 10 nM). 0.1 mg/mL infusion test sample and reference Trastuzumab expressed as percentage viability of maximum uninhibited cell viability (no drug) set to 100% 188
Figure 12 Plot showing normalised dose-response with reduced scale (0 – 10 nM). 21 mg/mL concentrate test sample from original vial and reference Trastuzumab expressed as percentage viability of maximum uninhibited cell viability (no drug) set to 100% 189

Tables

Chapter 2

Table 1 Trastuzumab retention time compared to co-eluted molecular weight markers 55
Table 2 SE-LC calibration data of instrument response (peak area) using UV detection at 280 nm for Trastuzumab 59

Chapter 3

Table 1 pH at 5 ºC reported for each time-point of study for the of 6 mg/mL and 0.5 mg/mL infusion bag samples 85
Table 2 Visual appearance reported as Pass/Fail with reference to acceptance criteria for 6 mg/mL and 0.5 mg/mL infusions 87
Table 3 Percentage aggregate dimer at each time point for 6 mg/mL and 0.5 mg/mL infusions 81
Table 4 SE-LC determination of Trastuzumab monomer as percentage of initial Trastuzumab assay for 6 mg/mL and 0.5 mg/mL infusions 92
Table 5 Visual appearance of gel plate reported as Pass/Fail with reference to acceptance criteria for the 6.0 mg/mL and 0.5 mg/mL infusions 99

Table 6 Percentage monomer with relative standard deviation for 3 injections and pH at each time-point for 0.1 mg/mL Trastuzumab infusion. 101
Table 7 Percentage monomer and dimer by relative peak area for the 0.1 mg/mL Trastuzumab infusion 102
Table 8 Percentage dimer for the original vial concentrate (21 mg/mL) over the study period. 106
Table 9 Stability of clinically relevant infusions
The pH at room temperature (RT): after exposure to light (24 hours), without light (24 hours) and agitation with exposure to light for 6 hours 107
Table 10 Aggregate and fragmentation analysis of clinically relevant infusions. Electrophoresis of samples taken from infusion bags after being subjected to stress conditions at room temperature (RT) 108
Table 11 Percentage loss of monomer as determined by SEC-LC after further stability testing of infusions 109

Chapter 4

Table 1 Results of the vertical deviation calculation for each cell number for Crystal Violet calibration 133
Table 2 Results of the vertical deviation calculation for each cell number for CCK8 calibration 134
Table 3 Results of the vertical deviation calculation for each cell number for calibration 1 140
Table 4 Results of the vertical deviation calculation for each cell number for the calibration 2 141

Chapter 6

Table 1 Biological activity of stored infusions for Plates A and B (bags 1 and 2 combined giving replicates = 8 for each plate) 180
Table 2 Biological activity of stored infusions using pooled data (combined data for bags and plates A and B: replicates = 16) 181
Table 3 Normalised percentage cell viability is shown for 0.5 mg/mL test infusion sample and compared to reference viability at point of measurement (1 and 2 nM) 185
Table 4 Normalised percentage cell viability is shown for 6 mg/mL test infusion sample and compared to reference viability at point of measurement (1 and 2 nM) 186

Table 5 Normalised percentage cell viability is shown for 0.1 mg/mL test infusion sample and compared to reference viability at point of measurement (1 and 2 nM) 190
Table 6 Normalised percentage cell viability is shown for 21 mg/mL test infusion sample and compared to reference viability at point of measurement (1 and 2 nM) 191
Table 7 Summary of normalised biological activity results for day 119. The table shows % viability difference at 1 nM and 2 nM assay concentrations for test infusions and concentrate stored in original vial 192

Schemes

Scheme 1 The succinimide reaction mechanism 28
Scheme 2 Isomerism of aspartic acid side chain by the hydrolytic cleavage of succinimide to give aspartic acid and isoaspartic acid 29
Scheme 3 Aspartyl hydrolysis of the peptide bond 32
Scheme 4 The mechanism of disulphide exchange 32
Scheme 5 Methionine oxidation mechanism 34
Scheme 6 The para-glutamate (pGlu) formation 35

List of abbreviations

ADCC	Antibody Dependent Cell Cytotoxicity
Asn	Asparagine
Asp	Aspartyl
ATCC	American Type Cell Culture
ATR	Attenuated total reflectance
Balb/c	Bagg albino (stock) c
BFWI	Bacteriostatic Water for Injection
BT474	Breast Tumour cell-line 474
C	Constant (domain)
CCK-8	Cell Counting Kit-8 (Water Soluble Tetrazolium-8)

CDR	Complementarity Determinant Region
CHO	Chinese Hamster Ovary
CV	Crystal Violet
Cys	Cysteine
D	Aspartyl
DEHP	di-(2-ethylhexyl) phthalate
DLS	Dynamic Light Scattering
DP	Degradation Product
DNA	Deoxyribonucleic Acid
E	Glutamate
EBC	Early Breast Cancer
ECD	Extra-Cellular Domain
EGFR	Epidermal Growth Factor Receptor
ELISA	Enzyme-Linked Immunosorbent Assay
EMA	European Medicines Agency (formerly EMEA)
EMEA	European Medicines Evaluation Agency
Fab	Fragment antigen binding of an immunoglobulin molecule
F(ab')$_2$	Immunoglobulin molecule fragment with two antigen binding sites
Fc	Fragment crystallisable
FcγR	Fragment crystallisable gamma Receptor
FTIR	Fourier Transform Infra-red
G1	Gamma (class) 1
γ1	Gamma (heavy chain type) 1
GHPMP	Good Hospital Pharmacy Manufacturing Practise
Gln	Glutamine
Glu	Glutamate
GMP	Good Manufacturing Practise
H	Heavy (chain polypeptide)
HER1	Human Epidermal Growth Factor Receptor 1
HER2	Human Epidermal Growth Factor Receptor 2
HER3	Human Epidermal Growth Factor Receptor 3
HER4	Human Epidermal Growth Factor Receptor 4
His	Histidine

HRP	Horse Radish Peroxidase
HVR	Hyper variable Regions
ICH	International Conference on Harmonisation
IgG1	Immunoglobulin Gamma (class) 1
INN	International Nonproprietary Name
IR	Infra-red
kDa	kiloDaltons
kJ mol^{-1}	kilo Joule per mole
L	Light (chain polypeptide)
L	Laevorotatory
LEC 13	Lectin resistant (cell-line) 13
MAPK	Mitogen Associated Protein Kinase
mAb	monoclonal Antibody
MBC	Metastatic Breast Cancer
Met	Methionine
MGC	Metastatic Gastric Cancer
MTS	4-[5-[3-(carboxymethyloxy)phenyl]-3-(4,5-dimethyl-1,3-thiazol-2-yl)tetrazol-3-ium-2-yl]benzenesulfonate
MTT	Methylthiazoletetrazolium bromide (2-(4,5-Dimethyl-1,3-thiazol-2-yl)-3,5-diphenyl-2,3-dihydro-1H-tetrazol-4-ium bromide)
mumAb4D5-8	murine monoclonal Antibody (clone number)
N	Asparagine
NAD	Nicotinamide Adenine Dinucleotide
NADH	Reduced form of Nicotinamide Adenine Dinucleotide
NADP	Nicotinamide Adenine Dinucleotide Phosphate
NADPH	Reduced form of Nicotinamide Adenine Dinucleotide Phosphate
NHS UK	National Health Service United Kingdom
NK	Natural Killer (cells)
PI3K	Phosphatidylinositol 3-kinase
PDB	Protein Data Base
P	Proline
PBMC	peripheral blood mononuclear cells

pGlu	para glutamate
Phe	Phenylalanine
PMS	Phenizinium methylsulphate
PVC	Polyvinyl chloride
Pro	Proline
Q	Glutamine
Q	Quality (ICH guidelines)
QCNW	Quality Control North West
rhumAb 4D5-8	recombinant humanized monoclonal Antibody (clone number)
RCSB	Research Colloboratory for Structural Bioinformatics
RSC	Royal Society of Chemistry
RT	room temperature
SDS-PAGE	Sodium dodecyl Sulphate-Poly Acrylamide Gel Electrophoresis
SE-LC	Size Exclusion-Liquid Chromatography
SFPO	Société Française de Pharmacie Oncologique **(**French Society of Oncology)
SIAM	Stability Indicating Assay Methods
SOP	Standard Operating Procedure
SPC	Summary of Product Characteristics
SPR	Surface Plasmon Resonance
SWFI	Sterile Water For Injection
TMB	(3, 3, 5', 5')-tetramethylbenzidine
TKR	Tyrosine Kinase Receptor
Trp	Tryptophan
Tyr	Tyrosine
V	Variable (domain)
VEGF	Vascular Endothelial Growth Factor
WST	Water Soluble Tetrazolium
WST-8	Water Soluble Tetrazolium-8 (Sodium 4-[3-(2-methoxy-4-nitrophenyl)-2-(4-nitrophenyl)-2H-tetrazol-3-ium-5-yl]-1,3-benzenedisulfonate)
XTT	3,3'-[5-(Phenylcarbamoyl)-2H-tetrazol-3-ium-2,3-diyl]bis(4-methoxy-6-nitrobenzenesulfonate)

Statement of contribution

The research described in this thesis is, to the best of my knowledge, original except where due reference has been made.

Ian Michael Shropshire

Abstract

There is a lack of stability data for in-use parenteral drugs. Manufacturers state a shelf-life of 24 hours for infusions based on microbiological contamination. The lack of data is of particular significance with protein-based drugs where action is determined by their complex structure. A range of techniques are required to assess stability, including biological assessment to support other data. There has been an increase in published data but often the few studies that address in-use stability are incomplete as they do not employ biological assessment to assess potency.

Trastuzumab is an antibody-based drug used to treat cancers where the Epidermal Growth Factor Receptor 2 (HER2) is over expressed or over abundant on the cell surface. Trastuzumab infusions have been assigned by the manufacturer to be stable for 24 hours at temperatures not exceeding 30 ^{o}C. If stability is shown beyond this point it would enable extended storage and administration. To this end, methods were selected and developed with biological assessment central to the approach to assess clinically relevant infusion concentrations (0.5 mg/mL and 6.0 mg/mL) and a sub-clinical infusion concentration (0.1 mg/mL). This may enhance instability and provide opportunity to study degradation.

A Cell Counting Kit CCK8 (Sigma Aldrich) was ultimately adopted as a basis for a colorimetric assay to assess cell viability. Attenuated Total Reflectance Infra-Red Spectroscopy and Size Exclusion Chromatography methods were developed to evaluate secondary structure and aggregation respectively. These methods were applied to a shelf-life study (43 days) as a collaboration with Quality Control North West (NHS) and Clatterbridge Centre for Oncology NHS Foundation Trust, Clatterbridge Hospital. There was no evidence of degradation and no loss efficacy for clinically relevant infusions (0.5 mg/mL and 6.0 mg/mL) over 43 days, whilst the sub-clinical infusions (0.1 mg/mL) developed particles after 7 days of storage between 2 ^{o}C and 8 ^{o}C. Furthermore, evidence of stability at day 119 gave increased confidence for the data from earlier time points. This work assisted in the shelf-life being recommended to be extended to 28 days for Trastuzumab stored in polyolefin IV bags at concentrations between 0.5 mg/mL and 6.0 mg/mL with 0.9% saline between 2 ^{o}C and 8 ^{o}C. However, infusions with concentrations below 0.5 mg/mL were not recommended for storage.

Acknowledgments

I would like to express my gratitude to the following people for their assistance in this research:

Dr Alan-Shaun Wilkinson for his continual assistance, advice and encouragement.

Dr Heidi Sowter for her guidance and advice.

Prof Mike Allwood for his continual guidance and support.

Prof Paul Lynch for his help and encouragement.

Dr Richard Toon for his support.

University of Derby School of Science (BFS) for funding the Graduate Teaching Assistant position.

BUPA for reconstituted Herceptin® vials, Quality Control Northwest (QCNW) NHS for the Herceptin® drug and Clatterbridge Hospital NHS for supply of infusion bags.

I would also like to express my gratitude for the support from family and friends.

Marilyn, Colin and Aimee Ridding and Joan Davies.

Dr Andrew Wallace, Linda Roberts, Mike Pearson, Dr Atul Nayak, Paul Landon, Stephen Smethurst, Walter Brown, Anthony Mullin and Monika Kopf.

Finally, I would like to dedicate this thesis to the memory of my parents Doris and Ernest Shropshire, my Aunt Marion Rose and Prof Roger J. Mortimer.

CHAPTER 1

1. GENERAL INTRODUCTION

1.1 Rationale for study

Stability studies by the manufacturer provide sufficient information for regulatory purposes of the manufactured product but may have limited relevance in practical use. Clinical requirements may be very different from those needed for licensing purposes. Indeed out of necessity practical use conflicts with the manufacturers specifications for use such as for patient-ready preparations (Bardin et al. 2011). Therefore there is a need to show drugs continue to be safe and efficacious in clinical practise.

The determination of physicochemical stability for drugs based on relatively simple robust chemical compounds is a relatively straightforward and established process (Allwood & Wilkinson 2013). However, new drugs are increasingly based on proteins which are innately more susceptible to instability (Allwood & Wilkinson 2013). The complex variable structure of these molecules determines their clinical effect. Therefore changes in structure may decrease efficacy or initiate an inappropriate response by the immune system. Consequently the complex structure of these molecules requires a multifaceted approach to the assessment of stability. However, there has been a lack of consensus in the approach to this class of drugs (Bardin et al. 2011). This state of affairs can be illustrated by the drug Herceptin® (Roche) which has been selected for this study.

Herceptin® (Trastuzumab (international nonproprietary name (INN)) is an antibody-based drug used to treat cancers where the Epidermal Growth Factor Receptor 2 (HER2) is over expressed or over abundant on the cell surface. Trastuzumab typifies the expense of this class of drug. For example the drug cost alone for treatment of early breast cancer by Norfolk and Norwich University Hospital NHS UK Trust in 2006 equated to £1.9 million for 75 patients (Barrett et al. 2006). If other expenditure associated with treatment are added, including pharmacy preparation, the cost

becomes £2.3 million (Barrett et al. 2006). Thus it is apparent that any improvements in efficiency of drug use would have significant financial benefit.

It can be seen from the example that acceptable stability data beyond this time would enable an extension of the assigned shelf-life. This would aid a safer and cost effective compounding of the drug in practise.

To measure the stability of protein-based drugs is complex and thus requires a range of techniques. Techniques selected must be stability indicating assay methods (SIAMs) to determine physicochemical stability and biological activity (Barnes 2012). Analytical techniques are required to detect sub-visible aggregation as this may lead to particles. It has been suggested that particle formation will determine the shelf-life of the product and therefore should be studied more methodically (Bardin et al. 2011). The determination of biological activity has been largely ignored. This approach has been identified by the NHS UK, in their document A Standard Protocol for Deriving and Assessing Stability Part 2 Aseptic Preparations, as an essential part in determining the overall stability profile (Barnes 2012) and is therefore a focus in this study.

An appropriate study design would entail applying these techniques at suitable time points to assess the integrity of the drug. The NHS recommends that a study has a minimum of four sampling points in addition to the baseline or time zero data (Barnes 2012). Stored samples at each time point would be tested together with standards (day = 0) prepared on the same day.

1.2 General Stability issues and existing guidelines

1.2.1 Hospital Pharmacy Practice and In Use Drug Stability

Hospital pharmacists are required to prepare safe and efficacious doses of parenteral drugs. Ready to administer preparations need to be prepared sufficiently in advance to meet patient needs and for efficient organisation of hospital resources; including staff workload management and reducing wastage of drug (Bardin et al. 2011). This may

entail advanced preparations for an individual treatment over several days, weekends and holiday periods or for dose banding (Bardin et al. 2011). This situation is particularly the case for cytotoxic drug infusions where a short shelf-life, typically 24 hours, has been arbitrary or provisionally assigned on bacteriological grounds (Bardin et al. 2011). Furthermore, there is no documentary indication or data supporting evidence that physicochemical stability is compromised after 24 hours. A shelf-life of over 28 days would be appropriate for most clinical situations for efficient use of infusions (Bardin et al. 2011; Sewell et al. 2003).

Hospitals observe Good Hospital Pharmacy Manufacturing Practise (GHPMP) which is complementary to Good Manufacturing Practise (GMP) observed in drug production. GHPMP ensures that drugs continue to be safe and efficacious within the clinical setting. This means drugs are of the correct dosage and possess appropriate microbiological stability. Therefore the remaining uncertainty resides in the physicochemical stability of the compounded drug. Physicochemical stability is unlikely to have been altered but this needs to be obviously confirmed with appropriate studies. This has been the case with conventional cytotoxic cancer drug infusions such as paclitaxel, a drug used to treat ovarian and breast cancer (Donyai & Sewell 2006).

New cytotoxic cancer drugs are increasingly based on monoclonal antibody structures (Weinberg et al. 2005). These are protein-based drugs which are members of the biologic family of drugs which include hormone drugs. These newer monoclonal antibody-based biologics are more complex than previously approved biologics and conventional chemical drugs. Furthermore, due to their complex structure, monoclonal antibodies are more susceptible to change. Thus there is a need to assess infusions of these drugs under clinically relevant conditions. Conventional drug infusion stability has set the precedence for these new studies to increase shelf-life of this drug class (Kaiser & Kramer 2011; Paul et al. 2012 (a); Paul et al. 2012 (b); Paul et al. 2013; Pabari et al. 2013). However, the methods employed may differ to reflect the distinct instability in this class of drug. In addition, methods will need to be selected on an individual drug basis and, due to the targeted mechanisms of these therapeutic molecules, should include evaluation of biological activity. Assessment of both physicochemical stability and biological activity may offer the best approach for

both safe and efficacious monoclonal antibody-based drugs and other biologics in practical clinical use.

In-use stability studies of protein-based drugs are becoming even more relevant because this class of drug continues to grow in importance. Furthermore, the patents of established biologics are currently coming to the end of their lifetime (Cornes 2012). Indeed, it has been reported Chemistry World (Royal Society of Chemistry) that the very first biosimilar monoclonal antibody-based drugs have been approved in Europe (Anon 2013). These are two biosimilars, manufactured by Celltrion South Korea (Remsima) and Hospira UK (Inflectra), of Johnson and Johnson's Remicade (Infliximab) used to treat autoimmune diseases. It was reported that 'these drugs are the most complex biosimilars yet to be approved in Europe'(Anon 2013). Additionally, it was reported that approval in the US has being delayed due to inadequate guidance for the approval of biosimilars from the Food and Drugs Administration (Anon 2013; Mukhopadhyay 2011). Biosimilars have to show functional similarity to the parent drug (Weise et al. 2012; European Medicines Agency 2014). This is a complicated process and comparable for that of approval for an innovator drug (Mellstedt et al. 2008). In contrast to drugs based on relatively simple chemical structures the biosimilar version will not be identical to its parent drug (Weise et al. 2014). Furthermore, the manufacturing processes will be different to the original drug (European Medicines Agency 2014). Therefore the drug must be considered a new entity (Weise et al. 2012). Hence the term biosimilar is preferred to that of generic or biogeneric (European Medicines Agency 2014; Mellstedt et al. 2008).

Celltrion and Hospira had to complete human trials to ensure that their biosimilar Infliximab was safe and efficacious as Remicade (Anon 2013). Additionally, as with any biosimilar, a comprehensive stability profile should be established as the 'generic' version may behave differently to that of the parent drug. This is due to the inherent variation of structure of these complex molecules and in part to some biosimilars being an improved version of the parent drug. Consequently this has generated an additional need for stability data of these new drugs within a clinical context.

However, there needs to be guidance to ensure stability studies are fit for purpose so as to furnish appropriate data. The limited body of stability data published may only partly meet this need (Allwood & Wilkinson 2013). This is often due to unsuitable methodology and inadequate evaluation measures or unavailability of data from the manufacturer (Barnes 2012). This situation must change so that clinically pertinent stability data can be available. This can be achieved by building on the existing guidelines to produce a post-licensure approach to practical stability. This has been recognised by European hospital pharmacists and various NHS bodies (Allwood & Wilkinson 2013; Bardin et al. 2011; Barnes 2012).

1.2.2 Guidelines for stability assessment

Information on the stability of the diluted drug is limited as the available documentation, including the product insert, is focused on the marketing requirements of the drug rather than its deployment within a clinical setting. In these documents it is presumed the drug will be used immediately (European Agency for the Evaluation of Medicinal Products (EMEA) 2010) and consequently infusions are often designated a shelf-life of 24 hours for bacterial contamination reasons (European Agency for the Evaluation of Medicinal Products (EMEA) 2010).

The International Conference on Harmonisation of Technical Requirements for Registration of Pharmaceuticals for Human Use (ICH) publishes the ICH harmonised tripartite guidelines (ICH 2012). These documents generally refer to the requirements for licensing and offer only a limited guidance for biological products (European Medicines Agency 2006). ICH Q1A Stability Testing of New Drug Substance and Products is concerned with the information required for applications for new molecular entities and drug products (European Medicines Agency 2003). This parent guide refers to ICH Q5C Stability Testing of Biotechnological/Biological Products for further guidance concerning stability of biological-based products (European Medicines Agency 2006). These general guides are concerned with the manufacturing process and the drug as marketed. Nevertheless, the ICH Specifications guides such as ICH Q6B Specifications Test Procedures and acceptance criteria for biotechnological/biological Products, which are a list of tests, references to analytical

procedures, and proposed acceptance criteria, does provide a more explicit guidance (European Medicines Agency 1999).

However, this official guidance is complementary to in use stability and provides a platform to create a more appropriate approach post-licensure. This has been recognised by a European consensus conference in 2010 sponsored by the French Society of Oncology (SFPO) to propose adapted rules based on the existing guidelines to facilitate an approach to anti-cancer drug practical stability (Bardin et al. 2011). The consensus conference identified the need to assign acceptance criteria with respect to degradation products on an individual case. In particular, there was a focus on biologically-based therapies. The acknowledgment of this area of therapeutics is important as there is no such framework in place at present for this class of drugs. It was identified that validated stability indicating assay methods (SIAMs) should be used (Bardin et al. 2011). Moreover consideration should be given that an accepted analytical procedure from a pharmacopoeia may not be sufficiently a SIAM. The method would have been originally developed for the determination of synthesis or process impurities rather than degradation products (DPs). Therefore it is important to show that a proposed procedure is able to distinguish DPs being formed in practical clinical use (Bardin et al. 2011).

The NHS has also recognised the need for an approach to practical stability especially for use of biologically-based drugs. To meet this need the NHS Pharmaceutical Quality Assurance Committee, the NHS Pharmaceutical Production Committee and the NHS Pharmaceutical Aseptic Services Group have commissioned a protocol for deriving and assessing stability of biopharmaceuticals (Barnes 2012). The document was created by the NHS Pharmaceutical Research and Development Working Group. This has resulted in a standard protocol for aseptic preparation of licensed biopharmaceuticals (Barnes 2012). The focus of the protocol is on monoclonal antibodies although much will be relevant to other proteins. The document does not refer to cell-based therapies, vaccines or blood components and is intended only for aseptic manipulation post-licensure use.

In conclusion it is apparent that the need of stability data for infusion-based drugs is in the process of being addressed. This is particularly important for innovator and

biosimilar monoclonal antibody drugs, where their structure makes them potentially more vulnerable to change. This fact combined with their high cost more than justifies the need for an extended shelf-life for efficient use and to reduce unnecessary wastage.

1.3 Trastuzumab Case Study

1.3.1 Trastuzumab and Cancer

Trastuzumab belongs to the relatively new class of antibody-based drugs. Antibody-based drugs are part of the biologic family of drugs (Goldenberg 1999). Biologics are manufactured using recombinant DNA technology and have been engineered to treat a variety of diseases including cancer. Trastuzumab is an anti-Human Epidermal Growth Factor Receptor 2 (HER2) humanized monoclonal immunoglobulin G1 (IgG1) antibody (rhuMAb 4D5-8).

Trastuzumab was generated by immunization of Balb/c mice with cells and membranes containing the HER2 protein. This was achieved by using an antibody producing hybrid cell-line (hybridoma). The resultant murine parent of Trastuzumab (muMAb 4D5) was humanized by genetic engineering (Carter et al. 1992). The humanized Trastuzumab (rhuMAb 4D5-8) retains only the HER2 recognition site of the original murine antibody and is produced in recombinant Chinese Hamster Ovary cells by hybridoma technology (European Agency for the Evaluation of Medicinal Products (EMEA) 2005b).

Trastuzumab has been designed to bind with high affinity and specificity to the extra-cellular domain of the HER2 receptor (Human Epidermal Growth Factor Receptor 2) (Carter et al. 1992). The binding of Trastuzumab to the HER2 receptor interrupts its role with other HER receptors in the intra-cellular signaling process and marks out the cell for destruction by antibody dependent cell cytotoxicity (ADCC) (Goldenberg 1999). Trastuzumab is only indicated for cancers where the HER2 receptor number is found to be higher than normal (European Agency for the Evaluation of Medicinal Products (EMEA) 2010). The HER2 gene is amplified affording an increase in the

number of HER2 molecules at the surface of the cells. Tumours which show this are therefore termed as over-expressing HER2 or HER2 positive. Furthermore, the large difference between normal levels and over-expressed levels make the receptor a prime therapeutic target (Maple et al. 2004). HER2 over-expression is found in 30% of breast cancers as determined by Slamon et al. (1987) and cited by Nahta (2012).

HER2 over-expression is also found in other tumours besides breast such as ovarian, non-small-cell lung and bladder cancer (Scholl et al. 2001). Trastuzumab is indicated for the treatment of patients with the following cancers: metastatic breast cancer (MBC); early breast cancer (EBC) and metastatic gastric cancer (MGC) (European Agency for the Evaluation of Medicinal Products (EMEA) 2010). HER2 positive cancer is linked with rapid tumour growth and increased ability of the disease to spread. Initially licensed for HER2 positive breast cancer, treatment with Herceptin has been extended to other HER2 positive cancers.

1.3.1.1 HER2 and Cell Signalling

HER2 is a trans-membrane protein and is a member of the Tyrosine Kinase Receptor family (TKR). These receptors are structurally related comprising of an ligand binding extra-cellular domain (ECD), a membrane spanning region and an intra-cellular signalling region reviewed by Hynes and MacDonald (Hynes & MacDonald 2009). The TKR group is involved in the control of cellular processes such as proliferation, differentiation, migration and apoptosis or cell death. Control is provided by the transduction of a chemical messenger or peptide ligand and interaction between one of the other receptor molecules. The HER2 receptor molecule has a key role due to being a preferred partner in this interaction (Gijsen et al. 2010). HER2 is always present in the activated conformation whilst the other receptor molecules need to be activated by ligand binding to allow interaction with HER2.

The receptor family comprises of HER1 (commonly referred to as EGFR), HER2, HER3 and HER4. Ligand activation of the HER1, 3 and 4 causes dimerisation of these receptors with HER2. Figure 1 shows the HER2:HER3 dimerisation and the resultant phosphorylation of HER3 which initiates intra-cellular signalling. HER2 is

responsible for activating the mitogen associated protein kinase (MAPK) signalling pathway. A mitogen is a substance which causes nuclear and cell division. Increase in this process results in cell proliferation. Each possible combination initiates a different signalling pathway through the activated EGFR tyrosine kinase of the receptor. A protein kinase is an enzyme which adds a phosphate to a specific amino acid such as tyrosine. The activated EGFR tyrosine kinase undergoes autophosphorylation of its C-terminus tyrosine residues (phosphotyrosine sites) within the cell. This allows numerous proteins (protein kinase) to bind to the phosphotyrosine sites on the cytoplasmic tail of the receptor, thus enabling the propagation of the intra-cellular signalling cascade (Busse et al. 2000). The regulation of the interaction of signalling pathways is intimately controlled by the presence and identity of the ligand, the heterodimer partners and the availability of proteins that can bind to the phosphotyrosine sites (Kruser & Wheeler 2010).

The HER2:HER3 heterodimer may be the most effective coupling for the generation and development of the tumour (Genentech 2015). This dimer activates cell proliferation and survival pathways. The HER3 dimer partner activates the phosphatidylinositol 3-kinase (PI3K) pathway. The HER3 receptor is the only HER member that can directly initiate the PI3K pathway. This kinase phosphorylates a membrane phospholipid on the insositol group at carbon 3 of its ring structure. This signal pathway leads to an increase in cell survival and resistance to programmed cell death (apoptosis).

Content removed for copyright reasons.
Genentech, 2015. HER2 HER3 Dimerization | BioOncology. Available at: http://www.biooncology.com/research-education/her/dimer [Accessed January 9, 2015].

Figure 1 Schematic representation of the HER2:HER3 heterodimer. HER2 phosphorylates (transphosphorylation) the tyrosine kinase domain of HER3. This results in intra-cellular signalling leading to proliferation, increased cell survival and resistance to programmed cell death. Source: adapted from Genentech Reaction HER Pathways [online] (Updated 2009) (Genentech 2015).

1.3.1.2 Mechanisms of Trastuzumab Action

The mechanisms of action of Trastuzumab are not completely known. The action of Trastuzumab is thought to involve the binding of the Trastuzumab molecule to the HER2. This event prevents the dimerisation of HER2 with other HER molecules. The intra-cellular signalling is therefore interrupted, inhibiting cellular proliferation (Genentech 2015). The bound Trastuzumab may also stop the loss of the extracellular domain (ECD) of HER2 (Molina et al. 2001). The loss of the ECD is an activation mechanism of HER2 (Zabrecky et al. 1991). However, there is strong evidence that an

immune response is a major element of the action of Trastuzumab (Gijsen et al. 2010; Colombo et al. 2010). The summary of product characteristics states that 'Trastuzumab is a potent mediator of antibody-dependant cell-mediated cytotoxicity (ADCC)'(European Agency for the Evaluation of Medicinal Products (EMEA) 2010). This is consistent with the mode of action of antibodies in general. In this process the surface bound antibody molecules mark these cells out for destruction by the immune system (Elgert 2009; Collins et al. 2012). This process is mediated by the Fc region of the antibody with Fc receptors of the immune cells (Elgert 2009). In addition, Trastuzumab may cause the cell membrane to surround the HER2 receptor taking it within the cell (Valabrega et al. 2007). This process is called endocytosis and as a result down-regulates the HER2 expression and function.

1.3.1.2.1 Inhibition of tumour cell proliferation

Trastuzumab is an anti-HER2 antibody which means it will recognize and then bind specifically to the extra-cellular domain of the HER2 protein. This highly specific binding interaction is enabled through the fragment antigen binding (FAB) residing on the Trastuzumab molecule (Cho et al. 2003). Figure 2 shows the structure of the extra-cellular domain (ECD) of HER2 alone and in complex with the Herceptin FAB (Cho et al. 2003). Once bound to the HER 2, Trastuzumab prevents the formation of a dimer with HER3 (figure 2) or one of the other receptor molecules. Thus phosphorylation of the receptor is prevented and signalling cascade halted. This results in inhibition of cellular proliferation and cell growth (figure 3).

Content removed for copyright reasons.

Cho, H.-S. Mason, K., Ramyar, K. X., Stanley, A. M., Gabelli, S. B., Denney, D. W., & Leahy, D. J., 2003. Structure of the extracellular region of HER2 alone and in complex with the Herceptin Fab PDB 1n8z. Nature, 421(6924), pp.756–60.

Figure 2 X-ray crystal structure of (A) Trastuzumab Fab fragment (Fragment antigen binding) bound with (B) extra-cellular domain of HER2 (Cho et al. 2003). PDB access code 1n8z; resolution 2.5Å.

Content removed for copyright reasons.

Genentech, 2015. HER2 HER3 Dimerization | BioOncology. Available at: http://www.biooncology.com/research-education/her/dimer [Accessed January 9, 2015].

Figure 3 Bound Trastuzumab prevents the formation of the dimer with HER3. Phosphorylation of the receptor is prevented and signalling cascade halted. The result of this is inhibition of cellular proliferation and cell growth. Source: adapted from Genentech Reaction HER Pathways presentation [online] (Updated 2009) (Genentech 2015).

Recent research has shown that Trastuzumab does not decrease HER2 phosphorylation (Gijsen et al. 2010). Furthermore, is has been reported that Trastuzumab given alone to HER2 positive cells can increase HER2 phosphorylation (Scaltriti et al. 2009; Junttila et al. 2009). This may be an important factor in acquired immunity when Trastuzumab is given as a monotherapy (Gijsen et al. 2010).

1.3.1.2.2 Antibody-dependant cell-mediated cytotoxicity (ADCC)

ADCC is a process where the cell bound antibody marks the cell out for destruction by the immune system cells. The immune cells primary involved in this process are the natural killer (NK) cells (Strome et al. 2007). These are large granular lymphocytes which are white blood cells. The process is reliant on the antibodies Fc region γ heavy chain being recognised by the NK cells corresponding Fc gamma receptor (FcγR). ADCC is initiated when Fc binds to the lymphocyte FcγR.

1.3.1.3 Formulation and practice aspects of drug compounding

Herceptin® in Europe contains Trastuzumab (150 mg) and is formulated with the excipients α, α trehalose dehydrate (136.2 mg), L-histidine hydrochloride (3.36 mg), L-histidine (2.16 mg), and polysorbate 20 (0.6 mg) as a lyophilised powder. The powder is contained in a clear glass Type I borosilicate glass vial (15ml capacity) with butyl rubber stopper laminated with fluoro film resin (European Agency for the Evaluation of Medicinal Products (EMEA) 2010).

Trastuzumab is reconstituted for administration with 7.2 mL of sterile water for injection (SWFI) in the original vial. This gives a single dose solution of Trastuzumab at a concentration of approximately 21 mg/mL and a volume of 7.4 mL representing a 4% volume overage. The overage is provided to ensure that the full dose of 150 mg of Trastuzumab can be removed from the vial if necessary. The actual volume of solution removed relates to the dosage required which in turn depends on patients weight and the regimen followed. Calculations for a weekly and three-weekly regimens are adapted from the product information supplied in the summary of product characteristics (European Agency for the Evaluation of Medicinal Products (EMEA) 2010). The requisite volume is withdrawn from the vial and is always diluted for intra-venous infusion by addition to an infusion bag containing 250 ml of 0.9% saline solution.

1.4 Structure of Trastuzumab

1.4.1 General Protein Structure

The compact structure of a protein is determined by the interaction between the constituent amino acid groups and the water present. The hydrophilic polar side chains interact with the water solvent through hydrogen bonding. This aids the burial of hydrophobic non-polar groups within the protein, a thermodynamically favoured process (Stryer 1995)**.**

In contrast, hydrogen bonding between amino acid residues gives rise to the various structures found within proteins. The amino acid group can hydrogen bond through the main chain CO and NH groups. In addition, some of the side chain groups are able to form hydrogen bonds within the core. Therefore structure can be described in terms of amino acid sequence and the 3-dimensional structures that emerge. There are four levels of increasing complexity that describe protein structure: primary, secondary, tertiary and quaternary (Stryer 1995) (figure 4).

1.4.1.1 Primary

Primary structure is the sequence of amino acids and encodes the folding instructions for the protein. The peptide bond which forms the sequence is rigid. This pre-determines the number of conformations available on rotation of the adjacent bonds. This may result in the polypeptide chain folding into distinct structures (Stryer 1995).

1.4.1.2 Secondary (Stryer 1995)

What is called secondary structure? This process is driven by the formation of hydrogen bonds between amino acid residues to give a repeating pattern or motif. These motifs are termed α-helix and β-sheet (figure 4). These are present within small regions of relatively disordered coils. The α-helix is a tightly coiled helix formed by the main chain CO and NH forming inter-molecular hydrogen bonds. The β-sheet is

formed from a series of β-strands. A β-strand is an almost fully extended polypeptide chain. Inter-molecular hydrogen bonds between individual β-strands stabilise the β-sheet. The polypeptide chain may run in the same or opposite direction. The resulting structures are termed parallel and anti-parallel β-sheets respectively. To conserve the compact structure of the protein a β-strand has to reverse its direction. This gives rise to the β-turn resulting in a β-sheet running in the opposite direction (figure 4).

1.4.1.3 Tertiary

Tertiary structure is the overall folded structure of a polypeptide. This consists of various secondary structural elements forming domains, regions of less ordered structure and distribution of disulphide bonds (Stryer 1995).

1.4.1.4 Quaternary

The final organisational level is the quaternary structure. This refers to the relationship of discrete polypeptide sub-units (Stryer 1995).

Content removed for copyright reasons.
Egan, W.M., 2009. Analytical Techniques for Characterizing Follow-on Protein Products NDA and BLA Pathways for Biologics. PharmaNet Boston.

Four levels of protein structure also described and illustrated in Stryer, L., 1995. Biochemistry. In Biochemistry. New York: W H Freeman, pp. 17–41.

Figure 4 Schematic of the four levels of protein structure. Primary structure: amino acid sequence. Secondary structure: folding of sequence into distinct structures such as α-helix (red) and β-strand (blue). Tertiary structure: overall folding of the polypeptide with interaction of secondary structures. β-strands form sheets with turns (A). Quaternary structure: relationship between polypeptide sub-units. Source: adapted from the presentation Analysing Techniques For Characterising Follow-on Protein Products (Egan 2009).

1.4.2 IgG Antibody Structure

1.4.2.1 Antibody fragments

The model of antibody structure and its terminology originates from work in the late 1950's and early 1960's (Elgert 2009). Porter in 1959 selectively fragmented IgG using the enzyme papain (figure 5). Three fragments were produced each having a mass of 50 kiloDaltons (KD). Two of the fragments were able to bind antigens. These were termed fragment antigen binding (Fab). In contrast, the third fragment was unable to bind an antigen and crystallised on storage at low temperature. This part was the stem portion and called fragment crystalliable (Fc) (Elgert 2009).

Corresponding studies by Alfred Nisonoff cited by Elgert (2009) investigated antibody structure with the enzyme pepsin. The site of hydrolysis by pepsin cleaves the molecule at a different site to papain (figure 5). In this case one large fragment was yielded and many very small fragments. The molecular weight of this large fragment was 100 KD, twice that of the Fab. This fragment was termed $F(ab')_2$.

1.4.2.2 Chain Structure Heavy and light chains (Elgert 2009)

In a different approach, Edelman used a reducing agent and solvent treatment to determine the polypeptide structure of the IgG. Dithiothreitol was used to reduce the disulphide bonds. An addition of iodoacetamide prevented disulphide bonds from reforming by alkylating the sulphur. A denaturant was used to disrupt non-covalent interactions. After a separation step two polypeptide sub-units of different mass were identified in equimolar ratio. The larger sub-unit was named heavy (H) and the smaller light (L). The molecular weights of the fragments were 50 KDa and 23 KDa respectively. Edelman concluded that the IgG comprised of two heavy and two light polypeptides. Additionally, it was concluded that these subunits are linked by a disulphide bridge and non-covalent interactions.

Figure 5 shows a representation of the IgG molecule indicating the positions of enzymatic cleavage by papain and pepsin. Fab and $F(ab')_2$ fragments are generated by pepsin and papain respectively.

Content removed for copyright reasons.
Elgert, K.D., 2009. Antibody structure and function. In Immunology: understanding the immune system. John Wiley and Sons, pp. 58–78.

Figure 5 Schematic representation of the IgG molecule: showing light and heavy chains with positions of enzymatic cleavage indicated. Cleavage with papain releases the individual Fab units. Cleavage with pepsin generates the $F(ab')_2$. L = light chain and H = heavy chain polypeptides. Based on figure 4-2 Antibody structure and function Chapter 4 (Elgert 2009).

The polypeptide is further arranged into domains. These are regions which fold into a compact structure. The domains are defined by disulphide bridges across one point of the chain to another point on the same polypeptide chain. In between the domains the peptide chain is less ordered.

1.4.2.3 Glycosylation

The carbohydrate content of an antibody is in the form of two nitrogen-linked oligosaccharides on the Fc heavy chains. The presence of these oligosaccharides and their structure is essential for ADCC. This aspect of action is important in the efficacy of therapeutic mAbs (Goswami et al. 2013). The composition of the carbohydrate includes variable amounts of fucose, galactose and sialic acid.

1.4.3 Trastuzumab structure (Elgert 2009; Magdelaine-Beuzelin et al. 2007)

The quaternary structure of a Trastuzumab IgG molecule consists of two identical polypeptide chains of 214 amino acids (light chain), two identical polypeptide chains of 446 amino acids (heavy chain) and 2-3% carbohydrate. Each chain is divided into domains of variable or constant primary structure. The light chains consist of a variable (V) and constant (C) domain. The heavy chains have one V and three C domains. The heavy chains pair and the light chains pair with the heavy chains. The chains and domains are linked by disulphide bonds and non-covalent interactions forming the characteristic Y shape. The N-terminal (amino terminal) of the polypeptide chains are on the arm tips whilst the C-terminal (carboxylic acid terminal) is at the opposite end. The arm tips of the Y are highly variable in amino acid sequence and vary between different antibodies.

The variable regions are organised into three distinct hypervariable regions (HVRs). These are called complementarity determinant regions (CDRs) and are termed CDR1, CDR2 and CDR3. Between each HVR the amino acid sequences are of limited variability and define each separate CDR. The variable regions of the light and heavy chains fold to form a cleft. The CDRs are exposed on the cleft surface and are

important in determining its shape. The specific shape is essential in binding an antigenic determinant or site on an antigen. The distinctive shape of the cleft is responsible for the high specificity of Trastuzumab in binding to the HER2 protein (Elgert 2009).

Trastuzumab is the result of the humanisation of its parental murine monoclonal antibody (mumAb 4D5) during the production process. This means only the CDRs are of mouse origin in Trastuzumab. The humanisation process resulted in a 3-fold increase in binding affinity (European Agency for the Evaluation of Medicinal Products (EMEA) 2005b). The primary structure determines the proteins 3-dimensional structure. Therefore changes in amino acid sequence of the variable regions may modify the cleft shape, change specificity and binding affinity. The hinge region connects the arms of the molecule to the stem. This allows greater flexibility facilitating simultaneous binding of different sites (Magdelaine-Beuzelin et al. 2007).

The stem portion of the heavy chains has a constant amino acid sequence. The heavy chains are identical within an antibody class or isotype. In the IgG1 isotype, which Trastuzumab belongs, they are called γ chains and determine its biological action or effector functions. The IgG1 stem region mediates the immune systems response. This arises when the antibody covers the cell, marking it for destruction, and the Fc binds to the immune cells. This process recruits various types of white blood cells, especially the natural killer (NK) cells, to kill the antibody-targeted cells. The process is called antibody dependent cell cytotoxicity (ADCC). Furthermore, the humanisation of mumAb 4D5 maximise the immune response of Trastuzumab by incorporating the human IgG1 heavy chains (γ1) for the Fc (European Agency for the Evaluation of Medicinal Products (EMEA) 2005b). This ensures recognition and attack by the human immune system for which the Fc has a critical role (Liu et al. 2008).

Glycosylation and its structure are essential for this function. This aspect of action is important in the efficacy of therapeutic mAbs. The composition of the carbohydrate includes variable amounts of fucose, galactose and sialic acid. The carbohydrate content has been modified in therapeutic mAbs to improve affinity with the immune system (Carter 2006). This has enhanced anti-tumour activity (Liu et al. 2008). In

particular, the fucose content has an effect on ADDC effectiveness. The absence of fucose in the oligosaccharide has been shown to increase ADDC (Jefferis 2009). This was shown with Trastuzumab when produced in a mutant CHO cell-line (LEC 13). However, the cell-line was not suitable for production of the drug (Jefferis 2009).

1.5 Protein stability

Conventional drugs are based on relatively simple robust chemical entities. Their structure enables them to withstand processes such as tableting, encapsulation and packaging (Wang 1999). In contrast protein-based drugs have physical and chemical properties that make them more prone to structural change (European Medicines Agency 2006). These differences can be attributed to the types of chemical bonding which define the active structure (European Medicines Agency 2006). The biologically active protein structure, referred to as the native state, is the result of the highly specific organisation of the primary, secondary and tertiary structures (Stryer 1995).

Stability is classed and described in terms of physical or chemical processes. This classification is useful in providing a mechanistic understanding of the principal processes involved. In actuality, physical and chemical instabilities are linked (Manning et al. 2010). Changes in conformation may expose a chemically reactive site or conversely a chemical change at the primary level will influence structural changes at higher levels (Manning et al 2010.). This may lead to loss of efficacy or increased immunogenicity. A more complete understanding of these processes will aid the production of more stable formulations, effective monitoring and the assessment of protein drugs in-use.

The understanding of protein-based drug stability is becoming increasingly important as new biologics are developed. More specifically, as patents are beginning to expire on current biologics, the field of biosimilar or biogeneric protein-based drugs is likely to expand. Manning et al (1989) wrote a review on protein stability which has been frequently cited (Manning et al. 1989). The review has been recently updated

(Manning et al. 2010) which reflects how knowledge has progressed with a corresponding increase in dominance of protein-based drugs.

1.5.1 Physical Stability

Physical stability refers to the ability of the protein to retain its 3-dimensional biologically active or native structure. The protein superstructure is only slightly stable and is in constant flux of different folded states. Unfolding of the protein molecule may make the protein drug product susceptible to degradation through the mechanisms of denaturation, adsorption, aggregation and precipitation (Manning et al. 2010).

1.5.1.1 Adsorption

Surface induced instability of a protein molecule begins with adsorption of a native or partially unfolded protein molecule (Manning et al. 2010). The adsorption of the IgG1 molecule is a particular favoured process due to its structural complexity and flexibility irrespective of surface charge or surface energy. Surface adsorption may result in a lowering of the bulk Trastuzumab concentration and thus reducing the administered effective dose or efficacy of the preparation. Additionally, adsorption may induce changes in conformation leading to denaturation and loss of efficacy of the Trastuzumab molecule.

1.5.1.2 Conformational stability

The native folded conformation is achieved by the combination of attractive forces and hydrophobic interactions. Attractive forces involved are electrostatic forces, Van der Waals forces and hydrogen bonds. The native folded state of the protein is not static and involves a distribution of many different states of folding or partial unfolding. The dynamic native structure is a balance between the stabilising interactions and tendency for entropy of the conformation to increase. Entropy is the

drive for the unfolding of the protein. The large and complex structure of the protein gives scope for disorder of the system to increase. This is manifest in the range of different folded states centered on the native conformation.

The thermodynamic stability of the native structure of a protein is minimal (~21-84 kJ mol^{-1}) under physiological conditions (Chi et al. 2003). To put this into context the staggered and eclipsed conformations of a hydrocarbon only differ by a 12 kJ mol^{-1}. The rotation about the carbon-carbon single bond readily takes place at 25^{o}C with frequency of approximately $10^{12}s^{-1}$. In contrast, the thermodynamic stability of covalent and ionic bonds is considerably greater (~627kJ mol^{-1}) (Chi et al. 2003). For example the bond energy of a C-C single bond energy in ethane is 347 kJ mol^{-1} and that of the C=C double bond in ethene is 598 kJ mol^{-1}.

1.5.1.3 Aggregation

1.5.1.3.1 Low Order Aggregation (Dimers, trimers and other low order oligomers)

The native monomer in solution has a tendency to form reversible native conformation aggregates which are the result of association and disassociation of the protein molecules (Philo & Arakawa 2009). The constituent monomers of these aggregates retain their original structure and biological activity. The reversible native conformation dimers are innate within the formulation and are present in protein solutions from the time of production to administration. The antibody molecule is inherently self-complementary and will have a tendency to naturally associate forming reversible oligomeric species such as dimers and trimers. These oligomers may become irreversible (non-native) over time by the formation of covalent bonds between the monomeric units. Further aggregate growth of these small oligomers by the addition of monomers is thermodynamically disfavored due to an energy barrier to assemble or nucleate (Chi et al. 2003). However, overtime may eventually lead to particulate formation and ultimately precipitation.

1.5.1.4 Denaturation

1.5.1.4.1 High Order Aggregation (Precipitation)

Non-native or irreversible aggregation is a process whereby the protein molecules associate. This process occurs via a partly unfolded intermediate which reveals the hydrophobic core. The core is normally bound and not accessible to the water solvent. Binding of this internal structure to another molecular core can lead to irreversible collapse of the protein structure and aggregation.

Irreversible aggregation is a common way physical instability is demonstrated within a formulation (Chi et al. 2003). The aggregation process results in reduced activity and more significantly an increase in immunogenicity of the drug system. Aggregates can form in both liquid and solid forms under a variety of conditions experienced during processing, storage and use (Arakawa et al. 2006). Conditions which may promote aggregation include concentration, pH, temperature, lyophilisation, freeze-thaw processing and mechanical stress.

Mechanical stress is of particular interest as it is encountered at each step of production and use of the protein. Liquid formulations are stirred and pumped during the manufacturing process. In use, the drug will be administered by injection or infusion. Mechanical stress includes sheer forces induced by mixing (stirring and shaking) and injection. The large velocities of these processes have been described as capable of denaturing the structure of the protein leading to aggregation and cleavage of the amide backbone (Jaspe & Hagen 2006).

Studies using Horse cytochrome c exposed to laminar flow high shear forces showed no change in structure (Jaspe & Hagen 2006). Horse cytochrome c is a small and compact globular protein of 104 amino acids and therefore may be more resistant to sheer forces. Conversely, the antibody molecule may be more susceptible to shear forces. This view is consistent with the fact that the antibody molecule is considerably larger, more complex and flexible than simpler globular proteins. A study of the rheological and syringeability properties of polyclonal antibodies were not affected by irreversible aggregation (Burckbuchler et al. 2010).

In considering these types of studies it is important to be sure other factors are not contributing to the observed effect. Shear forces are often applied over an extended period of time. This may give time for surface adsorption denaturation to contribute or affect the amount and type of aggregates (Jaspe & Hagen 2006; Kiese & Papppenberger 2008). In contrast to simple shear force models, shaking and stirring of IgG1 may generate aggregates (Kiese & Papppenberger 2008).

Precipitation is the macroscopic result of molecular association whereby the aggregate size exceeds the limit for solubility. This is particularly important issue for long term storage. Precipitation may also occur by the concentration exceeding the solubility product.

1.5.2 Chemical stability

In contrast to physical instability, chemical instability within a protein molecule can be manifest in bond formation or disassociation generating a new chemical entity. Degradation may involve the following discrete chemical reactions; deamination (scheme 1), aspartic acid isomerisation (scheme 2), proteolysis (scheme 3), oxidation (scheme 4), disulphide exchange (scheme 5), Maillard reaction and para-glutamine residue (p-Glu) formation (scheme 6).

1.5.2.1 Chemical Degradation

1.5.2.1.1 Deamination to succinimide

Deamination is a common degradation path for peptides and proteins (Manning et al. 2010). Trastuzumab formula at pH 6 the mechanism will involve an acid catalyzed intra-molecular cyclization of the Asparagine (Asn or N) or glutamine (Gln or Q) residues with the back-bone amide nitrogen. The reaction of Asn residue is considerably faster than that for the Gln side chain amide and is probably due to the conformational stability of the succinimide 5-membered heterocyclic ring at pH6 (scheme 1).

The scheme shows the reaction of the Asparaginyl forming a succinimide with concomitant irreversible loss of ammonia from the amide. The steps involved in the intra-molecular cyclization are described below.

Step 1: Base abstraction of hydrogen from the back bone amide N generates a nitrogen nucleophile. This is stabilised by delocalisation of negative charge in a π-allyl system over the back bone amide bond. Stabilisation of the anion intermediate can be further enhanced by conformation (Robinson & Robinson 2004) and effects such as hydrogen bonding.

Step 2: Nucleophillic attack on the carbon of the side chain amide to give a cyclic intermediate.

Step 3: Protonation of the amine group (regeneration of base) and its loss as ammonia to give the succinimide.

Contents removed for copyright reasons.

Robinson, N.E. & Robinson, A.B., 2004. Molecular Clocks – Deamidation of asparaginyl and glutaminyl residues in peptides and proteins, Cave Junction OR: Althouse Press.

Scheme 1 The succinimide reaction mechanism: showing the intra-molecular cyclization of the Asparaginyl residue with the amide back bone (Asparaginyl residue in green) (Robinson & Robinson 2004).

1.5.2.1.2 Hydrolysis of succinimide and isomerism of aspartic acid product

The L-succinimide an identifiable degradation product in its own right, may be cleaved by hydrolysis at either side of the N atom of the heterocyclic moiety giving a mixture of aspartic and isoaspartic acid (scheme 2). Inter-conversion or isomerism is then made possible by imide ring intermediate shown in scheme 1 and 2. This process of isomerism has been reported to take place often in the recent literature for monoclonal antibodies (Manning 2010).

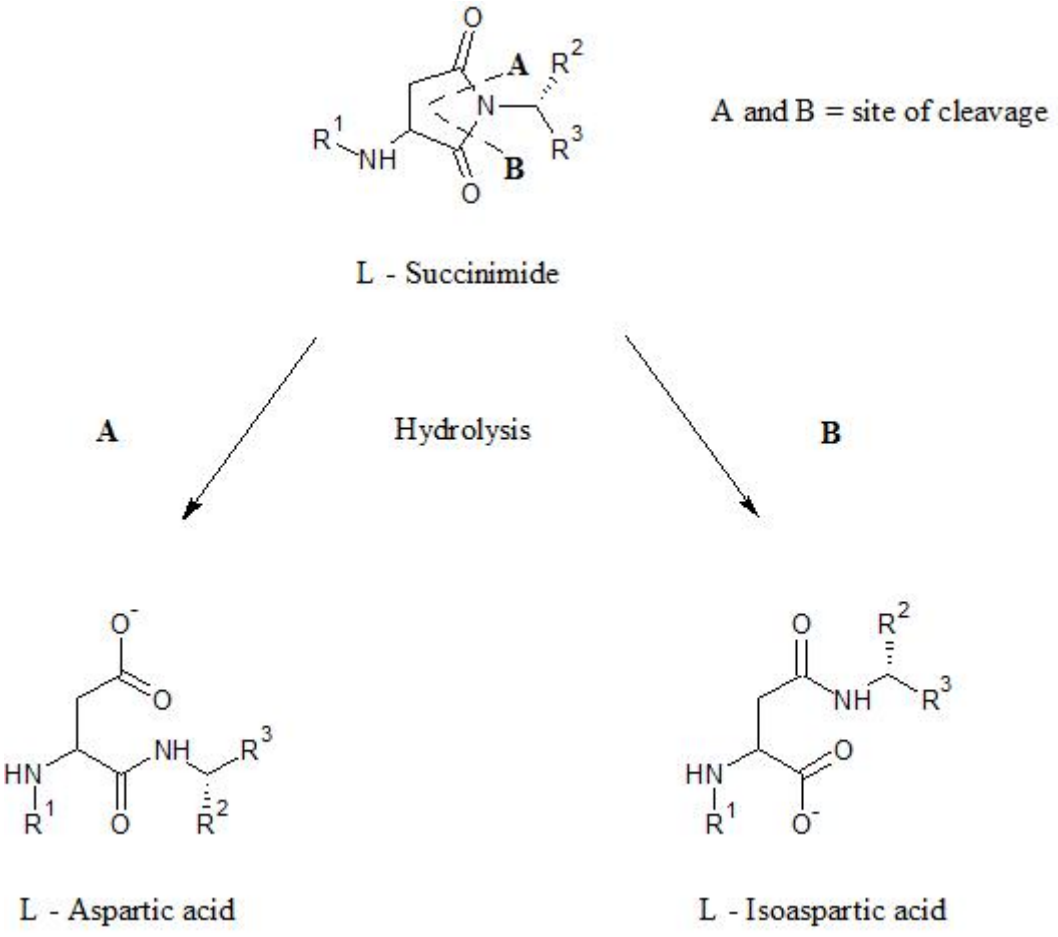

Scheme 2 The scheme shows isomerism of aspartic acid side chain by the hydrolytic cleavage of succinimide to give aspartic acid and isoaspartic acid. Cleavage can take place either side of the ring nitrogen atom at position A or B.

1.5.2.1.3 Proteolysis

Aspartyl (Asp or D) residues may induce hydrolysis of the peptide bond of the backbone at either N and C terminals or both (scheme 3). Peptide cleavage may lead to inactivation of protein (Manning et al. 1989). The Asp-Pro Proline (Pro or P) sequence is particularly prone to hydrolysis in the presence of ammonia. The mechanism involves an intra-molecular cyclization and as the deamination process discussed above is pH dependent.

Degradation by hydrolysis not involving Asp occurs in the hinge region. This process is different to the enzymatic cleavage reactions usually used to prepare fragments of antibodies for study and characterization. Cleavage in the case of hydrolysis involves a residue sequence range within the hinge location and has been associated with the inherent flexibility of the protein in this location and instability of the fragment antigen binding Fab unit itself (Manning 2010).

Contents removed for copyright reasons.

Manning, M.C., Patel, K. & Borchardt, R.T., 1989. Stability of Protein Pharmaceuticals. Pharmaceutical research, 6 (11), p.903 818.

Scheme 3 Aspartyl (Asp or D) residues may induce hydrolysis of the peptide bond of the backbone at either the N or C terminals. Aspartyl residues may form 6 and 5-membered ring intermediates with N-peptide and C-peptide bond fission of the respective intermediates. Source: Stability of protein pharmaceuticals (Manning et al. 1989).

1.5.2.1.4 Disulphide exchange

Trastuzumab as with many protein molecules contain important sulphur bonds. These can be disrupted or scrambled leading to change in structure. Sulphur bonds are important in defining and stabilizing the globular structure of the protein and hence its ability to recognize and bind with other proteins. Therefore alteration or mismatching of sulphur bonds will lead to changes in 3-dimensional structure and loss of activity. The mechanism of disulphide exchange in neutral and alkaline media is shown in scheme 4.

Contents remove for copyright reasons.
Manning, M.C., Patel, K. & Borchardt, R.T., 1989. Stability of Protein Pharmaceuticals. Pharmaceutical research, 6(11), p.903 818.

Scheme 4 The mechanism of disulphide exchange under neutral and alkaline conditions. Source: Stability of protein pharmaceuticals (Manning et al. 1989).

During SDS-PAGE under reducing conditions the disulphide bonds of an antibody are broken apart to furnish the individual light and heavy chains of the protein. This contrasts with enzymatic treatment where the Fab and Fc fragments of an antibody molecule are generated instead.

1.5.2.1.5 Oxidation

Another major protein degradation route is that of oxidation. A solution of protein drug will have a head space which increases after initial use and therefore on storage presents an increased opportunity for aerial oxidation. The residues that are most susceptible to oxidation are the sulphur containing Cysteine (Cys) and Methionine (Met) side chains. The sulphur containing side chains are hydrophobic and therefore buried within the core of the globular protein. Rate of reaction is dependent on oxygen solubility and diffusion. Cys will form disulphides and radical species and in contrast Met will give sulphoxides. Oxidation of Met residues has been shown to occur in the constant region of monoclonal antibodies and may impact on the functionality of therapeutic antibodies (Manning 2010). The mechanism of Met with different oxidation agents is shown in scheme 5.

Contents removed for copyright reasons.

Manning, M.C., Patel, K. & Borchardt, R.T., 1989. Stability of Protein Pharmaceuticals. Pharmaceutical research, 6(11), p.903 818.

Scheme 5 Met oxidation mechanism under (a) mild condition: hydrogen peroxide and (B) strong condition: performic acid to give sulfoxide and sulfone respectively. Source: Stability of protein pharmaceuticals (Manning et al. 1989).

1.5.2.1.6 Maillard Reaction

The Maillard reaction or non-enzymatic browning is the result of a reducing sugar reacting with the amino group on a lysine side chain. For this reason formulation of excipients avoids reducing sugars. However, sucrose present in excipient formulations may be hydrolysed to glucose and fructose. Non-enzymatic browning is a result of the formation of a carbohydrate–protein adduct. The reaction may occur at all temperatures. The reaction mechanism is a complex series of reactions which involve the formation of a Schiff's base as an intermediate (Kumar & Banker 1998).

1.5.2.1.7 Para-glutamate formation

Glutamate (Glu, E) can react to give para-glutamate (pGlu). This is a five membered N-terminal cyclised product. It is frequently seen in monoclonal antibodies due to the prevalence of Glu in the N-terminal light chain. In particular, it is seen during long term storage. The reaction involves a nucleophilic attack by the amine on the carbonyl of the N-terminal Glu side chain with concomitant loss of water (scheme 6) (Manning et al. 2010).

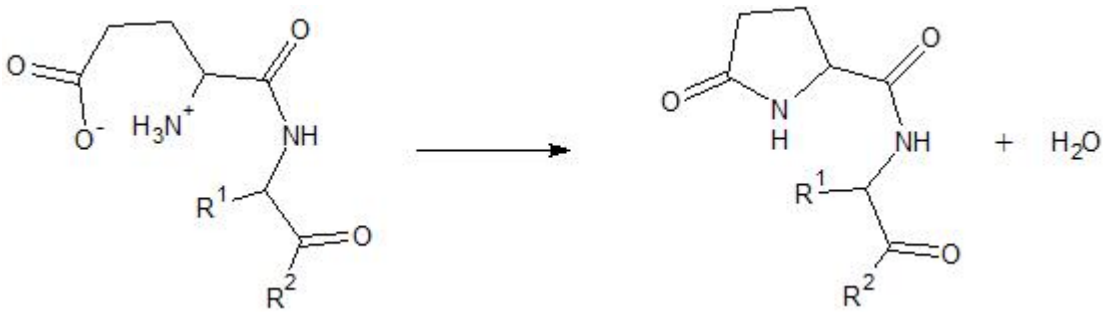

Scheme 6 The para-glutamate (pGlu) formation. This stable product is formed by a nucleophilic attack by the amine on the carbonyl of the N-terminal Glu side chain of the light chain.

1.6 Generic Techniques for determining Stability

1.6.1 Physical techniques

Physicochemical studies of proteins using a selection of techniques enable the complexity of physical and chemical instability to be investigated. Techniques should be stability-indicating and complementary. The measurement of different parameters and chemical markers of instability can provide a more satisfactory stability profile. There are numerous techniques available for the study of protein stability. Many approaches initially characterise the protein in terms of its chromatographic and electrophoretic behaviour (Arakawa et al. 2001). Other techniques which may be useful for a specific protein become evident during initial characterisation (Arakawa et al. 2001). A selection of techniques which are often applied to protein characterisation are reviewed.

1.6.1.1 Size Exclusion Liquid Chromatography

SE-LC is generally accepted as a very suitable method for determining protein size. It is used for both detection and quantitative determination of aggregates and fragments in biologic pharmaceuticals. Furthermore, it is virtually always a regulatory requisite for drug approval (Arakawa et al. 2001).

Separation is achieved by the differential residing time of proteins within the silica-based porous column packing. For example a monoclonal antibody (mAb) sample containing monomer, aggregates and fragments will elute in the order of size of species. Aggregates will elute first followed by the monomer or parent mAb and lastly fragments.

Protein adsorption has been a problem as the technique requires separation to be based only on size. This has been largely addressed by manufacturer column design and method development (Bond et al. 2010).

1.6.1.2 Ion Exchange chromatography (IEX)

This technique performs separation using a proteins net charge. The process is advantageously carried out under non-denaturing conditions. Electrostatic interactions mediated by the amino acid side chains and the charged surface of the ion exchange resin. The net charge of the protein has been used to explain retention. However, separation can be achieved when the net charge is zero. It is one of the commonly used methods for the detection of charge variants (Weinberg et al. 2005). Therefore this would be an appropriate way of following changes within a protein under non-denaturing conditions.

1.6.1.3 Sodium Dodecyl Sulphate-Polyacrylamide Gel Electrophoresis (SDS-PAGE)

SDS-PAGE is used to separate proteins (Lord 2003). This involves first denaturing the protein in the sample with the detergent SDS and heated. This produces unfolded polypeptide strands which migrate under the influence of an electric field through a polyacrylamide gel. Due to the loss of tertiary structure the polypeptides are impeded through the gel network to the same degree. Therefore separation is achieved solely on a mass basis (Grabski & Burgess 2001).

SDS-PAGE may detect fragments and aggregates (Arakawa et al. 2006). Fragments will travel further while aggregates will be impeded by their size. A variation of this technique is to perform it under reducing conditions. This entails adding a reducing agent at the denaturing step with the SDS detergent. Any disulphide bonds present will be will be broken producing single polypeptide chains. An antibody will be rendered into its Fab and Fc component polypeptides. A consequence of this process is that any disulphide bonded aggregates present will be separated under reducing conditions.

1.6.1.4 Attenuated Total Reflectance Fourier Transform Infra-Red Spectroscopy (ATR-FTIR)

The infra-red (IR) spectroscopy depends on bonds in the protein having a dipole, and therefore able to absorb in the infra-red region (Barth & Zscherp 2002). The result is a vibrational spectrum. The amide I normal vibrational mode or region of the IR spectrum is usually used to study protein structure. This region originates mainly from the carbonyl stretching vibration and depends on the conformation of the polypeptide backbone. Therefore this can give information on secondary structure within the protein.

However, when operating in normal transmission mode the IR travels through the protein solution. Water is a good absorber of IR and obscures protein absorption in the amide region even with a cell of small path length. Increasing concentration of the protein does not offset this because dispersive effects are introduced. This problem has been overcome by using attenuated total reflectance FTIR. The IR beam is guided through an IR transparent germanium crystal by total internal reflection and due to quantum effects the electromagnetic field penetrates into the crystal to the depth of about one micron. This vanishing or evanescent wave interacts with the surface protein which then contributes to the absorption without involvement from the bulk water.

One approach is to quantitatively analyse the amide I region of the spectrum (figure 6). The amide I region can be analysed in terms of the percentage component of secondary structure using band fitting. If there are significant structural changes in the molecule these will be reflected in changes in secondary structural motifs. Monoclonal antibodies such as Trastuzumab have a mainly ordered beta sheet structure, some alpha-helix, with the remaining being random coil. Therefore an increase in random coil is expected to be seen at the expense of the more ordered beta sheet during degradation. This can be an effective tool to assess these changes on a molecular level.

Contents removed for copyright reasons.
IMB, 2014. IMB Jena Image Library: Determination of secondary structure in proteins by FTIR spectroscopy. Available at: http://jenalib.fli-leibniz.de/ImgLibDoc/ftir/IMAGE_FTIR.html.html#Bandassignments [Accessed August 28, 2014].

Figure 6 Amide regions of the FTIR spectrum showing position of the amide I which originates form the carbonyl bond vibrations of the amide backbone. Source: IMB Jena Image Library (IMB 2014)

An alternative approach (Barth & Zscherp 2002) is to look for differences in the whole spectrum and not specific signals from chromophores or infra-red active groups. The principle of analysis involves correlating the whole spectral signature (a multivariate response) with biological activity.

1.6.1.5 Dynamic Light Scattering

An important area of studying aggregation is the characterisation of particles which are not detectable by SEC-LC or visual examination. This can be effectively achieved by Dynamic Light Scattering (DLS) which determines particle size and distribution. This is achieved by measuring fluctuations in the intensity of scattered light originating from Brownian motion on laser illumination of the test solution. The fluctuations in scattering can be correlated to the diffusion coefficient. Therefore the hydrodynamic radius of the particle can be determined through the Stokes-Einstein equation:

$$D = k T / 6 \pi \eta R_H \qquad \text{Equation 1}$$

Solve for the hydrodynamic radius:

$$R_H = k T / 6 \pi \eta D \qquad \text{Equation 2}$$

Where R_H = radius, k = Boltzmann constant, T = absolute temperature, η = solvent viscosity and D = diffusion coefficient.

Additionally, the experiment is not intrusive and therefore is a suitable method for monitoring the same sample over a period of time. Trace amounts of aggregates can be detected due to the scattering intensity being proportional to the square of the molecular weight of the protein. DLS has been shown to be a useful technique for monoclonal antibodies allowing their study under native conditions. In particular the study of the monomer-dimer equilibria is of interest (Nobbmann et al. 2007).

1.6.1.6 Electrospray Mass Spectroscopy

Electrospray Mass Spectroscopy can be used to probe changes in primary structure during degradation such as amino acid sequence and chemical modifications of the protein (Beck et al. 2005; Manning et al. 2010). The Mass spectrometer consists of three basic units; ionizer, analyser and detector (Harris 2003). The ionization step utilized in this particular mass spectroscopy technique is electrospray. It is well suited to fragile protein molecules which have a tendency to fragment. The sample must first be dissolved in a polar volatile solvent and nebulized at high voltage. The resultant charged droplets decrease in size as the volatile solvent evaporates eventually releasing charged sample ions. The ionized sample enters the analyser which is under

high vacuum to allow the ions to travel unimpeded. The ions are separated according to their mass/charge ratios under the influence of a quadrupole magnetic field. The signals generated from the detector are stored and displayed as mass/charge ratios and their relative abundance as a spectrum.

1.6.2 Biological Techniques

There are three types of biological assays biochemical, cell-based and animal-based. An animal-based assay is unlikely to be used (Barnes 2012). Therefore the cell-based assay is the most direct way of evaluating how much drug is still intact and functional. This approach has been largely ignored and physicochemical methodology has been the sole strategy to assess stability of diluted protein-based drug infusions such as the Kaiser and Kramer (2011).

A cellular approach which measures the biological response to the drug or efficacy is preferable to biochemical methods which only assess the binding of the antibody such as an enzyme-linked immunosorbent assay (ELISA). However, the biological response selected must reflect the clinical mechanism of drug action using an appropriate cell-line which expresses the receptor target for the disease, in the case of Trastuzumab a cell-line which overexpresses the HER2.

1.6.2.1 ELISA

The use of the ELISA provides information on the success of the binding interaction but does not report on biological effects (Crowther 2000; Barnes 2012). In the ELISA method for Trastuzumab Maple et al. (2004) used monoclonal antibodies which are Fab specific to the cytoplasmic domain of the HER2 receptor. These are absorbed onto the bottom of the micro-plate well surface. A full complement of HER2 protein is then added which is captured by the antibody surface. This system ensures the correct orientation of the protein enabling the extracellular domain (ECD) to be presented with a binding opportunity to the Trastuzumab FAB region during the assay. Trastuzumab that successfully binds to the ECD of HER2 will be detected by

an antihuman IgG-horse radish peroxidise (HRP) conjugate reporter and a (3, 3, 5', 5')-tetramethylbenzidine (TMB) substrate which turns blue on reaction with peroxidase (figure 6). Absorbance can be measured at 652 nm and is proportional to the amount of Trastuzumab which is bound to the HER2.

Contents removed for copyright reasons.
Maple, L., Lathrop, R., Bozich, S., Harman, W., Tacey, R., Kelley, M., &, 2004. Development and validation of ELISA for herceptin detection in human serum. Journal of immunological methods, 295(1-2), pp.169–82.

Figure 7 Schematic of the Trastuzumab-ELISA. 1. Mouse anti-C terminal part of HER2 antibody. 2. Trastuzumab. 3. Antihuman IgG conjugated with horse radish peroxidase (HRP) reporter. 4. TMB substrate turnover (Maple et al. 2004).

Key steps in a general ELISA for Trastuzumab (Maple et al. 2004):

1. Micro-plate coated with mouse anti-C terminal part of HER2 antibodies.
2. HER2 receptor captured in cell lysate ensuring correct orientation with Trastuzumab binding to HER2 N-terminal part representing extra cellular domain (ECD).
3. Antihuman IgG conjugated with horse radish peroxidase (HRP) reporter.
4. TMB substrate turnover signals Trastuzumab binding.

1.6.2.2 Cellular Assay

Biological activity can be determined by measuring viability or proliferation of the BT474 cells. These two parameters are subtlety but importantly different. Cellular proliferation relates to the number of dividing cells and therefore the ability to form colonies whilst viability relates to the number of living cells within a sample. Cellular proliferation may be determined by performing a colony formation assay which tests each cell's ability (Franken et al. 2006) to produce progeny and therefore to form colonies. The colonies are fixed and stained to aid examination. The size and number of colonies will be related to the inhibitory effect of a chemical or physical agent and therefore a gauge of reproductive capability. This approach is standard for biological assessment of cytotoxic agents such as chemical compounds. The colony formation assay is not biased towards any specific mechanism of death if the cytotoxic agent affects the cells' ability to reproduce (Franken et al. 2006).

Cell viability can be determined using a colorimetric reporter to indicate differences in absorbance and hence cell number. Colorimetric cell viability methods include the water soluble tetrazolium (WST) analogues, MTT, MTS and XTT (Serra et al. 2008; Budman et al. 2007; Nahta et al. 2004; Ozbay et al. 2010). These methods work on the principle of the conversion of a water soluble tetrazolium (WST) analogue to a formazan dye by living or viable cells. For example the WST-8 assay works by the conversion of a yellow tetrazolium salt, using an electron coupling agent, to form a soluble orange formazan dye by metabolically active cells and therefore only occurs in viable cells (figure 8). The formazan dye concentration is determined by absorbance between 450 nm and 500 nm using a spectrophotometer.

Contents removed for copyright reasons.
Held, P., 2009. An Absorbance-based Cytotoxicity Assay using High Absorptivity, Water-Soluble Tetrazolium Salts. Available at: http://www.biotek.com/assets/tech_resources/An_Absorbance-based-Cytotoxicity_App Note.pdf [Accessed August 14, 2014].

Figure 8 Mechanism of a WST-8 formazan dye assay. Schematic showing conversion of a water soluble tetrazolium (WST) analogue to a formazan dye by living or viable cells. Source : BioTek instruments (Held 2009).

Cell viability can also be determined by colorimetric absorbance by stain release of cells. This method is appropriate because the colonies are fixed and stained for a colony formation assay. The stain can be easily released and re-stained if required. For a crystal violet stain absorbance is measured at 570 nm (Eichhorn et al. 2008).

1.7 Method Rationale

1.7.1 Selection of Physical Techniques

A common route to drug degradation when stored is aggregation (Philo & Arakawa 2009). Aggregation is a process whereby the protein molecule self-associate reversibly or irreversibly and may lead to particulates or precipitation of the protein within the formulation (Philo & Arakawa 2009). Aggregation has been reported as a common concern during the storage and use of therapeutic proteins (Kiese & Papppenberger 2008; Manning et al. 2010; Arakawa et al. 2006; Chi et al. 2003). The aggregation process results in reduced activity by decreasing the concentration of the active drug and more significantly an increase in immunogenicity. Aggregates are antigenic and consequently recognised by the immune system which may lead to anaphylaxis. This is an instant reaction, produced by immunoglobulin E (IgE) of the immune system, which causes local or systemic attack. This immune reaction has been associated with increased patient morbidity and mortality (Manning et al. 2010).

Accordingly aggregate detection and characterisation became a focus in the selection of the methodology (Bardin et al. 2011). There is an extensive range of physico-chemical techniques which are suitable. Ideally a range of methods are needed for aggregate characterisation, but practicality requires a manageable number of techniques. The approach adopted in this study has used a small set of techniques. The selection is appropriate for the different ways instability is revealed within the drug. This is a practical approach rather than an exhaustive characterisation of the drug. This means differences in the drug will be monitored and not the determination of absolute structural change of the protein molecule. However, this will involve determining the stability indicating properties of the molecule such as shape (conformation), size (aggregation, particulates and fragmentation) and chemical modification.

The various chromatography and spectroscopic techniques applied to protein secondary structure determination and aggregation have been assessed (Arakawa et al. 2006; Brousseau 2008; Hawe et al. 2009; Nobbmann et al. 2007).

Size exclusion chromatography and infra-red spectroscopy have been identified as the most promising in terms of studying the changes in the protein and further developing the use of these techniques within Trastuzumab drug stability (Bond et al. 2010; Kong & Yu 2007). This combination of methods allows the opportunity to study the physico-chemical nature of instability in terms of aggregation and secondary structure.

Size exclusion chromatography of protein based drugs (Arakawa et al. 2006) provides to assess the condition of the formulation in terms of aggregate size distribution and to aid the prediction of particle formation. The appearance and increase in multimeric species are of significance as they may be indicative of instability of the drug solution. Furthermore, these species may lead to higher order aggregates and subsequent precipitation. Particle formation has been identified as a limiting factor in shelf-life (Bardin et al. 2011).

Infra-red spectroscopy (FTIR) has been a choice method for secondary structural determination and work has focused on the fundamental evaluation of spectral information of proteins in general. FT-IR has been applied to the assessment of stability of protein-based drugs during the lyophilisation process and upon reconstitution (Arakawa et al. 2001; Andya et al. 2003). Additionally, it has been utilised to study the effects of stress after reconstitution (Kiese & Papppenberger 2008). Thus it is appropriate to extend the application of infra-red spectroscopy for stability studies of further diluted Trastuzumab during storage.

1.7.2 Selection of Biological Assay

A cell-based approach was selected as this models the mechanism of the disease. Knowing the HER2 is the target of Trastuzumab an appropriate cell-line can be chosen. There are several suitable cell-lines but BT474 was selected as this overexpresses HER2 and is therefore Trastuzumab responsive (Neve et al. 2006; Holliday & Speirs 2011). Determination of biological activity using a cell-based approach enables the assessment of the activity of the drug with respect to its binding to a receptor and the subsequent effects on cellular processes which are detected and

measured. Proliferation and viability are usually assessed with various readouts of these cellular properties being employed. Both cell viability and cell proliferation approaches were selected.

1.8 Quality Assurance and Quality Control

1.8.1 Quality Assurance

These are the measures to ensure that quality control activities related to Quality Control are implemented correctly. This is a management process that involves documentation of procedures which have relevance to the quality of the data, thus allowing those procedures to be monitored and therefore enabling quality to be maintained.

Laboratory books and standard operating procedure documentation are a main part of ensuring quality of procedures and consequently data. Also log books documenting items such as cell stocks which aid traceability.

Equipment calibration and maintenance should be on a regular basis and fully documented. General care of the laboratory is important for ensuring overall quality.

These measures were employed in this study

1.8.2 Quality Control

Quality control can be achieved through the determination of accuracy and uncertainty of data which informs on the precision or closeness of a series of measurements.

Accuracy is the closeness or agreement of measurement and a true or accepted reference value. Accuracy may be inferred once precision, linearity and specificity are determined (ICH 2005). Uncertainty or error of data may originate systematically or randomly in an experiment (Harris 2003). Linearity of an analytical method is its

ability to obtain a test result, within a given range, which is directly proportional to the amount of analyte (ICH 2005). The range is the upper and lower limit of analyte amount that shows suitable precision, accuracy and linearity. Specificity is the ability to assess the analyte in the presence of other components such as excipients or degradants (ICH 2005)

These validation characteristics are regarded as the most important for assay validation and are the characteristics normally evaluated (ICH 2005)

1.9 Aim and objectives

Aim:

To provide experimental evidence to support an extended shelf-life of Trastuzumab infusions under clinical in-use conditions.

The objectives of this study are to:

- Develop and validate a cell-based analytical method to detect and measure changes in activity in Trastuzumab (Herceptin) after reconstitution and dilution;

- Select, develop and validate physico-chemical methods to characterise Trastuzumab (Herceptin). This includes development of FTIR to monitor changes at the secondary structural level and Size Exclusion Chromatography to monitor dimers leading to aggregation,

- Evaluate the stability-indicating capability of the biological and physicochemical methods,

- Apply these methods to evaluate the stability of Trastuzumab (Herceptin) after reconstitution and dilution in infusion solutions during extended storage and administration.

1.10 Hypothesis

Trastuzumab is sufficiently robust to remain unaltered following reconstitution or dilution to clinically relevant concentrations when stored in appropriate containers under controlled normal conditions of storage.

Note: When diluted to high dilution, below clinically relevant concentrations, at 0.1mg/ml or lower increased interactions between protein and container become important in limiting shelf-life than at lower dilution.

CHAPTER 2

2. METHOD DEVELOPMENT OF PHYSIOCHEMICAL CORE TECHNIQUES FOR STABILITY ASSESSMENTS

2.1 INTRODUCTION

Particulate formation is an important indicator of injection solution quality. In use it is essential to assess particulates in injections as in parenteral administration the drug is introduced directly into the body, typically into the blood stream. The presence of particles, which may be product related or a contaminant, will present a serious risk for patient safety. Protein-based drug products have the additional properties of drug aggregation and increased immunogenicity. Furthermore, the degree of immunogenicity increases with aggregate size with dimers and trimers being inefficient at initiating immune reaction (Rosenberg 2006). Therefore aggregate characterisation has been identified as an important indicator of particle formation and consequently the safety of the Trastuzumab formulation. This has informed the selection of the core techniques identified and discussed in Chapter 1 General Introduction (Section 1.7 Method rationale). The nature and extent (size) of aggregation can be assessed using the selected core techniques of infra-red spectroscopy and size exclusion chromatography, respectively.

Aggregates may be native, i.e. where folding of the protein structure remains unaltered, or non-native, i.e. when unfolding results in abnormal secondary and irregular higher order structure within the aggregate (Manning et al. 2010). The detection of aggregates and changes in their size distribution may aid prediction of instability. An increase in higher order aggregates or aggregate growth, i.e. greater than dimeric or trimeric species, should rationally precede particle formation of the protein (Manning et al. 2010). Particulate formation has been identified as a restrictive factor in determining a shelf-life for protein-based drugs (Bardin et al. 2011). Therefore the ability to monitor the aggregate profile of the reconstituted and diluted

Trastuzumab formulation was the main objective of physicochemical assessment method development.

2.2 METHODS AND MATERIALS

2.2.1 Preparation of Trastuzumab (Herceptin® Roche)

Trastuzumab (150 mg) previously reconstituted with water for injection (WFI) (7.2 mL) in single dose vials (triplicate vials clear glass type I vial was supplied for use by BUPA home healthcare UK). The vials were fitted with butyl rubber stoppers coated with a fluoro film resin, batches HO636 with expiry date 07/13) and H3144 with expiry date 07/15. These vials were supplied and used within a few days following reconstitution for the early preliminary work only. Fresh Trastuzumab solution was used in the remainder of the work.

Two batches of lyophilised Trastuzumab were used (batches H4008 and H3144 with expiry date 2015).

Trastuzumab was reconstituted under aseptic conditions for reference and test purposes by weighing accurately using a four place analytical balance approximately 20 mg of drug and adding 1 ml nominal volume of sterile water for injection (SWFI). The actual volume of SWFI was adjusted to give 21 mg/mL of Trastuzumab and corresponds to the approximate vial concentration.

2.2.2 Size exclusion liquid chromatography (SEC-LC)

2.2.2.1 Instrumentation

Size exclusion liquid chromatography was performed using a Dionex MAb Pac SEC1™ (Dionex; a Fisher Scientific company) size exclusion column with a packing particle size of 5 μm with a 300 Angstrom (0.03 μm) pore size. Instrumentation comprised of Gynkotek Gina 50 HPLC system with quaternary pump and vacuum

degasser (Gina 50). Gynkotek ultraviolet UV340S Diode array detector (Type: UVD 340S). Kontron Instruments 422 HPLC Pump operated under by Opus software under a Chromeleon operating system. A Shimadzu LC-10 system was also used operated by Lab Solutions Chromatography system under Windows XP environment performed the analysis.

2.2.2.2 Conditions for chromatographic separation

The mobile phase was 300 mM sodium chloride and 50 mM disodium hydrogen phosphate solution adjusted to pH 6.8. The elution rate was 0.2 mL/minute with dual wave length UV detection at 280 nm and 220 nm.

2.2.2.3 Chromatogram processing and analysis

Chromatographic data was converted and exported for further processing in Microsoft EXCEL (2003). This enabled the comparison of chromatograms at UV detection of 280 nm and 220 nm.

2.2.3 Development of Attenuated Total Reflectance Fourier Transform Infra-red (ATR-FT-IR) Spectroscopy for the analysis of Trastuzumab

2.2.3.1 Instrumentation

Infra-red spectra were acquired using Fourier Transform Infra-red (ATR-FT-IR) Spectroscopy (Spectrum One spectrophotometer Perkin-Elmer) with a fast recovery deuterated triglycine sulphate (FR-DTGS) detector operated by Spectrum 1 software (Spectrum version 5.0.1), under Windows XP environment. Attenuated total reflectance infra-red spectra were acquired using a germanium crystal ATR accessory with liquid sample recess (Specac Silver Gate™ Evolution) mounted on the ATR base plate (Specac Benchmark™ base plate).

Optical performance: range 7,800 to 350 cm^{-1}, resolution 0.5 to 64 cm^{-1} and accuracy 0.1 cm^{-1} at 1,600 cm^{-1} within the Amide I region.

2.2.3.2 ATR plate installation, set-up and optimisation of throughput signal

The transmission base plate and cell holder was removed and replaced with the ATR base plate (Specac Benchmark™ base plate). The optical unit with the ATR crystal top plate in position (Specac Silver Gate™ Evolution) was mounted on the base plate and secured by a screw into the front column of the base plate support. The optical path was finely aligned to optimise throughput energy. This was achieved by adjusting the mirror screws and monitoring the resultant energy (detector current) until a maximum level was obtained.

2.2.3.3 Spectra acquisition

Final acquisition parameters were as follows; 256 continuous scans for each spectrum at a resolution of 4 cm^{-1} and scan range of 4,000 cm^{-1} to 1,000 cm^{-1} wave numbers.

The sample (20 μL) was introduced into the recess within which the germanium crystal is housed ensuring full surface coverage of crystal. The crystal was cleaned between samples with deionised water (ten times) followed by acetonitrile (three times) (HPLC grade Fisher Scientific).

2.2.3.4 Spectra processing and analysis

Water vapour background subtraction and ATR correction were carried out by the Spectrum One software (Spectrum version 5.0.1). The ATR correction function transforms the spectrum to a form comparable to that of transmission spectroscopy where the infra-red beam passes through the sample. The spectral peaks resulting from attenuation of the infra-red beam are broadened due to the variation of penetration depth with frequency or wave number.

Spectra were converted and exported as ASCII (American Standard Code for Information Interchange) files for further processing in Microsoft EXCEL (2003). The corresponding blank spectra were subtracted from the sample spectra and the resultant spectrum normalised to 1,850 cm^{-1}; the baseline wave number adjacent to the amide I envelope and graphed as Microsoft EXCEL (2003) charts. This enabled the direct comparison of the Amide I region by spectrum overlay of all sample spectra.

2.3 Quality Assurance and Quality Control

2.3.1 Trastuzumab

Two independent batches of lyophilised Trastuzumab, within the expiration date, were used. Trastuzumab concentrate was accurately prepared under aseptic conditions as described in section 2.2.1.

2.3.2 Size exclusion liquid chromatography (SE-LC)

Trastuzumab (21 mg/mL) was diluted accurately with water for injection WFI to the desired concentration. The chromatographic separation was performed in triplicate. Calibration of instrument response to Trastuzumab concentration was performed to confirm satisfactory linearity, accuracy and precision. Specificity of the method to the analysis of the monomer was shown in the presence of degradation products and excipients. Absence of analyte carry-over was assured by blank column runs following Trastuzumab analysis. Table 1 shows the retention time of Trastuzumab with reference to co-eluted molecular weight marker proteins.

Sample	MW (kDa)	Retention Time (min)
Trastuzumab	148	12.6
Apoferritin	443	11.5
Carbonic anhydrase	29	14.8

Table 1 Trastuzumab retention time compared to co-eluted molecular weight markers

2.3.3 Attenuated Total Reflectance Fourier Transform Infra-Red (ATR-FT-IR) Spectroscopy

The accuracy specification of the FT-IR instrument is 0.1 cm^{-1} at 1,600 cm^{-1}. Furthermore, the accuracy specification resides within the Amide I region and therefore should enable small but significant changes in absorbance and hence secondary structure to be detected.

After optimisation of instrument throughput signal, a spectrum of the ATR crystal in air was obtained to confirm 100% transmission for the germanium crystal, i.e. without sample. Signal to noise ratio was improved by increasing scan number from 128 to 256 continuous scans. Signal to noise was assessed by subtracting two spectra obtained in air to see residual instrument noise level.

Blank background (air) spectra were collected before and after sample analysis. A blank spectrum with a 100% transmission line, i.e. zero absorbance, with no spectral features showed that the crystal was clean prior to further samples being analysed.

A representative sub-sample of the heat stressed Trastuzumab solution was obtained from the original sample used for SE-LC. This assured that stressed Trastuzumab had been sampled.

2.4 Results and Discussion

2.4.1 Size exclusion chromatography (SE-LC) of reconstituted Trastuzumab with ultraviolet (UV) detection at 220 nm and 280 nm

After commissioning and conditioning the column an acceptable resolution with repeatability was observed for the Trastuzumab monomer appearing at 12.3 minutes and the dimer at 11.3 minutes (figure 1 and 2). Species elute in order of decreasing size. The excipient buffer peak is free of the peaks associated with Trastuzumab monomeric and multimeric peak system. This gives a sufficient retention window for peaks associated with fragmentation to be seen.

The selection of a dual wavelength approach to improve sensitivity of aggregate characterisation has been cited in the literature (Bond et al. 2010). This approach allows the monomer peak to be on scale at 280 nm (figure 2) and the smaller aggregate and fragment peaks detected with greater sensitivity at 220 nm (figure 1). At 280 nm the aggregate and fragment peaks are very small and give inaccurate indication of their quantity. The use of dual ultraviolet wavelength detection SE-LC with the system has confirmed that this mode of analyte detection gives an improved analytical procedure in terms of the accurate and sensitive determination of percentage purity of the monomer. Calibrations of reconstituted Trastuzumab over a range of concentrations prepared from a stock of 21 mg/mL were performed. The resulting calibrations of instrument response (peak area) as a function of Trastuzumab concentration were linear with a correlation coefficients approaching unity. A characteristic calibration with a correlation coefficient of 0.9997 is shown in figure 3. The SE-LC data and statistical analysis for this calibration are presented in table 2.

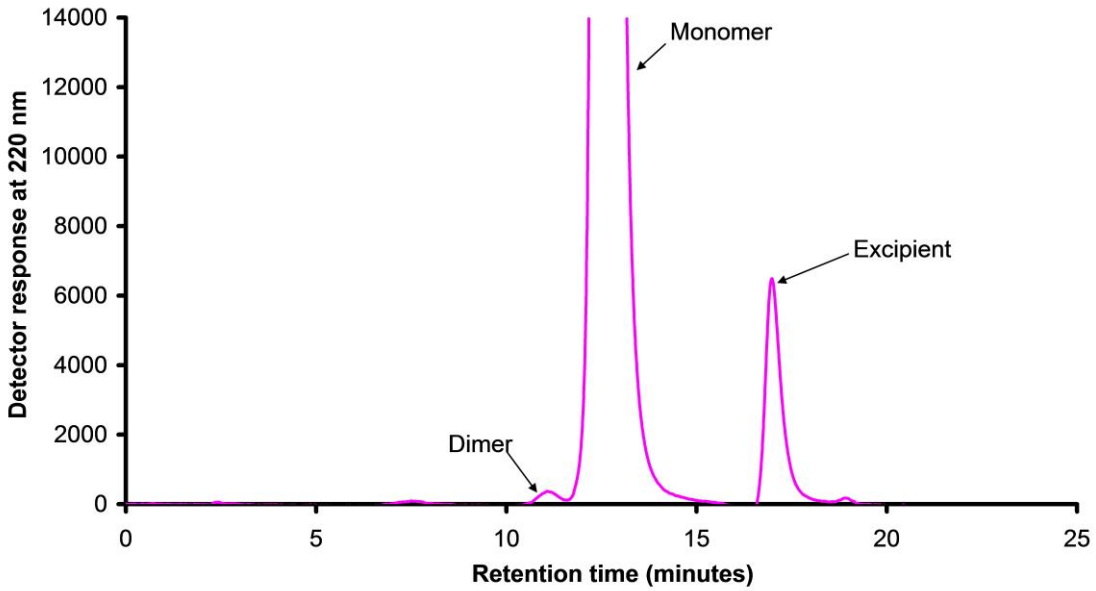

Figure 1 Representative SE-LC chromatogram of Trastuzumab with UV detection at 220 nm showing peaks for monomer (off scale), dimer and excipient buffer. Dionex (Fisher Scientific) MAbPac^{TM} SEC-1 size exclusion column with a column packing particle size of 5 μm with a 300 Angstrom (0.03 μm) pore size. The mobile phase was 300 mM sodium chloride in a 50 mM disodium hydrogen phosphate adjusted to pH 6.8 with an injection volume of 10 μL. The elution rate was 0.2 mL/minute with dual wave length UV detection at 280 nm and 220 nm.

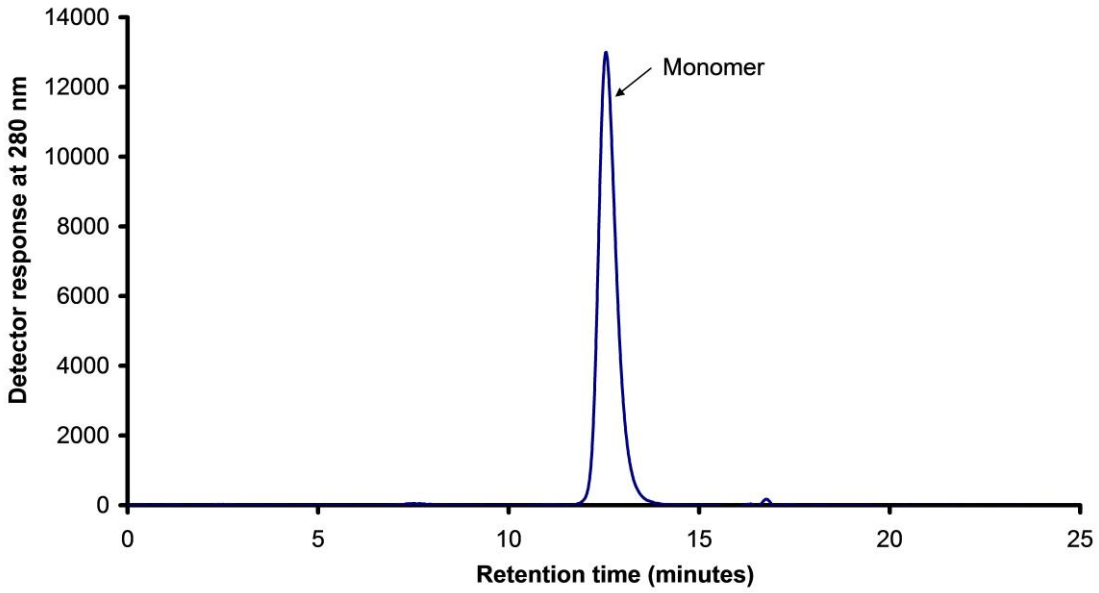

Figure 2 Representative SE-LC chromatogram of Trastuzumab with UV detection at 280 nm showing peaks for monomer (on scale). Conditions for analysis as in figure 1.

Trastuzumab concentration mg/ml	Area injection 1	Area injection 2	Area injection 3	Mean Area	Standard Error	Standard Deviation	Variance
4.20	-	180.63	184.12	182.38	1.75	2.47	6.09
2.10	88.70	87.13	89.77	88.53	0.77	1.33	1.76
1.05	42.19	42.69	42.44	42.44	0.14	0.25	0.06
0.53	20.73	20.91	20.89	20.84	0.06	0.10	0.01
0.26	9.99	9.88	9.85	9.91	0.04	0.07	0.01
0.13	4.58	4.60	4.57	4.58	0.01	0.02	0.00
0.07	2.10	2.10	2.10	2.10	0.00	0.00	0.00

Table 2 SE-LC calibration data of instrument response (peak area) using UV detection at 280 nm for Trastuzumab showing integration of peaks and statistical analysis for each standard concentration of drug.

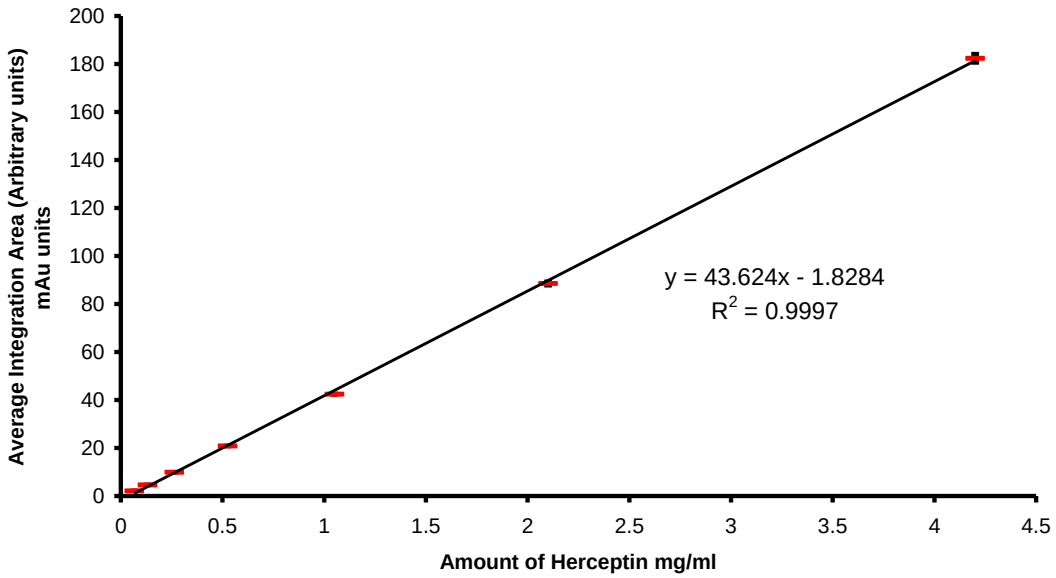

Figure 3 SE-LC calibration of instrument response (UV detection at 280 nm) to Trastuzumab for a range of concentrations. Standard error of replicate analysis is shown with inferential error bars (injections per concentration n = 3 for all concentrations except for the 4.2 mg/mL sample n = 2). Conditions as previously stated.

2.4.1.1 Assessment of forced degradation (aggregate induction) of reconstituted and diluted Trastuzumab using Size exclusion chromatography (SE-LC) with ultraviolet (UV) detection at 220 nm and 280 nm

To assess the stability indicating ability of SE-LC in terms of detecting aggregate formation a Trastuzumab sample was heated to 75 ^{o}C for 5 minutes. The rationale for this was that a temperature of 75 ^{o}C approximates the melting temperature (T_m) of the Trastuzumab molecule (Matheus, et al. 2006; Pabari et al. 2013). At this temperature the protein molecule population is in equilibrium between native and denatured (loss of native secondary structure) states (Arakawa et al. 2001(b); Manning et al. 2010). Aggregation may occur below this temperature, as the sample heats, via partial unfolding of the protein molecule (Chi et al. 2003) and retain native secondary

structure (Pabari et al. 2011). As the sample temperature approaches the T_m the extent of unfolding increases with associated aggregation probability and rate increasing (Vermeer & Norde 2000).

Therefore the adopted method was to perturb the system for a sufficiently short time to initiate aggregation whilst not to induce complete denaturation or chemical degradation. Furthermore, aggregates formed by a relatively mild perturbation are likely to be representative of the species formed under the conditions of this study (Barnes 2012). This approach is in contrast with the standard method of thermal degradation used for conventional drugs (Blessy et al. 2014). This entails application of a thermal stress for prolonged periods which would result in an unrepresentative decomposition mechanism and products (Barnes 2012). This method may have some relevance to drugs based on more robust chemical compounds but is completely inappropriate with protein-based drugs (Allwood & Wilkinson 2013).

Mechanical stress was considered as a means to induce aggregation but is a less defined stress mechanism involving a complex combination of shear and interfacial effects (Jaspe & Hagen 2006). Additionally, mechanical stress would be appropriate for stability studies pertaining to the manufacturing process (Kiese & Papppenberger 2008; Pabari et al. 2011).

Figure 4 and 5 shows a chromatogram overlay with UV detection at 220 nm of a heat treated sample of Trastuzumab (0.1 mg/mL) which had been heated in a water bath at 75 ^{o}C for 5 minutes and an untreated standard drug chromatogram at full scale (figure 4) and reduced scale (figure 5). The degraded sample has a peak area of ~90% of that of the untreated Trastuzumab sample (figure 4). On the reduced scale (figure 5) an increase in multimeric species is apparent. There is an increase in the size of the peak assigned to the dimer and an appearance of a broad peak system extending from the shoulder of the dimer peak. This is indicative of aggregate growth and consistent with the formation of trimers and other higher order multimeric species (Bond et al. 2010). Also, there is a new peak system between the monomer and excipient peak (figure 5). This region corresponds to large species but smaller than the monomer, i.e. fragmentation of the Trastuzumab antibody molecule possibly by the loss of a sub-unit (Bond et al. 2010; Vlasak & Ionescu 2011). This infers that the forced degradation experiment was not completely successful. However, peaks indicating

smaller fragments indicating additional unrepresentative degradation were absent (Bond et al. 2010). This type of fragmentation ought to be found at retention times greater than that for the excipient buffer peak. Indeed, in thermal stressing experiments discussed in the Chapter 5 (forced degradation studies of Trastuzumab) these peaks appear at retention time greater than the excipient peak.

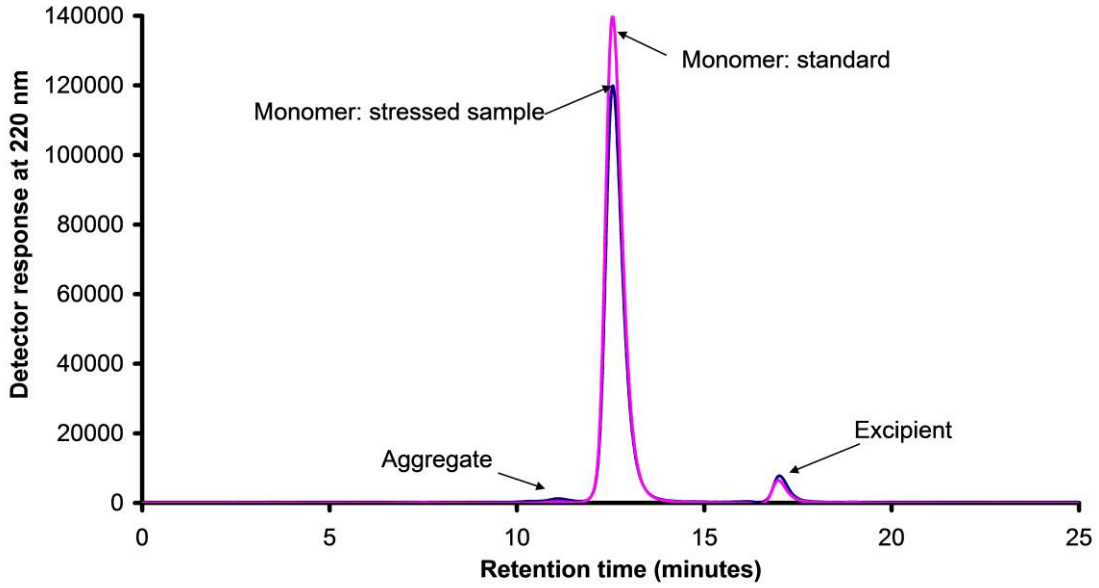

Figure 4 SE-LC chromatogram with UV detection at 220 nm (showing peaks for monomer on scale) of Trastuzumab (0.1 mg/mL) after heating in a water bath at 75 ^{o}C for 5 minutes compared with an overlaid chromatogram of an untreated Trastuzumab (0.1 mg/mL) reference. The heat treated sample has a monomer peak area of ~90% of that of the untreated reference sample. Chromatographic conditions as previously stated.

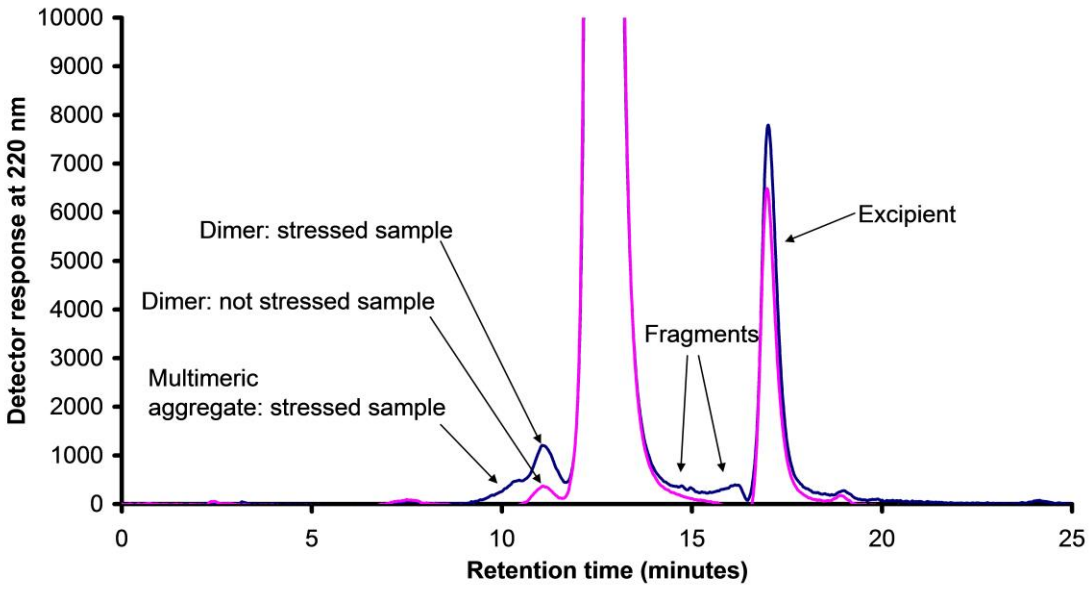

Figure 5 SE-LC chromatogram with UV detection at 280 nm (showing peaks for monomer off scale) of Trastuzumab (0.1 mg/mL) after heating in a water bath at 75 ^{o}C for 5 minutes compared with an overlaid chromatogram of an untreated Trastuzumab (0.1 mg/mL) reference. The heat treated sample shows an increase in peak system assigned to the dimer and appearance of a peak system attributed to aggregate growth. Fragmentation of the monomer is indicated by the peak system between the monomer and excipient peaks. Chromatographic conditions as previously stated.

2.4.2 Attenuated Total Reflectance Fourier Transform Infra-red (ATR-FT-IR) Spectroscopy for the analysis of Trastuzumab

2.4.2.1 System optimisation

Signal to noise was assessed by subtracting two spectra obtained in air to see residual instrument noise level. The noise is randomly or normally distributed around zero absorbance. Signal to noise ratio was improved by increasing scan number from 128 to 256 continuous scans. Figure 6 shows spectrum of the ATR germanium crystal in air within a wavenumber range of 2,000 cm^{-1} to 1,000 cm^{-1}.

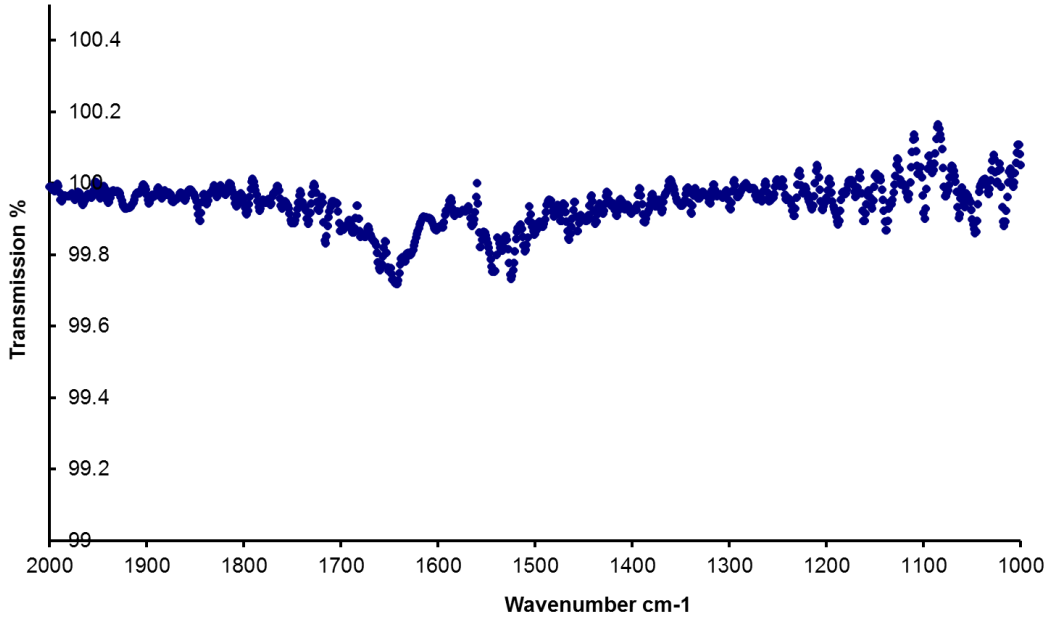

Figure 6 ATR-FT-IR spectrum from 2,000 cm^{-1} to 1,000 cm^{-1} of germanium crystal ATR in air i.e. no sample. Scan range of 4,000 cm^{-1} to 450 cm^{-1} wave numbers 256 continuous scans at a resolution of 4 cm^{-1} and with an accuracy of +/- 0.1 cm^{-1} at 1,600 cm^{-1}. Spectrum normalised to wavenumber 1,850 cm^{-1} and background, water vapour and ATR corrected.

A greater number of scans didn't produce any observable improvements and significantly increased analysis time. Multiple scans and precise replication of wave numbers during each scan enables the instrument to average the signals from each scan (Harris 2003). This improvement assists in the identification of slight differences in spectra (Harris 2003). Averaging 256 scans produces an improved signal to noise ratio by a factor of 16, i.e. the square root of the scan number (Harris 2003). The improved signal and inherent instrument accuracy of 0.1 cm^{-1} at 1,600 cm^{-1} (Perkin Elmer Life and Analytical Sciences 2004) within the Amide I region provided acceptable conditions to acquire and compare spectra of Trastuzumab.

2.4.2.2 Acquisition of Trastuzumab spectra

It is important that the spectra acquired originate from the sample alone and that Trastuzumab does not change during sample manipulation. This was ensured as no preparation, including dilution, of the sample was required. The original sample was introduced to the recess in the top plate which houses the crystal and may be recovered and reserved for further testing if required. However, it is imperative the sample recess was thoroughly cleaned to avoid absorbance artefacts from sample carry over. This was particularly important as the antibody molecule was expected to adsorb to an extent onto the crystal surface (Philo & Arakawa 2009). Complete removal of protein from a previous sample was shown by acquiring a blank spectrum of the cleaned and dried crystal.

Figure 7 shows the complete spectrum (4,000 cm^{-1} to 1,000 cm^{-1} wave numbers) and figure 8 shows the Amide I region (1,800 cm^{-1} to 1,500 cm^{-1} wave numbers) for two different vial samples of 21 mg/mL Trastuzumab. The Amide I region, originating mainly from carbonyl stretching vibration, is the most commonly selected reporter of secondary structure conformation due to its almost sole dependence on the orientation of the polypeptide backbone (Barth & Zscherp 2002). Therefore the Amide I band has been selected as a marker of conformational change. If there are significant functional changes of Trastuzumab, i.e. loss of efficacy, these may be related to the structural change within the molecule and reflected in the spectrum in this region.

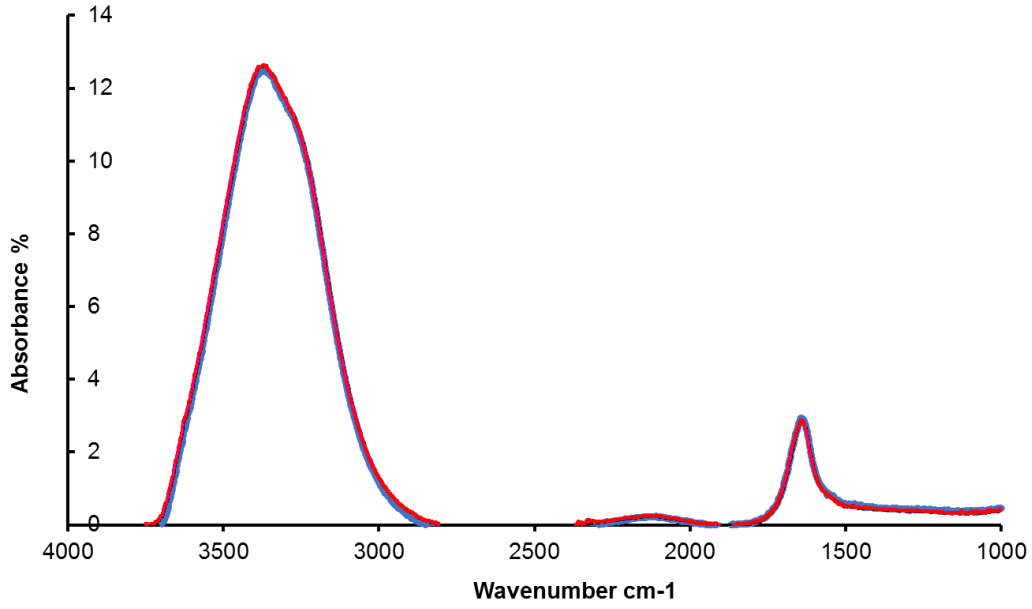

Figure 7 ATR-FT-IR spectrum of reconstituted Trastuzumab 21 mg/mL from two vials (red and blue plots). Scan range of 4,000 cm^{-1} to 1,000 cm^{-1} wave numbers 256 continuous scans at a resolution of 4 cm^{-1} and with an accuracy of +/- 0.1 cm^{-1} at 1,600 cm^{-1}. Spectrum normalised to wavenumber 1,850 cm^{-1} and background, water vapour and ATR corrected.

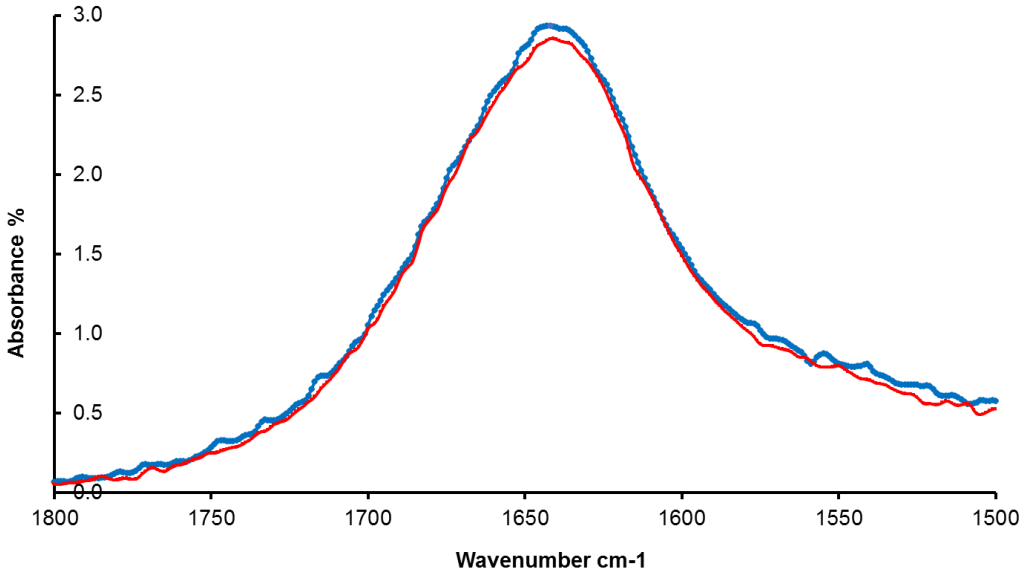

Figure 8 ATR-FT-IR representative spectra of reconstituted Trastuzumab 21 mg/mL from two vials (red and blue plots) showing Amide I region (1,800 cm^{-1} to 1,500 cm^{-1} wave numbers). Scan range of 4,000 cm^{-1} to 1,000 cm^{-1} wave numbers, 256 continuous scans at a resolution of 4 cm^{-1} with an accuracy of +/- 0.1 cm^{-1} at 1,600 cm^{-1}. Spectrum normalised to wavenumber 1,850 cm^{-1} and background, water vapour and ATR corrected.

2.4.2.3 Interpretation and analysis of Trastuzumab spectra

Trastuzumab has a mainly ordered β-sheet structure with the remaining being random coil. Therefore an increase in random coil is expected to be seen at the expense of the more ordered β-sheet during degradation. Furthermore, it has been stated previously that aggregate species may develop non-native structures (Chi et al. 2003) which often contain intermolecular β-sheet structures in high levels irrespective of the initial secondary structure (Carpenter et al. 1998; Chi et al. 2003). Therefore it is likely that if there is any difference in the structure of whole or part of the molecular population this will manifest itself as a change in the shape of the Amide I envelope or shift in

wave number of the peak profile (Barth & Zscherp 2002). A method to enhance any differences in the spectra is to calculate the second derivative of the Amide I spectrum (Barth & Zscherp 2002). This method does not distort the spectrum and preserves the original spectral information (Dong et al. 1995).

The change in peak profile can be followed over time to give information on the secondary structure of the stored reconstituted and diluted Trastuzumab. This may be achieved by overlaying spectra or generating difference spectra; i.e., spectrum at time point n minus spectrum at time point 0 = difference spectrum. The new difference spectrum may show small, complex and difficult to detect global changes between the two spectra in the Amide I profile or complete spectrum and hence changes within the formulation (Grdadolnik 2002).

An additional approach available to monitor changes in the protein is to assign structural motifs to their corresponding regions in the Amide I envelope and calculate their relative quantities hidden there in (Barth & Zscherp 2002). This entails using an iterative band fitting approach of the Amide I envelope (Jackson & Mantsch 1995). The structural elements are hidden within the broad Amide I envelope and can be thought of as being separate peaks of combined area equal to the Amide I area (Barth & Zscherp 2002). Thus knowing that the initial state of the antibody molecule has β-sheet (60-70%) at 1,642cm^{-1} and 1,624cm^{-1}, β-turn (~30%) at 168 cm^{1}, 1,680cm^{-1}, 1,672 cm^{-1} and 1,666 cm^{-1} and random coil at 1,648cm^{-1} (Kong & Yu 2007), percentile changes of secondary structure may be determined.

A great disadvantage of band fitting is its inherent subjectivity (Jackson & Mantsch 1995; Carpenter et al. 1998). Furthermore, reorganization of the molecular structure may result in a significant change in peak shape although band fitting may show no change in the relative proportions of secondary structure (Carpenter et al. 1998). This behaviour has been observed in lyophilised-induced stress studies (Carpenter et al. 1998). Dehydrated α-chymotrypsinogen was found to have an extremely disturbed structure although the whole relative secondary structure was unaffected (Carpenter et al. 1998). The authors indicate that quantitative analysis using band fitting is normally not required, may lead to increased subjectivity in data analysis and misleading (Carpenter et al. 1998). However, quantitative analysis may be useful for determining

percentage of intermolecular β-sheet which may form between aggregated monomers or increase in random coil (Vonhoff et al. 2010; Carpenter et al. 1998).

2.4.2.4 Assessment of forced degradation (aggregate induction) of reconstituted and diluted Trastuzumab using Attenuated Total Reflectance Fourier Transform Infra-red (ATR-FT-IR) Spectroscopy

ATR-FT-IR assessment of the heat treated Trastuzumab showed no difference in the spectral signature compared to that of an unstressed Trastuzumab. Generating a difference spectrum, which would enhances any change, did not reveal new spectral structures (figure 9). This observation was consistent with the interpretation that the secondary structure had not changed significantly.

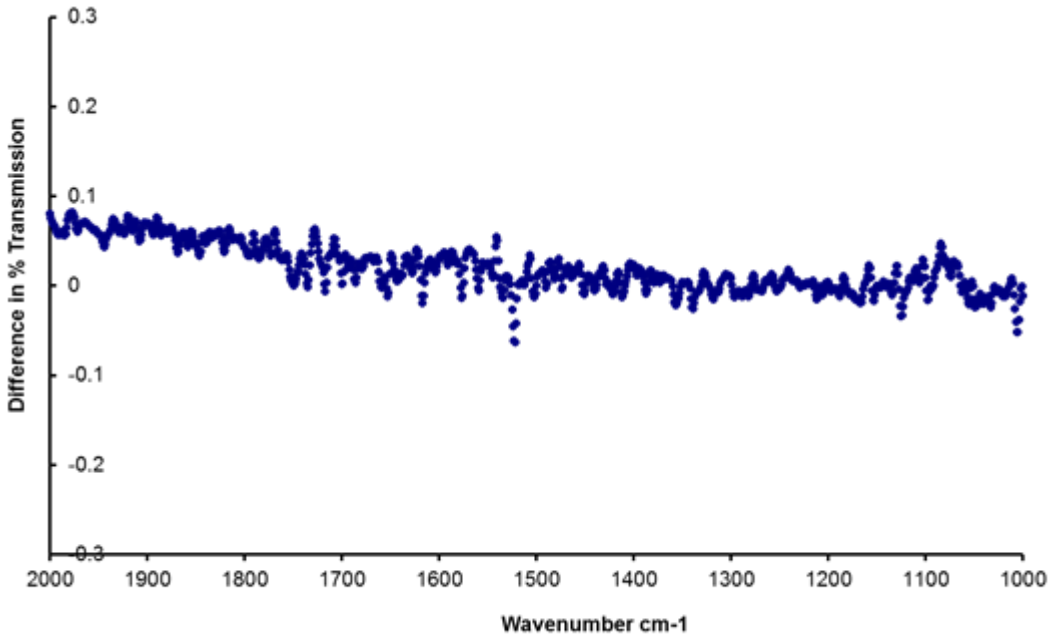

Figure 9 ATR-FT-IR difference spectrum of reconstituted Trastuzumab (heat-stressed and not heat-stressed) at 0.1 mg/mL concentration. Showing region 2,000 cm^{-1} to 1,000 cm^{-1} wave numbers. Scan range of 4,000 cm^{-1} to 1,000 cm^{-1} wave numbers, 256

continuous scans at a resolution of 4 cm^{-1} with an accuracy of +/- 0.1 cm^{-1} at 1,600 cm^{1}. Spectrum background, water vapour and ATR corrected.

SE-LC confirmed that Trastuzumab monomer aggregation had increased after application of thermal stress (figure 5). This inferred that the aggregates generated have retained their secondary structure whilst increasing in size from the dimeric species inherently present in the reconstituted and diluted formulation. The retention of native structure has been found in shear-stressing experiments (Kiese & Papppenberger 2008). Furthermore, shear force is more stressful than heating and has been found to be more effective in generating insoluble aggregates (Xenopoulos 2013).

It is possible changes in secondary structure were not detected due to a limit in instrument sensitivity. Yet the FTIR spectrometer instrument has an accuracy specification of 0.1 cm^{-1} at 1,600 cm^{-1} (Perkin Elmer Life and Analytical Sciences 2004).

Alternatively, the aliquot used for the ATR-FTIR measurement may not be representative of the stressed bulk sample. However, the stressed protein solution used for analysis was a representative sample.

An additional possibility is that the aliquot was not fully sensed or probed and consequentially changes are undetected in the bulk solution (Goldberg & Chaffotte 2005). This view is consistent with the short-lived wave (Hsu 1997) only being able to penetrate to the depth of protein adsorbed on the crystal surface or crystal-solution interface and thus not sensing the bulk protein (Goldberg & Chaffotte 2005). Consequently, changes in bulk concentration were not detected when spectra were acquired for a series of concentrations (figure 10). None proportionality of absorbance was observed at each concentration with identical absorbance (figure 10). Providing that the crystal surface-associated protein molecules were representative of that of the bulk Trastuzumab solution assessment of the sample in terms of structure should be possible (Goldberg & Chaffotte 2005). This appeared to be the case due to the observed spread of sample over the crystal surface enabling efficient sampling of the ATR recess contents (Hsu 1997).

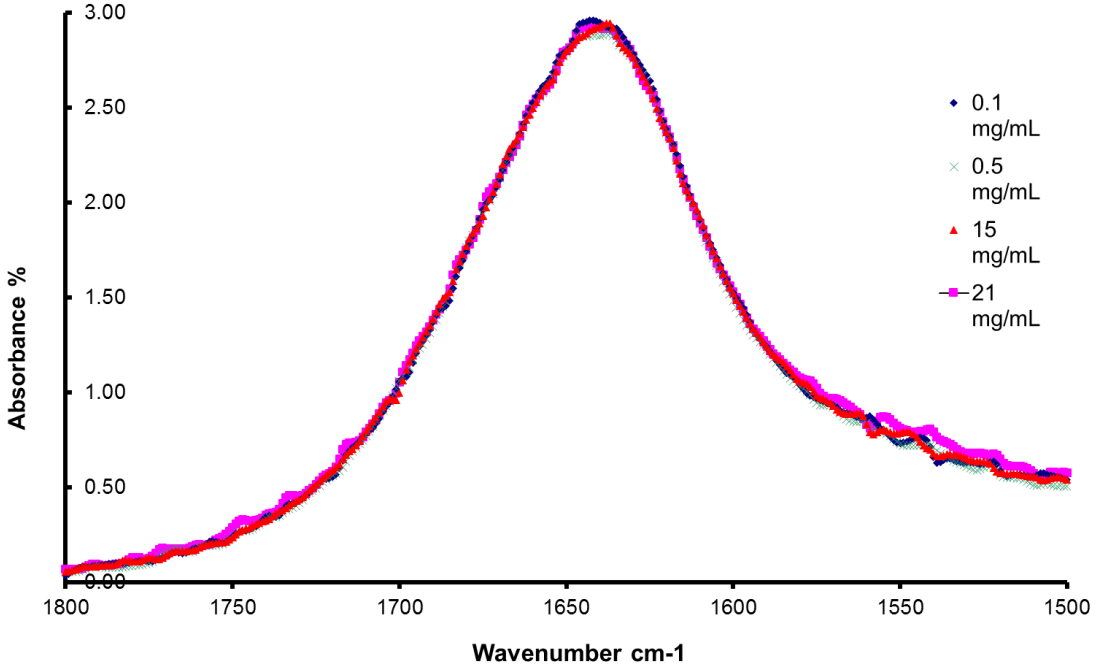

Figure 10 ATR-FT-IR spectra of reconstituted Trastuzumab at 0.1 mg/mL, 0.5 mg/mL, 15 mg/mL and 21 mg/mL showing Amide I region (1,800 cm^{-1} to 1,500 cm^{-1} wave numbers). Scan range of 4,000 cm^{-1} to 1,000 cm^{-1} wave numbers, 256 continuous scans at a resolution of 4 cm^{-1} with an accuracy of +/- 0.1 cm^{-1} at 1,600 cm^{-1}. Spectrum normalised to wavenumber 1,850 cm^{-1} and background, water vapour and ATR corrected. Coincidental plots indicate concentration independence of infra-red absorbance.

2.5 Conclusions

Dual ultra-violet wavelength detection size exclusion chromatography (SE-LC) enabled the detection of both monomer and dimer at retention times of 12.3 minutes and 11.3 minutes respectively (figure 1 and 2). Accurate determination of monomer was shown (table 1 and figure 3).

The stability indicating ability of the method was shown by a decrease in monomer peak after application of thermal stress (figure 4). Loss of monomer peak was

accompanied by an increase in dimer peak (figure 5) and appearance of an adjacent new peak system (figure 5). The appearance of a further peak system between the monomer and excipient peaks is consistent with fragmentation of the antibody molecule (figure 5).

ATR-FTIR spectroscopy showed acceptable residual instrument noise after subtraction of spectra obtained in air with 256 continuous scans (figure 6). Spectra can be acquired of Trastuzumab samples (figure 7) and comparisons made over the Amide I region (figure 8).

ATR-FTIR assessment did not reveal any significant change after forced degradation of Trastuzumab as shown in the difference spectrum (figure 9). Additionally it was found that the absorbance was insensitive to Trastuzumab concentration (figure 10).

CHAPTER 3

3. USE OF PHYSICOCHEMICAL TECHNIQUES TO DETERMINE TRASTUZUMAB STABILITY

3.1 INTRODUCTION

Physicochemical testing is the standard approach in assessing stability of drug substance and drug product. Assessment of physical and chemical stability is obligatory for regulatory purposes. The importance of physical and chemical stability is reflected in the quality of medicines guidelines published by the European Medicines agency: the International Conference on Harmonisation of Technical Requirements for Registration of Pharmaceuticals for Human Use (ICH) (ICH 2012). However these comprehensive guidelines and the pharmacopoeial texts of the ICH regions European (Ph. Eur.), United States (USP) and (Japan (JP)) are specific to the manufacturing process and the drug as marketed. Nevertheless, this guidance for chemical product stability can be used as a basis to develop an approach to in-use stability. More specifically aid the selection of standard techniques which can be employed to characterise properties which are stability indicating. In the case of in-use parenteral infusions and injections assessment of visual appearance, sub-visible particles and pH are of particular importance in determining acceptable drug quality.

Visual appearance

Colour, turbidity and visible particle levels should be assessed. The presence of visible particles is an important indicator of instability and quality of parenteral infusions and injectables. The requirement for these products is that the infusion should be “essentially free from visible particulates” according to the harmonised pharmacopoeial text (USP 2009). This statement has caused some confusion within the pharma community and requires clarification on definition with additional guidance on lot sampling and inspection (FDA Visual Inspection of Parenterals Advisory Panel Meeting, Purpose of Visual Inspection) (Madsen et al. 2009; Madsen

2010). Particulate contamination can be assessed using a standard method such as European Pharmacopoeia standard 2.9.20. (Ph. Eur. 2.9.20) (Ph. Eur 2000) and equivalent standards of USP and JP. However, other validated methods may be used. The test for assessing visible particles described in Ph. Eur. 2.9.20. (Ph. Eur 2000) entails examination using none glare white and black background with white-light illumination.

Sub-visible particle

Parenteral infusions must be assessed for sub-visible particles not including bubbles or dissolvable material. Light obscuration liquid particle count test can detect particles of 10 µm and 25 µm in size but requires large samples (25mL) (USP 788) (USP 2006). Acceptance criteria are "the average number of particles present in the units tested does not exceed 6000 per container equal to or greater than 10 µm and does not exceed 600 per container equal to or greater than 25 µm" (USP 2006). The USP 788 specifies the light obscuration particle count test and the microscopic particle test. The former is preferred for assessment of parental infusions but may be used in conjunction with the microscopic particle test to reach a conclusion on conformance USP 788 (USP 2006). The USP 788 is equivalent to the European Pharmacopoeia standard 2.9.19. (Ph. Eur. 2.9.19.) (Ph. Eur 2000). Sub-visible particles may also be detected using size exclusion chromatography or dynamic light scattering.

pH

The pH should be monitored as changes in value may indicate instability. The solution will have a pH influenced by the drug substance, product-related substances and product-related impurities. Chemical degradation may be influenced by the pH. The tendency of the drug product to undergo hydrolysis will vary over a pH range and therefore should be assessed (Allen 2011 (a); Allen 2011 (b); European Medicines Agency 2003).

The assessment of the aforementioned characteristics may be applied to an in-use parenteral injections or infusions with little or no alteration. However, with protein-based drugs the approach and methodology used must be adapted to reflect their specific nature. The International Conference on Harmonisation of Technical Requirements for Registration of Pharmaceuticals for Human Use (ICH) provides

general guidance for protein-based drugs with Q5 and Q6 documents (European Medicines Agency 1995; European Medicines Agency 1999). These documents are specific to the manufacturing process and the drug as marketed but do provide guidance for stability studies and test procedures respectively.

Particles are of specific importance as they are indicative of quality and safety of the parenteral infusion. Proteins inherently form aggregates including dimers and higher order aggregates. In the case of protein-based infusions aggregation of protein molecules will lead to sub-visible and visible particles. Particulates will impact on safety and efficacy and must be thoroughly evaluated and a focus of a stability study. The USP General Chapter Injections <1> (USP 2009) states the following, "the Pharmacopoeial definitions for sterile preparations for parenteral use generally do not apply in the case of the biologics because of their special nature and licensing requirements."

Moreover, the USP Visual Inspection of Parenterals Advisory Panel Meeting, Purpose of Visual Inspection History and revision of General Chapter Injections <1> (USP 2009) does not address assessment of protein particulates (USP 2009; Madsen et al. 2009). A panel member commented in their presentation that, "protein products can contain visible proteinaceous particles due to high concentrations or simply the nature of the protein. These particles are shown not to impact safety or efficacy during development" (Madsen 2010). However, this is not compatible with clinical requirements where intrinsic protein particles are of prime concern due to patient safety.

The absence of specific guidance for biologic or protein-based drug sterile preparations and more specifically for in-use clinical applications has been addressed by the NHS UK Pharmaceutical Research and Development Working Group with the document A Stability Protocol for Deriving and Assessment of Stability Part 2 – Aseptic Preparations (Biopharmaceuticals) (Barnes 2012).

One important aspect highlighted by this document is the use of an appropriate container in a stability study. This must reflect what is used within the clinical setting, such as a polyolefin, because the interaction of the protein may change with a

different container material and consequently affect the stability profile (Barnes 2012). Moreover, materials such as polyvinyl chloride (PVC) contain plasticisers which pose a health risk of leaching out di-(2-ethylhexyl) phthalate (DEHP) (US Food and Drug Administration 2001) into the infusion and may interact with the protein (Bee et al. 2011).

Interaction of Trastuzumab with the hydrophobic surface of the plastic material of the infusion bag would likely involve adsorption to some extent (Manning et al. 2010). It is well known that hydrophobic interactions between the surface and hydrophobic patches on a protein initiate adsorption (Pinholt et al. 2011). Surface activity of an antibody (mouse IgG1) molecule has been shown to be accompanied by partial unfolding on a hydrophobic Teflon surface (Vermeer et al. 1998). This process may involve unfolding of the fab fragment whilst conserving the native-fold of the Fc (Vermeer et al. 2001). Whilst the contribution of surface activity of proteins, with regard to instability has been established to a degree, applicable pH and excipient surfactant effects have not been fully investigated (Couston et al. 2012). Studies have been generally confined to model monoclonal antibodies and surfaces which represent those encountered after preparation of the drug (Couston et al. 2012; Kapp et al. 2015). Couston et al. (2012) showed that a human monoclonal antibody (identified as Mab 1) adsorbed on hydrophobic octadecyl-coated silica surfaces as a thin irregular monolayer using total internal reflectance fluorescence measurements. This is consistent with minimum interaction of the antibody with the surface; when the hydrophobic core remains buried in the native form (Couston et al. 2012).

Interaction may be further decreased by end-on orientation of the antibody molecule (Kapp et al. 2015) and also by the presence of the polysorbate excipient competing for adsorption sites (Garidel et al. 2009). Additionally, the limited contact point of the antibody may make displacement by the polysorbate more facile (Kapp et al. 2015). The effect of an hydrophobic surface on the extent of adsorption can be illustrated by the following example from Couston et al. (2012). Their study found that the surface loading of the Mab was highest on silica at a value of ~5.5 mg/m^2 and lowest on hydrophobic octadecyl-coated silica with a loading of ~2 mg/m^2 at a solution concentration of 0.01 mg/mL and pH 5.4. Furthermore, the authors showed that the affinity for the hydrophobic surface does not markedly increase with an increase of

bulk concentration, thus retaining a monolayer structure. These results are consistent with the view that at clinically relevant concentrations the dose will not be compromised due to the low level of adsorption (Kapp et al. 2015).

Another factor to consider is the effect of prolonged or inadvertent exposure to light of the Trastuzumab solution and clear polyolefin bag under in-use conditions, such as during infusion (Qi et al. 2009; Barnes 2012). Specifically this will mean exposure to UV-A and cool white light within the visible region (European Medicines Agency 1998; Kerwin & Remmele 2007). Photo-induced damage of proteins has been widely documented and has been reviewed by Pattison et al. (2012). However, there has been a limited number of studies relating to protein-based drugs (Kerwin & Remmele 2007) and have not included marketed drugs until a recent study by Hernández-Jiménez et al. (2016). This study examined the photo-induced forced degradation of Bevacizumab, Cetuximab, Infliximab, Rituximab and Trastuzumab infusions at therapeutic relevant concentrations (2 mg/mL and 5 mg/mL). Aggregation was assessed as dimer content by SEC-LC after exposure to simulated in-use light conditions (European Medicines Agency 1998) between a wavelength range of 320-800 nm with an irradiance of 250 W/m^2 (Hernández-Jiménez et al. 2016). The authors reported that light exposure caused aggregation in all drugs and was monitored each day until turbidity was observed. Trastuzumab infusions showed the greatest resistance to aggregation as dimer percentage was highest before the onset of turbidity after 17 hours of continuous light exposure (Hernández-Jiménez et al. 2016).

The interaction of UV with the protein will be via the absorption of radiation by the amide backbone and specific amino acid residues (Schmid 2001) The major UV absorbing amino acids are tryptophan (Trp), tyrosine (Tyr), phenylalanine (Phe), histidine (His), methionine (Met), cysteine (Cys) and disulphide bonds (Pattison et al. 2012). Absorption is greatest for UV-B (280-320 nm) and to a lesser degree with UV-A (320-400 nm) (Pattison et al. 2012). . Most other amino acids only weakly absorb UV at wavelengths >230 nm (Davies 2003). Trp is the predominate amino acid that absorbs UV (Creed 1984a). Trp and Tyr are mainly responsible for the observed absorbance maxima of proteins with a small contribution to the absorbance from the disulphide bond (Schmid 2001). Therefore the photophysics and photochemistry of these amino acids have been extensively reviewed and continue to be of interest due

to their role in protein analysis and degradation (Creed 1984a; Creed 1984b; Creed 1984c; Pattison et al. 2012).

Absorption of UV-A may result in direct photo-oxidation of these specific amino acids via the generation of excited states and radical-cations (Davies & Truscott 2001). Additionally there can be secondary oxidation reactions involving peroxy radicals and singlet oxygen with the other amino acids (Laustriat & Hasselmann 1975; Kerwin & Remmele 2007; Gracanin et al. 2009). These processes are limited due to the relatively weak absorption, in the UV-A region (>290 nm) (Davies 2003), that they are normally exposed to in the absence of sensitisers (Kerwin & Remmele 2007). However, oxidation products of the amino acid side-chain, notably Trp, are more efficient at generating triplet oxygen (Davies 2003).

Susceptibility of Trp has been recognised in recombinant monoclonal antibodies (Nowak et al. 2016). If the amino acid sequence of a recombinant antibody such as Trastuzumab is examined it is evident that there are two Trp on each light chain and nine Trp on each heavy chain (Drug Bank 2016). This further implicates this amino acid residue's potential role in degradation of Trastuzumab. On absorption of UV Trp will be excited and may relax to the singlet state followed by fluorescence, convert to the first triplet state by the non-radiative process of intersystem crossover or eject an electron (Kerwin & Remmele 2007). Furthermore, Phe and Tyr can transfer their excitation energy to Trp (Creed 1984b; Kerwin & Remmele 2007). Electron transfer is facile from the triplet state Trp to a thiyl anion giving a disulphide radical anion (Davies & Truscott 2001). The Trp radical-cation deprotonates to a neutral Tryp indolyl radical (Kerwin & Remmele 2007; Pattison et al. 2012). The neutral Trp indolyl radical may abstract a hydrogen from a Tyr to give a Tyr phenoxyl radical, form a peroxyl radical by reacting with oxygen or react with other amino acids (Kerwin & Remmele 2007). The reaction of the peroxyl radical may further react with oxygen to give N-formylkyneurenine and kyneurenine (Creed 1984a; Kerwin & Remmele 2007). These photo-products absorb at longer wavelength compared to Trp and therefore act as sensitisers, thus increasing damage (Kerwin & Remmele 2007). Alternatively the Trp radical cation may oxidise a nearby Tyr residue to the Tyr phenoxyl radical, thus reducing back to Trp (Creed 1984a).

Trastuzumab has one adjacent Trp and Tyr on each heavy and light chains (Drug Bank 2016). This observation suggests a possible intramolecular path of electron transfer for sensitisation of Tyr by the formation of the Tyr phenoxyl radical (Creed 1984a; Aubert et al. 1999). The Tyr radical is particularly stable and therefore may combine with another Tyr radical giving a dityrosine (Creed 1984b; Malencik & Anderson 2003). This radical termination reaction may result in either intramolecular or intermolecular crosslinking (Balasubramanian & Kanwar 2002; Malencik & Anderson 2003). Other crosslinking reactions include thiyl cross coupling to give a disulphide (Creed 1984c; Roy et al. 2009) and reactions of histidine (His) and lysine (Lys) with singlet oxygen via an endoperoxide intermediate generating His-His or His-Lys crosslinking (Davies & Truscott 2001). Intermolecular crosslinking has been identified as an important mechanism for photo-induced aggregation (Kerwin & Remmele 2007; Qi et al. 2009; Wang et al. 2010; Hernández-Jiménez et al. 2016).

This physicochemical stability study was a collaboration with Quality Control Northwest (QCNW) (Liverpool NHS Primary Care Trust). This association has enabled an approach to obtain stability data which can be used in clinical practise.

The approach to physicochemical assessment of Trastuzumab infusion stability employed some techniques not associated with general chemical stability. These were Electrophoresis (SDS-PAGE) and Infra-Red Spectroscopy (FTIR). These techniques are specific to the protein nature of Trastuzumab where determination of aggregate levels and secondary structure allow assessment of these indicators of stability.

3.2 Materials and Methods

3.2.1 Materials

Trastuzumab (150 mg in a single dose vial clear glass type I vial) fitted with butyl rubber stopper laminated with fluoro-film resin, batch H4008 with expiry date 2015.

Trastuzumab was reconstituted as described in Chapter 2 Method Development of Physicochemical Core Techniques for Stability Assessments, Methods and Materials page 51.

Two intravenous (IV) polyolefin bag types, with a volume of 50 mL, were used for the Trastuzumab infusions: Viaflo (Baxter no. FE1306, lot 11614663 with an expiry date of 09/2012) and Freeflex® (Fresenius Kabi no. B248941, lot 13EIS025 with an expiry date of 08/2013).

Viaflo (Baxter) IV bag Trastuzumab infusions

These infusions comprised of two bags at a Trastuzumab concentration of 6 mg/mL (batch numbers ML1103024 and ML1103027) and two bags at a concentration of 0.5 mg/mL (batch numbers ML1103020 and ML1103018). The expiry date of the infusions was 05/11/2011.

Freeflex® IV bag Trastuzumab Infusions

The Freeflex® IV bag infusions consisted of two bags (batches) of Trastuzumab at a concentration of 0.1 mg/mL (batch numbers ML1103042 and ML1103002) with an expiry date of 05/11/2011.

Trastuzumab infusion IV bags with 0.9% sodium chloride were aseptically prepared by Clatterbridge Centre for Oncology (pharmacy code CCOCH634JY and IMS number 18612) according to Summary of Product Characteristics (SPC).

Sampling and testing

All infusion bags were stored in a refrigerator between 2 ^{o}C and 8 ^{o}C to reproduce conditions encountered during in-use storage. Physicochemical testing of samples was carried out at 0, 7, 14, 28, 35, 43 days. Physiochemical testing comprised of assessment of appearance, pH and Trastuzumab monomer and dimer determination by SE-LC.

Techniques more specific to the protein nature of Trastuzumab were also employed to assess aggregate levels and secondary structure. These were Electrophoresis (SDS-PAGE) and Infra-Red Spectroscopy (Attenuated Total Reflectance Fourier Transform Infra-red Spectroscopy (ATR-FTIR) respectively.

After day 43 of the study QCNW subjected their infusions to further testing for stability at room temperature. The conditions used were 24 hours at room temperature in dark and light conditions and mechanical agitation in light for 6 hours. Tests carried out were pH, SDS-PAGE and SE-LC monomer assay. The remaining samples were stored for long term stability assessment for over 119 days.

3.2.2 Methods

3.2.2.1 pH

Measurements of pH performed by QCNW.

A combination electrode glass probe (Mettler Toledo InLab 413SG IP67) and pH meter (Mettler Toledo SevenMulti™ pH meter) was used to record sample pH at each time point (QCNW).

3.2.2.2 Visual Appearance

The infusions stored in the IV bags were examined for visible particles, clarity and colour with a magnifier using white light illumination and both a black and white background according to standard method (Pharmacopoeia Europaea Ph.Eur 2.9.20.) (Ph. Eur 2000). The acceptance criteria are that the infusion remained free of none dissolvable particles or precipitation and retains colour and clarity of initial infusion examination (day 0).

3.2.2.3 Sub-visible Particle Analysis and Trastuzumab Assay

Due to the sampling burden determination of sub-visible particles by light obscuration was impractical. However, sub-visible particles may be detected by Size Exclusion liquid chromatography (SE-LC). SE-LC also allows monomer assay which provides information on the integrity of the Trastuzumab molecule and aggregate analysis.

The two SE-LC methods employed had a different focus. Method 1 (University of Derby) had the aim of providing information on higher aggregates, whilst method 2 (NHS (UK) QCNW) was concerned solely with quantitative assay.

3.2.2.3.1 Size Exclusion Chromatography (SE-LC) method 1

SE-LC method was performed as described in chapter 2 Method Development of Physicochemical Core Techniques for Stability Assessments, Methods and Materials.

The chromatographic separation was performed in triplicate at 20 ^{o}C. Standards were prepared from a freshly reconstituted Trastuzumab solution (21 mg/mL) by dilution with 0.9% saline solution to the desired concentrations of 15, 10.5, 5.3, 2.6 and 1.3 mg/mL. Trastuzumab infusion samples were injected undiluted.

3.2.2.4 Size Exclusion Chromatography (SE-LC) method 2

3.2.2.4.1 Instrumentation

Size exclusion liquid chromatography was performed using a Tosoh TSKgel G3000SWXL size exclusion column (Hichrom). Instrumentation comprised of gradient pump (Kontron 325), auto sampler (Kontron 360) and UV detector (Kontron 332).

3.2.2.4.2 Conditions for chromatographic separation

The mobile phase was 100 mM sodium chloride, 50 mM potassium dihydrogen phosphate and 50 mM dipotassium hydrogen phosphate solution adjusted to pH 6.0 with orthophosphoric acid. The elution rate was 1.0 mL/minute with UV detection at 220 nm and injection volume of 20 µL. The chromatographic separation was performed at 20 ^{o}C. Standards were prepared from a freshly reconstituted Trastuzumab solution (21 mg/mL) by dilution with 0.9% saline solution to give concentrations of 0.08, 0.12, and 0.15 mg/mL.

3.2.2.4.3 Chromatogram processing and analysis

Data collection and analysis was performed using EZChrom Version 2.6.1. software.

3.2.2.5 Attenuated Total Reflectance Fourier Transform Infra-red (ATR-FT-IR) Spectroscopy

ATR-FT-IR was performed as described in chapter 2 Method Development of Physicochemical Core Techniques for Stability Assessments, Methods and Materials.

3.2.2.6 Electrophoresis: SDS-Page (Sodium Dodecyl Sulphate Poly Acrylamide Gel Electrophoresis)

SDS-PAGE analysis of test samples and reference sample at each time point was performed by QCNW. Electrophoresis with 9% resolving gel under both non-reducing and reducing conditions (2-mercaptoethanol) at 200 volts. Molecular weight markers (ColorBurst™) were resolved with test samples. Visualisation of protein bands using Coomassie Blue (Fisher). Gels stained for 2 hours and de-stained in water overnight.

Acceptance criteria are that the band pattern or distribution under none reduced and reduced electrophoresis conditions coincided with those obtained for the reference Trastuzumab.

3.3 Results and Discussion

3.3.1 Results for clinically relevant infusions

Results are presented and discussed including statement of compliance to acceptance criteria for the clinically relevant samples: 0.5 mg/mL and 6 mg/mL infusions. It is difficult to assign acceptance limits for biologics. The NHS Pharmaceutical Research and Development Working Group suggest size exclusion chromatography (SE-LC) acceptance limit should be a maximum of 5% loss in active protein and a maximum of 2% relative loss in degradant peak. Physical appearance should not change and there should be no significant change in pH (Barnes 2012).

3.3.2 pH

The initial pH of the 0.5 mg/mL and 6 mg/ml infusion samples were 6.04 and 6.23 pH units respectively (table 1). These values were consistent with the pH of Trastuzumab being reported as approximately 6 pH units (European Agency for the Evaluation of Medicinal Products (EMEA) 2010). Furthermore, the pH of Trastuzumab may vary between 5.4 and 6.6 pH units for reconstituted Trastuzumab at the 21 mg/mL vial concentration as stated in the Roche safety data sheet for Trastuzumab (Roche 2006). Additionally, dilution with 0.9% saline solution of the Trastuzumab and excipient concentrate in the infusion may be expected to have an effect on pH (Pabari et al. 2013). Indeed the 0.5 mg/mL infusion was 0.19 pH units lower than that for the 6 mg/mL infusion sample at the initial measurement on day 0 (table 1). The difference in pH profile between 0.5 mg/mL and 6 mg/mL infusions was shown to be significant ($p = 0.0001$) by using a t-Student test with a significance threshold of < 0.0500.

The pH of all infusion samples remained within specification of the concentrate value within the study period (table 1). However, a small statistically non-significant decrease in pH was observed compared to the initial pH readings for both concentrations of infusion samples at day 14. This behaviour was almost mirrored in the pH differences between the two infusion concentrations approaching a maxim after day 14 (table 1). The pH data for both 0.5 mg/mL and 6 mg/mL infusions gave a mean and standard deviation of 5.94 +/- 0.06 and 6.24 +/- 0.03 pH units respectively.

Day	pH at 5 ºC		Difference in pH between infusion concentrations
	0.5 mg/mL infusion	6 mg/mL infusion	
0	6.04	6.23	0.19
7	5.99	6.21	0.22
14	5.88	6.19	0.31
28	5.90	6.25	0.35
35	5.91	6.24	0.33
43	5.94	6.29	0.35

Table 1 pH at 5 ºC reported for each time-point of study for the of 6 mg/mL and 0.5 mg/mL infusion bag samples. Performed by NHS QCNW.

The pH of biological-based pharmaceuticals is critical to their stability and consequently symptomatic of adverse conditions and instability (Barnes 2012). Accordingly pH measurements should be performed as part of an assessment of stability.

The pH during storage remained consistent with the value being reported as approximately a value of pH 6 (European Agency for the Evaluation of Medicinal Products (EMEA) 2005b). Specifically, the pH of Trastuzumab may vary between 5.4

and 6.6 pH units for reconstituted Trastuzumab at the 21mg/mL vial concentration as stated by the manufacturer (Roche 2006). The pH values of the infusions ranged from 6.0 to 5.9 and 6.2 to 6.3 over the storage period for 0.5 mg/mL and 6.0 mg/mL concentrations respectively.

Pabari et al. (2013) and Kaiser and Kramer (2011) also found the pH remained within the acceptance limit. Whereas the measurement of pH was not included in the study by Paul et al. (2013).

The assessment of pH fundamentally supports that these infusions stored within their containers are stable. Although judgement on stability must of course include the examination of data from other tests. An illustration of this is that of the 0.1 mg/mL infusions where pH remained within specification but developed particles.

3.3.3 Appearance

All infusions at clinically relevant concentrations, i.e. 6 mg/mL and 0.5 mg/mL infusions, remained clear and colourless after 43 days (table 2). Other studies with visual assessment showed similar findings for stored Trastuzumab infusions (Kaiser & Kramer 2011; Pabari et al. 2013). These studies showed that the appearance of Trastuzumab infusions, at concentrations of 0.4 mg/mL and 4 mg/mL, did not change over a 28 day storage period (Kaiser & Kramer 2011; Pabari et al. 2013).

Day	Visual appearance Pass/Fail	
	0.5 mg/mL infusion	6 mg/mL infusion
0	Pass	Pass
7	Pass	Pass
14	Pass	Pass
28	Pass	Pass
35	Pass	Pass
43	Pass	Pass

Table 2 Visual appearance reported for 6 mg/mL and 0.5 mg/mL infusions over the 43 day study period.

Assessment of visual appearance is a requirement common to both small molecule and biologic infusions (USP 2009). Changes in colour, clarity and appearance of particulates are indicative of changes in the quality of the infusion and accordingly their assessment should be part of a minimum testing protocol. Indeed in clinical practise an infusion will be routinely inspected visually before use. If the infusion is free of particulates or precipitates and shows no colour change it will be administered to the patient.

The USP document does not include visual assessment as it is concerned with reference procedures and their validation which are specific to the characterisation of Trastuzumab. However, this assessment should be included in a stability study design that sets out to increase the shelf-life of a drug infusion. The acceptance criteria in this context are that the infusion must remain free visible particles or precipitation and retain colour and clarity of initial infusion examination (day 0) (USP 2009).

In this study there were no noticeable changes in appearance for all infusion bags at concentrations of clinical relevance (6.0 mg/mL and 0.5 mg/mL) over 43 day's storage. In contrast the Trastuzumab infusions at the concentration of 0.1 mg/mL developed visible particles with the solution remaining clear and colourless. This could be observed with the naked eye in all 0.1 mg/mL bags after 14 days. This suggests that the appearance of particulate matter may be a result of the Trastuzumab and excipients being highly diluted at this infusion concentration.

Subsequent studies by other authors showed that Trastuzumab infusions remained unchanged during storage with respect to their visual appearance (Kaiser & Kramer 2011; Pabari et al. 2013). Although the method details are not stated and therefore it is not known if a compendia method was employed as in this study. All these studies, having various storage periods, used a range of concentrations which appropriately included therapeutic high and low concentrations of Trastuzumab. Kaiser and Kramer (2011) used 0.4 mg/mL and 4 mg/mL with a 28 day storage period. Whilst Pabari et al. (2013) used the same concentrations with the addition of a 1.0 mg/mL infusion with a 28 day test period. The final study to be compared is a long-term stability study of Trastuzumab infusions (Paul et al. 2013). Paul et al. (2013) stored Trastuzumab infusions at the concentrations of 0.8 mg/mL and 2.4 mg/mL for 6 months but did not include or reported on visual examination as part of the study design.

The consensus conclusion of the published work, where visual examination was included, and with this study is that the visual appearance of the stored Trastuzumab infusions did not change over a period of 28 days. Furthermore, in this study it was shown that the appearance remained clear and colourless with no precipitate beyond the study period of 43 days.

3.3.4 Sub-visible particle analysis

Sub-visible particles as soluble aggregates, Trastuzumab monomer concentration and degradation were assessed using size exclusion liquid chromatography (SE-LC). Trastuzumab dimer is presented as a percentage of the initial Trastuzumab monomer

concentration (table 3), thus allowing the monomer purity to be determined. Aggregate content did not increase over time during the study. This is indicative of the Trastuzumab infusions retaining stability in terms of a relatively stable dimer concentration and absence of larger aggregates. This behaviour is consistent with the dimer being in dynamic equilibrium with the monomer which will be concentration dependent (Cromwell et al. 2006). This is shown in table 3 where the dimer content is greater at the higher concentration of 6 mg/mL. The larger aggregate species may become precursors of macroscopic sub-visible particles as the latter must grow from smaller aggregates such as the dimer via higher order or intermediate aggregates (Philo & Arakawa 2009). Thus it may be expected that if the aggregate levels remain unchanged the probability of visible particles forming should remain low. However, visible particles were observed early in the study after 7 days with the sub clinical infusion at the concentration of 0.1 mg/mL. This concentration is discussed separately in section 3.4.1 page 100.

Day	Percentage Trastuzumab Aggregate (dimer)/ %	
	0.5 mg/mL infusion	6 mg/mL infusion
0	0.1	0.27
7	0.2	0.29
14	0.2	0.29
28	0.0	0.22
35	0.0	0.30
43	0.2	0.28
119	0.1	0.30

Table 3 Percentage aggregate dimer at each time point for 6 mg/mL and 0.5 mg/mL infusions over the 43 day study period.

The results of the quantitative assay of the Trastuzumab monomer is shown in table 4. It can be seen that there is no evidence of degradation of the stored samples had occurred. On the contrary monomer content appeared to have increased. This may indicate that the Trastuzumab aggregates have dissociated over time during storage. After dilution these aggregates would be expected to dissociate or re-dissolve over time due to their none-covalent nature. Furthermore, the extent of dissociation or dimer content would be expected to be dependent on concentration or dilution of Trastuzumab as stated previously. This is supported by the difference in aggregate content between the 6 mg/mL and 0.5 mg/mL infusions (table 3 and figure 1). The difference in dimer content between these infusions was significant ($p = 0.007$, using a t-Student test with a significance threshold of < 0.050). However, the apparent increase in Trastuzumab monomer was not accompanied by a decrease in percentage aggregate content (table 3). A non-significant positive correlation was found with both concentrations between monomer and dimer content (Pearson's correlation coefficient (r) was 0.19 and 0.35 for 0.5 mg/mL and 6 mg/mL infusions respectively). This is illustrated by the correlation graphs for each infusion which show no relationship between monomer and dimer content (figures 2 and 3).

These observations may indicate that other aggregate species are present in the freshly prepared infusions which are too large to be detected by SE-LC. Indirectly this infers the presence of sub-visible particles which may dissolve and increase monomer content. This seems a reasonable assumption as the freshly reconstituted Trastuzumab will likely contain aggregates originating from the lyophilised solid form and may form new aggregates during reconstitution at the vial concentration (21 mg/mL) (Webb et al. 2002; Daugherty & Mrsny 2006). Furthermore, due to the reliance on self-mixing full dissolution of particulates may take some time.

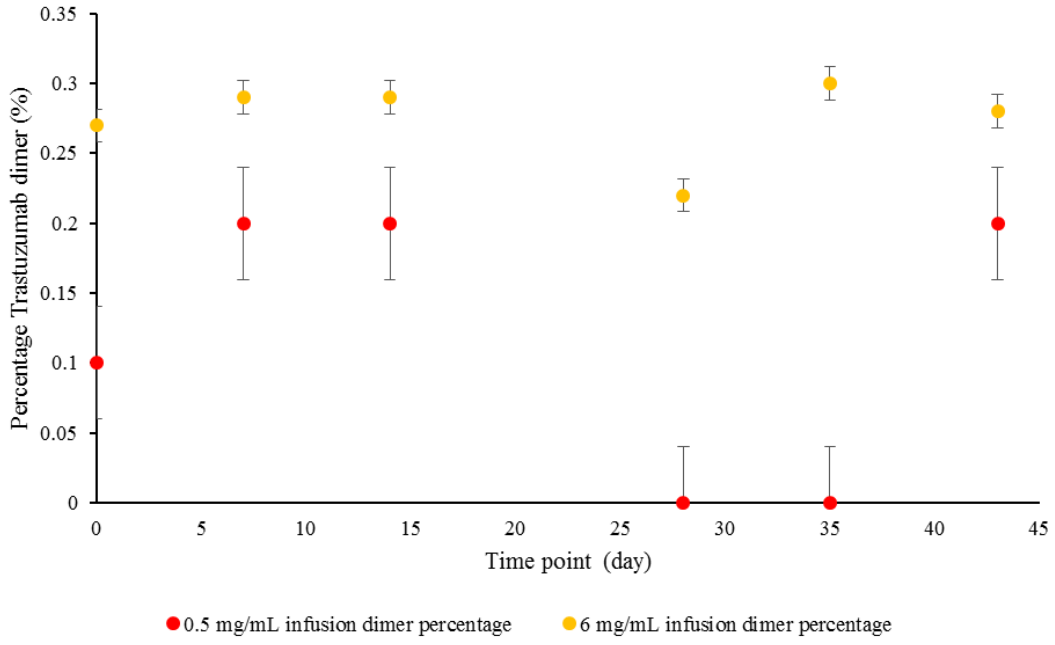

Figure 1 Percentage dimer at each time point for 0.5 mg/mL and 6 mg/mL infusions. Standard error is shown with inferential error bars.

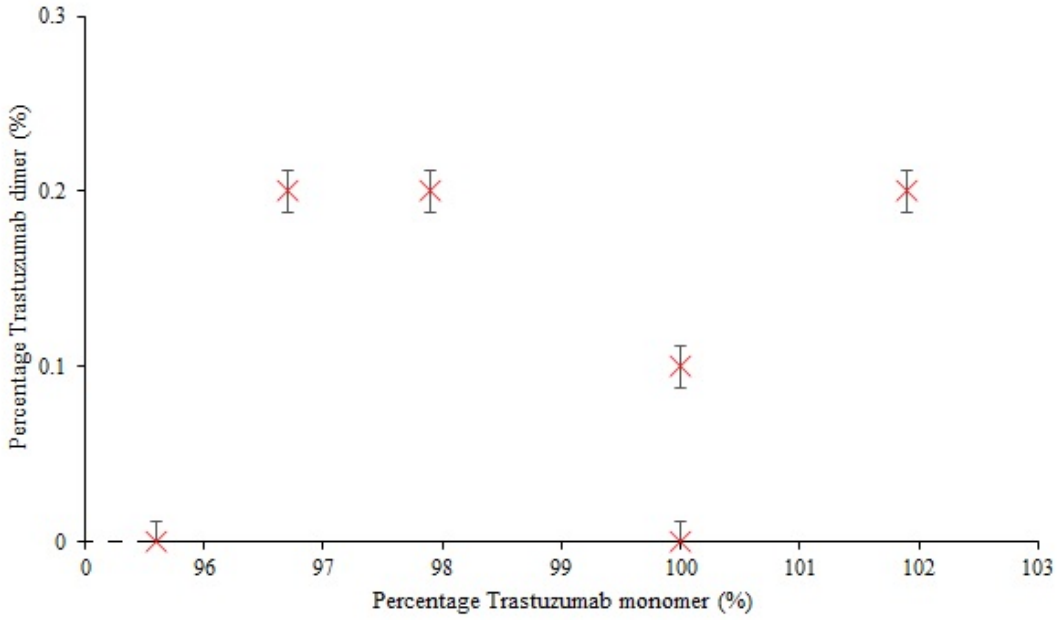

Figure 2 Correlation graph of dimer content with monomer content for the 0.5 mg/mL infusion. Standard error bars shown

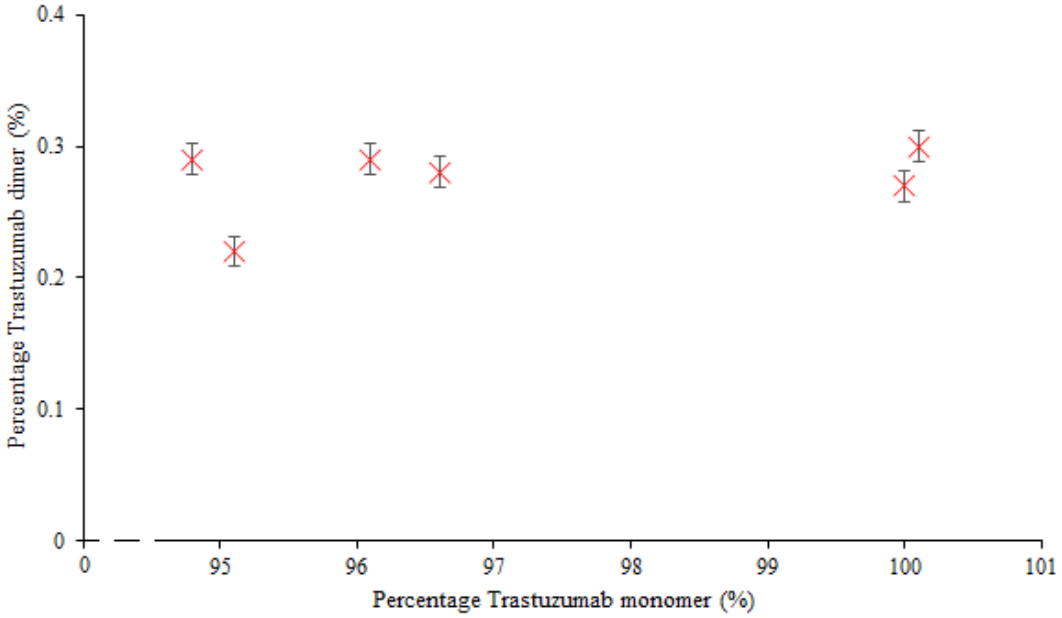

Figure 3 Correlation graph of dimer content with monomer content for the 6 mg/mL infusion with standard error bars.

Day	Percentage Trastuzumab (monomer) / %			
	0.5 mg/mL		6 mg/mL	
0	Method 1 100.0	Method 2 100.0	Method 1 100.0	Method 2 100.0
7	96.7 (3.1)	100.4 (0.6)	94.8 (0.5)	102.3 (1.2)
14	97.9 (3.4)	100.6 (0.3)	96.1 (0.9)	101.1 (1.9)
28	95.6 (3.6)	99.8 (0.7)	95.1 (0.4)	100.9 (1.2)
35	100.0 (3.6)	100.4 (0.2)	100.1 (1.1)	101.6 (1.1)
43	101.9 (8.0)	101.2 (0.4)	96.6 (1.0)	101.9 (1.1)

Table 4 SE-LC determination of Trastuzumab monomer as percentage of initial Trastuzumab assay (relative standard deviation for 3 injections each for two infusion bags) at each time point for 6 mg/mL and 0.5 mg/mL infusions over the 43 day study period.

Size exclusion chromatography is employed as one of the reference procedures in the proposed USP summary validation report for Trastuzumab (USP 2013). The role of SE-LC in the USP document is to detect product related impurities, referred to as species with a higher molecular mass than that of Trastuzumab, in freshly reconstituted Trastuzumab. These impurities correspond to the aggregate species which may dissociate or form and increase in size when in-use and in storage. Therefore these species should be monitored to aid the assessment of the condition of the stored Trastuzumab infusions.

The size exclusion chromatography methods employed showed that there was no evidence of degradation of Trastuzumab infusions at therapeutic concentrations during storage. There was no significant loss in Trastuzumab monomer concentration or increase in aggregation and an absence of fragmentation peaks in all these infusions.

In fact an increase in Trastuzumab monomer concentration was apparent during the study. The increase in monomer content was observed after day 7 with method 2 (QCNW) and day 35 with method 1 for both 0.5 mg/mL and 6.0 mg/mL infusions. This behaviour may be due to the differences in sample preparation between the two methods.

In method 2 the test solutions were highly diluted before chromatographic separation. This treatment may increase dissolution rate of aggregates which occurs over time. Furthermore, this view may be supported by the delayed increase in monomer content found by method 1. This behaviour may in some part be reflected in and consistent with the measured variance and relative standard deviation differences between the methods.

The monomer assay for the 6.0 mg/mL infusion, using method 1, gave a variance of 5.7 % and relative standard deviation of 2.2 % with initial measurement set at 100 %. Whereas analysis of the 6.0 mg/mL infusion by method 2 gave a variance of 0.6 % and relative standard deviation of 0.7 %. The 0.5 mg/mL infusion showed a similar difference between the variance and relative standard deviation for the two methods. Method 1 gave 4.6 % and 2.2 % for variance and relative standard deviation

respectively. Whilst method 2 had a variance and relative standard deviation of 0.2 % and 0.4% respectively.

The other studies which have been compared to this study also show no evidence of degradation with SEC-LC under controlled in-use storage conditions between 2 ^{o}C and 8 ^{o}C (Kaiser & Kramer 2011; Pabari et al. 2013; Paul et al. 2013). Furthermore, Paul et al. (2013) state that no significant changes in the chromatogram, with detection at 280 nm, occur when stored at 20 ^{o}C under light protection for 6 months. However, SE-LC with detection at 280 nm is not sensitive to aggregation (Bond et al. 2010).

3.3.5 Attenuated Total Reflectance Infra-Red Spectroscopy (ATR-FT-IR): Assessment of changes in Trastuzumab secondary structure

The Amide I spectrum remained unchanged for all stored samples. This may indicate that no significant secondary changes had occurred. This was consistent with the view that aggregation resulted in aggregates that retained secondary structure. This was supported by the results of the monomer assay and aggregate SE-LC analysis showing reversibility of the dimer. However, very small changes may have occurred within the infusion and are undetectable. Therefore a difference spectrum method was applied which can reveal very small changes between spectra.

The difference spectrum is the result of subtracting two spectra of two different states. If there are no changes the resultant spectrum will be featureless and centred on the zero datum. In this case a spectrum from time point 0 was subtracted from the spectrum acquired at different time points for day 7, 42 and 119. Small changes are revealed and can become manifest as positive or negative spectral features. For example, increase or appearance of new structure will be revealed by a positive spectral signature. Conversely loss of structure will result in a negative spectral features.

The difference spectrum for the samples resulted in the appearance of new spectral features at day 7. These were predominantly two peaks in the Amide A and Amide I regions. A control difference spectrum of two different 0.1 mg/mL infusion bags spectra acquired for day 0 showed no new spectral features. This confirmed that the new spectral features had appeared during the first week of storage.

The amide peak at ~1,640 cm^{-1} is within the intramolecular β-sheet region (Vonhoff et al. 2010). This indicates β-sheet content has increased. This implies that the Trastuzumab molecule has undergone conformational rearrangement and increased in order (Sethuraman & Belfort 2005). The amide A band originates exclusively from NH stretching and is isolated from the polypeptide back bone and therefore indifferent to conformation (Barth & Zscherp 2002).

There was no discernible relationship between the extent of these peaks, which varied in intensity, and the concentration. Figure 1 shows difference spectra relative to day 0 for a 0.1 mg/mL infusion for spectra acquired at day 7, 43 and 119. For this series of spectra the amide peak disappeared after 7 days (figure 4). In figure 5 for a 6 mg/mL infusion sample the amide I peak has been retained for all time point samples. For another 6 mg/mL infusion bag there was no discernible peak at 1,640 cm^{-1}. The amide A peak was prominent and showed a time dependency increase for each day. In one of the two 0.5 mg/mL infusion bags there was a small loss in structure, evident by the small negative peak in the amide I region. A similar observation was also apparent in one of the four 0.1 mg/mL infusions. This may be related to the lower concentration and is discussed in section 3.3.1.

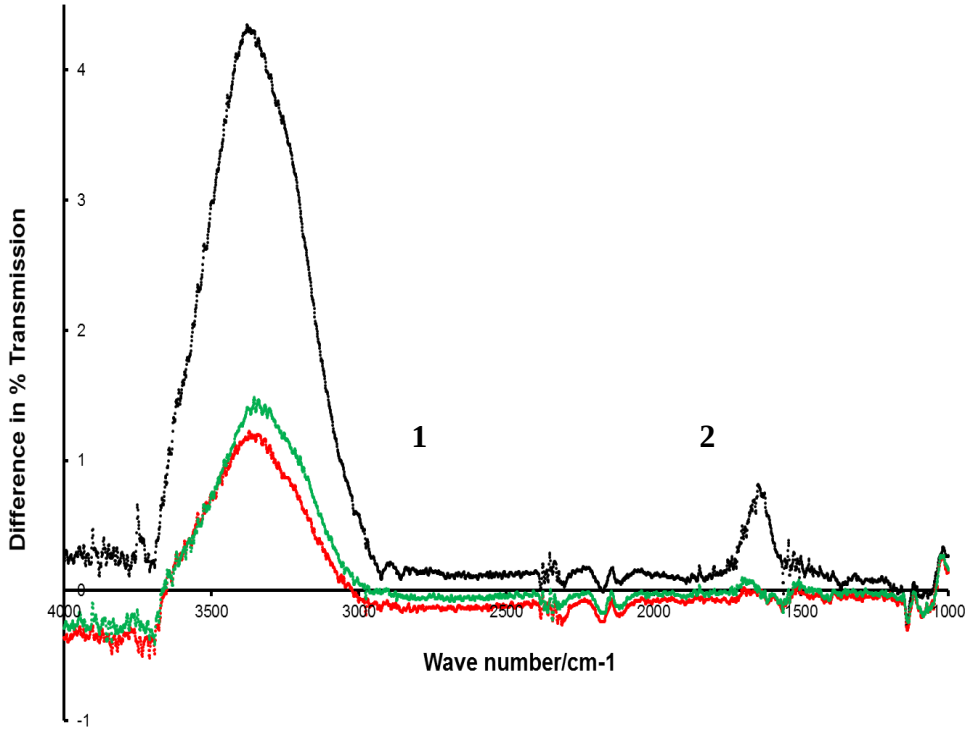

Figure 4 ATR-FT-IR difference spectra of 0.1 mg/mL infusion. Spectrum from time point 0 was subtracted from the spectrum acquired at different time points for day 7 (black), 42 (red) and 119 (green). Spectra shows amide A (1) and amide I (2) peaks. Amide I peak has diminished for day 42 and 119.

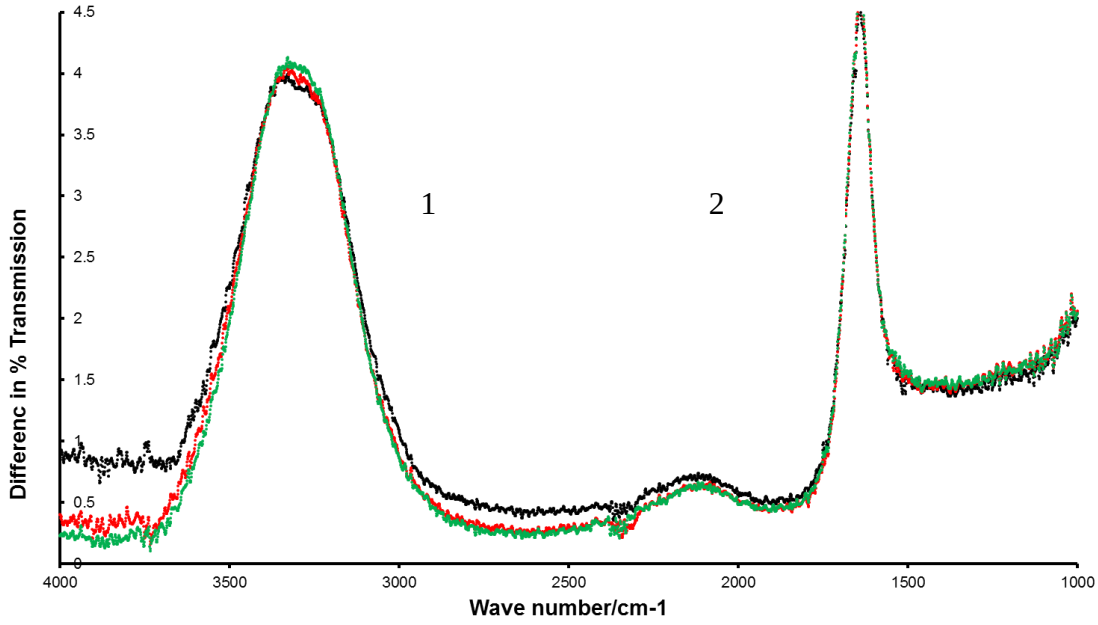

Figure 5 ATR-FT-IR difference spectra of 6.0 mg/mL infusion sample. Spectrum from time point 0 was subtracted from the spectrum acquired at different time points for day 7 (black), 42 (red) and 119 (green). Spectra shows amide A (1) and amide I (2) peaks. Amide I peak has stayed constant for day 7, 42 and 119.

Although not stability indicating the ATR-FTR-IR results do indicate that Trastuzumab has changed in structure to a varying degree on dilution within an infusion solution. Furthermore, these changes are generally indicative of increased order within the molecule.

ATR-FT-IR spectroscopy was used to assess the secondary structure of the stored infusions. This entailed examination of the conformation sensitive Amide I region (1600 cm^{-1} - 1700 cm^{-1}).

The ATR-FT-IR spectra for both reference spectra acquired using freshly prepared Trastuzumab solutions and from samples from each time-point were superimposable.

When difference spectra were generated new spectral features after day 7 were observed. These were in the Amide A and Amide I regions. The amide peak at ~1640cm^{-1} is within the intramolecular β-sheet region (Vonhoff et al. 2010). Although there was no apparent trend with respect to peak size of these features with concentration this may indicate a minor change in structure. This may have resulted from internal reorganisation of the Trastuzumab molecule following dilution and hydration. This view is consistent with the appearance of the Amide A band in the difference spectrum. This peak originates from the NH stretch doublet, which is insensitive to conformation, but sensitive to hydration and thus obscured by the OH stretching band from H_2O molecules in the resultant difference spectrum.

Paul et al. (2013) also found reference and sample spectra superimposable during their study. Although Pabari et al. (2013) did not perform FTIR in their study they did assess the secondary structure using circular dichroism (CD). Pabari et al. (2013) found that the CD spectra did not change and this result is consistent with native structure being maintained throughout the 28 day storage period. The CD spectral signature also originates from the amide but is in the far-UV region (190 – 250 nm). The CD signal is determined by the amide group being in an ordered molecular environment and therefore reports on secondary structure (Barnes 2012).

These studies provide convincing evidence that the secondary structure of Trastuzumab infusions stored between 2 ^{o}C and 8 ^{o}C have remained unchanged. Furthermore, the results of these studies are consistent with the apparent conformational stability at 20 ^{o}C reported by Paul et al. (2013).

3.3.6 Electrophoresis SDS-PAGE: Trastuzumab degradation (fragmentation and aggregation)

Electrophoresis under both none reducing and reducing conditions of 0.5 mg/mL and 6 mg/mL infusion samples at each time point showed no change in band distribution compared to reference Trastuzumab. This indicates no observable levels (within

sensitivity range of 5 to 50 ng) of Trastuzumab degradation products, such as higher aggregation or fragmentation, were present in the samples from the infusion bags.

Day	Visual appearance of gel plate Pass/Fail	
	0.5 mg/mL infusion	6 mg/mL infusion
0	Pass	Pass
7	Pass	Pass
14	Pass	Pass
28	Pass	Pass
35	Pass	Pass
43	Pass	Pass

Table 5 Visual appearance of gel plate reported as Pass/Fail with reference to acceptance criteria for the 6.0 mg/mL and 0.5 mg/mL infusions over the 43 day study period.

Sodium dodecyl sulphate-polyacrylamide gel electrophoresis may detect degradation by the appearance of band smearing but is often qualitative in its interpretation (Barnes 2012).

SDS-PAGE was performed under both none-reducing and reducing conditions to assess the infusion samples at each time point. The resultant gels showed no change in band distribution or presence of band smearing and were equivalent to those of the freshly prepared reference Trastuzumab gels within sensitivity range of 5 to 50 ng. Under none-reducing conditions a single band at ~150 KD was observed which is consistent with the molecular weight of the intact Trastuzumab molecule. In contrast,

under reducing conditions the Trastuzumab molecule degrades into the component light and heavy chains as anticipated. This results in two bands corresponding to the light and heavy chains at 25 KD and 50 KD respectively.

This result was also shown in the studies by Pabari et al. (2013) and Kaiser and Kramer (2011). The use of SDS-PAGE in all these studies, including this study, may provide evidence that Trastuzumab remains intact as commented by Kaiser and Kramer (2011). However, it is questionable that small changes in glycan content could be detected using this technique (Nebija et al. 2014). This is an important issue as the glycan profile is known to be influential on the functionality of the Trastuzumab molecule (Barnes 2012).

3.4 Stability of sub-clinically relevant infusion (0.1 mg/mL) and original vial concentrate (21 mg/mL)

3.4.1 Stability of sub clinically relevant infusion (0.1 mg/mL)

The 0.1 mg/mL showed instability early in the study. Visible particles were observed in all bags within 14 days of the study and increased as the study progressed. This was accompanied by loss of Trastuzumab monomer and a decrease in pH (table 6). However, the pH values remained in the specification range of 5.4 to 6.6 pH units for reconstituted Trastuzumab at 21 mg/mL vial concentration (Roche 2006) (table 6). In contrast both reducing and none reducing electrophoresis (SDS PAGE) showed no evidence of degradation (table 6). This is consistent with aggregate disassociation which may occur during the considerable sample manipulation with this technique (Philo 2006; Das 2012). Furthermore, particles must be solubilised in the SDS detergent for any changes to the protein to be detectable (Das 2012).

	0.1 mg/mL infusion			
Day	Visual appearance Pass/Fail	Percentage Trastuzumab (monomer) / %	pH	SDS PAGE Visual appearance of gel plate
0	Pass	100.0	6.11	Pass
7	Fail	98.8 (1.1)	5.73	Pass
14	Fail	97.3 (0.7)	5.71	Pass
28	Fail	95.5 (0.7)	5.66	Pass
35	Fail	95.2 (1.2)	5.70	Pass
43	Fail	94.2 (0.7)	5.87	Pass

Table 6 Percentage monomer with relative standard deviation for 3 injections and pH at each time-point for 0.1 mg/mL Trastuzumab infusion.

The decrease in pH on day 7 is maintained until a recovery on day 43. The pH data gave a mean and standard deviation of 5.80 +/- 0.17, thus presenting a significant change in pH greater than measurement scatter. The loss of monomer with time was highly linearly correlated (Pearson's correlation coefficient (r) = -0.99). In addition the correlation of monomer loss with pH was strong (Pearson's correlation coefficient (r) = 0.78) up to day 35 and decreased to moderate (r = 0.51) with inclusion of pH at day 43. These results are consistent with decreased stability at lower concentration. This may be due to the further dilution of excipients decreasing buffering capacity and the protection of polysorbate (Garidel et al. 2009; Bee et al. 2011).

Evidence of degradation was also shown by the percentage monomer and dimer by relative peak area (table 7). The data gives a strong negative correlation of monomer content over time (Pearson's correlation coefficient (r) = -0.69). The converse is

shown for the dimer content due to the relative relationship between monomer and dimer.

	Percentage monomer and dimer for 0.1 mg/mL Trastuzumab infusion	
Day	Monomer / %	Dimer / %
0	99.98	0.02
7	99.96	0.04
14	99.89	0.11
28	99.98	0.02
35	99.99	0.01
43	99.61	0.39
119	99.67	0.33

Table 7 Percentage monomer and dimer by relative peak area for the 0.1 mg/mL Trastuzumab infusion.

In contrast no significant changes in the secondary structure was shown by ATR-FT-IR. However, difference spectra revealed a small negative change in spectral feature, in the amide I region, in one of the four 0.1 mg/mL Trastuzumab infusions (figure 6A). This was also found with a 0.5 mg/mL infusion shown in figure 6B for comparison.

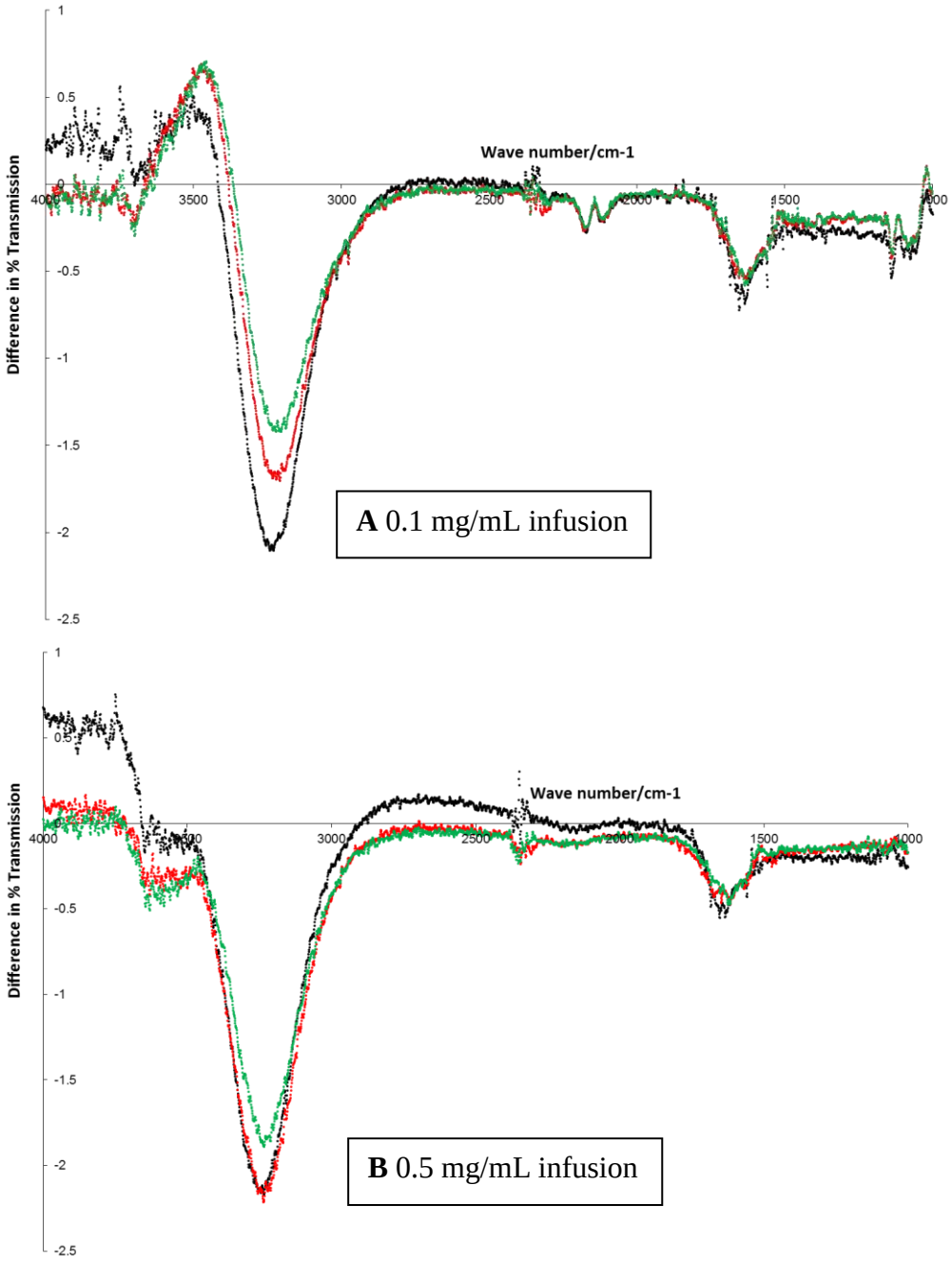

Figure 6 Difference spectra of A 0.1 and B 0.5 mg/mL infusions for day 7 (black), 42 (red) and 119 (green).

These features were accompanied by a relatively large negative change in the amide A region. This may indicate a decrease in hydration (Barth & Zscherp 2002). The

remainder of the 0.1 mg/mL infusions showed positive changes (figures 7, 8 and 9) similar to the 6 mg/mL infusions (figure 2).

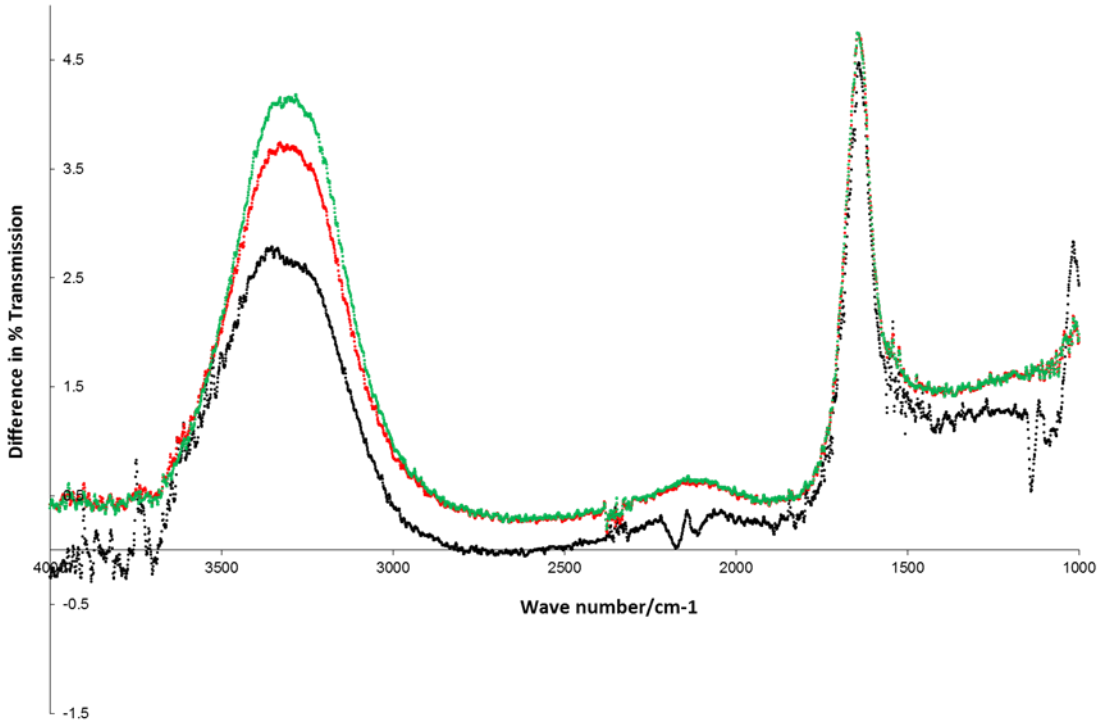

Figure 7 Difference Spectra for 0.1 mg/mL infusion (bag 1).

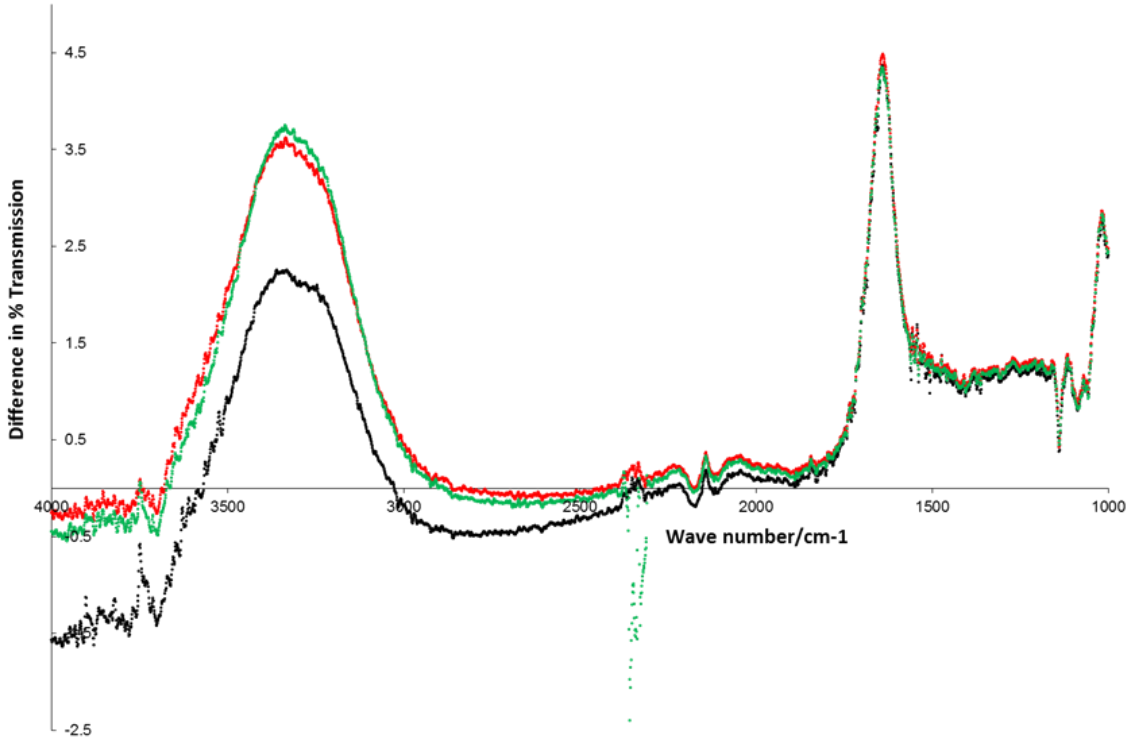

Figure 8 Difference spectra for 0.1 mg/mL infusion (bag 2).

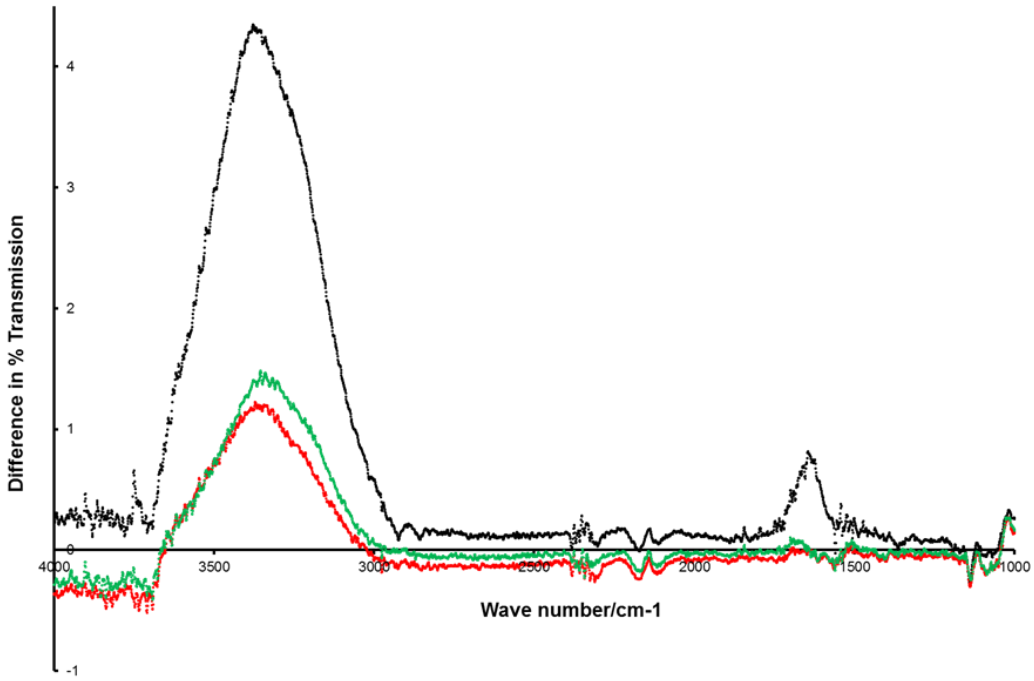

Figure 9 Difference spectra for 0.1 mg/mL infusion (bag 4).

3.4.2 Percentage dimer content of original vial concentrate (21 mg/mL)

The percentage dimer content by SE-LC remained constant during the study period of 43 days (table 8). Furthermore there was no change in dimer content during long term storage after 119 days under conditions of refrigeration (table 8).

Day	Percentage Trastuzumab (dimer) / %
0	0.1
7	0.3
14	0.4
28	0.3
35	-
43	0.3
119	0.3

Table 8 Percentage dimer for the original vial concentrate (21 mg/mL) over the study period.

3.5 Stability of clinically relevant infusions at room temperature

The NHS QCNW infusions showed satisfactory stability at room temperature with light and agitation. The pH remained within specification (table 9). The initial pH at the beginning of the study is shown for comparison (table 9). The pH after stress generally remains in the range found during the study (5.88 to 6.04 for the 0.5 mg/mL infusion and 6.21 to 6.29 for the 6 mg/mL infusion). However, the 0.5 mg/mL infusion showed an increase in pH for the light exposure test compared to the light

protected result at room temperature. This gave two approximate standard deviations higher from the mean (5.94+/-0.06) for the 6.07 result. Although a relatively small difference, this may reflect the dilution of excipients. This view is reasonable as the pH for the 6 mg/mL infusions with light protection and light exposure was very similar, although showing a small decrease for light exposure. Agitation showed little effect on pH.

Conditions	pH of Trastuzumab infusions	
	0.5 mg/mL	6 mg/mL
Initial	6.04	6.23
Day 43	5.94	6.29
Exposed to light for 24 hours at RT	6.07	6.21
Light protected for 24 hours at RT	5.98	6.23
Exposed to light with agitation for 6 hours at RT	5.95	6.20

Table 9 Stability of clinically relevant infusions. The pH at room temperature (RT): after exposure to light (24 hours), without light (24 hours) and agitation with exposure to light for 6 hours.

The SDS-PAGE showed no differences between stressed and control plates (table 10).

Conditions	SDS PAGE analysis of Trastuzumab infusions Visual appearance of gel plate Pass/Fail	
	0.5 mg/mL	6 mg/mL
Exposed to light for 24 hours at RT	Pass	Pass
Light protected for 24 hours at RT	Pass	Pass
Exposed to light with agitation for 6 hours at RT	Pass	Pass

Table 10 Aggregate and fragmentation analysis of clinically relevant infusions. Electrophoresis of samples taken from infusion bags after being subjected to stress conditions at room temperature (RT).

SEC-LC did not show evidence of degradation (table 11) compared to the variation of monomer content during the study period (table 4). This was reported as percentage loss of monomer (table 11). The percentage decrease of monomer was within the acceptance limit of 5% (Barnes 2012).

Conditions	Percentage loss of Trastuzumab monomer / %	
	0.5 mg/mL	6 mg/mL
Exposed to light for 24 hours at RT	1.0	1.2
Light protected for 24 hours at RT	1.7	1.1
Exposed to light with agitation for 6 hours at RT	1.5	0.5

Table 11 Percentage loss of monomer as determined by SEC-LC after further stability testing of infusions.

3.6 Conclusions

The clinically relevant concentration infusions, 0.5 mg/mL and 6 mg/mL, remained free of visible particles (table 2). Furthermore, the clarity and colour observed at day 0 was retained (table 2). Sub-visible particles as soluble aggregates, as determined by SE-LC, did not increase during the study (table 3). Additionally, there was no indication of monomer loss (table 4). SDS-PAGE did not show evidence of aggregation or fragmentation (table 5). The pH of the clinically relevant infusions was relatively constant during storage (table 1), with the 0.5 mg/mL infusion giving a slightly lower pH over the study period (table 1).

The sub-clinically relevant 0.1 mg/mL concentration infusions developed particles from day 7 (table 6). Whilst SDS-PAGE did not detect aggregation or fragmentation

(table 6). Particulate formation was accompanied by a decrease in monomer (table 6) and increase in dimer content during storage (table 7). In contrast, the original vial concentrate showed no change in dimer content during the study period of 43 days and long term storage after 119 days (table 8).

All infusions showed very small positive (figures 4, 5, 7, 8 and 9) or negative changes (figures 6A and 6B) in their difference spectra.

The NHS QCNW infusions showed satisfactory stability at room temperature with light and agitation in terms of pH, aggregation levels and loss of monomer (tables 9, 10 and 11).

CHAPTER 4

4. DEVELOPMENT OF CELLULAR ASSAY

4.1 INTRODUCTION

The aim of this study was the development of a cellular assay that is appropriate to measure changes in potency of Trastuzumab. It is essential to consider the mechanism of action of Trastuzumab with an appropriate cell line to select the most suitable end reporter assay.

Trastuzumab binds to the HER2 receptor on the cell surface inhibiting dimerisation and is targeted towards cells that over-express this cellular receptor (Goldenberg 1999; Nahta 2012). Dimerisation is the key step in the cell signalling pathways which stimulate cell reproduction (Sundaresan et al. 1999; Genentech 2015). Therefore in assay design cellular growth (viability and proliferation) was selected as an end reporter of effective binding and action of Trastuzumab. There are other processes subsequent to Trastuzumab binding to the HER2 receptor. These processes involve the immune system *in vivo* and are not detected by the cellular assay used in this study.

The selection of the level of dose for an assay can prove demanding (Barnes 2012), whilst referring to the equilibrium dissociation constant (k_D) may aid this process. The equilibrium dissociation constant k_D for Trastuzumab is 5 nM (De Lorenzo et al. 2004). This means a concentration of 5 nM gives a 50% binding of the HER2 receptors. Thus this gives some idea of what may be a clinical and sub-clinical dose.

Another factor in designing the assay was the selection of an appropriate read-out to assess cellular growth. There are different types of assay read-out which include colony counting (Franken et al. 2006) or measurement of the enzymatic turnover of a substrate to a coloured product (Riss et al. 2004).

In the case of Trastuzumab a number of cell-lines could be used (Subik et al. 2010). The BT474 cell line which over-expresses the HER2 receptor (Sundaresan et al. 1999; Subik et al. 2010) was selected. This receptor is the therapeutic target for the drug (European Agency for the Evaluation of Medicinal Products (EMEA) 2005b; Reichert 2012). Following the cell line selection the type of assay has to be selected with careful consideration. Cell proliferation was originally selected as a reporter of drug potency for the BT474 cell line. Following initial work this was later changed to viability. It should be noted that preliminary work was performed using the MCF7 cell line. MCF7 is an example of an adherent breast cancer cell line. Although this cell line does not over-express the HER2 receptor and is therefore unsuitable, it enabled the development of cell culture techniques and also methodology of the proliferation assay. Due to significant differences in growth characteristics between MCF7 and BT474 the early work had ultimately little relevance to the work with BT474.

In a proliferation assay the ability of an individual cell to form colonies is assessed, i.e. the number of cells that are dividing to form colonies. These colonies will increase in size at a rate determined by the ability of the cell to divide. After an incubation or growth period colonies will vary in size depending on their individual capability for cellular division. If a lower limit of colony size is defined a count of colonies above this size threshold will be a measure of the number of actively dividing cells within the cellular population.

Figure 1 shows colony counting in practise from this study. In this example colonies are counted using an inverted light microscope using phase contrast. The micrograph shows fixed and stained BT474 colonies at x100 magnification after a 14 day incubation or growth period within a 6-well micro-plate. Wells were filled with a cell suspension in media to give 100,000 cells per well. This process is termed seeding. The 50 μm diameter circles defines the size of a colony that may be included in a colony count. The circles numbered 1 and 2 are colonies that are below the size threshold. The circles numbered 3 and 4 would be included in a count.

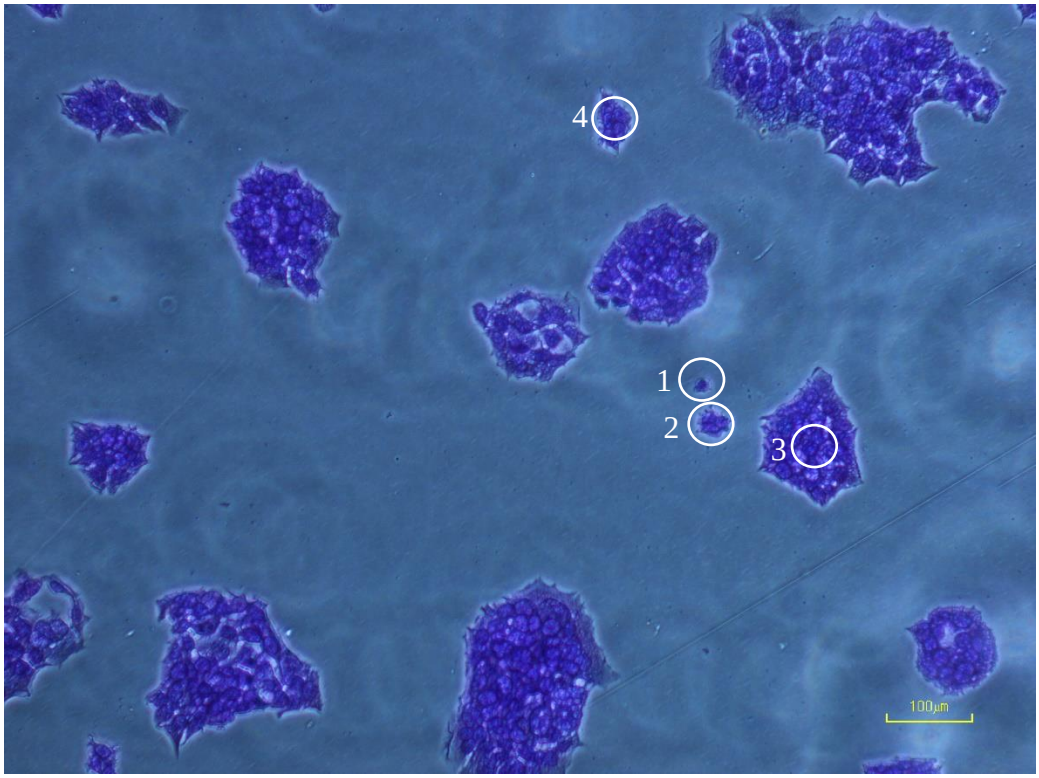

Figure 1 Micrograph of fixed and stained BT474 colonies at x100 magnification after a 14 day incubation or growth period within a 6-well micro-plate. Wells were seeded with a cell density of 100,000 cells per well. The 50 µm diameter circles defines the size of a colony that may be included in a colony count. The circles numbered 1 and 2 are colonies that are below the size threshold. The circles numbered 3 and 4 would be included in a count. Colonies were imaged using an inverted microscope and imaging system (Nikon Eclipse T100 binocular phase contrast microscope fitted with Digital Sight DS Fi1 imaging system).

In contrast cellular viability was reported from a measure of the number of live or metabolising cells following incubation with and without the presence of Trastuzumab (Kawa et al. 2009). Changes in the biological potency of Trastuzumab can be described in terms of the effect on cellular viability. With fully active Trastuzumab, freshly prepared, cell proliferation and viability will be affected by the greatest extent. Any degradation of drug during storage could result in a decreased effect on cell proliferation and viability.

The ability of detecting a change in proliferation and viability is dependent on the sensitivity of the methods employed and the magnitude of change. In this study a colorimetric reporter read-out was used to assess cellular viability. The reporter chemistry selected was a commercial kit supplied by Sigma Aldrich (CCK8) which has high sensitivity in terms of read-out and is a variant of the much published MTT assay (Lin et al. 2005; Brescia & Banks 2009; Budman et al. 2007; Barnes 2012). Sensitivity will be affected by both repeatability in precision of the number of cells used in replicate experiments and the intrinsic sensitivity of the readout method employed. With the colorimetric readout approach adopted in this study the variability in the optical density measurement between successive readings of the same well provides an indication of the uncertainty in measurement. This uncertainty will limit the sensitivity of measurement.

A significant amount of time was devoted to developing a robust cell delivery technique to ensure consistency in seeding cells within the 96-well plates used for the cellular assays. The cell seeding consistency was evaluated by using the same CCK8 cell counting kit (Sigma Aldrich) and a Haemocytometer to measure the numbers of cells in each well of a 96-well plate. The approach that was developed in the study allowed characterisation of cell growth and provided a means to quantify viability using repeatable calibration curves over range of cell densities. This enabled both qualitative and quantitative assessment of cell growth. The strategy taken forward in this study included both cell viability and cell proliferation approaches were initially developed and cell viability selected for the final study.

4.2 MATERIALS AND METHODS

4.2.1 Preparation of Trastuzumab (Herceptin®)

Trastuzumab was reconstituted as described in Chapter 2 section 2.2.1 page 51.

4.2.2 Cell lines

The MCF7 breast cancer cell line was a kind gift from Dimitra Dafou (University College London). This cell line originates from the Massachusetts Cancer Foundation (MCF7) and was selected because the cells express the HER2 receptor which is the therapeutic target of Trastuzumab and this cell line is often used and cited in breast cancer literature (Holliday & Speirs 2011). The MCF7 cells exhibited rapid cell growth which was a desirable feature as this aided the development phase when establishing the cell culture methods.

The BT474 breast tumour (human ductal tissue (epithelial) carcinoma) cell line from ATTC (HTB-20; lot: 58471910) was selected as the actual cell line for performing the potency testing of Trastuzumab. This cell line is superior to the MCF7 cell line for testing because BT474 cancer cells over-express the HER2 surface cell receptor which is the therapeutic target for Trastuzumab (anti-HER2 antibody) (Sundaresan et al. 1999; Subik et al. 2010).

4.2.2.1 Reviving cells from cryogenic storage

The selected vial was retrieved from cryostasis and warmed in a water bath (37 $^{\circ}$C) for a few minutes until contents had liquefied. The submerging of the vial was avoided to reduce risk of contamination. Once the vial contents were completely thawed, the contents (~1 ml) were removed and diluted into a cell culture flask, containing pre-warmed (37 $^{\circ}$C) media. The cells were incubated overnight to allow attachment of cells and the media exchanged (6 ml). Both cell lines were further passaged as and when required. Passaging is the process where the adherent cells are released and/or transferred between flasks when the growth area is beginning to merge or become confluent. The cells were passaged at approximately 60% confluence or coverage of the area available for growth described in section 4.2.2.4 page 116.

4.2.2.2 Maintenance of BT474 Cells

The BT474 cells were cultured in RPMI 1640 base growth media with stable glutamine and phenol red pH indicator (PAA Labs; E15-885: E88510-3009) supplemented with 10% foetal bovine serum FBS Gold (PAA Labs FBS; A11-151; lot: A15111-2028) and 1% Penicillin/streptomycin (PAA Labs; P11-010; lot: P01009-2794). BT474 cells were incubated at 37 $^{\circ}$C in a humidified 5% carbon dioxide incubator (Sanyo NC0-19AIC (UV)). The cells were grown and maintained in 75 cm^2 (growth area) tissue culture flasks (SPL Life Sciences; PAA 430641) until 60% confluence and then passaged (released to give a cell suspension). The suspension was then transferred and distributed within two or three 75 cm^2 tissue culture flasks (SPL Life Sciences; PAA 430641) or used in an assay.

4.2.2.3 Maintenance of MCF7 Cells

The MCF7 cells were cultured under the same conditions as the BT474 cell line (section 4.2.2.2 page 116)

4.2.2.4 Cell Passage and Seeding of BT474 cells

The BT474 cell growth media was removed by aspiration using a glass Pasteur pipette attached to plastic tubing and connected to plastic waste reservoir which was connected to a pump (Progen: article number 31200005 serial number 0638002367). The BT474 cells were then washed once with phosphate buffered saline (5 mL) (PBS, Dulbecco H00211-0079) delivered using a sterile disposable serological pipette or Strippete® (Corning Costar® Blue 4051 5 mL). Washing the BT474 cells removes any residual media which would otherwise inhibit the action of the trypsin. The BT474 cells were then released from the flask growth surface using an addition of 0.05% trypsin in 0.02% ethylene diamine tetra-acetic acid/phosphate buffered saline (EDTA/PBS) solution (2 mL) (PAA Labs; L11-004; lot: L00410-2467). The cells were incubated at 37 $^{\circ}$C for 5 minutes to assist release and then the trypsin was neutralised using an addition of growth media (20 mL) to the BT474 cell suspension.

The serum present in the media inhibits trypsin activity. The BT474 cellular suspension was gently agitated by the action of a rocking motion of the flask combined with the careful use of a sterile disposable serological pipette or Strippete® (Corning Costar® Red 4251 25 mL) to repeatedly withdraw and expel the suspension to ensure separation of cells to give a single cell suspension. The resultant BT474 cell suspension is either distributed between a numbers of flasks depending on the degree of splitting required or diluted to required concentration and used for seeding plates.

A uniform BT474 cell suspension is required for accurate cell counting and consistent seeding. The cell density or number of cells per unit volume was then determined using a Bright-Line Haemocytometer (20 µL loading capacity, Sigma Aldrich; product code Z359629) and standard counting protocol (Sigma Aldrich, 2012). The BT474 cell suspension was then serially diluted to a concentration of 50,000 cells/mL. The BT474 cell suspension was continually agitated during this process, as described above, to ensure a uniform distribution of cells and hence the target cell density or cell number would be achieved. For the final protocol a 0.2 mL aliquot of the same cell suspension was added to each of the 96 wells of a micro well plate (NunclonΔ Tissue Culture 96F; 167008; batch: 075127) using an 8-channel multi-pipette (Biohit, 30-300 µL serial no: 725140 Cat No: 6545280) giving 10,000 cells per well. The 96 well plates were incubated for 24 hours to give time for the cells to attach or adhere on the growth surface and adopt normal cellular activity. The wells were inspected to assess the quality of seeding and health of cells using an inverted microscope (Nikon Eclipse T100 binocular phase contrast microscope fitted with Digital Sight DS Fi1 imaging system).

4.2.2.5 Fixing and staining colonies of BT474 cells (Eichhorn et al. 2008)

Media was aspirated or removed from the wells and the cells were washed twice with a phosphate buffered saline (PBS) to remove traces of media. The colonies were fixed with acetic acid and methanol solution (1:3) and stained with aqueous 0.5% crystal violet (Fisher Scientific) 25% methanol (Fisher Scientific). The wells were then filled with acetic acid/methanol (1:3) fixative solution and the BT474 cells plus acid/methanol (1:3) fixative solution incubated on the bench for 5 minutes. After this

time the fixative solution was removed and the stain solution was applied using a multi-pipette to each well (60 µL). The micro- well plates containing the staining solution were left undisturbed for 15 minutes to allow the staining process to take effect, then washed with copious amounts of water (tap water) to remove excess stain, rinsed with distilled deionised water (DI) and then drained and allowed to air dry partially inverted on a draining board. The fixing and staining process allows colonies to be preserved and aids visualisation for the colony formation assay (Eichhorn et al. 2008).

4.2.2.6 Method of stain release of crystal violet from BT474 cells and absorbance measurements of crystal violet at 540 nm as a measure of cell number/viability to calibrate instrument response for comparison to CCK8 reporter chemistry data

The BT474 cells that were stained with crystal violet solution were treated with aqueous acetic acid (10%) to release the stain into solution and the released stain measured using a Biotek micro well plate reader (Biotek Epoch, operating Gen 5 Software, version 1.10.8 under windows XP environment, service pack 2) at 540 nm. The method followed was that of a published method by Eichhorn et al (2008). The absorbance data was collected and then analysed using Microsoft Excel from Microsoft Office 2003. Re-staining of BT474 cellular colonies was performed when required using the same process as given above (Eichhorn et al. 2008).

4.2.2.7 BT474 cell line colony formation assay

The BT474 cell line was seeded in to a 6 well micro-plate format at cell densities ranging from 1000 to 500,000 cells per well. This level of seeding density proved optimal for colony counting purposes in the assay for the BT474 cell line.

BT474 colonies (>0.1 mm) were counted using an inverted microscope (Nikon Eclipse T100 binocular phase contrast microscope fitted with Digital Sight DS Fi1 imaging system) in ten random user defined fields (~1 mm) at x10 magnification (Wu

et al. 2002a; Hermanto et al. 2001) in addition to efforts to count colonies on the whole well surface.

4.2.2.8 MCF7 cell line Colony formation assay

The MCF7 cell line was seeded in to a 6 well microplate format at cell densities ranging from 50 to 600 cells per well. A seeding density 300 cells per well proved optimal for colony counting purposes in the assay for the MCF7 cell line. Seeding and passage procedure as for BT474 cell line.

4.2.2.9 Method for assessing potency of an inhibitor of the MCF7 cell line for the development of colony formation assay protocols

The MCF7 cell line was seeded at 300 cells per well in a 6 well-plate format. Resultant colonies were counted using either all of the surface area available on the micro well plate or using a user defined area and a low powered light microscope (Nikon Eclipse T100 binocular phase contrast microscope fitted with Digital Sight DS Fi1 imaging system) to aid counting. For the initial development work methanol was used as a known inhibitor of cell growth for the MCF7 cell line and was used at concentrations of 0%, 1.5% and 2.0% which were added to test micro wells within the 6 well-plate to limit cellular growth in those wells. In this way it proved possible to establish a protocol for assessment of different chemical inhibitors of the cell line MCF7 and development of the assay protocols for use with the BT474 cell line.

4.2.3 Method of cell counting using a commercial cell counting kit (Sigma Aldrich, CCK8) assay

The BT474 cell line growth media was exchanged for either fresh media (200 μL) for the zero drug control (negative control) or seeding (calibration experiments) i.e. cells and media, reference Trastuzumab (positive control) which was freshly reconstituted in sterile water for injection (SWFI) and diluted in BT474 cell line growth media (200

μL) or test Trastuzumab solutions which following re-constitution in sterile water for injection were diluted in BT474 cell line growth media (200 μL).

The micro well-plates were then aspirated to remove the media before the test samples were added using the glass Pasteur pipette aspirator system described in section 4.2.2.4 page 96. The micro well-plate was inclined vertically as possible and the media withdrawn from the side of the well to avoid contact with cells. The drug solution was added in tissue culture media (0.2 mL addition) at the appropriate concentration. The micro-plates were then returned to the humidified incubator at 37 ^{o}C, 5% CO_2 (Sanyo NC0-19AIC (UV)). The cells were incubated for 4 days to allow for growth of BT474 colonies or tested immediately. The plates were removed from the incubator and the cellular reporter substrate CCK8 (increased from 10 μl to 30 μl) (Sigma Aldrich CCK8 cell counting kit instruction leaflet) was added to each well using an 8-channel micro-pipette (Biohit, serial no: 725140 Cat No: 6545280) and incubated at 37 ^{o}C, 5% CO_2 (Sanyo NC0-19AIC (UV)) for 1, 2, 4 and 20 hours. The absorbance was then read at 450nm according to the manufacturer's instructions using a Biotek micro-plate reader (Biotek Epoch, operating on Gen 5 Software, version 1.10.8).

4.2.4 Optimisation of a commercial cell counting kit (Sigma Aldrich, CCK8) assay method

Seeding experiments using a range of cell densities were performed to assess the effect of an extended test period on the resultant absorbance measurements following addition of CCK8 reagent. This entailed testing immediately after seeding or after a growth period of 4 days. Absorbance was monitored at 1, 2, 4 and 20 hours after addition of CCK8 to monitor signal build-up and determine a working range of response.

4.2.5 Stability indicating capability of using a commercial cell counting kit (Sigma Aldrich, CCK8) to distinguish between differences in viability induced by changes in active Trastuzumab concentrations by thermal degradation

The BT474 cell line growth media was exchanged for either fresh media (200 µL) for the zero drug control (negative control) or seeding (calibration experiments) i.e. cells and media, reference Trastuzumab (positive control) which was freshly reconstituted in sterile water for injection (SWFI) and diluted in BT474 cell line growth media (200 µL) or test Trastuzumab (0.1 mg/mL) solutions which following re-constitution in sterile water for injection had been thermally degraded and then diluted in BT474 cell line growth media (200 µL) to determine the level of change in biological activity which may be observable. Trastuzumab was thermally stressed by heating in a water bath at 75 ^{o}C for a range of times (5, 10, 15 and 20 minutes)

A colony formation assay using a seeding density of 10,000 cells/well, identical to the CCK8 assay, was performed to assess changes in proliferation and to identify the optimum drug concentration and stressing time for subsequent CCK8 proliferation assay.

Samples were serially diluted in the complete cell culture media, which was used to maintain the cells prior to the assay, to a nominal concentration of 1 µM before serial dilution to the appropriate concentration range used in the stability indicating assay. The stressed sample and unstressed control were diluted in the range of 0.5, 1, 2 and 100 nM. The reference Trastuzumab was diluted in tissue culture media in an equivalent manner to the samples.

The micro well-plates were then aspirated to remove the media before adding the test samples as described in section 4.2.2.4 page 96. The micro well-plate was inclined vertically as possible and the media withdrawn from the side of the well to avoid contact with cells. The drug solution was added in tissue culture media (0.2 mL addition) at the appropriate concentration. Each sample of drug in media was added using replicate (n = 24) stressed drug wells to the 96 well micro-plate including reference standards (n = 24) and controls (no drug) (n = 32) for each plate. The micro-

plates were then returned to the humidified incubator at 37 ºC, 5% CO_2 (Sanyo NC0-19AIC (UV)). The cells were incubated for 4 days to allow for growth of BT474 colonies. The plates were removed from the incubator and the cellular reporter substrate CCK8 (increased from 10 µL to 30 µL) (Sigma Aldrich CCK8 cell counting kit instruction leaflet) was added to each well using an 8-channel micro-pipette (Biohit, serial no: 725140 Cat No: 6545280) and incubated at 37 ºC, 5% CO_2 (Sanyo NC0-19AIC (UV)) for up to 4 hours. The absorbance was then read at 450 nm according to the manufacturer's instructions using a Biotek micro-plate reader (Biotek Epoch, operating on Gen 5 Software, version 1.10.8).

A seeding calibration was performed for each stability indicating assay in duplicate with replicate wells (n = 16) for each seeding density. The purpose of this was to determine the relationship between cell density and absorbance after the 4 day test period. The final projected cell densities (0 to 320,000 cells per well) of the calibration encompass the cell density range at the assay end-point to enable the determination of relative cell numbers within the wells which had a drug addition or none. The data from the assay and calibration was exported using Microsoft Excel 2003 for further analysis.

4.3 QUALITY ASSURANCE AND QUALITY CONTROL

The BT474 cell line obtained had been thoroughly tested and authenticated by ATCC. In-house training and webinars ensured competence in cell culture knowledge and techniques. Documentation was kept and included SOPs, pipette calibration, details of feeding, frozen stock and passage number. A frozen stock from an early passage provided assurance of a homogeneous cell supply. Microscopic examination of cells on feeding, passaging and seeding provided assurance of culture health.

The seeding operation was followed by cell counting, with a haemocytometer, gave assurance of an acceptable precision of seeding within a 6-well plate format. However, the absolute number of cells within the wells will be unknown. The colorimetric method of the CCK8 assay improves assessment of accuracy and

precision of seeding experiments. Linearity was assessed by calculating vertical deviation of data and plotted against cell number.

4.4 STUDY LIMITATIONS

The processes of Trastuzumab action which involve the immune system *in vivo* are not assessed in the cell-based assay. The processes assessed in this study induce apoptosis or normal cell death. Apoptosis shows variability between cells. This is shown even with genetically identical cells under the same growth conditions (Raj & van Oudenaarden 2008).

The cost of Trastuzumab was a major limitation for this study putting constraints on repeating work outside of the main study and use of hospital compounding facility.

4.5 RESULTS AND DISCUSION

4.5.1 MCF7 and BT474 propagation and proliferation assessment

4.5.1.1 MCF7 seeding and colony growth characteristics

The MCF7 cell line has a rapid and evenly distributed growth characteristic allowing the implementation of numerous tests to aid development of test methodology. The MCF7 cell line was seeded at 50 - 600 cells per well in a 6 well micro-plate format to find the optimal level of cell density to facilitate the counting of colonies. To aid singular and even distribution of the cells during seeding agitation of cell suspension was employed. Resultant colonies were distributed with varying success. There was a tendency for cells to preferentially form around the edge leaving the centre devoid of colonies or to gather in the centre. Delivering the cells with no agitation or a controlled figure of eight movement of the plate to aid distribution did not appear to correlate with the resultant cell or colony distribution. After many attempts some wells did appear to have an even distribution of diffuse and large colonies. The best

seeding was achieved at a density of 300 cells per well which gave a relatively even spread of colonies (figure 2).

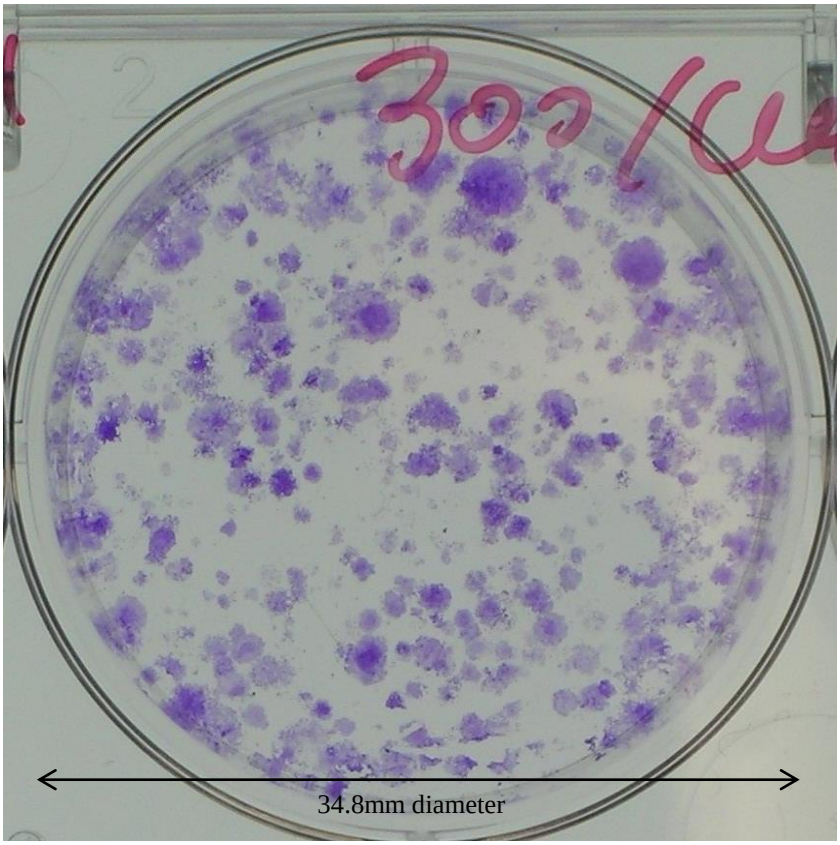

Figure 2 MCF7 colonies resulting from an initial seeding density of 300 cells per well. The photograph shows a top view of a well of a 6 well-plate with a 34.8 mm diameter and approximate growth area of 9.5 cm^2. Cells were fixed with acetic acid/methanol (1:3) and stained with aqueous 0.5% crystal violet (CV) 25% methanol solution.

4.5.1.2 BT474 seeding and colony growth characteristics

The growth characteristics of this cell type were very different to that of the MCF7 cell line. The initial revival of BT474 from cryostat stocks showed low viability and

slow growth as confluence or coverage was not achieved after several days' propagation. On subsequent propagation viability and growth rate had improved possibly due to recovery from the revival procedure. Cellular growth produced inconsistent areas of stacked or layered of cells which were very unlike the behaviour of the MCF7 cell line. BT474 cells were seeded at densities ranging from a 1000 to 500,000 cells per well in a 6 well microplate format. The resultant colonies were very small but well defined (figure 3). This was in contrast to the morphology of that found with the MCF7 colonies (figure 2).

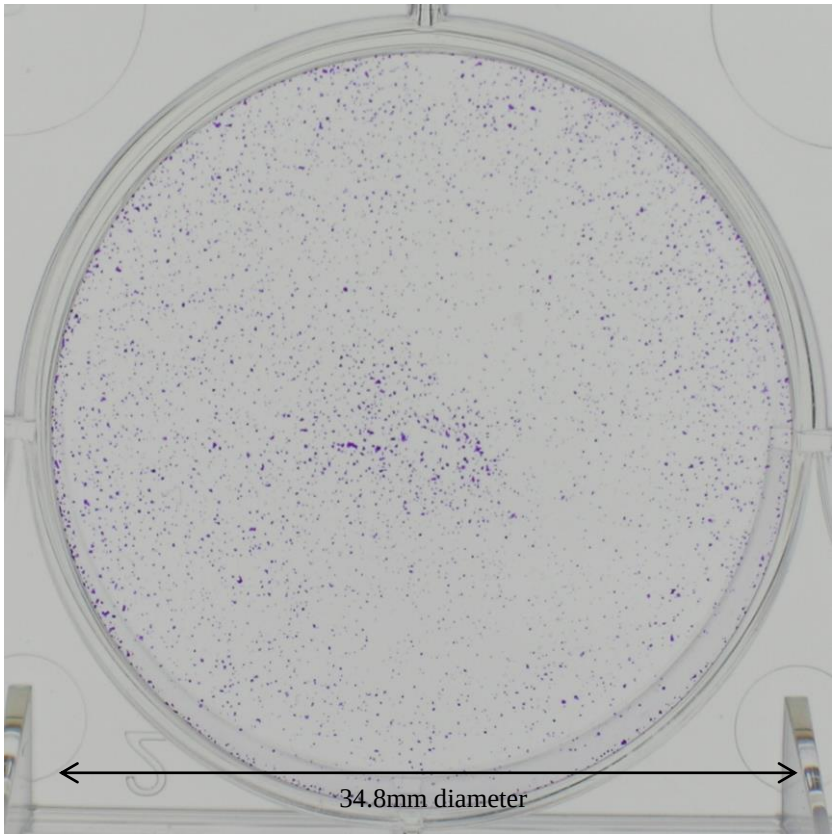

Figure 3 BT474 colonies resulting from an initial seeding density of 14,000 cells per well. The photograph shows a base view of a well of a 6 well-plate with a 34.8 mm diameter and approximate growth area of 9.5 cm^2. Cells were fixed with acetic acid/methanol (1:3) and stained with aqueous 0.5% crystal violet (CV) 25% methanol solution.

The point-like appearance of the colonies was consistent with the tendency of the BT474 cells to stack or layer upon each other rather than spread over the flask growth surface during propagation.

4.5.2 Development of MCF7 and BT474 colony formation assays

4.5.2.1 MCF7 cell-line colony counting with and without methanol inhibitor

Colony counting of the whole well surface was attempted but the diffuse colonies and overlap made the task of identifying individual colonies difficult which gave a highly variable and non-reproducible count. Colony counts resulting from a 300 cells per well seeding may vary, for example, between 113 and 154 units. Figure 4 shows the colonies resulting from a 300 cells per well seeding using methanol as a test inhibitor.

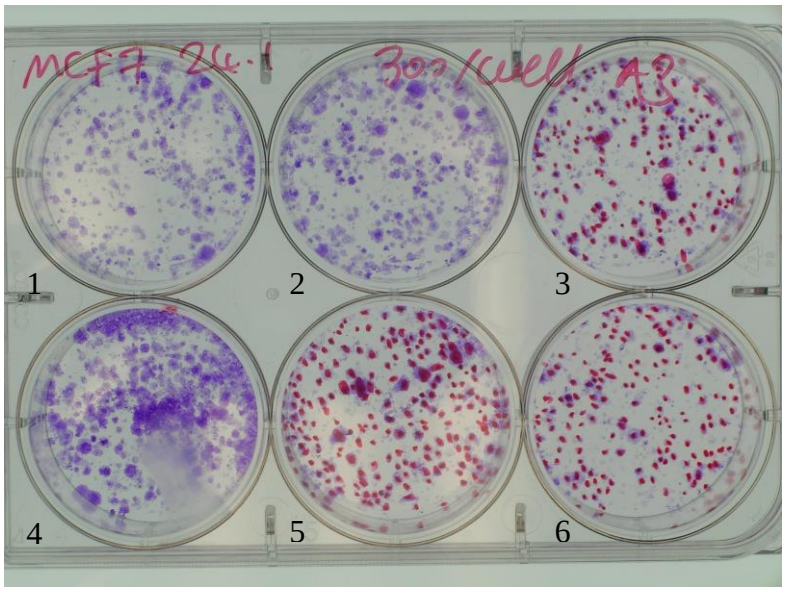

Figure 4 MCF7 colonies resulting from an initial seeding density of 300 cells per well. The photograph shows a top view of a 6 well-plate in the process of colony counting aided by pen marking. The wells have a 34.8 mm diameter and approximate growth area of 9.5 cm^2. Cells were fixed with acetic acid/methanol (1:3) and stained with aqueous 0.5% crystal violet (CV) 25% methanol solution. Well 1: 1.5% methanol, well 2: 2.0% methanol, well 3: 2.0% methanol, well 4: 2.0% methanol, well 5: no methanol and well 6: no methanol.

The selection of a pre-defined randomised count area was also investigated but proved ineffective due to many wells having an uneven distribution of colonies. Nevertheless, the development of the colony formation work was continued by progressing to the BT474 cell-line.

4.5.2.2 BT474 cell-line colony counting following exposure to Trastuzumab and placebo respectively

BT474 is the target cell line which will allow the testing of Trastuzumab. Initially seeding experiments were carried out to determine if consistency of cell number could be achieved. This stage is essential before progressing to experiments assessing the action of inhibitors. Success of seeding was determined both quantitatively and qualitatively by releasing and counting cells using a haemocytometer and examining the resultant fixed and stained colonies respectively. The fixing and staining process allows unsatisfactory seeded wells to be rejected before attempting to count colonies or further analysis. Additionally a qualitative correlation of the degree of final colony growth with the level of initial seeding can be observed. Typical repeated cell counts for a single well were $199x10^4$, $200x10^4$, $180x10^4$, and $197x10^4$ cells per 20 µl volume for one seeding experiment (mean count 194 and standard deviation 8). In another experiment using a different flask the count was $209x10^4$, $207x10^4$, $198x10^4$, $207x10^4$ and $151x10^4$ cells per 20 µl volume (mean count 194 and standard deviation 22). The last count was low due to intentionally allowing settling to show the importance of mixing to the procedure. Both experiments were at a 100,000 seeding and counted after 14 days growth. Generally cell counting with the aid of a haemocytometer was acceptable for assessing development of seeding technique but would be impracticable for the determination of viability for the shelf-life study.

Colony counting of the whole well surface was attempted for seeding experiments and experiments using Trastuzumab and methanol as inhibitors but was found to be impracticable due to the large numbers involved and overlapping of colonies. The use of user-defined random count areas was also investigated (Wu et al. 2002; Hermanto et al. 2001). This was unsuccessful showing high variability. A variation of this method involved counting in a field of view defined by a microscopic image

(representing an area of ~1 mm area) of the well surface but showed limited success. This method was applied to the assessment of the activity of Trastuzumab (figure 5).

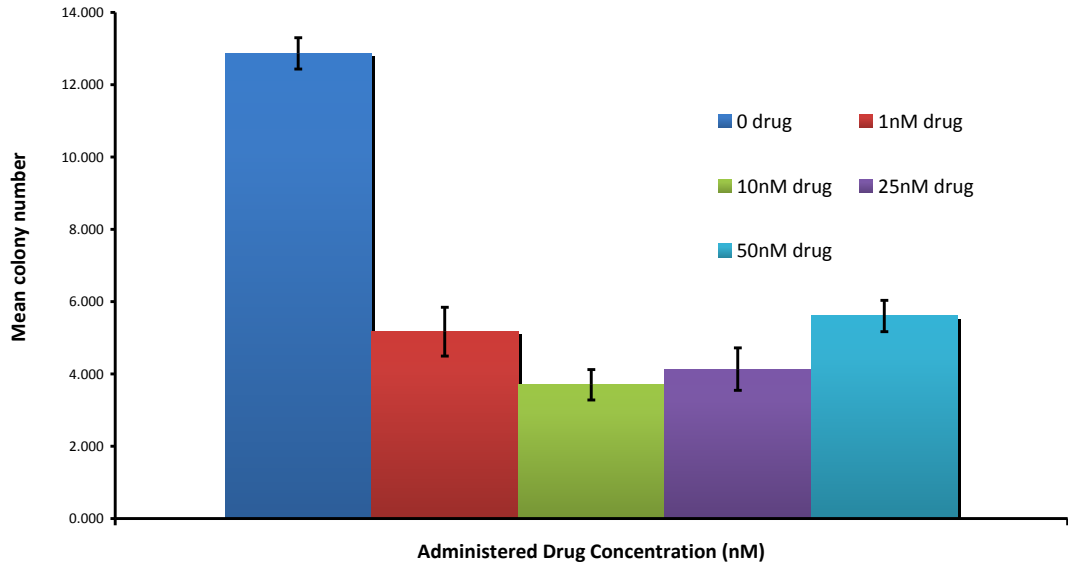

Figure 5 Colony formation assay bar chart showing action of Trastuzumab on colony count as a function of well drug concentrations in a 6 well-plate format. Control (12) and inhibitor (12) wells distributed over 4 plates. Standard error of replicate analysis of random count areas is shown with inferential error bars (replicate control (no drug) random area counts = 120 and replicate drug addition random area counts = 30 for each well drug concentration).

Difference between drug and no drug was shown to be highly significant ($p < 0.001$) by using a t-Student test with a significance threshold of $p < 0.05$, although control data showed variability giving a mean and standard deviation of 13 +/- 5 respectively. However, there is no distinction between concentrations of drug. The colony count data for the 1 nM, 10 nM, 25 nM and 50 nM concentrations gave a mean and standard deviation of 5 +/- 4, 4 +/- 2, 4 +/- 3 and 6 +/-3 respectively. Moreover, a weak negative Pearson's correlation coefficient (r) was shown ($r = -0.37$). This would suggest that relatively small changes in drug concentration anticipated during storage

would not be detected. Another approach attempted was to select evenly distributed areas for counting purposes but this approach also showed a high degree of innate subjectivity and inconsistency.

Automated colony counting using programs such as Image J (V1.46i) and Cell profiler (V2.0) were also considered. A preliminary investigation on developing these platforms adequately for colony counting was time consuming and appeared, at the stage of development, not very promising. Furthermore, due to the large number of plates, counting and collating the colony formation data would be prohibitively time consuming even for a relatively small sample of plates or even wells. Attention was directed to determining viability using colorimetric methods.

4.5.3 BT474 viability assessment using colorimetric methods

Viability or counting cells using a colorimetric method removes the subjectivity encountered with the colony formation assay. Additionally, instrumentation and system software provide a manageable means to assess a large number of samples in terms of data collection, processing and analysis. Two approaches have been investigated. The first approach investigated was to release or re-solubilise the crystal violet (CV) from the fixed and stained colonies generated for the colony formation assay and make an absorbance measurement (Eichhorn et al. 2008). The second method utilised a commercial chromogenic enzyme reporter system which transforms a substrate to a formazan dye with its absorbance measured at 450 nm. The colorimetric determination of released stain was explored in both a 6 well and 96 well formats whereas the commercial enzyme reporter was only used for the 96 well microplates. This was due to the substrate reagent burden in the 6 well format and consequential cost incurred. The commercial reporter system selected was the Cell Counting Kit CCK8 (Sigma Aldrich) which is from a range of commercially available colorimetric-based assays.

The concentration of the formazan dye and CV is normally directly proportional to the number of living cells. This condition is met if the cells are seeded consistently

and have uniform growth. Thus the first stage in method development requires the optimisation of a calibration protocol of adequate precision and sensitivity**.**

4.5.3.1 Comparison of Crystal violet (CV) stain release method and CCK8 assay

The calibration curves of absorbance as a function of cell number for CV and CCK8 assay are presented from initial investigations (figure 6). A linear calibration infers that the cell numbers after the growth period relate to a consistent initial seeding and supports the view that the cell population as undergone uniform cell growth between wells for the CV (R^2 = 0.9082) and CCK8 (R^2 = 0.9854) experiments. The CCK8 assay is performed first on the cells then they are fixed and stained. Following this the CV was released and absorbance measured. Thus the experiment is performed on the same population of cells and consequently the difference in the two methods may be exposed. One evident distinction between the two plots is the slope or gradient. The slope is indicative of the sensitivity of the calibration and it can be clearly seen that the CV assay has little sensitivity over the dynamic seeding range.

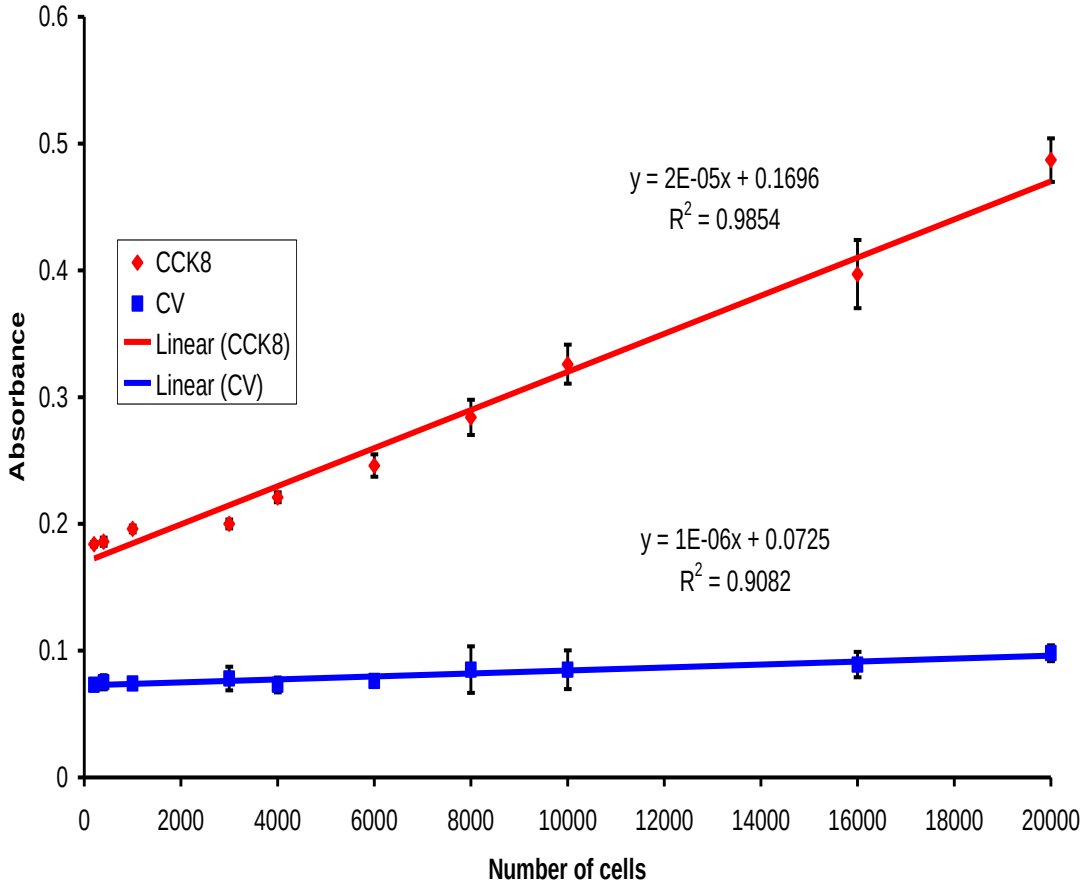

Figure 6 Cell seeding calibration in 96 well-plate format for re-solubilised CV stain and CCK8 formazan dye absorbance at 540 nm and 450 nm respectively as a function of cell number. Standard error of replicate analysis of wells is shown with inferential error bars (replicate wells = 8).

Standard error of replicate wells for each calibration is shown with inferential error bars (replicate wells = 8 for each cell number). The inferential error bars further support an acceptable precision or consistency in the initial seeding and a subsequent uniform growth rate in each well. The R^2 values obtained from the calibration exercise appear to be acceptable but are these values sufficiently close to unity to assert a linear relationship between cell number and absorbance within a reasonable level of uncertainty? R^2 values above 0.995 or 0.999 have been reported (Harris 2003) as a suitable measure for the determination of linearity for most purposes but to represent a truly linear fit for a data series the R^2 value must be very close to unity (Harris

2003). An alternative and superior marker of linearity is a plot of the vertical deviation of the experimental data points from those calculated from the equation for the least-squares line (Harris 2003).

In support of this view to assess linearity of the calibration more vigorously the ICH Harmonised Tripartite Guideline Validation of Analytical Procedures suggests data from a regression line may provide a mathematical estimation of linearity and with an analysis of the deviation of the actual data points from the regression line will be useful in evaluating linearity (ICH 2005). Vertical deviation for each data point was obtained from the difference in observed absorbance from the instrument response or readout and the absorbance calculated from the computed least-squares line ($y_{observed} - y_{calculated}$). The calculation of y for each x value of cell density involves using the linear regression equation obtained from the output from the Microsoft EXCEL (2003) regression analysis function.

The cell number for each experimental data point was substituted for x in equation (1) to obtain each value of y for the straight lines of each calibration:

$$y = mx + c \qquad \text{equation (1)}$$

Crystal Violet regression analysis equation $y = 1.0E\text{-}06x + 0.0725$

CCK8 regression analysis equation $y = 2E\text{-}05x + 0.1696$

Where y = absorbance, m = slope and c = intercept on y axis, x = cell number, slope m from regression analysis of Crystal Violet linear plot = 1.0E-06 and slope m from regression analysis of CCK8 linear plot = 2E-05.

Tables 1 and 2 show the vertical deviations for each data point of the crystal violet and CCK8 calibration respectively. This result is then plotted as a function of cell number to facilitate data judgement (figure 7).

Cell number	**$y_{observed}$**	**$y_{calculated}$**	**Vertical deviation ($y_{observed} - y_{calculated}$)**
20000	0.098	9.25E-02	0.0055
16000	0.089	8.85E-02	0.0005
10000	0.085	8.25E-02	0.0025
8000	0.085	8.05E-02	0.0045
6000	0.076	7.85E-02	-0.0025
4000	0.073	7.65E-02	-0.0035
3000	0.078	7.55E-02	0.0025
1000	0.074	7.35E-02	0.0005
400	0.075	7.29E-02	0.0021
200	0.073	7.27E-02	0.0003

Table 1 Showing results of the vertical deviation calculation for each cell number for crystal violet calibration. Values of vertical deviation are small in magnitude indicating closeness of experimentally determined y values compared to the y values calculated from that obtained from the linear regression analysis.

Cell number	$y_{observed}$	$y_{calculated}$	Vertical deviation ($y_{observed} - y_{calculated}$)
20000	0.487	0.5696	-0.0826
16000	0.397	0.4896	-0.0926
10000	0.326	0.3696	-0.0436
8000	0.284	0.3296	-0.0456
6000	0.246	0.2896	-0.0436
4000	0.221	0.2496	-0.0286
3000	0.2	0.2296	-0.0296
1000	0.196	0.1896	0.0064
400	0.186	0.1776	0.0084
200	0.184	0.1736	0.0104

Table 2 Showing results of the vertical deviation calculation for each cell number for CCK8 calibration. Values of vertical deviation are small in magnitude indicating closeness of experimentally determined values of y compared to the y values calculated from that obtained from the linear regression analysis.

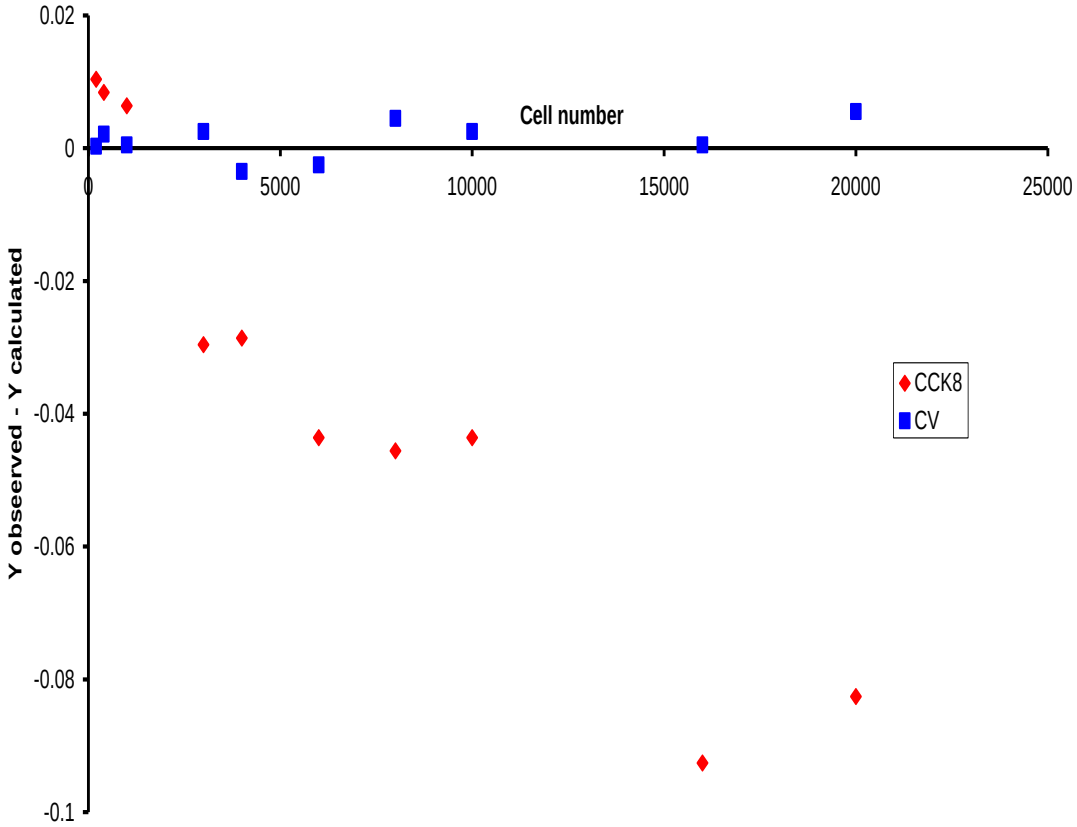

Figure 7 Plot of vertical deviation ($y_{observed} - y_{calculated}$) of observed y data point values from calculated y values of the least-squares line y = m x + c. Data points represent the difference between experimental and calculated values of absorbance for each cell number for the CCK8 and CV calibration.

Visualisation of the deviation of the observed data from data calculated from the regression analysis (figure 5) facilitates the identification of systematic differences, which may be present in the data set, and therefore establish if there is any significant departure from linearity. Nonlinearity is detected if the vertical deviation of data points form a pattern, i.e., clustering of negative or positive points in different areas. In contrast linearity is evidenced by a random spread of points around the datum line of zero deviation.

Values of vertical deviation for the CV calibration are small in magnitude indicating closeness of experimentally determined values of y compared to the y values calculated from that obtained from the linear regression analysis. However, the vertical deviations tend to positive values, i.e., y observed is larger than predicted. Nevertheless the data is relatively centred on the datum. This result is consistent with the apparent low sensitivity of the CV system. In contrast on examination of the vertical deviation plot for the CCK8 calibration a pattern is evident. The data set tends to increasingly negative value with increase in cell number, i.e., y observed is smaller than predicted. This represents a deviation from linearity albeit of low magnitude and appears at first not consistent with the R^2 value obtained for CCK8 of 0.9854 compared to that for CV of 0.9082. This difference can be explained by the sensitivity or slope of the each assay. The CCK8 plot shows an absorbance difference over the calibration range of 0.303 units. This gives more capacity for systematic or random error to manifest itself. Conversely, the small slope of the CV calibration gives an absorbance difference of 0.025 units over the seeding range and therefore any error may be masked.

The CV assay with its low sensitivity appeared to offer little scope for development into an acceptable assay. The CCK8 assay was selected for further development.

4.5.3.2 Development of CCK8 assay

Two parameters were identified to be developed and optimised; a suitable seeding density for testing the Trastuzumab and improvement of instrument response or absorbance. Although it must be considered that an absorbance approaching the limit of the instrument represents very little light entering the detector. This is the case with absorbance readings at the top of the instrument working range (~3 units) and consequently this would increase measurement error.

Considering the working range of the instrument a series of seeding densities were investigated adding the CCK8 reagent immediately after seeding. This identified a seeding of 10,000 cells per well as producing an absorbance of 1.8 read at 20 hours

comparable to early seeding calibration work. Figure 8 shows the relationship between absorbance and reading time for two seeding plates from a single cell stock. At 20 hours the absorbance is starting to level out. The two seeding experiments show low variation.

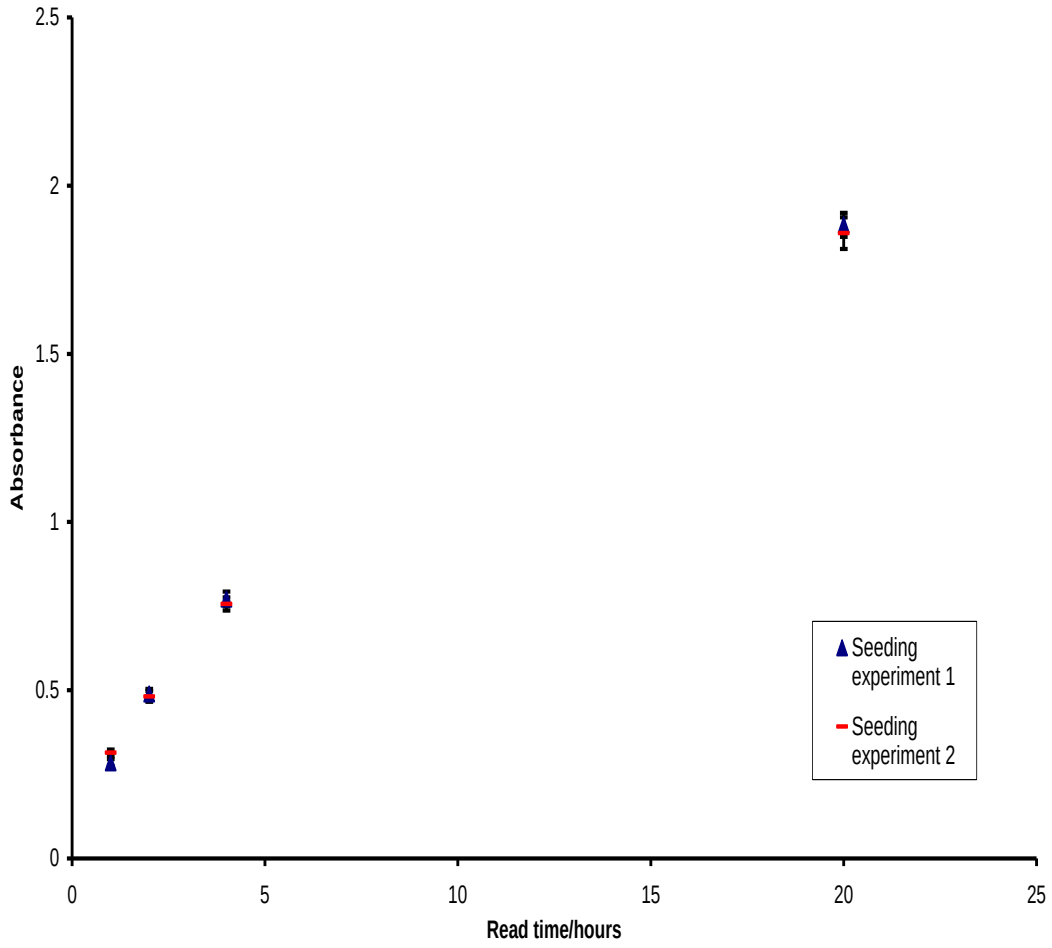

Figure 8 Graph showing absorbance as a function of read time. Seeding density 10,000 cells per well. Standard error of replicate analysis of wells is shown with inferential error bars (replicate wells = 16).

The absorbance values obtained from these seeding experiments sit well inside the working range of the instrument. Therefore there was sufficient potential capacity to increase the instrument response.

The concentration of the formazan dye generated in the assay is related to the ability of the cells to turn over the substrate and the number of cells present. Therefore if the CCK8 is added after the cells have multiplied an increase in absorbance would be expected. This was found to be the case as after a 4 day growth period the absorbance had reached a value of 3.32 and 3.53 for two seeding experiments for the 20 hour read (figure 9). This amplification step was subsequently used for all CCK8 calibrations and assays. This enabled the seeding range of the calibration to use the maximum working absorbance. In addition the projected cell number from the initial seeding for an assay maximises the sensitivity and decreases variation by utilising the absorbance working range available. Furthermore, the degree of difference in absorbance between killed cells and those proliferating freely will become increasingly pronounced with growth time.

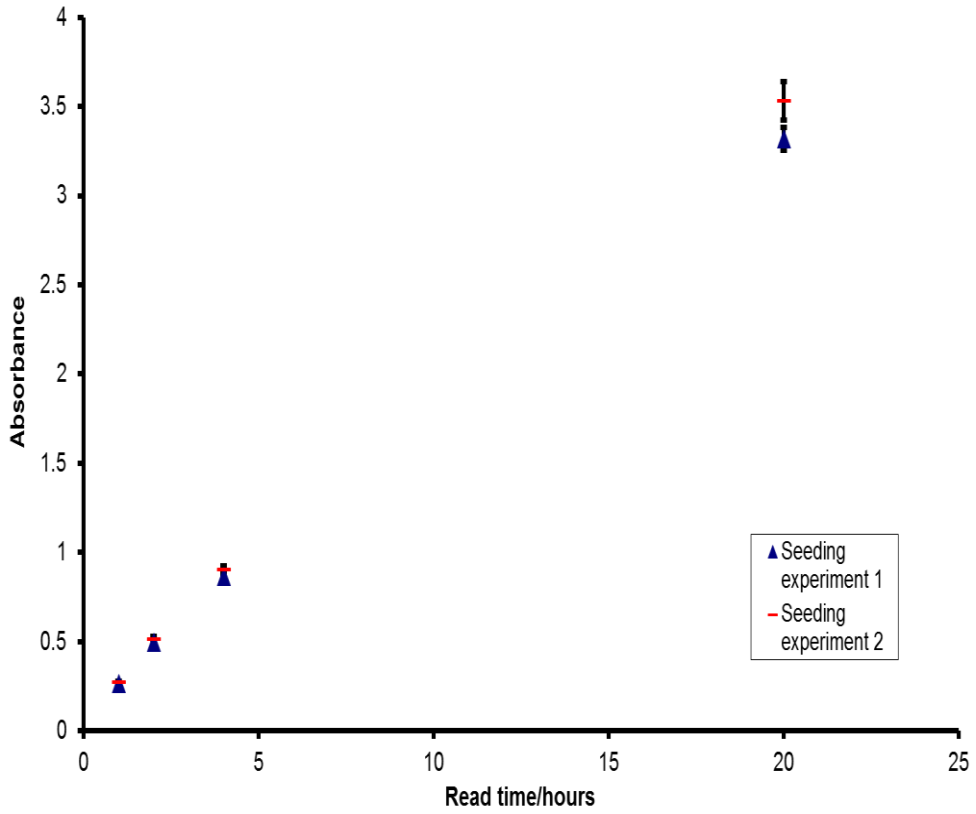

Figure 9 Graph showing absorbance as a function of read time after a 4 day growth period. Other details as for figure 8.

4.5.3.3 Optimised CCK8 assay

Following the development work seeding experiments were performed to assess the improvements in the assay. The calibration curve of absorbance as a function of cell number was linear (R^2 = 0.997 6) for both micro-plates (figure 10). The agreement of R^2 values shows a high degree of inter-plate precision. Furthermore, the calibration set infer that the cell numbers after the growth period relate to a consistent initial seeding and supports the view that the cell population as undergone uniform cell growth between wells and plates.

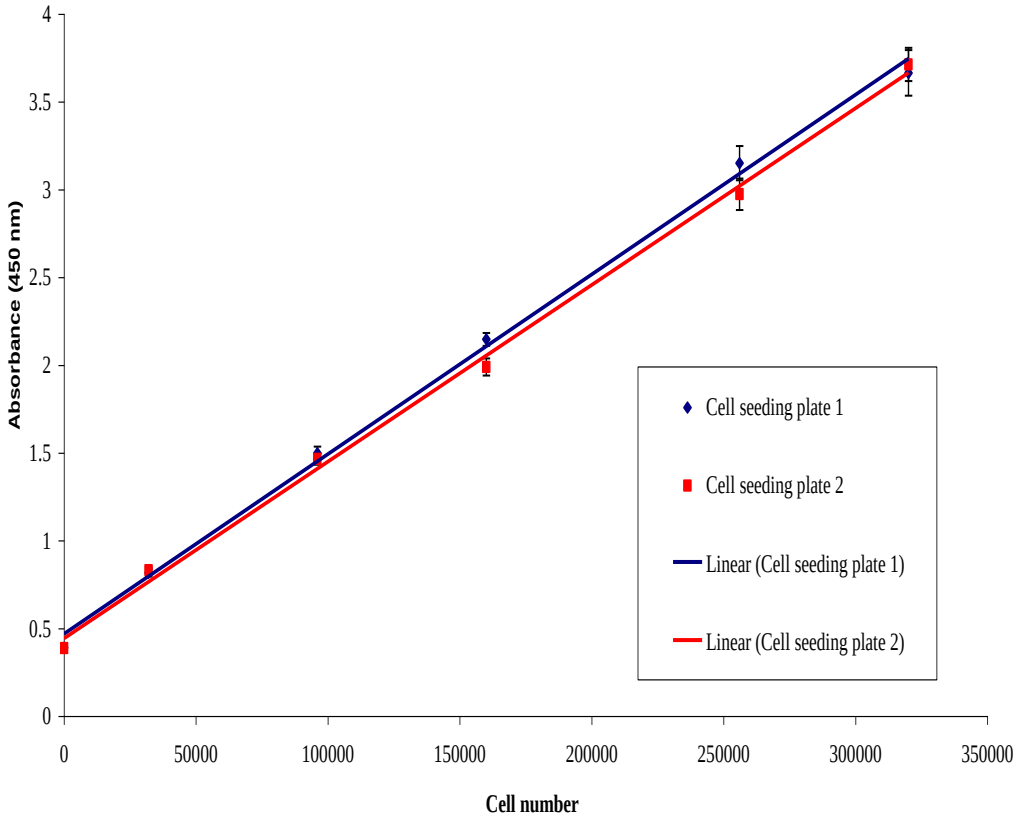

Figure 10 Representative biological assay calibration plot showing the relationship between projected BT474 cell number after a 4 day uninhibited growth period and absorbance at 450 nm. Duplicate calibration plots are shown originating from a single cell culture stock solution (number of independently performed experiments: n = 1). Standard error of replicate analysis of wells is shown with inferential error bars (replicate wells = 16).

Analysis of vertical deviation of the y data for the calibration set is shown in tables 3 and 4. The data presented is also shown graphically in figure 11.

Cell number	**$y_{observed}$**	**$y_{calculated}$**	**Vertical deviation ($y_{observed} - y_{calculated}$)**
0	0.391625	0.4714	-0.07978
32000	0.818	0.799027	0.018973
96000	1.499375	1.454281	0.045094
160000	2.147875	2.109535	0.03834
256000	3.151438	3.092416	0.059021
320000	3.665727	3.74767	-0.08194

Table 3 Showing results of the vertical deviation calculation for each cell number for calibration 1. Values of vertical deviation are small in magnitude indicating closeness of experimentally determined values of y compared to the y values calculated from that obtained from the linear regression analysis.

Cell number	**$y_{observed}$**	**$y_{calculated}$**	**Vertical deviation ($y_{observed} - y_{calculated}$)**
0	0.38825	0.4443	-0.05605
32000	0.832438	0.766545	0.065893
96000	1.466375	1.411034	0.055341
160000	1.990438	2.055524	-0.06509
256000	2.974563	3.022258	-0.0477
320000	3.714182	3.666748	0.047434

Table 4 Showing results of the vertical deviation calculation for each cell number for the calibration 2. Values of vertical deviation are small in magnitude indicating closeness of experimentally determined values of y compared to the y values calculated from that obtained from the linear regression analysis.

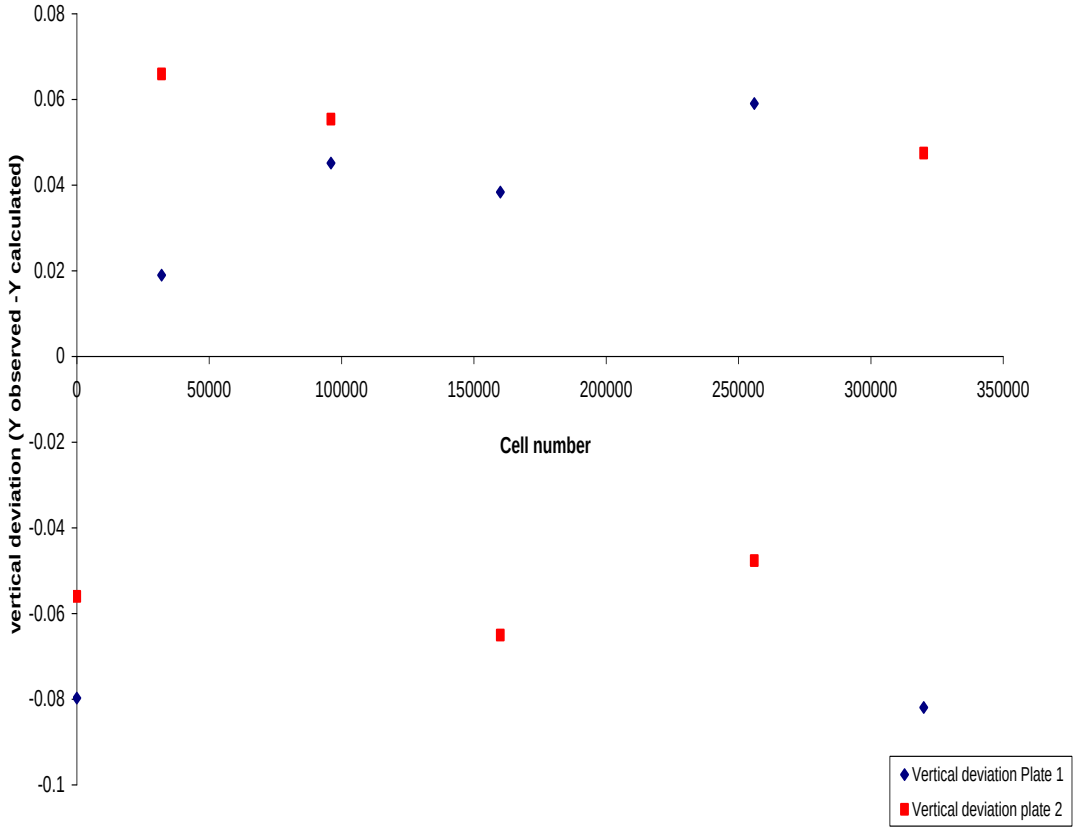

Figure 11 Plot of vertical deviation ($y_{observed} - y_{calculated}$) of observed y data point values from calculated values of y of the least-squares line $y = m x + c$. Data points represent the difference between experimental and calculated values of absorbance.

Vertical deviations from plate 1 data have a slight positive bias which is almost mirrored by the negative deviations for plate 2 and covers the working range of the assay (~90% to ~50% viable cells). Looking at the vertical deviations collectively for the complete calibration set and considering the magnitude of the individual deviations it can be concluded that the calibration is adequately linear. Moreover the distribution is indicative of the high degree of sensitivity of the assay.

4.5.3.4 The stability indicating capability of CCK8 assay

A colony formation assay was performed with stressed and not stressed Trastuzumab (0.1 mg/mL) to determine an appropriate dose for the assay. Stressed and not stressed samples were diluted to 0.5, 1, 2 and 100 nM and tested by a colony formation assay. After fixing and staining the colonies showed no apparent difference in colony size between stressed and not stressed samples for the 1, 2 and 100 nM concentrations. At these concentrations the quantity of active drug may have saturated the HER2 receptors (Watts 2012). In contrast the 0.5 nM concentration gave an observable decrease in colony size. This identified a well dosing drug concentration of 0.5 nM to be optimal; showing the greatest differentiation in colony size between stressed and unstressed drug at a stressing time of 15 minutes in a water bath heated to 75 ^{o}C. Therefore the optimal dose should allow loss of activity to be detectable and measurable with the CCK8 assay.

Heating for 20 minutes decreased the potency to approximately 25% of fresh Trastuzumab as determined by the CCK8 assay. This work is expanded on in Chapter 5: forced degradation studies of Trastuzumab.

Sources of Error

Cell counting is an important possible source of error and will propagate through subsequent assay steps. This may occur if the sample from the flask is unrepresentative of the cell population concentration and could be due to clumping of cells or insufficient mixing. The use of a haemocytometer may add further errors. The total volume of the counting chamber should represent a random sample. This is only the case if the single cells are in suspension. The error contributed by pipetting and sampling can be as high as 55% and for chamber and counting error 45% (Freund et al. 1964). This was for the same person counting duplicate plates of sperm cells. Additionally, pipetting may cause cell damage and impact on viability. This will decrease the expected cell number. Frothing of media can be a problem when pipetting, giving liquid and cell transfer error. These errors will decrease assay performance.

4.6 CONCLUSIONS

Following assessment the CCK8 system was adopted as the best method to determine viability within a 96 micro-plate format due to its sensitivity and repeatability as shown in the seeding calibration data set (figure 8)

CHAPTER 5

5 FORCED DEGRADATION STUDIES OF TRASTUZUMAB

5.1 INTRODUCTION

A forced degradation study normally entails subjecting a drug (drug substance, product or placebo) to extreme chemical and environmental conditions to determine the extent of degradation, to try to identify decomposition products, mechanism or mechanisms involved, and thus establish a stability indicating profile and fitness of the analytical method employed (Blessy et al. 2014). The degradation species formed in a forced degradation experiment are referred to as potential breakdown products which could be present under normal conditions but they may or may not represent the true degradation products and degradation mechanism encountered under different storage conditions over time (Blessy et al. 2014).

One of the main approaches to degradation studies is to thermally stress the product by heating to accelerate decomposition (European Medicines Agency 2003). However, whilst this produces breakdown products in distinct chemical entities with small molecule drugs, for proteins this is inappropriate and will lead to fully denatured protein precipitate (Barnes 2012). This approach is a legacy from conventional chemical drug stability testing (European Medicines Agency 2003). The requirement to perform this test more reflects the lack of any guidance for testing stability of biological drugs which is yet to be addressed by the regulatory authorities than a scientific basis for this test (Allwood & Wilkinson 2013). Shown below is an overview of conditions which have been used for forced degradation of traditional drug products and drug substances (figure 1).

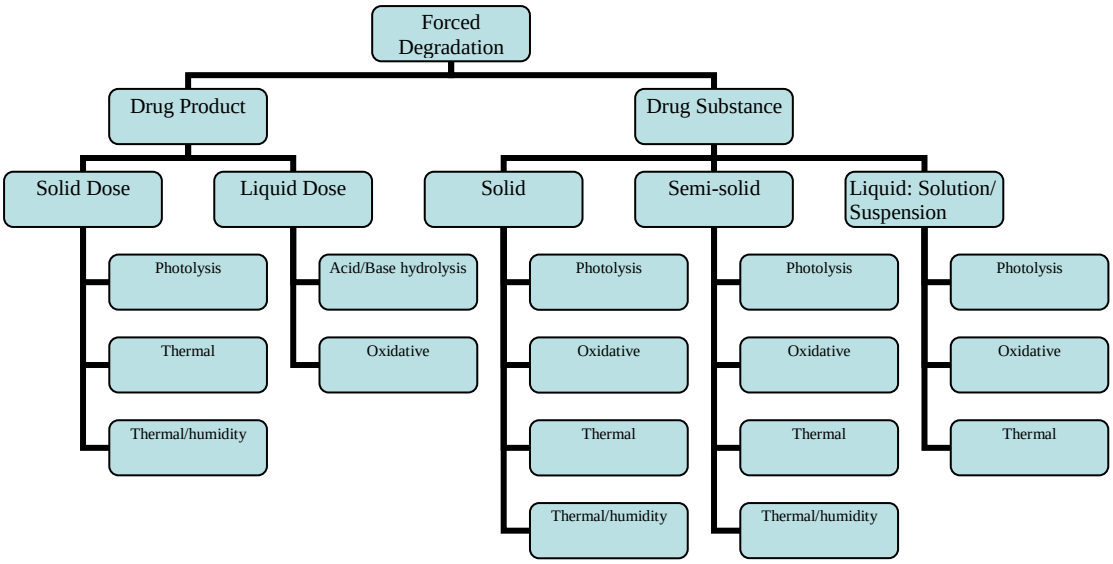

Figure 1: Forced degradation conditions used to test drug product and drug substance. Chart adapted from a Power Point presentation by Rhami Dharati entitled Forced Degradation concerning regulatory affairs (2007).

In addition, a forced degradation study may validate the analytical procedures applied to the in-use shelf-life extension studies and inform on product integrity and degradation mechanism following accidental exposure to detrimental conditions; such as temperature excursions during transportation or storage (European Medicines Agency 2003). Current regulatory documents concerning forced degradation offer general guidance and are aimed at the development and manufacture of new drugs (European Medicines Agency 2003). Furthermore, the Tripartite Guideline provides a basis for condition selection but may not be appropriate for biologics (European Medicines Agency 2003; Allwood & Wilkinson 2013). The ICH Topic Q5C Biological Products document states that study conditions selection should be on a case-by-case basis (European Medicines Agency 2006).

However, it has been stated that stability testing of a new drug should include the effect of temperature, humidity, oxidation, photolysis and pH dependant hydrolysis depending on the drug product and drug substance (European Medicines Agency 2003). Taking this information into account an approach to a proposed forced degradation study can be developed that is sufficiently appropriate to clinically

relevant conditions and appropriate for the Trastuzumab shelf-life extension study. The experimental approach adopted and its rationale is presented in the following section.

The potential stresses likely to be encountered within a clinical setting are associated with mishandling of the drug during reconstitution, storage and administration (Liu et al. 2011). The stresses encountered represent a complex combination of shear and interfacial stresses involved during dissolution, mixing and transfer to infusion bag (Pabari et al. 2013). The drug may also experience temperature excursions during transportation or if inadvertently left out in the ward or due to refrigerator malfunction in the pharmacy (Bardin et al. 2011). Therefore these stresses can be broadly classified into mechanical and thermal stresses respectively.

Thermal stresses are more likely to be encountered as the formulation is relatively sufficiently robust to the range of handling by trained staff (Bardin et al. 2011). This view is consistent with the recommendations by the ICH to include effects of temperature during the development and manufacture of new drugs (European Medicines Agency 2003). The models selected to represent thermal stresses were heating in a water bath at 75^{o}C for a range of times (5, 10, 15 and 20 minutes) and storage in ambient conditions for 4 days. The former conditions are clearly not particularly realistic but do give the opportunity to investigate degradation products which may have a mechanistically limited relationship to that of an aged sample within an in-use temperature study. Furthermore, the range of times selected for thermal stressing will affect the degree of unfolding and therefore form a series of aggregation profiles which may provide mechanistic information.

In contrast, the latter experimental conditions present a more realistic scenario where a 0.1 mg/ml sample was stored for 4 days in the laboratory approximate the conditions encountered on a hospital ward. Furthermore, the low concentration, which is not clinically relevant, may accelerate any degradation under these conditions and be more representative of the appropriate mechanism encountered during an accidental temperature excursion (Barnes 2012). The excipients will be at a relatively low concentration and will be less effective in stabilising the proteins' native state by preferential hydration through surface tension effects (Rowe 2001). This choice of

infusion concentration is supported by the reported stability of a 0.4 mg/mL concentration infusion after exposure to 170^{o}C by Pabari et al. (2011). Subsequently, it was reported by Paul et al. (2013) that Trastuzumab infusion stability was retained until degradation was detected after 2 years of storage at 20 ^{o}C. Additionally, the authors stated that 96 hours at 60 ^{o}C was required to allow the detection of instability. The infusion concentrations investigated were 0.8 mg/mL and 2.4 mg/mL. Therefore the 0.1 mg/mL infusion may be more susceptible to degradation than the higher concentration infusions.

It is expected that heat stressing at 75 ^{o}C, due to the experimental temperature being in the region of the transition temperature (T_m) of the unfolding reaction or melting point of the protein (Matheus et al. 2006), will involve initiation of aggregation by an atypical increase in the population of less stable conformations leading to initial intermediates in a 50% unfolded state as compared to normal storage temperature (Wang 1999). The T_m of a protein is indicative of its thermal resistance (Wang 1999; Wang et al. 2010). However, there is no specific relationship between T_m and protein stability as determined thermodynamically by the free energy changes between folded and unfolded states (Dill et al. 1989; Wang 1999).

Unfolded species may recruit native monomers and possibly propagate aggregation in a similar fashion to that encountered during aging under normal kinetically controlled conditions considerably below the T_m (Vermeer & Norde 2000). This may be even more the case when the stress is removed and when the aggregation process is likely to continue after critical nucleation driven by mass action involving the native antibody population (Vermeer & Norde 2000; Wang et al. 2010). Therefore SE-LC characterisation of the aggregate species within the sample immediately after stressing and after a period of storage under conventional storage conditions along with ambient exposure may give insight into any post stressing aggregation and associated mechanism or mechanisms encountered after an accidental temperature excursion.

5.2 Materials and Methods

Forced degradation at elevated temperature

Initial experiments involved exposing Trastuzumab at a concentration of 0.1 mg/ml to heat in a water bath for 5, 10 and 15 minutes at 75 ^{o}C to 79 ^{o}C in the region of the transition temperature (T_m) of the unfolding reaction or melting point of the protein. The stressed sample and unstressed control were diluted in the range of 0.5, 1, 2 and 100 nM mirroring the concentrations used for the CCK8 cellular assay in the shelf-life study. A colony formation assay using the standard seeding density of 10 000 cells/well was performed to assess changes in proliferation and to identify the optimum drug concentration and stressing time for subsequent CCK8 proliferation assay. Degradation was confirmed by size exclusion chromatography showing an increase in higher order aggregates and concomitant decrease in monomer or active drug molecule as compared to an unstressed control sample. The wavelength of 220 nm was selected for optimum sensitivity in measuring the changes in low abundance products. Measurements were also made at 280 nm to confirm the products were protein in origin. Degradation was compared for each stress time point and a comparison made between chromatograms of stressed Trastuzumab which was analysed immediately with stressed Trastuzumab which had been stored under refrigeration (5-8 ^{o}C) for 4 days before analysis by size exclusion chromatography.

The thermal degradation experiment was repeated using the optimum conditions and with an increased heating time of 20 minutes to further ensure sufficient degradation. A CCK8 assay was performed using the standard seeding density of 10,000 cells per well in a 96 well micro-plate. Replicates for drug treated wells were 28 wells and 32 replicate for no-drug addition wells. The absorbance was read at 1 hour 2 hours and 4 hours incubation following addition of CCK8 reagent. A seeding calibration was performed using a series of cell densities; 100,000, 80,000, 50,000, 30,000, 10,000 and 0 cells per well with 16 replicates per cell density. The highest useable absorbance readings for the calibration of cell number as a function of absorbance at 450 nm was obtained after 2 hour incubation. After this time absorbance is at the limit of the instrument and for the higher seeding densities at the top of the calibration

range absorbance was not measurable and gave an overflow result rather than a numerical readout of absorbance.

Degradation under ambient conditions

A 0.1 mg/mL sample of Trastuzumab was stored, maintaining aseptic conditions, for 4 days under ambient conditions and degradation was assessed by size exclusion liquid chromatography (SE-LC).

5.2.1 Size exclusion liquid chromatography (SE-LC)

Size exclusion liquid chromatography was performed using a Dionex MAb Pac SEC1^{TM} (Dionex; a Fisher Scientific company) size exclusion column with a packing particle size of 5 μm with a 300 Angstrom (0.03 μm) pore size. The column is specifically designed for the quantitative separation of monoclonal antibodies and the aggregates. A Shimadzu LC-10 system operating a Lab Solutions Chromatography system with Windows XP was used to perform the analysis. The mobile phase was 300 mM sodium chloride in a 50 mM disodium hydrogen phosphate adjusted to pH 6.8. The elution rate was 0.2 mL/minute with dual wave length UV detection at 280 nm and 220 nm. Analysis was performed in triplicate.

5.2.2 Attenuated Total Reflectance Fourier Transform Infra-red (ATR-FT-IR) Spectroscopy and protein secondary structure determination

Spectra were acquired for stressed and standard Trastuzumab. Changes in the Amide I band, which is indicative of changes in secondary structure of the protein, may be detected by amide I band spectra overlay of each sample. Acquisition parameters were as follows; 256 scans for each spectrum was found to give good spectra at a standard resolution of 4 cm^{-1} and scan range of 4,000 cm^{-1} to 450 cm^{-1} wave numbers. Water vapour background subtraction and ATR correction were carried out by the on-board Spectrum One functions. The sample (20 μL) was introduced into the recess

within which the germanium crystal is housed ensuring full surface coverage of crystal. The crystal was cleaned between samples with ten washings of demineralised water and with three washings of HPLC grade acetonitrile (Fisher Scientific). Blank spectra were collected to show that the crystal was clean prior to the sample being loaded. Spectra were converted and exported as ASCII files for further processing in Microsoft EXCEL (2003). The corresponding blank spectra were subtracted from the sample spectra and normalised to 1,850 cm^{-1}; the baseline wave number adjacent to the amide I envelope and graphed as Microsoft EXCEL (2003) charts. This enabled the direct comparison of the amide I region by spectrum overlay of all sample spectra.

5.3 Results and Discussion

Thermal degradation

<u>Biological Activity of Trastuzumab reconstituted and diluted to 0.1 mg/mL</u>

The colony formation assay gave an observable decrease in colony formation efficiency and identified a well dosing drug concentration of 0.5 nM to be optimal; showing the greatest differentiation in colony size between stressed and unstressed Trastuzumab at a stressing time of over 15 minutes in a water bath heated to 75 ^{o}C. Changes in colony size between stressed and unstressed drug were noticeable by the naked eye but can be seen more clearly by microscopic examination (figure 2).

Figure 1A shows increased colony size of the BT474 cell line indicating increased cellular proliferation when exposed to thermally stressed Trastuzumab as compared to figure 1B showing the colony formation resulting from treatment with the freshly prepared Trastuzumab which shows smaller colonies and therefore decreased proliferation. This observation is consistent with Trastuzumab being fully active and that after heating to 75 ^{o}C for over 15 minutes the efficacy has decreased as compared to the untreated control.

(A)

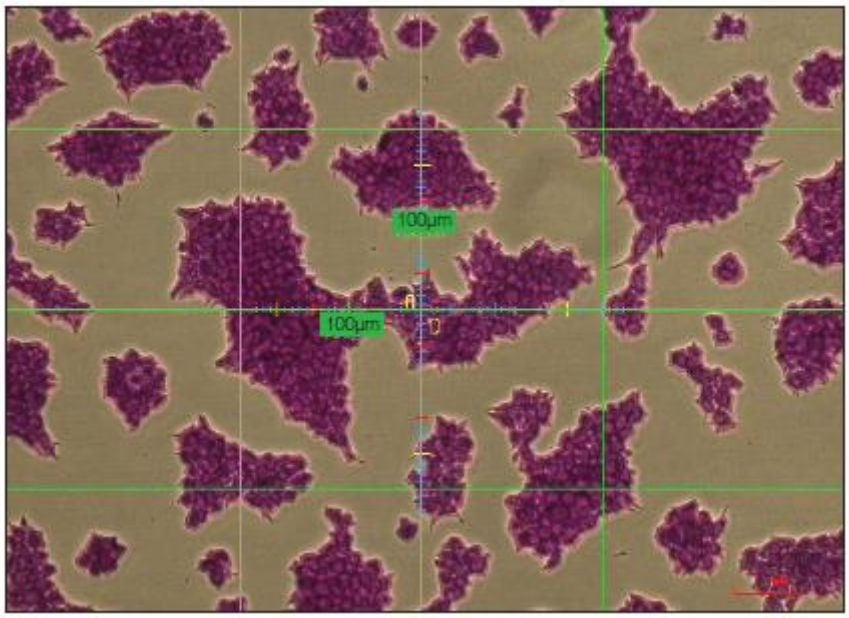

(B)

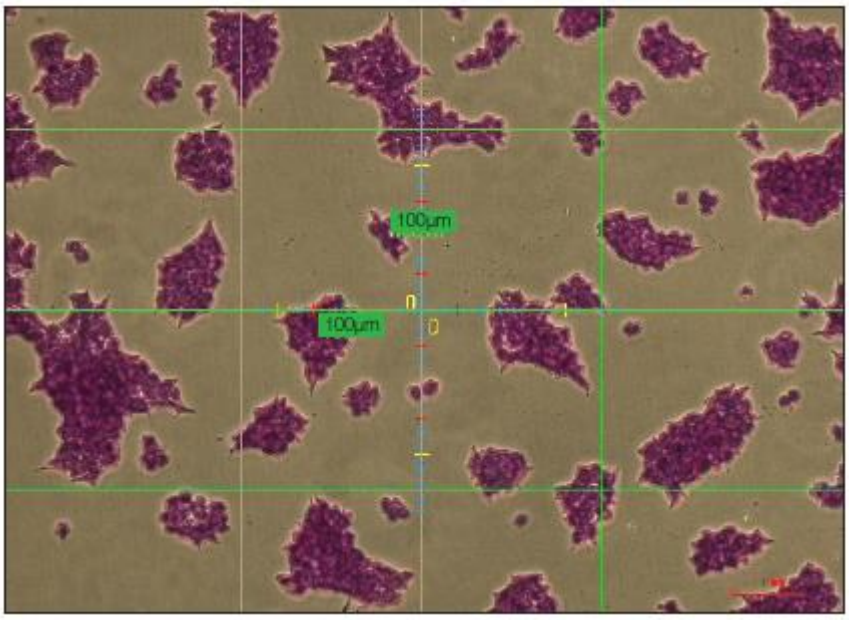

Figure 2. Micrographs of BT474 colony formation: with (A) Trastuzumab that was thermally stressed at 75^{o}C and (B) Trastuzumab that was not stressed as a control. Micrograph of crystal violet stained BT474 colonies (Magnification x100 with height at 750 µm for both micrographs)

The plot of absorbance at 450 nm versus cell number was linear ($R^2 = 0.9776$) (figure 3) thus confirming the cells were proliferating at the same rate for each initial seeding density and inferring similar behaviour with the cells used in the assay. This was a reasonable assumption as the cells came from the same flask with a low passage number and therefore generation.

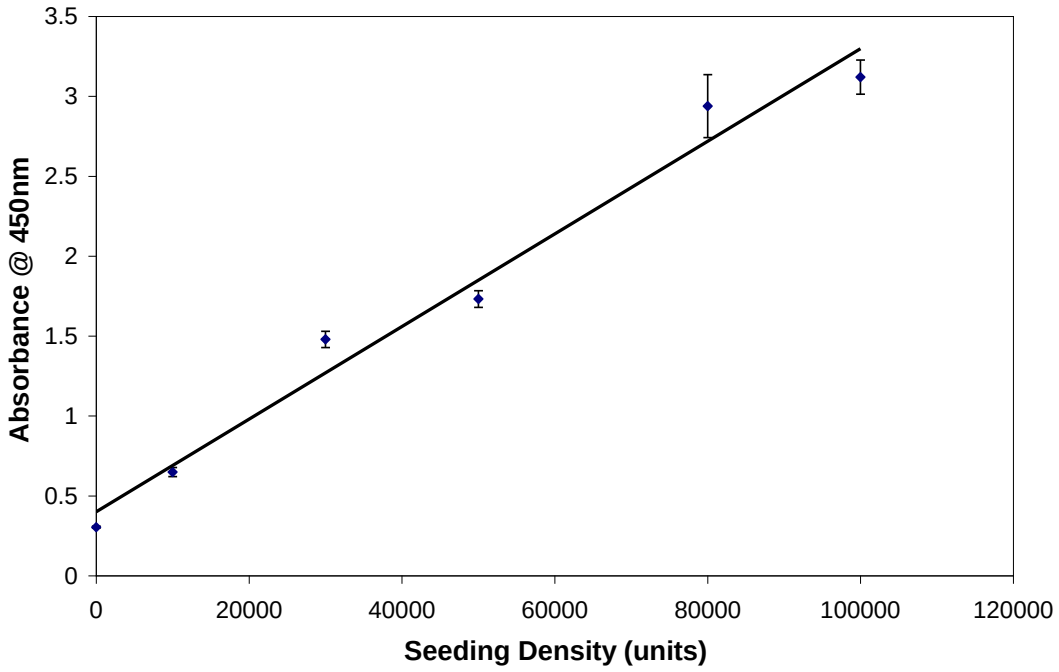

Figure 3. Calibration plot showing absorbance measured at 450 nm versus initial cell count for BT474 at low passage number. $R^2 = 0.9776$ for the data series. Standard error bars shown.

Figure 4 shows the effect of thermal stress on the 0.1 mg/mL Trastuzumab infusion. The absorbance readings obtained were after 2 hours of incubation with the CCK8 reagent. The mean absorbance readings decreased in the order of no drug, stressed and unstressed Trastuzumab with the mean absorbance values of 1.907 (0.403, n = 32), 1.792 (0.206, n = 28) and 1.443 (0.320, n = 28) units respectively with standard deviation and number of readings (n) in brackets. However, the standard deviations appear too great for the result to be significant. This variability may be due to

inconsistent seeding of wells, although the seeding calibration performed in parallel with the assay was satisfactory.

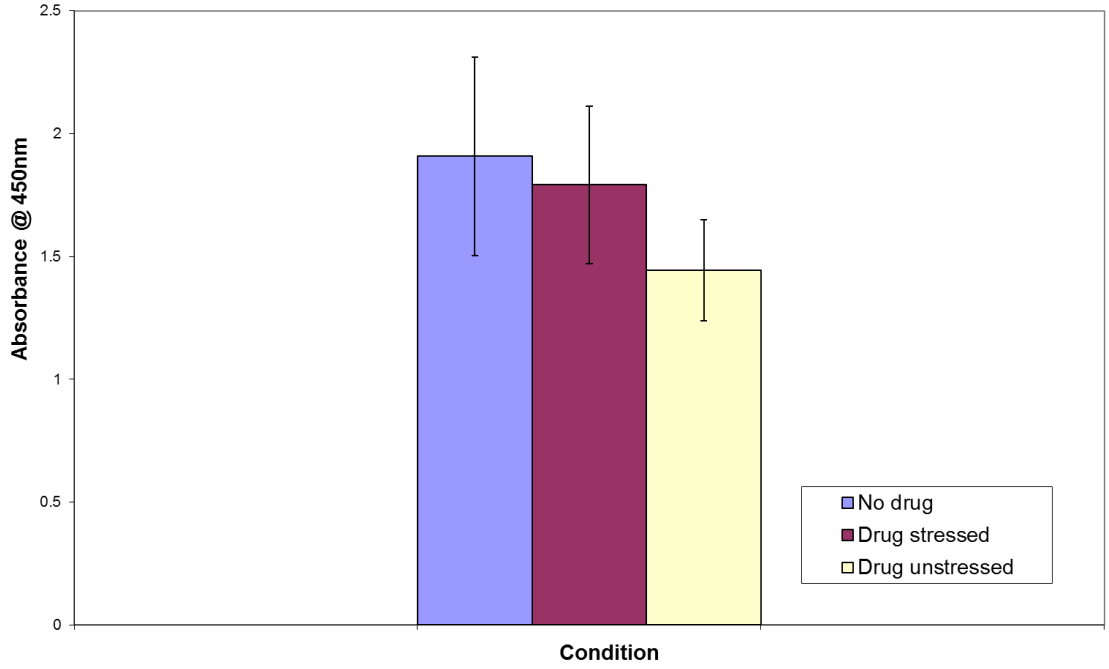

Figure 4 Plot showing the effect of thermally stressed Trastuzumab (0.1 mg/mL) on cellular viability as measured by CCK 8 absorbance at 450 nm after 2 hours incubation with reagent. Results show absorbance for the conditions: no drug, stressed drug and unstressed drug. Descriptive statistics shown as standard deviation error bars.

After a further 2 hours incubation the difference between stressed drug and unstressed drug has become apparent: 3.120 (0.350) and 2.309 (0.289) absorbance units respectively. The absorbance for uninhibited growth of the cells was 3.158 (0.453). In figure 5 the absorbance for the stressed drug is approaching the reading for the uninhibited cells. In contrast the difference between the aforementioned absorbance readings and unstressed drug is greater. This is consistent with a decreased viability for the cells treated with the unaltered Trastuzumab compared to untreated and stressed drug. A t-Student test comparing the stressed and not stressed drug data sets gave $p < 0.001$ with a significance threshold of $p = 0.050$. The p value provides

evidence against there being no difference in cell absorbance between the fully active drug and stressed drug measurements.

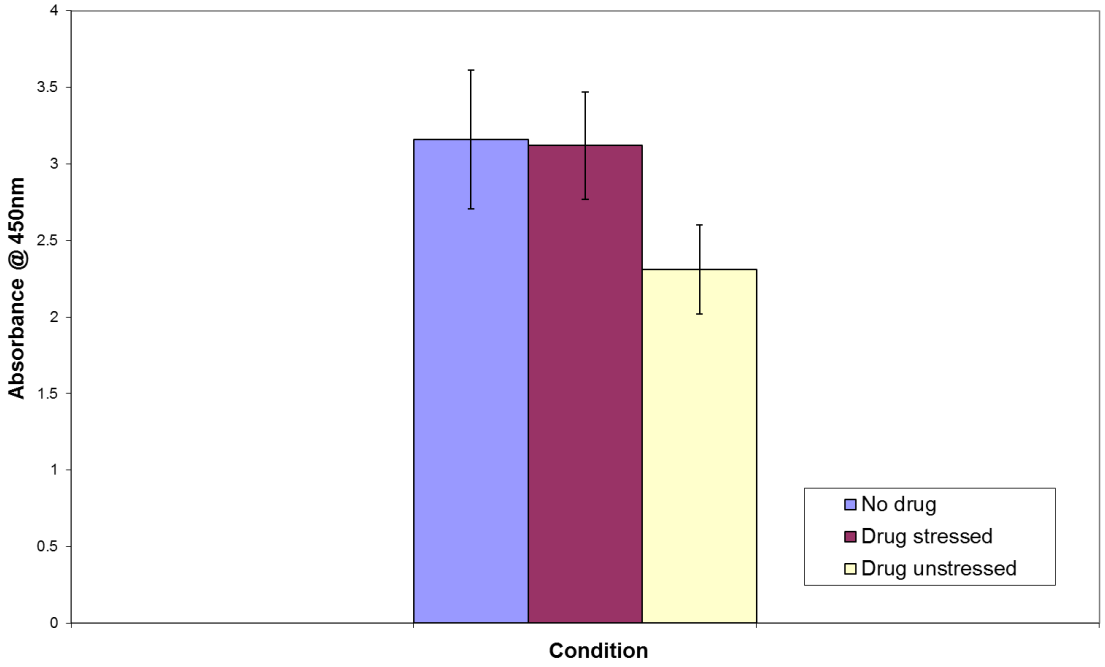

Figure 5 Plot showing the effect of thermally stressed Trastuzumab on cellular viability as measured by CCK 8 absorbance at 450 nm after 4 hours incubation. Standard deviation error bars shown.

Physicochemical Stability of Trastuzumab reconstituted and diluted to 0.1 mg/mL

SE-LC results

Trastuzumab as manufactured inherently contains a small amount of its dimeric form along with the active monomer (Philo & Arakawa 2009). Monitoring the formulation for changes in the monomer, dimer and appearance of other aggregate species enable the assessment of the stability or condition of the drug. Size exclusion chromatography (SEC) shows the monomer eluting at a retention time of 12 minutes

and the dimer at a retention time of about 10 minutes. The elution time of 12 minutes is consistent with the monomer but the dimer identity is unconfirmed.

Figure 6 shows that after thermal stress the dimer peak increases in intensity and higher molecular weight species, which imply the formation of aggregates, begin to form with concomitant decrease in monomer peak area and height which is off scale. The generation of higher order aggregates is consistent with drug degradation.

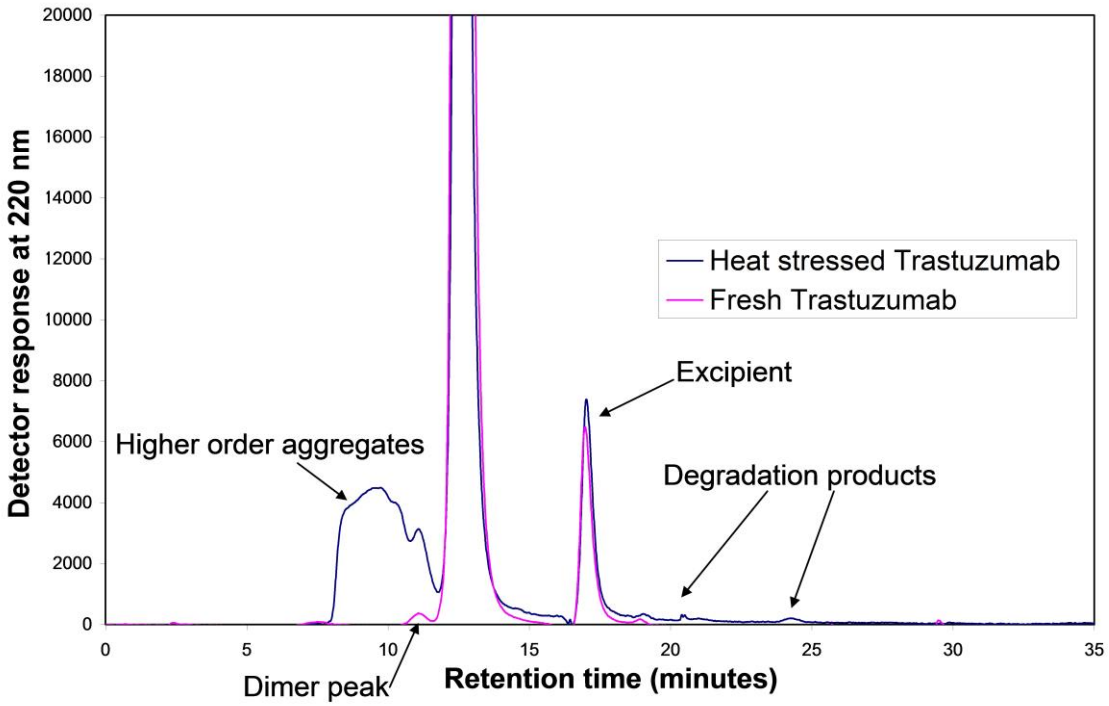

Figure 6. Size exclusion chromatogram of Trastuzumab at 0.1 mg/ml concentration thermally stressed at 75 ^{o}C for 20 minutes compared to fresh Trastuzumab at 0.1 mg/ml. A broad range of higher order aggregates form and an apparent increase in dimer on stressing which is evident left of the monomer peak which is off scale at a 12 minutes retention time (blue trace).

When Trastuzumab was stressed for 10 minutes and then analysed after a 4 day period by SEC the distribution of higher molecular weight species had changed compared to the aggregate profile of a stressed sample analysed immediately (figure 7). A shift to higher molecular species and a continued loss of monomer had occurred after the stress was removed and during storage under refrigeration. This observation supports the view that aggregation involves the native monomer in its propagation after the process is initiated. In contrast for a 15 minute heat stress experiment with SEC analysis after 4 days the monomer has decreased considerably more and the higher order aggregate peaks are hardly visible after 4 days (red trace) (figure 8). The dimer is not resolved possibly due to very low levels of monomer. This is consistent with the reversible dimer being in equilibrium with the monomer. Conversely immediate analysis after 15 minutes of heat stress produces the typical broad aggregate profile.

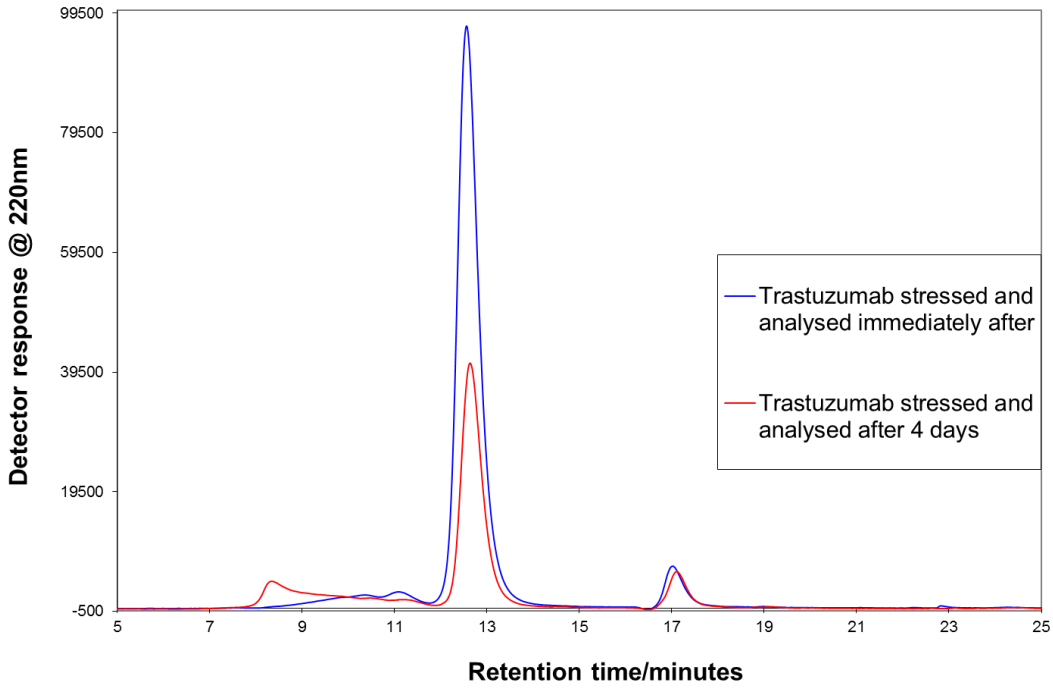

Figure 7 Size exclusion chromatogram of Trastuzumab at 0.1 mg/ml concentration thermally stressed at 75 ^{o}C for 10 minutes and analysed immediately (blue trace) and Trastuzumab at 0.1 mg/ml concentration thermally stressed at 75 ^{o}C for 10 minutes and analysed after 4 days. Monomer has decreased and higher order aggregates have increased after 4 days.

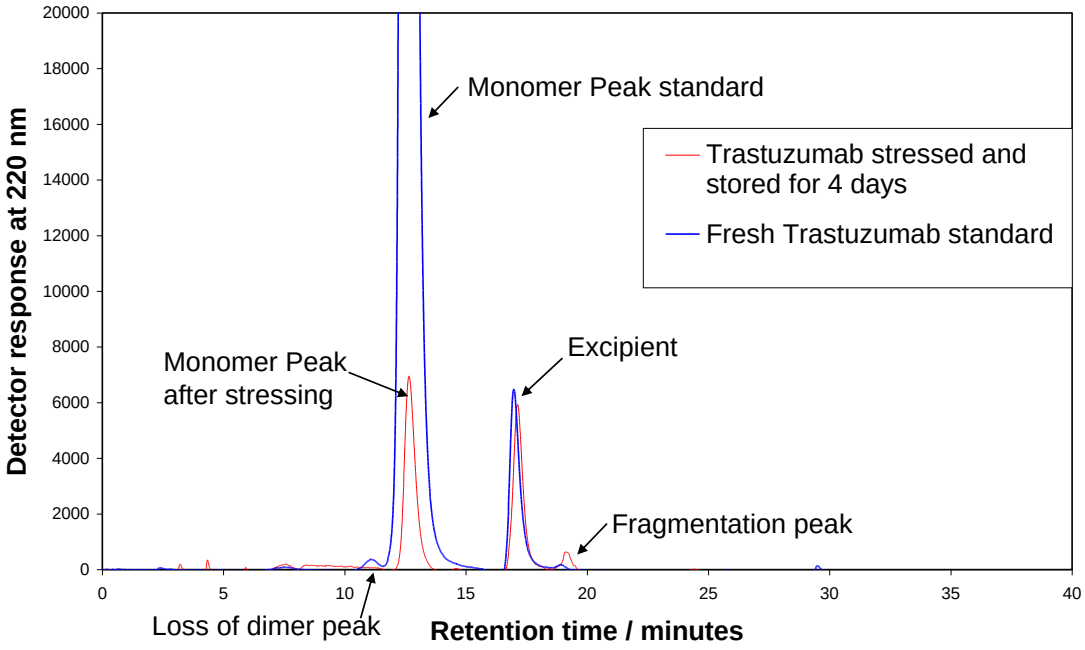

Figure 8. Size exclusion chromatogram of Trastuzumab standard at 0.1mg/ml concentration (blue trace) and Trastuzumab at 0.1 mg/ml concentration thermally stressed at 75ºC for 15 minutes and analysed after 4 days (red trace).

These results broadly correlate with the cellular assay data. The Trastuzumab monomer peak decreased as the higher order aggregates increased after storage under refrigeration (5–8 ºC) for the 10 minute heat-stressed sample. In contrast Trastuzumab that was heat-stressed for 15 minutes and analysed by SEC after 4 days revealed further monomer loss. Nevertheless, higher order aggregate peaks were barely visible with the dimer peak also absent. Moreover these peaks were detected when the analysis was performed immediately. These observations are consistent with the view that aggregation continued after the thermal-stress was removed and aggregate species became too large to be detected by SE-LC. This may explain, at least in part, why in a USP forced degradation study for their proposed Trastuzumab validation document,

that the degree of aggregation was not proportionate to the decrease in potency observed (USP 2013). Additionally, in the USP validation report SE-LC analysis was only performed on unstressed Trastuzumab and on Trastuzumab after 60 minutes of heating (USP 2013).

Degradation under ambient conditions

The 0.1 mg/ml sample of Herceptin stored for 4 days under ambient conditions (aseptic conditions maintained) showed a similar aggregate profile to the unstressed drug by size exclusion liquid chromatography (SE-LC) (figure 9).

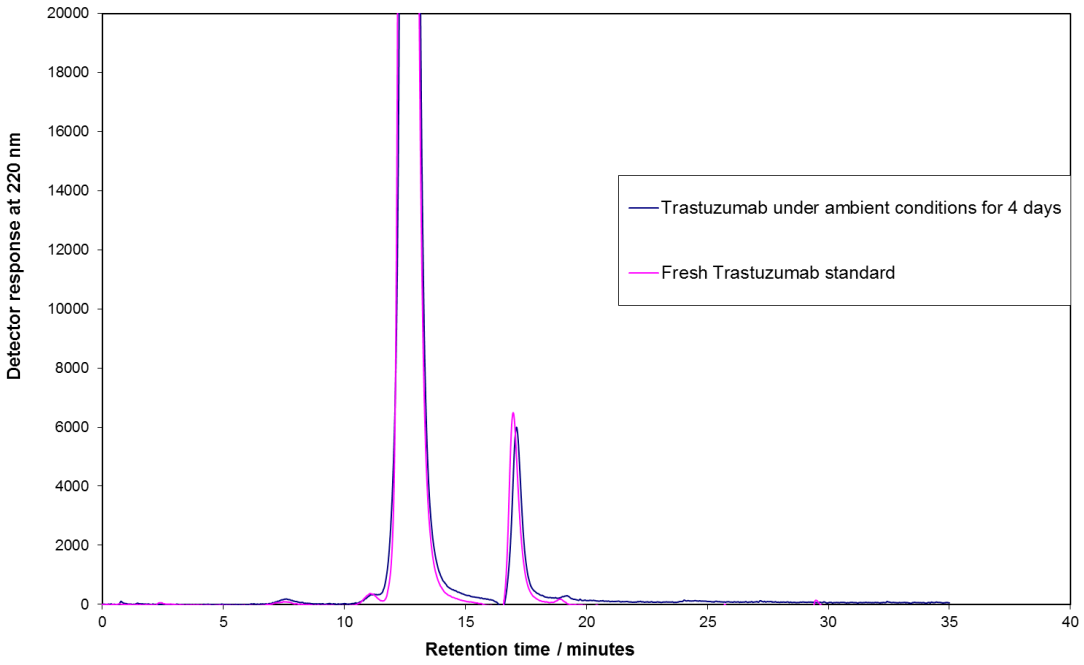

Figure 9 Size exclusion chromatogram for ambient storage of 0.1 mg/mL infusion sample compared to fresh Trastuzumab standard.

IR results

The ATR corrected infra-red spectra (figure 10) show no apparent difference between stressed and freshly prepared Trastuzumab. This observation suggests there has been no major change in the protein at the secondary structural level and is consistent with the aggregation process mainly recruiting native monomers.

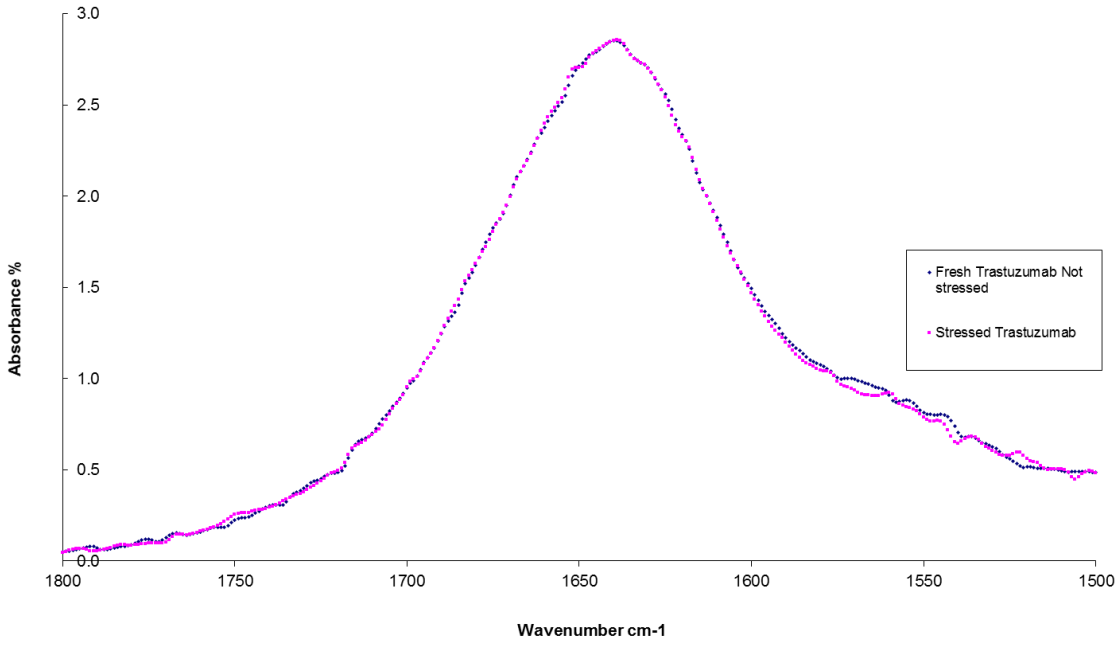

Figure 10. Attenuated Total Reflectance (ATR) Fourier Transform Infra-red spectrum of fresh standard of Trastuzumab at 0.1mg/ml and Trastuzumab at 0.1 mg/ml concentration stressed 75 ^{o}C for 20 minutes. Spectra were water vapour subtracted, air background corrected, ATR corrected and normalised to 1,850 cm^{-1}. Spectra are virtually coincidental for heat-stressed and freshly prepared Trastuzumab.

5.4 Conclusions

The difference between colony size in stressed and unstressed drug treated wells was apparent (figure 2). The CCK8 assay showed variability (figure 4), although an acceptable seeding calibration was obtained (figure 3). The difference in mean absorbance between stressed and unstressed drug became more apparent after 4 hours incubation before absorbance measurement (figure 5).

The SE-LC analysis of stressed Trastuzumab infusion showed an increase in the number and size of peaks at retention times (~10 minutes) immediately before the monomer (12 minutes) (figure 6). At retention times greater than 20 minutes small peaks were evident (figure 6). The appearance of these peaks was accompanied by a decrease in the monomer peak (figure 7). Further loss of monomer peak was shown after the 10 minute heat stress experiment on storage (figure 7). In addition, the peak system adjacent to the monomer shifted to shorter retention times (figure 6). A heat stressing time of 15 minute with SE-LC analysis after 4 days gave a further decrease in the monomer peak, however peaks at retention times < 12 minutes are hardly visible (figure 8). Storage under ambient conditions show no significant changes of the chromatogram (figure 8). The infra-red spectra show no apparent changes between stressed and freshly prepared Trastuzumab (figure 10).

CHAPTER 6

6. USE OF CELLULAR ASSAY TO DETERMINE TRASTUZUMAB STABILITY

6.1 INTRODUCTION

The manufacturers state that Trastuzumab reconstituted with sterile water for injection is physically and chemically stable for 48 hours at 2 ^{o}C to 8 ^{o}C and on further dilution for infusion, in 0.9% sodium chloride solution, may be stored up to 24 hours at temperatures not exceeding 30 ^{o}C (European Agency for the Evaluation of Medicinal Products (EMEA) 2010). In contrast the multi-dose form of Trastuzumab which is available outside Europe has a designated shelf-life of 28 days if reconstituted with bacteriostatic water containing benzyl alcohol as a preservative (European Agency for the Evaluation of Medicinal Products (EMEA) 2005b). This implies that the manufacture's stability limit is determined on a microbiological basis rather than physicochemical stability.

If physicochemical stability and functional activity can be shown beyond the current limit, even for a few days, wastage will be decreased. Thus offering the potential to utilise none administered infusions or partially used vials. In addition it will allow for a more efficient drug compounding in the form of dose banding for patient ready preparations. It has been stated that efficient dose banding has a clear requirement for longer shelf-life stability of 28 to 84 days for infusions (Bardin et al. 2011).

However, there is a lack of stability data for Trastuzumab to support an extended in-use shelf-life; in particular functional activity is overlooked in the relatively small number of studies that address in-use stability (Kaiser & Kramer 2011; Paul et al. 2013; Pabari et al. 2013). Biological assessment is an important aspect of assigning a shelf-life because it is a direct way of determining functional activity and supports

physicochemical stability data. This has been recognised in the NHS document guidance for deriving and assessment of stability of biopharmaceuticals which post-dates this study whilst sharing common principles (Barnes 2012).

It is important to consider the correct mode of action when selecting a biological assay. The mode of action of the drug must reflect its pharmaceutical action. Biological assessment may take the form of a binding assay for an enzyme or inhibitor. Whereas for more complex biological drugs, where binding to a receptor is followed by a cellular cascade with an extra-cellular response, there is a need to consider the complete mechanism of action. This may be multimodal which sometimes requires more than one cellular assay to fully assess the efficacy of the drug.

The drug concentrations selected should reflect clinical dosing at high and low concentrations. Thus if stability is found at high and low concentrations it may be possible to interpolate to intermediate concentrations (Barnes 2012). In this study Trastuzumab concentrations of 0.5 mg/mL and 6 mg/mL were selected. An additional concentration of 0.1 mg/mL was selected as this may enhance instability with the potential to study degradation products. There is a predisposition for lower concentrations of biologic drugs to be less stable. This may be the result of the dilution of excipients or decreased drug-drug interaction providing increased opportunity for adsorption on surfaces (Barnes 2012).

A study period of 119 days was chosen with test points at day 0, 7, 14, 28, 35, 43 and 119. The final test point at 119 days provides an increase in assurance of the 43 day data.

This chapter will now show the data of the cellular assay.

6.2 MATERIALS AND METHODS

6.2.1 Test materials

6.2.1.1 Reference Trastuzumab (Herceptin® Roche)

The reference Trastuzumab was the same batch supplied for the development work (chapter 4 Development of Cellular Assay Methods and Materials section 4.2 page 94).

The lyophilised Trastuzumab was reconstituted as described in Chapter 2 Methods and Materials section 2.2.1 page 51.

6.2.1.2 Infusion bag samples

The infusion bags were prepared aseptically according to the manufacturer's instructions which are described in the summary of product characteristics (SPC) (European Agency for the Evaluation of Medicinal Products (EMEA) 2010). Concentrations of 0.1, 0.5 and 6 mg/ml in 0.9% sodium chloride solution for infusion in intravenous (IV) Polyolefin infusion bags (Freeflex®) (50 ml) were prepared by Clatterbridge Centre for Oncology, Clatterbridge Hospital. All concentrations were made within acceptable tolerance for patient dosage.

6.2.2 Drug storage conditions and sampling protocol

The reconstituted and diluted samples were stored under refrigeration between 2 ^{o}C and 8 ^{o}C. Biological testing was carried out at each time point.

Samples were taken from the infusion bags by removing 1ml of the contents in duplicate with a 2 part syringe (Luer and Luer lock with no silicone) (B Braun) under aseptic conditions.

Each sample was serially diluted in the complete cell culture media RPMI 1640, which was used to maintain the cells prior to the assay, to a nominal concentration of 1 μMolar before further serial dilution to the appropriate concentration range used in the assay (1 pM to 100 nM). The reference Trastuzumab was diluted in tissue culture media in an equivalent manner to the samples.

6.2.3 Biological testing with the BT474 cell-line

The BT474 breast tumour (human ductal tissue (epithelial) carcinoma) cell line from ATTC (HTB-20; lot: 58471910) was selected for the testing of Trastuzumab because these cancer cells have an overabundance of the specific receptor which is the therapeutic target (HER2) on the cells' surface and is indicative of the cancer type for which Trastuzumab has been designed to treat.

6.2.3.1 Maintenance of cells

BT474 cells were maintained as described in Chapter 4 Method Development of Cellular Assay Methods and Materials section 4.2.2.2 page 116.

6.2.3.2 Seeding BT474 cells for biological testing

Cells were seeded at 10,000 cells per well in a 96 well micro-plate according to the protocol described in Chapter 4 Method Development of Cellular Assay Methods and Materials section 4.2.2.4 page 116.

The wells were inspected to assess the quality of seeding and health of cells using an inverted microscope (Nikon Eclipse T100 binocular phase contrast microscope fitted with Digital Sight DS Fi1 imaging system). Plates with an even and uninterrupted distribution of cells over the growth surface of the wells were selected for assay. The seeding method was validated by calibration in the development work and during the study.

6.2.3.3 Determination of BT474 Cell viability after addition of Trastuzumab using Cell Counting Kit CCK8

The BT474 cell-line growth media was exchanged for either fresh media (200 µl) for the zero drug control (negative control) i.e. cells and media, reference Trastuzumab (positive control) which was freshly reconstituted and diluted in media (200 µl) or test Trastuzumab which had been removed from the stored infusion bag at the appropriate time point and diluted in media (200 µl). The detail of the procedure was described in Chapter 4 Method Development of Cellular Assay Methods and Materials section 4.2.3 page 119.

Each sample of drug in media was added using replicate (n = 8) wells to the 96 well micro-plate including reference standards (n = 8) and controls (n = 8) for each plate. Additional control plates with untreated wells (n = 32) were produced. The micro-plates were then returned to the humidified incubator at 37^{o}C, 5% CO_2 (Sanyo NC0-19AIC (UV)). The cells were then incubated for 4 days to allow for growth of BT474 colonies. This time period allowed the degree of difference in cell growth between untreated and treated wells to be amplified.

Testing with the cellular reporter substrate CCK8 (Sigma Aldrich) was according to standard protocol documented in Chapter 4 Method Development of Cellular Assay Methods and Materials. The absorbance was then read at 450 nm using a Biotek micro-plate reader (Biotek Epoch, operating on Gen 5 Software, version 1.10.8) after 1, 2, 3, 4 and 20 hours incubation.

A seeding calibration was performed at each test time point in duplicate with replicate wells (n = 16) for each seeding density. The purpose of this was to determine the relationship between cell density and absorbance after the 4 day test period. The final projected cell densities (0 to 320,000 cells per well) of the calibration encompass the cell density range at the assay end-point to enable the determination of relative cell numbers within the wells which had a drug addition or none.

6.2.4 Colony Formation Assay

After the biological assay had been performed all microplate colonies were fixed and stained as a permanent record of cellular proliferation and provided an opportunity to assess if the colonies had remained evenly distributed and no cells had been lost before the micro-plates were read. This enabled the rejection of absorbance data from unsatisfactory populated wells. Fixing and staining preserves the cells in a form close to their original structure and facilitates further examination and assessment of colony numbers by unaided counting or instrumental-software based methods.

The colonies were fixed and stained as described in Chapter 4 Development of Cellular Assay Methods and Materials section 4.2.2.5 page 117.

6.3 QUALITY ASSURANCE AND QUALITY CONTROL

A standard reference solution of Trastuzumab was prepared using consistent dilutions at each time point. The standard reference determines the relative accuracy of subsequent measurements of test infusion samples. The additional control plates where the wells had no drug addition allow the demonstration of the uninhibited growth of the cells from the initial seeding for the assay. Furthermore, the control plates and the calibration plates enable the confirmation that the cells used from the stock culture were seeded and growing consistently and suggest that any differences between experimental cells and control cells should have originated from the drug addition of stored or standard Trastuzumab. The data from the assay and calibration were exported using Microsoft Excel 2003 for further analysis including uncertainty of data and inter-plate precision.

6.4 STUDY LIMITATIONS

Biological activity or potency of Trastuzumab, as determined by the CCK cell viability assay, during the storage period will be reported and discussed. Before this can be achieved appropriately it is provident to consider vigorously the nature of the experiment being performed and a justification of the approach to the analysis of the experimental results. The results for each time point cannot be compared collectively due to the inherent variation in cell growth at each time point. Furthermore, due to a single stock culture being used the multiple assays performed at each time point can only be considered as a single experiment with replicate cell cultures, i.e., n = 1 and therefore error bars or statistics are shown to report only on the consistency of seeding between wells of the single experiment (Cumming et al. 2007). Moreover, these errors do not inform on the reproducibility of the differences between experimental wells and control wells (Cumming et al. 2007). However, the comparison to freshly prepared standard concentrations does enable a direct comparison of aged drug performance or efficacy to the corresponding concentration of Trastuzumab at time zero at each time point of the study. Although, interpretation of the results should be exercised with great care due to the limited data points and concentration range used for measurement.

6.5 RESULTS AND DISCUSSION

6.5.1 Determination of cell viability as an indicator of potency of stored Trastuzumab

6.5.1.1 Assessment of biological activity day 0, 7, 14 and 28

Earlier data for days 0, 7, 14 and 28, using the concentration range 1 pM to 100 pM, showed a deficiency in the required sensitivity for assessing confidently changes in efficacy. This inferred that the dose-response had changed from that determined during pre-study validation and the concentration-absorbance response curve had been displaced to a higher concentration range. This resulted in the concentrations initially selected for the assay now coinciding within a plateau region of the curve,

i.e., a region insensitive to changes in concentration of the active drug or changes in potency. Figure 1 shows a typical response of the BT474 cells to Trastuzumab concentrations over a 0 to 700 pM range with the red double headed arrows showing the concentration range extension. The schematic also shows the shift in response from the linear portion of the curve (position 1) to the plateau section of low sensitivity (position 2) encountered with the early time points. To overcome this loss in satisfactory response to assess changes in efficacy the concentration range was extended from the 1 to 100 pM range up to 1 nM for days 35 and 43. For the final time point of day 119 a concentration range of 1 nM, 2 nM, 10 nM and 100 nM was selected. At these test points 1 nM and 2 nM was the concentration of maximum response of the drug as the response for these concentrations as they lay on the linear and steep portion of the dose response curve. In this region of the dose-response curve a small change in biological activity, such as a loss in potency or decrease in concentration of active Trastuzumab, will manifest itself in a relatively large change in absorbance. Therefore, changes in absorbance at 1 nM and 2 nM were selected to report efficacy as a percentage relative to fresh drug prepared and tested at each test point, i.e., 1nM for days 35 and 43 and with both 1nM and 2nM for day 119 for the final time point.

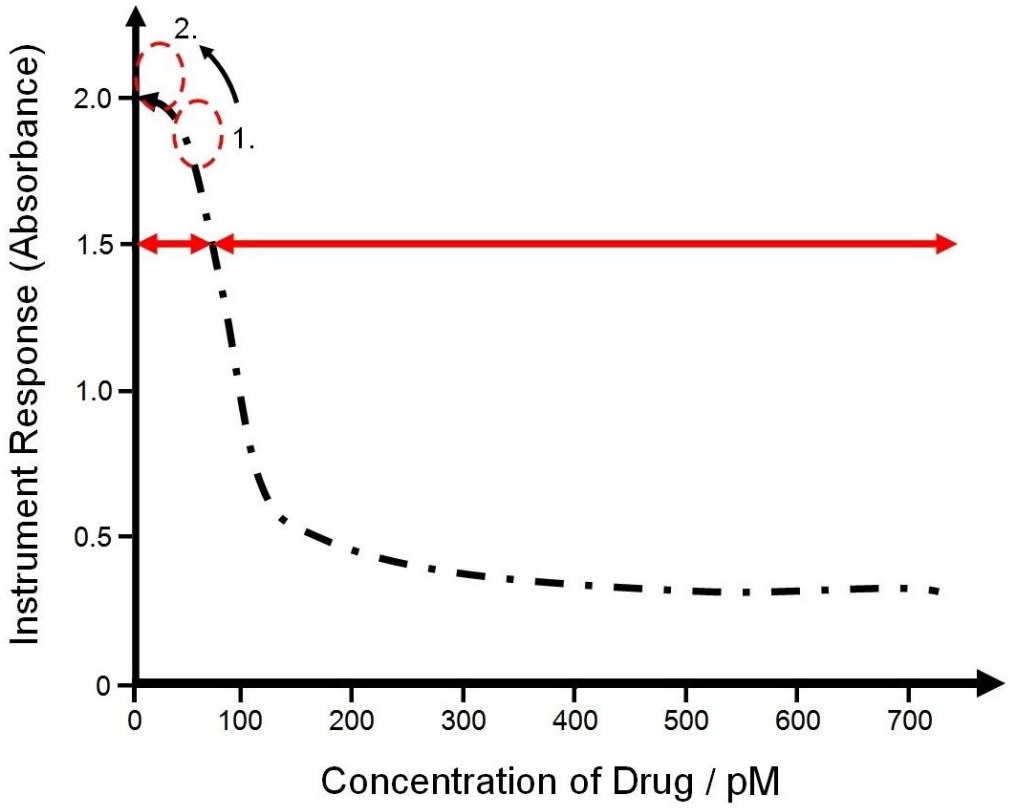

Figure 1 Schematic showing typical dose-response curve of BT474 cells over a 0 to 700 pM range. Also, the shift in response from the linear portion of the curve (position 1) to the plateau section of low sensitivity (position 2) found initially in the early time points when a Trastuzumab concentration range of 1 pM to 100 pM was used. The red double headed arrows show the concentration range eventually extending beyond 700 pM to 100 nM.

6.5.1.2 Assessment of biological activity day 35, 43 and 119

To characterise changes in efficacy at day 35 a concentration range of 1 pM to 1 nM was selected. The concentration range (1 pM to 100 pM) employed for the earlier time points (days 0, 7, 14 and 28) was found to be insensitive to changes in Trastuzumab concentration. Difference in absorbance at 1 nM (1000 pM) was used to assess any changes in Trastuzumab activity of the stored infusion bags at days 35 and 43. At the final test point of the study day 119 efficacy was determined at both 1 and

2 nM. The data set for the whole study shows no loss of efficacy over the period of 119 days.

Efficacy was reported as a percentage difference in absorbance between reference Trastuzumab, reconstituted and further diluted at the test point, and the stored Trastuzumab infusions (European Medicines Agency 2006). If there is no change in efficacy between the freshly prepared standard and the stored infusion then the result for the test infusion would be 100%. Conversely, a result of less than 100% would be indicative of an apparent loss of biological activity. However, a number of test samples showed an apparent increase in cell suppression or greater potency than the freshly prepared Trastuzumab (tables 1 and 2). For example the 0.5 mg/mL infusion recorded 153% cell growth suppression on day 35 compared to freshly prepared drug tested at the same time. The concentrations of 1 nM and 2 nM used to measure efficacy at the final time point define the sensitive portion of the dose-response curve and therefore a small change in active drug concentration within this region should give a large change in absorbance and facilitate detection of any changes in potency (USP 2013). However, this responsive region would also be expected to amplify any errors in the experiment such as variation in the cellular response or discrepancy of the original concentration in the infusion bag (Barnes 2012). This view is supported by the difference in measurement when 1 nM and 2 nM concentrations are used. The second measurement of potency was generally closer to the reference Trastuzumab.

The data for the clinically relevant concentrations of 0.5 mg/mL and 6 mg/mL have been collated and graphed for each concentration for each time point (figures 2 and 3). For each concentration two bags and two plates have been combined giving 16 replicates for each concentration. Efficacy at the assigned concentration for individual plates (replicates = 8) is also presented in table 1 for comparison of assay performance between duplicate plates A and B. Table 2 summarises the results obtained from the complete data sets for each concentration where replicates = 16 for each assay concentration.

The results for the 0.1 mg/mL infusion bags and the 21 mg/mL vial concentrate stored in the original vial are discussed separately. The results for day 119 will be presented. For the 0.1 mg/mL concentration data from four bags and two plates have been

combined giving 32 replicates for each assay concentration. The results for the 21 mg/mL vial concentrate have 4 replicates for each assay concentration. Rejection of data from wells that showed unsuccessful seeding and subsequent growth decreased the number of replicates available for analysis of the concentrate.

6.5.1.3 Day 35

Figure 2 shows a typical response of absorbance as a function of Trastuzumab concentration. The data presented in this graph is from two infusion bags of 0.5 mg/mL concentration. The relationship between dose and response is clear for both reference and test Trastuzumab. As the Trastuzumab concentration increased cell numbers became lower as evidenced by the lower absorbance; which was consistent with the view that cell growth had been suppressed or cell viability decreased as the dose increased. This trend is observed for both reference and stored infusions. The 0.5 mg/mL test infusion gave a 153% increase in activity at the 1 nM (1000 pM) assay concentration. The 6 mg/mL infusion test sample showed a similar response to drug dose (figure 3). This sample gave a 123% apparent potency increase at 1 nM (1000 pM).

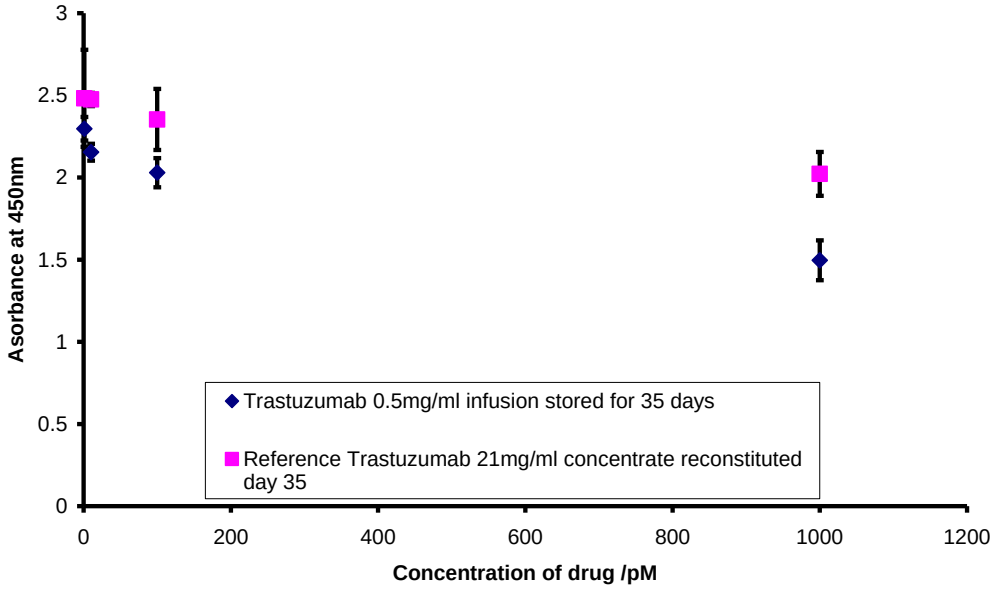

Figure 2 A plot of absorbance as a function of drug dose is shown for combined data for stored (day 35) infusion bags (replicates = 16) at a concentration of 0.5 mg/mL. Inferential error shown as standard error. The response is typical showing a decrease in absorbance with increase in Trastuzumab concentration.

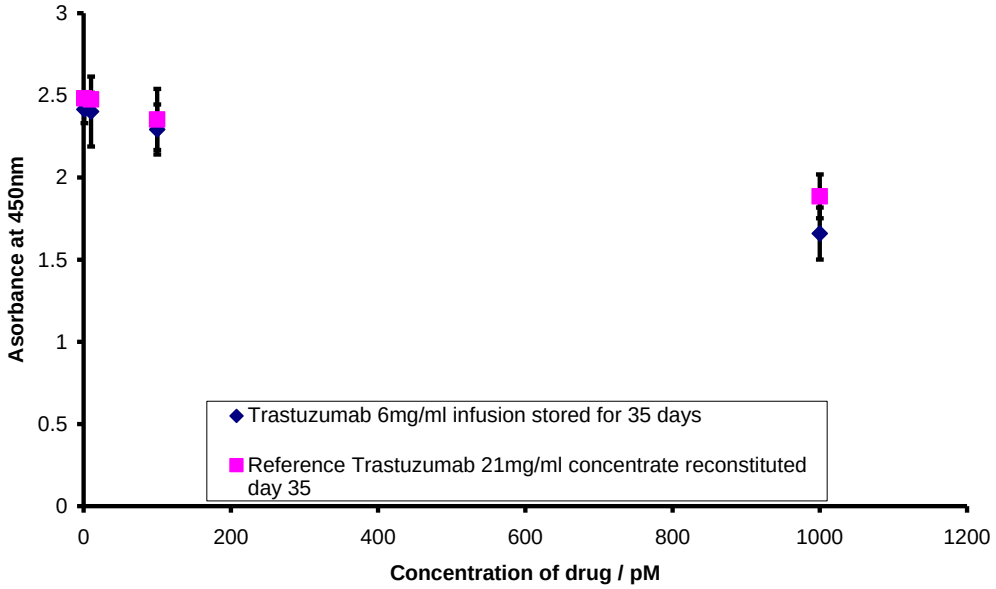

Figure 3 A plot of absorbance as a function of drug dose is shown for combined data for stored (day 35) infusion bags (replicates = 16) at a concentration of 6 mg/mL. Inferential error shown as standard error. The response is typical showing a decrease in absorbance with increase in Trastuzumab concentration.

6.5.1.4 Day 43

A comparable response to day 35 was found at day 43. The dose-response for the combined infusion bag data for each concentration of 0.5 mg/mL and 6 mg/mL stored test samples are shown in Figures 4 and 5 respectively. The percentage difference between sample and reference for 0.5 mg/mL and 6 mg/mL infusions were 87% and 103% correspondingly. This represents a decrease and increase in cell suppression respectively for the test samples.

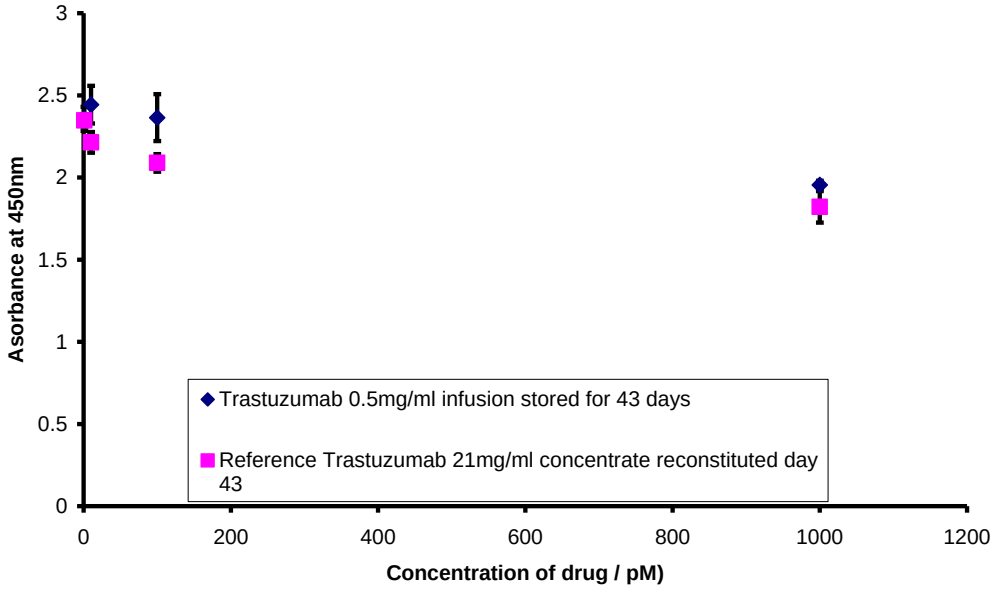

Figure 4 A plot of absorbance as a function of drug dose is shown for combined data for stored (day 43) infusion bags (replicates = 16) at a concentration of 0.5 mg/mL. Inferential error shown as standard error. The response is typical showing a decrease in absorbance with increase in Trastuzumab concentration.

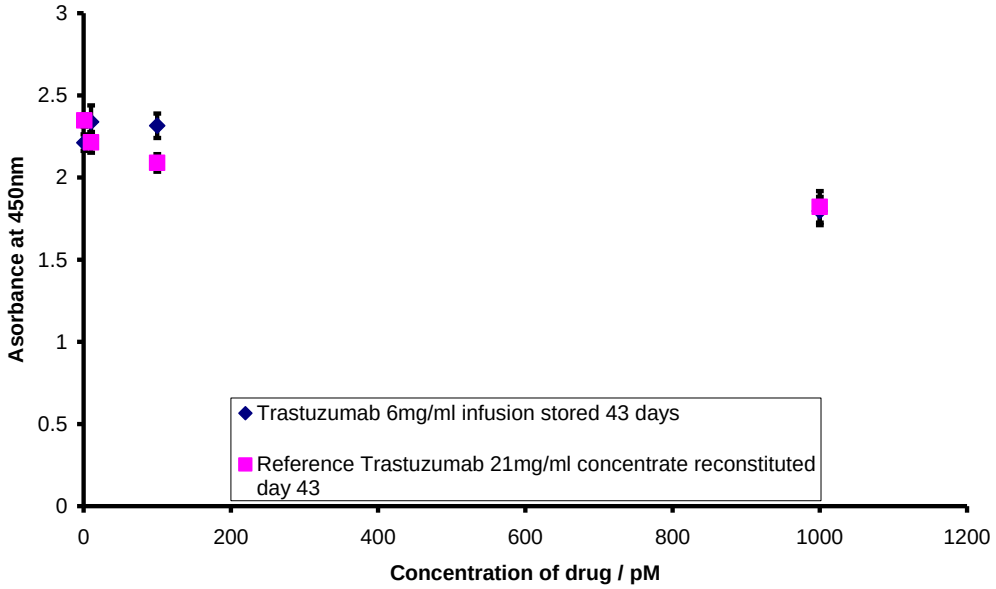

Figure 5 A plot of absorbance as a function of drug dose is shown for combined data for stored (day 43) infusion bags 1 and 2 for plate A and B (replicates = 16) at a concentration of 6 mg/mL. The response is typical showing a decrease in absorbance with increase in Trastuzumab concentration.

6.5.1.5 Day 119

At the final time point the concentration range for the assay was extended to 100 nM. Efficacy for the 0.5 mg/mL and 6 mg/mL infusion bags was determined at both 1 nM and 2 nM and showed greater cell suppression than the reference Trastuzumab. The 0.5 mg/mL test infusions recorded 149% at 1 nM and 114% at 2 nM. Whereas the 6 mg/ml test infusions recorded 136% at 1 nM and 123% at 2 nM. In all cases the 1 - 2 nM concentration range gave the maximum response for both reference and test Trastuzumab. After these concentrations the dose-response becomes limiting as the end point of biological response has been attained and the response levels out into a plateau region. Therefore this region also represents an additional concentration insensitive section of the dose-response profile mirroring the response at the lower concentration limit. After the response at the 1 - 2 nM concentration region of the

response plot the absorbance changes very little with increase in drug concentration as the response has maximised after the 2 nM and remains relatively insensitive to dose up to the 100 nM concentration. It can be seen that the experimental dose-response profile over the extended range (1, 2, 10 and 100 nM) (figures 6 and 7), even with a limited number of experimental data points, is suggestive of the theoretical dose-response shown in figure 1.

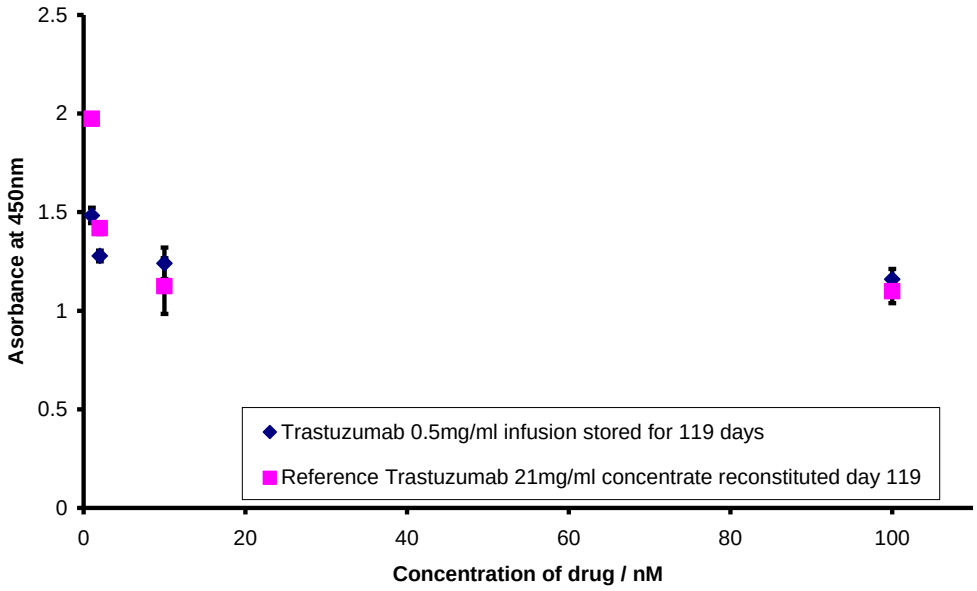

Figure 6 A plot of absorbance as a function of drug dose is shown for combined data for stored (day 119) infusion bags (replicates = 16) at a concentration of 0.5 mg/mL. Inferential error shown as standard error. The response is typical showing a decrease in absorbance with increase in Trastuzumab concentration. Cell suppression: 149% at 1 nM and 114% at 2 nM.

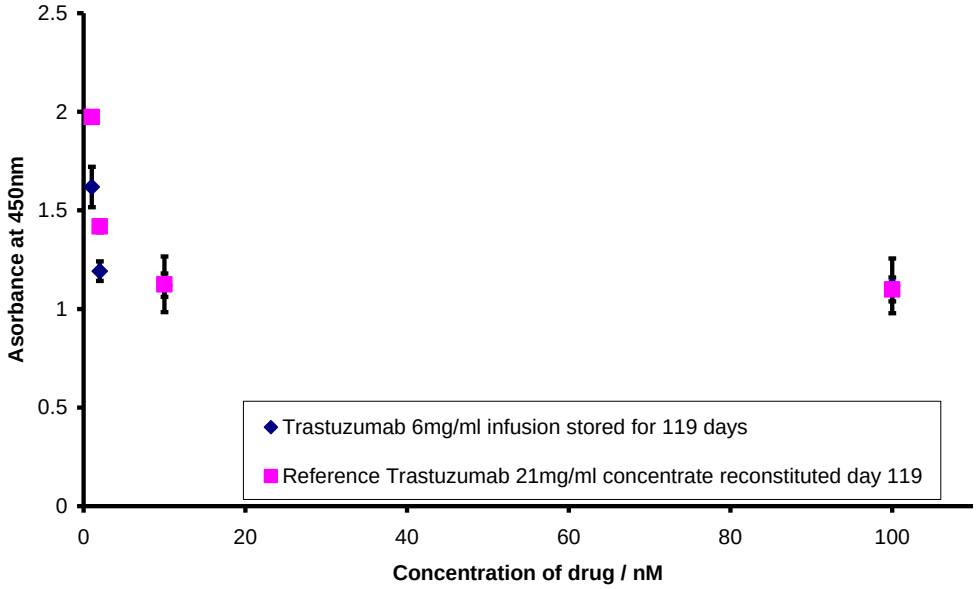

Figure 7 A plot of absorbance as a function of drug dose is shown for combined data for stored (day 119) infusion bags (replicates = 16) at a concentration of 6 mg/mL. Inferential error shown as standard error. The response is typical showing a decrease in absorbance with increase in Trastuzumab concentration. Cell suppression: 136% at 1 nM and 123% at 2 nM.

6.5.1.6 Summary of biological activity results

The results of biological activity expressed as percentage difference in absorbance between sample and reference show overall no loss in potency over 119 days (table 1 and 2). Results for the duplicate plates show some variation in response within a single time-point. In addition, response varies more between time-point which is consistent with the use of a different stock or population of cells. The difference between the nominal and actual concentration of the infusion was also considered as a possible source of error. However, this is not clear in this case because on examination of the data presented in table 1 and 2 there is no consistent or systematic variation for all time points or between plates which would originate from sampling from the same bag at each test point. The day 43 time point records results relatively

close to 100% while the results for the other time points vary between 114% and 153% (table 2).

Variations are most likely due to the range of responses an individual cell can initiate on the addition of drug. This view is supported by the growth characteristics of the uninhibited BT474 cells. The calibrations for each test point showed good linearity and repeatability and therefore indicates uniform growth of that particular stock of cells used in the experiment. Therefore if an extensive number of controls without drug are used to define maximum viability or cell number, and set to 100%, the relative cell numbers as a percentage can be assigned to the assay concentrations with the aid of the calibration and expressed as percentage of viable cells. This approach of normalising the data was adopted for the final time point of day 119 and is discussed in the following section 6.5.1.7 page 181.

Time Point (Day)	0.5 mg/mL IV bags				6 mg/mL IV bags			
	% difference in absorbance (viability) between sample and reference for microplates A and B (replicates = 8)				% difference in absorbance (viability) between sample and reference for microplates A and B (replicates = 8)			
	Measurement Concentration 1 nM		Measurement Concentration 2 nM		Measurement Concentration 1 nM		Measurement Concentration 2 nM	
	Plate A	Plate B	Plate A	Plate B	Plate A	Plate B	Plate A	Plate B
35	121	155	-	-	101	142	-	-
			-	-			-	-
43	79	94	-	-	103	102	-	-
119	157	141	134	94	151	120	121	124

Table 1 Biological activity of stored infusions for Plates A and B (bags 1 and 2 combined giving replicates = 8 for each plate): Absorbance reported at a drug dose of 1 nM for day 35 and 43 and at 1 nM and 2 nM drug concentration for day 119. Assay performed in duplicate (plates A and B). A percentage score below 100% represents an increase in absorbance (more cells) and hence an apparent decrease in drug activity for test sample compared to reference drug standard. Conversely, a percentage score greater than 100% represents an apparent increase in drug activity for test sample compared to freshly prepared drug.

Time Point (Day)	0.5 mg/mL IV bags		6 mg/mL IV bags	
	% difference in absorbance (viability) between sample and reference from combined data (plates A and B with replicates = 16)		% difference in absorbance (viability) between sample and reference from combined data (plates A and B with replicates = 16)	
	Measurement Concentration 1 nM	Measurement Concentration 2 nM	Measurement Concentration 1 nM	Measurement Concentration 2 nM
35	153	-	123	-
43	87	-	103	-
119	149	114	136	123

Table 2 Biological activity of stored infusions using pooled data (combined data for bags and plates A and B: replicates = 16): Absorbance reported at a drug dose of 1 nM for day 35 and 43 and at 1 nM and 2 nM drug concentration for day 119. A percentage score of 100% represents no change in absorbance and hence an apparent no change in drug activity for test sample compared to freshly prepared standard.

6.5.1.7 Percentage viability of BT474 cell count (normalised to base cell viability without drug)

In addition to the above treatment of the data for day 119 the biological response was normalised to uninhibited cell growth represented by the extensive controls of zero drug (replicates = 46) used at the final test point. The normalised percentage viability at 1 nM and 2 nM of both standard and test sample can then be directly related to unrestrained cell proliferation experienced by the cells without drug addition, i.e., 100%. This approach may give a more reliable indicator of potency changes by

assessing the relative response of reference and test samples compared directly to a zero drug response. Furthermore, the use of many controls may facilitate a more accurate datum line for uninhibited biological activity of the cells upon which to base the analysis on.

The dose-response profile expressed as a relative percentage viability for both 0.5 mg/mL and 6 mg/mL stored infusions is similar to the absorbance-concentration plots. Figure 8 shows the relative percentage viability dose-response profile for the 0.5mg/ml infusion test sample.

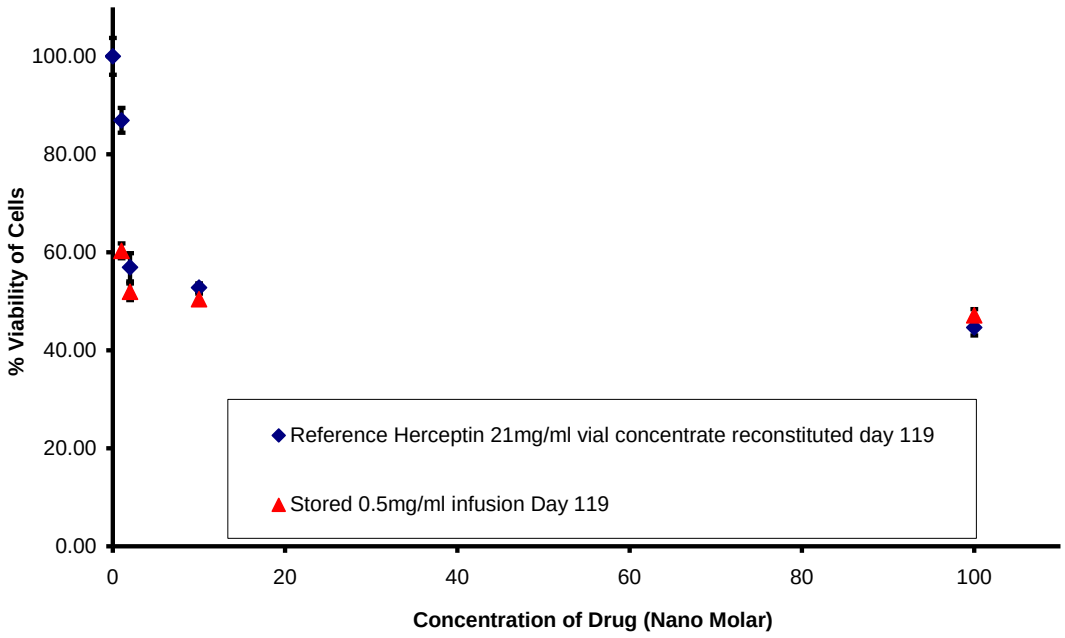

Figure 8 Plot showing normalised dose-response. 0.5 mg/mL infusion test sample and reference Trastuzumab expressed as percentage viability of maximum uninhibited cell viability (no drug) set to 100%.

The difference between standard and test sample is best seen on a reduced scale plot for both 0.5 mg/mL and 6 mg/mL stored infusions (figure 9 and 10). The percentage

viability at 1 and 2 nM for reference and test samples are shown in tables 3 and 4. The test samples show an apparent decrease in viability or increase in potency.

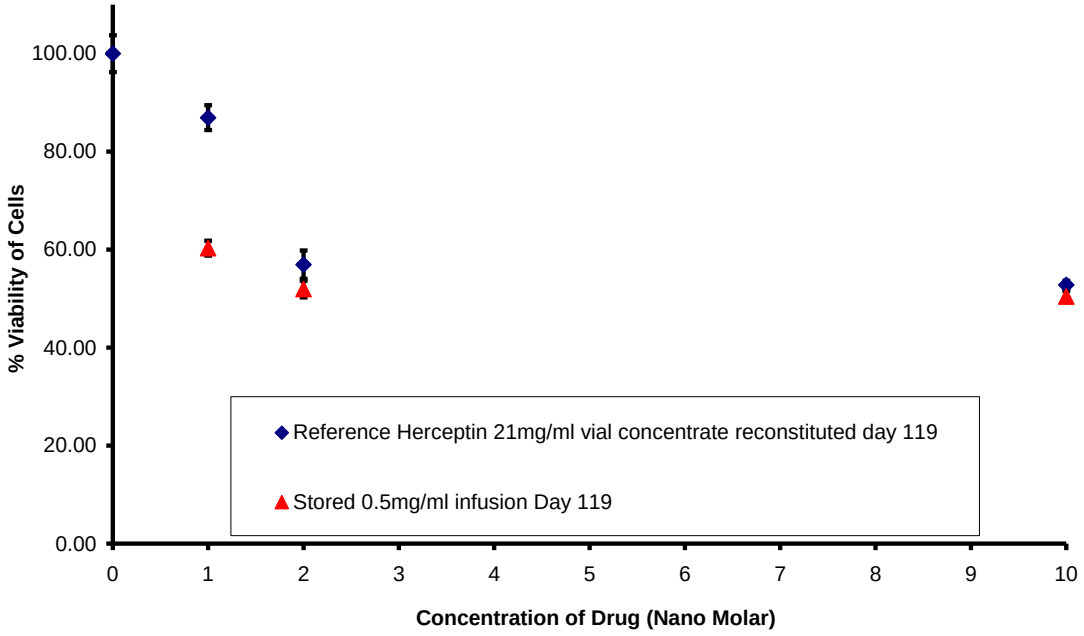

Figure 9 Plot showing normalised dose-response with reduced scale (0 – 10 nM). 0.5 mg/mL infusion test sample and reference Trastuzumab expressed as percentage viability of maximum uninhibited cell viability (no drug) set to 100%. The percentage viability can be seen at 1 and 2 nM for reference and test sample: reference 87% and 57%, test sample 60% and 52% respectively.

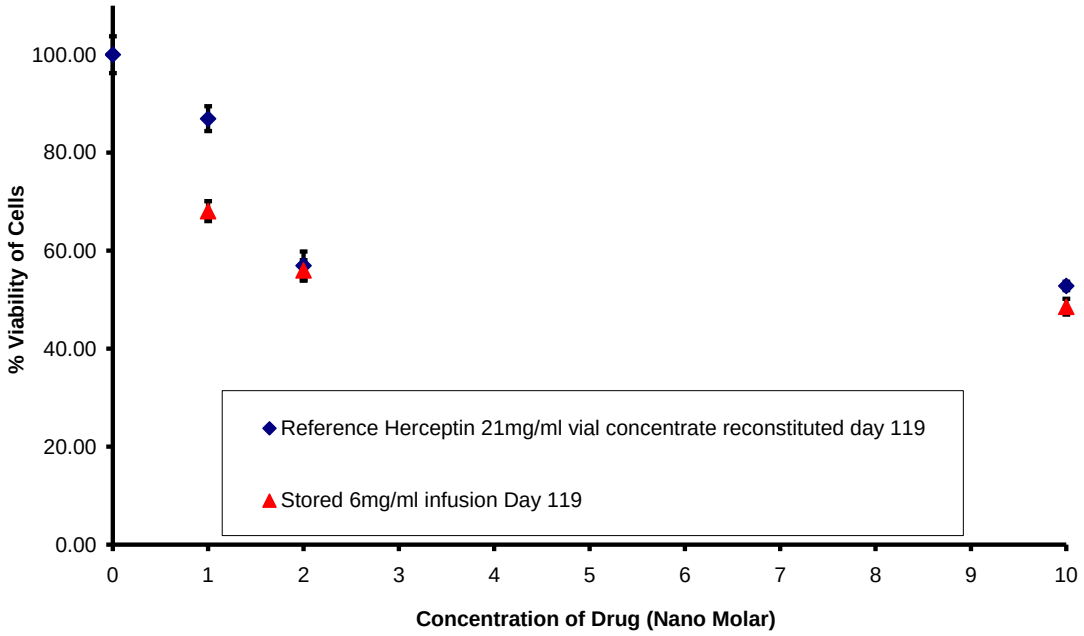

Figure 10 Plot showing normalised dose-response with reduced scale (0 – 10 nM). 6 mg/mL infusion test sample and reference Trastuzumab expressed as percentage viability of maximum uninhibited cell viability (no drug) set to 100%. The percentage viability can be seen at 1 and 2 nM for reference and test sample: reference 87% and 57%, test sample 68% and 56% respectively.

Trastuzumab concentration / nM	% Viable Cells Reference / control	% Viable Cells 0.5 mg/mL infusion	% difference (Reference - Test)
0	100		
1	87	60	27
2	57	52	5
10	53		
100	45		

Table 3 Normalised percentage cell viability is shown for 0.5 mg/mL test infusion sample and compared to reference viability at point of measurement (1 and 2 nM). Percentage difference is shown in the last column. A positive percentage difference indicates an apparent increase in potency.

Trastuzumab concentration / nM	% Viable Cells Reference / control	% Viable Cells 6 mg/mL infusion	% difference (Reference - Test)
0	100		
1	87	68	19
2	57	56	1
10	53		
100	45		

Table 4 Normalised percentage cell viability is shown for 6 mg/mL test infusion sample and compared to reference viability at point of measurement (1 and 2 nM). Percentage difference is shown in the last column. A positive percentage difference indicates an apparent increase in potency.

6.5.1.8 Stability of 0.1 mg/ml infusion bags and 21 mg/ml vial concentrate

A comparison of Trastuzumab at 0.1 mg/mL and the 21 mg/mL reconstituted concentrate in the original vial over the study period may provide insight into the stability at extremes of concentration which bracket the therapeutic range of concentration.

The manufacturers indicate a shelf life of up to 28 days post reconstitution of Trastuzumab when reconstituted with bacteriostatic water for injection (BWFI) containing benzyl alcohol (1.1%) in its original container in accordance with the United States Pharmacopoeial Convention (USP). This is indicative of acceptable stability with a preservative present which may actually decrease physical stability

(Philo & Arakawa 2009; Kaiser & Kramer 2011). This suggests a better physical and similar microbiological stability should be shown under aseptic conditions when reconstituted with sterile water for injection as is the practise in Europe. Moreover, this may support stability of 28 days in solutions more dilute than the concentrate as aggregate formation is less likely to occur at lower concentration (Shire et al. 2004). This may be supported by Kaiser and Kramer in their 28 day study where infusion concentrations 0.4 and 4.0 mg/mL showed no signs of physical instability (Kaiser & Kramer 2011).

In contrast, in this study visible particulates were found after 7 days with the 0.1 mg/mL infusion. In the Kaiser and Kramer study (Kaiser & Kramer 2011) the lowest concentration investigated was 0.4 mg/mL. This is consistent with the view that at a lower limit of concentration, i.e., below 0.4 mg/mL, the formulation becomes more susceptible to aggregation (Barnes 2012). The biological assay did not reflect the loss of active drug by showing a decrease in potency (figure 11 and table 5). The normalised cell viability difference was 21% and 2% at 1 and 2 nM respectively; showing an apparent increase in potency. This may imply that the assay has not detected these changes due to an error in the actual concentration of the test sample prior to dilution or is masked by systematic error in the performance of the assay. There is a relatively large positive difference (21%) or decrease in viability at 1 nM of the test sample compared to the reference which may infer a greater concentration for the 0.1 mg/mL infusion. This in part would explain the observed apparent increase in potency. Values of a similar magnitude at 1 nM were found with the rest of the infusion test concentrations whilst the concentrate in the original vial recorded a 5% increase in apparent potency at 1nM with a small decrease at 2 nM of -3% compared to reference drug (table 6). This observation when considered with the consistent preparation of all test samples, using identical dilution steps, infers that the source of error may originate in the formulation of the infusion bags and variation of biological response.

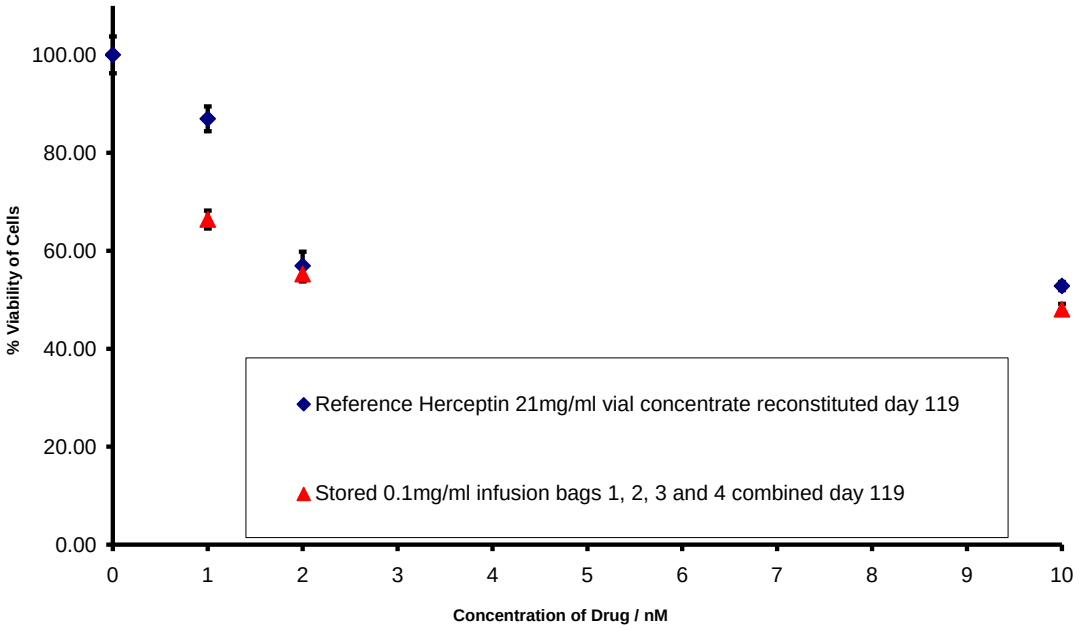

Figure 11 Plot showing normalised dose-response with reduced scale (0 – 10 nM). 0.1 mg/mL infusion test sample and reference Trastuzumab expressed as percentage viability of maximum uninhibited cell viability (no drug) set to 100%. The percentage viability can be seen at 1 and 2 nM for reference and test sample: reference 87% and 57%, test sample 66% and 55% respectively. Replicates = 32.

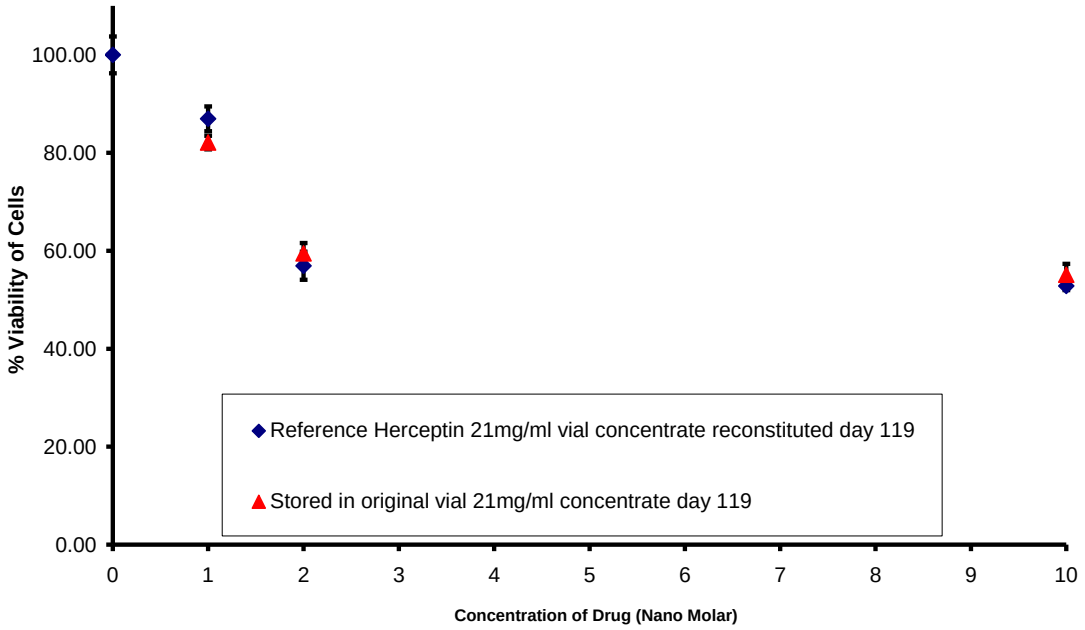

Figure 12 Plot showing normalised dose-response with reduced scale (0 – 10 nM). 21 mg/mL concentrate test sample from original vial and reference Trastuzumab expressed as percentage viability of maximum uninhibited cell viability (no drug) set to 100%. The percentage viability can be seen at 1 and 2 nM for reference and test sample: reference 87% and 82%, test sample 66% and 60% respectively. Replicates = 4.

Trastuzumab concentration / nM	% Viable Cells Reference / control	% Viable Cells 0.1 mg/mL infusion	% difference (Reference - Test)
0	100		
1	87	66	21
2	57	55	2
10	53		
100	45		

Table 5 Normalised percentage cell viability is shown for 0.1 mg/mL test infusion sample and compared to reference viability at point of measurement (1 and 2 nM). Percentage difference is shown in the last column. A positives value indicates an apparent increase in potency at 1 and 2 nM.

Trastuzumab concentration / nM	% Viable Cells Reference / control	% Viable Cells 21 mg/mL infusion	% difference (Reference - Test)
0	100		
1	87	82	5
2	57	60	-3
10	53		
100	45		

Table 6 Normalised percentage cell viability is shown for 21 mg/mL test infusion sample and compared to reference viability at point of measurement (1 and 2 nM). Percentage difference is shown in the last column. A negative value at 2 nM indicates an apparent decrease in potency.

6.5.1.9 Summary of normalised biological activity results for day 119

Table 7 shows a summary of the results for each concentration of infusion and the original vial concentrate. Values are relatively consistent between infusion samples with viability difference at 1 nM recording a higher value than at 2 nM which indicates an apparent increase in active concentration or potency. In contrast the concentrate stored in original vial mirrored this behaviour but showed only a relatively small increase in activity at 1 nM with a small decrease in activity at 2 nM. These observations are consistent with the view that the 1 nM and 2 nM concentrations cover the region of maximum dose response for all samples.

The apparent increase in efficacy with time could be related to dimer content; due to increased binding compared to the monomer (Wolff et al. 1993). This has been

reported as giving a 10 times increase in potency with thioether bonded dimers (Wolff et al. 1993). Furthermore, it has been reported that antibody dimers formed by introducing a thioether linkage become potent anti-tumour agents (Ghetie et al. 1997).

Trastuzumab concentration / nM	**% difference in viability (Reference - Test) Day 119**			
	0.1 mg/mL	**0.5 mg/mL**	**6 mg/mL**	**21 mg/mL**
1	21	27	19	5
2	2	5	1	-3

Table 7 Summary of normalised biological activity results for day 119. The table shows % viability difference at 1 nM and 2 nM assay concentrations for test infusions and concentrate stored in original vial compared to reference drug reconstituted and tested in parallel. Values are relatively consistent between infusion samples with activity at 1 nM recording a higher value. In contrast the concentrate stored in original vial showed a smaller increase in potency at 1 nM and a small decrease in potency at 2 nM. A t-Student test with a significance threshold of < 0.05 showed no significant difference between day 119 infusions and fresh drug: $p = 0.46$ for the 0.5 mg/mL concentration at 1 nM and $p = 0.62$ at 2nM, for the 6 mg/mL infusions $p = 0.71$ and 0.22 for the 1 nM and 2 nM respectively.

A biological assay is the most direct way to assess functional stability and thus became an important aspect of developing a strategy for studying the stability of Trastuzumab infusions.

There was no loss in biological activity of Trastuzumab indicating an acceptable functional stability during storage. The in-use stability studies which were compared to this study did not employ a biological assay. However Pabari et al. (2011) used a biological assay, in addition to physicochemical methods, to assess the effect on functional activity of various processing stresses. Pabari et al. (2011) showed that activity of Trastuzumab did not significantly change after sonication, freeze-thawing, lyophilisation, spray-drying and encapsulation. These results suggest that the Trastuzumab molecule can retain its biological activity, as determined by a cellular assay, under manufacturing and in-use conditions.

Paul et al. (2012) report that a direct cytotoxicity assay showed that Rituximab remained fully efficacious for 6 months at 4 ^{o}C. However, direct cytotoxicity is the incorrect mechanism that Rituximab exerts its effect *in vivo*. The results are presented as IC50, IC25 and area under the curve. It has been stated that using the data in this way would lack the necessary sensitivity over a long period of time (Watts 2012). Furthermore, small changes such as 5% would not be detected due to variation in data: IC50 time 0 = 137.2 +- 28.18 µg/mL versus time = 6 months 125.8_+- 36.5 µg/mL.

The biological activity of Pertuzumab, Rituximab and Infliximab was assessed at the limit of their SPC shelf-life, typically one or two days (Parry et al. 2014). The authors report greater or equal biological activity and fewer aggregates than freshly prepared infusions. Trastuzumab was also assessed and showed increase in functional activity at the concentrations tested. A Trastuzumab infusion at a concentration of 3.15 mg/mL showed just under a 5% increase in biological activity at the SPC shelf-life limit (Parry et al. 2014). These results may, at least in part, show agreement with this study.

Sources of error

A primary source of error was the cell counting and seeding process which has been discussed in chapter 4. However, satisfactory calibration data and control data may provide assurance that the cells are growing uniformly. Some error may originate with the variation in cell response to the drug. The cellular response should be shown in variation of cell numbers and therefore absorbance read out. If this is the case, the amplification step used in the CCK8 assay may magnify this error. High cell density may result in higher background signal which will contribute to instrumental inaccuracy (Bohn 2015). This error is mitigated by optimisation of cell density. Additionally variation may be between wells (Lundholt et al. 2003). Cells in the outer wells may react differently to the cells in the inner wells, showing uneven growth known as the edge effect (Lundholt et al. 2003). This may be due to a temperature differential when the plates are incubated (Bohn 2015).

6.6 CONCLUSIONS

The biological activity data for the whole study shows no loss of efficacy over the period of 119 days for all infusion bag concentrations. However, visible particulates were found after 7 days with the 0.1 mg/mL infusion. Although this concentration is below therapeutic relevant concentrations it does highlight the need to consider physicochemical stability data together with biological potency to provide a more complete profile of stability. The performance of the stored concentrate in the original vial compared to the reference sample, which originates from freshly reconstituted concentrate, displayed a similar dose-response profile to the infusion samples and recorded relatively small percentage differences in viability relative to the reference Trastuzumab. The similarities of the dose-response profiles suggest that this behaviour originates from cellular response rather than sample preparation. In contrast the infusion bag samples showed a larger deviation from the reference drug. This implies that the differences between the infusion and the reference may be in part an artefact of bag preparation.

CHAPTER 7

7. GENERAL DISCUSSION AND CONCLUSION

7.1 Introduction

There is an established body of published literature relevant to the in-use stability of injectable drugs that are defined as small molecules. Publications such as the Hand book on Injectables provide guidance in the form of summaries of this information regarding clinical use of parenteral medication (American Society of Health-System Pharmacists 2014). Additionally the Infostab website publishes an international database (Stabilis) of compatibilities and stabilities of injectable drugs (Infostab 2014).

The approach to conducting stability studies is documented to an extent but is generally confined to that applicable for the manufacturing of new drug substances and drug products (European Medicines Agency 2003). Furthermore, only limited reference is made to biologically-derived drugs known as biologics (European Medicines Agency 2006).

Biologic drugs require an unique approach to stability that takes into consideration their complex and labile protein nature where conventional testing such as accelerated testing may not be suitable (European Medicines Agency 2006). Without doubt, this necessitates a more thorough understanding of potential degradation pathways and of their mode of action than that for small molecule medications. Furthermore, application of suitable methodology and adequate assessment of criteria are essential to enable published data to be of value (Barnes 2012). These requirements have exacerbated the absence of in-use knowledge of biologics. Therefore there is a need for appropriate stability data for biologics including monoclonal antibodies such as Trastuzumab. Thus it is the aim of this study to some extent address this gap in knowledge for Trastuzumab once reconstituted and further diluted for use.

It is a common fact that manufacturers of parenteral drugs only disclose a limited amount of stability information which is relevant once the drug is reconstituted for use. This may take the form of statement, within the summary of product characteristics, limiting the use of a prepared infusion to 24 hours. This reflects stability from a microbiological perspective. Moreover, the manufacturer is not concerned with in-use stability and therefore may not possess pertinent data for the hospital pharmacist. Alternatively, if stability testing has been performed there may be a reluctance to disclose this information. This situation requires that studies must be performed to meet the need for in-use stability data. This is beginning to change although often published data is of limited value due to the use of inappropriate drug concentrations and inadequate number or selection of stability criteria investigated. More specifically, with Trastuzumab there have been some recent publications which have not included biological testing of potency (Paul et al. 2013; Pabari et al. 2013). These studies are therefore incomplete as they lack important information concerning stability in relation to the mode of drug action.

In July 2013 a reference procedure in the form of a USP summary validation report for Trastuzumab had been developed (USP 2013). At the time of writing this document is not yet an official USP document. The study described here precedes these publications but has some shared common aims with the USP principle requirements. A consensus is now evolving as to which tests should be included in a stability study for a biologic drug. A comparison of the findings of this study with other protein-based drugs and further studies on Trastuzumab are presented below.

This study was in agreement with other studies showing long-term stability of in-use marketed protein-based drugs beyond that stated in the summary of product characteristics. Long-term stability has been defined as an acceptable stability for a minimum of 2 weeks (Vigneron et al. 2014).

Paul et al. (2012 (a)) showed that re-packaged Bevacizumab in 1 mL syringes at a concentration of 25 mg/mL was stable at 4°C for 3 months. Although long term stability was reported no determination of biological activity was attempted. In contrast the choice of techniques used for physical stability was acceptable, although only data for time points 0 and 90 days are reported. SE-LC showed a similar

monomer and aggregate profile found in the Trastuzumab study. However, detection was at a single wavelength of 280 nm and not the sensitive dual method used in this study. A later study on Bevacizumab also showed continued stability on re-packaged drug for a period of 6 months at 5°C (Khalili et al. 2015). Determination of biological activity was included in this study, using a biochemical assay in the form of a binding assay. The binding of immobilised vascular endothelial growth factor (VEGF) to Bevacizumab was determined by surface plasmon resonance (SPR) (Huber & Mueller 2006). VEGF is the therapeutic target of Bevacizumab (European Agency for the Evaluation of Medicinal Products (EMEA) 2005a). This form of binding assay is more sensitive than an ELISA (Barnes 2012), although structural changes remote from the binding site are unlikely to be detected (Barnes 2012). It is more usual, as in this study, to use a cell-based assay to measure a biological end-point or action (Weinberg et al. 2005). SDS-PAGE and SE-LC analysis showed no changes in the presence of higher molecular weight species or degradants between time zero and 6 months. In contrast, in the Trastuzumab studies, including this study, aggregates were not detected by SDS-PAGE (Kaiser & Kramer 2011; Pabari et al. 2013). These results are consistent with reported silicone oil contamination from re-packaging into syringes which has been associated with increased levels of aggregates (Liu et al. 2011).

Rituximab was reported has showing a 6 months stability at 4°C (Paul et al. 2012). A cell-based assay was used employing a XTT colorimetric test and Raji cells expressing the CD20 receptor therapeutic target (Glennie et al. 2007). However, the direct cytotoxicity effect measured was not clinically relevant (Watts 2012). Paul et al. (2012) report that physical and chemical attributes remained unchanged. Rituximab showed only one peak by SE-LC with detection at 280 nm. The absence of higher molecular weight species is supported by the result of Hernández-Jiménez et al. (2016). Injecting undiluted samples, to prevent masking of results, they found no evidence of aggregates using a more sensitive UV detection of 214 nm.

The key findings of this study and the results of the other studies support the hypothesis: Trastuzumab is sufficiently robust to remain unaltered following reconstitution or dilution to clinically relevant concentrations when stored in appropriate containers under controlled normal conditions of storage. However, regarding the cellular assay CCK8 it must be stated that it is in the developing stages and the results are preliminary. Further experiments will be required before the usefulness of the CCK8 assay can be relied on.

Furthermore, Trastuzumab has been reported to be resistant to a range of processing stresses which supports an acceptable stability under the considerably less demanding conditions of pharmacy storage.

7.2 Future work

This study employed a relatively small number of techniques compared to the USP validation document. Whilst more techniques may garner more information the question should be which techniques are appropriate for an in-use stability study. For example the USP document has a significant number of methods for identification of Trastuzumab and assessing process related degradation or side-products resulting from oxidation and deamination reactions. These processes are more probable during manufacturing and therefore the associated methods may not be appropriate for an in-use stability study.

Pharmacists would generally attempt to decrease headspace in an IV bag to decrease contact with air. This may decrease oxygen absorption but more importantly may help to decrease protein adsorbing at the interface and undergoing a conformational change and aggregation. In fact, the unavoidable presence of dissolved oxygen in the infusion has not caused oxidation in the studies discussed. However, for home healthcare patients the transportation of infusions may expose the drug to stresses not normally found in a hospital and therefore requires more testing. This further highlights the difference between what is often the manufacturer's perspective and that of end-user. However, Genentech have recently presented a colorimetric assay for assessing transportation stress and the potential damage to a biologic drug in an IV bag at the

speciality cancer congress ECOP 2014 in Krakow. This represents a significant and unprecedented engagement by the manufacturing community into problems encountered by end-user.

The NHS guidance document suggests a suitable range of techniques covering physical and chemical aspects of in-use stability. However biological assessment, specific to the pharmaceutical effect of the drug, must always be included as it is central to the NHS stability criteria guidance and a complete stability assessment. Biological assessment may be best served utilising some of the newer cell-based and biochemical approaches which have become available. However, the selection of biological techniques ultimately depends on the drug and its mode of action.

Cell proliferation or viability assays assess the direct effect on the cancer cells but there are other functions involved in vivo. Another functional aspect of biologic drug action is the interaction with the immune system. In particular monoclonal antibody-based drugs may utilise antibody-dependent cellular cytotoxicity (ADCC) in their mechanism of action. The bound antibody mediates with the immune system via natural killer effector cells with the end point being cell lysis.

The ADCC function has been applied to a limited extent as a basis for a cell-based assay that utilised natural killer cells which are a component of the peripheral blood mononuclear cells (PBMC) (Timonen 1981). The assay is complex to perform and shows a high degree of variability which has led to the development of a ADCC-gene reporter alternative (Parekh et al. 2012). An engineered Jurkat cell-line was used for the effector cell and a luciferase reporter end-point generating a bioluminescence read-out. For read-out the antibody must be bound to the target cell and Fc receptor on the Jurkat cell (Parekh et al. 2012). The ADCC-gene assay has recently being developed into a kit format by Promega (2014).

Though often used for assessment of functionality of antibodies ELISA has recently been applied to assess higher order structure to aid biologic drug development (Wang et al. 2013). In this case the antibody itself is subjected to antibody interrogation by a panel of antibodies which report on its 3-dimensional structure or higher order structure. Polyclonal antibodies raised to the linear peptide sequence of the

monoclonal antibody interrogate the 3-dimensional structure of the therapeutic protein. A polyclonal antihuman antibody-biotin conjugate completes the sandwich ELISA. A streptavidin-HRP (horse radish peroxidase) conjugate detects the complex through the turnover of a TMB substrate read-out. If hidden epitopes are exposed, as little as 0.1%, due to structural change this will show itself in the ELISA read out (Wang et al. 2013).

The antibody array read-out would allow the determination of small structural changes between fresh and aged drug during storage. The ELISA kit-format (Array Bridge Inc.) has the ability to identify local changes in the molecule and the proportion of molecular population that has undergone these changes (Wang et al. 2013). In contrast physicochemical techniques are not as sensitive at detecting localised change in higher order structure and report on the average response (Wang et al. 2013).

The NHS (UK) shelf-life study showed that the secondary structure of Trastuzumab did not change and is indicative of a robust structure. ATR-FT-IR provided no evidence of change and equally circular dichroism (CD) in another study (Pabari et al. 2013). Thus it may be appropriate for techniques which probe secondary structure to be omitted from a study. Moreover, if other physicochemical techniques have been previously shown to give no evidence of change in a molecule during a study it may be provident not to include such tests in future studies.

The omission of redundant tests would allow other methods which provide pertinent stability information to take their place within a study design. One such technique would be glycan profiling using normal phase chromatography. Changes in glycan content have a profound effect on biological activity. This chemical change in the molecule can be correlated with the biological assay to provide structure-function information on changes in the glycan profile. The glycan profile may also influence the charge heterogeneity of the protein molecule and can have an important effect on stability and efficacy. Charge heterogeneity may be assessed by cation exchange chromatography. This technique has become more widely adopted and should be considered to be included in a future study.

Lastly, with the introduction of Trastuzumab for subcutaneous delivery by the NHS less Trastuzumab will be prepared in IV bags. However, the principles and approach developed in this study are applicable to monoclonal antibody drugs in general including Rituximab and Bevacizumab (Paul et al. 2012 (a); Paul et al. 2012 (b)). Studies have been published on these two important drugs, however as with Trastuzumab, there is either an absence of biological assessment or the assay selected is testing a none-clinically relevant effect. Thus highlighting a need for research into a better understanding of the important area of pharmaceutical action.

7.3 Conclusion

In conclusion it was found that Trastuzumab is a relatively robust molecule under storage conditions likely to be encountered in a hospital pharmacy. The outcome of this was the shelf-life of Trastuzumab was recommended to be extended to 28 days for Trastuzumab stored in polyolefin IV bags at concentrations between 0.5 mg/mL and 6 mg/mL with 0.9% saline at 2 ^{o}C to 8 ^{o}C. However, infusions with concentrations below 0.5 mg/mL are not recommended for storage.

The extension of the shelf-life of Trastuzumab infusions has enabled Clatterbridge Hospital to better utilise Trastuzumab drug resources by treating more patients and providing a substantial health economic benefit.

The potential of using the CCK8 assay as part of a shelf-life stability study has been explored. However, further work is required before its usefulness can be depended on.

References

(a) Allen, L.V.I.J. of P.C., 2011. pH and Solubility, Stability, and Absorption, Part 1. *Science and Technology for the Hospital Pharmacist*. Available at: http://compoundingtoday.com/Newsletter/Science_and_Tech_1111.cfm [Accessed July 25, 2014].

(b) Allen, L.V.I.J. of P.C., 2011. pH and Solubility, Stability, and Absorptin part 2. *Science and Technology for the Hospital Pharmacist*. Available at: http://compoundingtoday.com/Newsletter/Science_and_Tech_1112.cfm [Accessed July 25, 2014].

Allwood, M. & Wilkinson, A.-S., 2013. Assessing shelf life of injectable biologicals in ready-to-administer containers. *European Journal of Hospital Pharmacy*, 20(3), p.146.

American Society of Health-System Pharmacists, 2014. Handbook on Injectable Drugs L. A. Trisell, ed. , p.1,280. Available at: http://www.ahfsdruginformation.com/product-hid.aspx [Accessed September 3, 2014].

Andya, J.D., Hsu, C.C. & Shire, S.J., 2003. Mechanisms of aggregate formation and carbohydrate excipient stabilization of lyophilized humanized monoclonal antibody formulations. *AAPS pharmSci*, 5(2), p.E10.

Anon, 2013. Biosimilar drugs step up complexity. *Chemistry World*, p.16.

Arakawa, T., Philo, J. S., Ejima, D., Tsumoto, K., & Arisaka, F., 2006. Aggregation Analysis of Therapeutic Proteins, Part 1: General Aspects and Techniques for Assessment. *BioProcess International*, 4(November), pp.42–43.

Arakawa, T., Philo, J. S., & Kita, Y., 2001. Factors affecting short-term and long-term stabilities of proteins. *Advanced drug delivery reviews*, 46, pp.307–326.

Arakawa, T., Philo, J.S. & Kita, Y., 2001. Kinetic and thermodynamic analysis of thermal unfolding of recombinant erythropoietin. *Bioscience, biotechnology, and biochemistry*, 65(6), pp.1321–7.

Aubert, C. Mathis, P., Eker, A. P., & Brettel, K., 1999. Intraprotein electron transfer between tyrosine and tryptophan in DNA photolyase from Anacystis nidulans. *Proceedings of the National Academy of Sciences of the United States of America*, 96(10), pp.5423–5427.

Balasubramanian, D. & Kanwar, R., 2002. Molecular pathology of dityrosine cross-links in proteins: Structural and functional analysis of four proteins. *Molecular and Cellular Biochemistry*, 234-235(1), pp.27–38.

Bardin, C., Astier, A., Vulto, A., Sewell, G., Vigneron, J., Trittler, R., Pinguet, F., 2011. Guidelines for the practical stability studies of anticancer drugs: A European consensus conference. *Annales Pharmaceutiques Francaises*, 69(4), pp.221–231.

Barnes, A., 2012. A STANDARD PROTOCOL for DERIVING and ASSESSMENT of STABILITY Part 2 – Aseptic Preparations (Biopharmaceuticals) October 2012. , (October). Available at: http://mabstalk.com/a-standard-protocol-for-deriving-and-assessment-of-stability/ [Accessed September 26, 2013].

Barrett, A. Roques, T., Small, M., & Smith, R. D., 2006. How much will Herceptin really cost ? *British medical journal*, 333, pp.1118–1120.

Barth, A. & Zscherp, C., 2002. What vibrations tell about proteins. *Quarterly Reviews of Biophysics*, 35(4), pp.369–430.

Beck, A. Bussat, M.-C., Zorn, N., Robillard, V., Klinguer-Hamour, C., Chenu, S., Haeuw, J.-F., 2005. Characterization by liquid chromatography combined with mass spectrometry of monoclonal anti-IGF-1 receptor antibodies produced in CHO and NS0 cells. *Journal of chromatography. B, Analytical technologies in the biomedical and life sciences*, 819(2), pp.203–18.

Bee, J.S. Randolph, T. W., Carpenter, J. F., Bishop, S. M., & Dimitrova, M. N., 2011. Effects of surfaces and leachables on the stability of biopharmaceuticals. *Journal of pharmaceutical sciences*, 100(10), pp.4158–70.

Blessy, M. Patel, R. D., Prajapati, P. N., & Agrawal, Y. K., 2014. Development of forced degradation and stability indicating studies of drugs—A review. *Journal of Pharmaceutical Analysis*, 4(3), pp.159–165.

Bohn, J., 2015. 10 Tips for Successful Cell Based Assays - Enzo Life Sciences. Available at: http://www.enzolifesciences.com/science-center/technotes/2015/april/10-tips-for-successful-cell-based-assays/ [Accessed July 6, 2016].

Bond, M.D., Panek, M. E., Zhang, Z., Wang, D., Mehndiratta, P., Zhao, H., Volkin, D. B., 2010. Evaluation of a dual-wavelength size exclusion HPLC method with improved sensitivity to detect protein aggregates and its use to better characterize degradation pathways of an IgG1 monoclonal antibody. *Journal of Pharmaceutical Sciences*, 99(6), pp.2582–2597.

Brescia, P. & Banks, P., 2009. Quantifying Cytotoxicity of Thiostrepton on Mesothelioma Cells using MTT Assay and the Epoch™ Microplate Spectrophotometer. BioTek Instruments. *Inc. USA*. Available at: http://www.biotek.com/resources/articles/quontification-cell-viability-epoch.html [Accessed January 10, 2015].

Brousseau, J., 2008. Article: Detecting protein aggregates in biological actives using light scattering and chromatography. *European Laboratory Scientist*. Available at:

http://www.kdsi.ru/upload/iblock/de2/de23b4bdef75b808a0669b93bed7caa3.pdf [Accessed October 27, 2011].

Budman, D.R., Tai, J. & Calabro, A., 2007. Fluvastatin enhancement of trastuzumab and classical cytotoxic agents in defined breast cancer cell lines in vitro. *Breast cancer research and treatment*, 104(1), pp.93–101.

Burckbuchler, V. Mekhloufi, G., Giteau, a P., Grossiord, J. L., Huille, S., & Agnely,f., 2010. Rheological and syringeability properties of highly concentrated human polyclonal immunoglobulin solutions. *European journal of pharmaceutics and biopharmaceutics : official journal of Arbeitsgemeinschaft für Pharmazeutische Verfahrenstechnik e.V*, 76(3), pp.351–6.

Busse, D. Doughty, R. S., Ramsey, T. T., Russell, W. E., Price, J. O., Flanagan, W. M.,Arteaga, C. L., 2000. Reversible G(1) arrest induced by inhibition of the epidermal growth factor receptor tyrosine kinase requires up-regulation of p27(KIP1) independent of MAPK activity. *The Journal of biological chemistry*, 275(10), pp.6987–95.

Carpenter, J.F., Prestrelski, S.J. & Dong, A., 1998. Application of infrared spectroscopy to development of stable lyophilized protein formulations. *European journal of pharmaceutics and biopharmaceutics : official journal of Arbeitsgemeinschaft für Pharmazeutische Verfahrenstechnik e.V*, 45(3), pp.231–8.

Carter, P., Presta, L., Gorman, C. M., Ridgway, J. B., Henner, D., Wong, W. L., Shepard, H. M. 1992. Humanization of an anti-p185HER2 antibody for human cancer therapy. *Proceedings of the National Academy of Sciences of the United States of America*, 89(10), pp.4285–9.

Carter, P.J., 2006. Potent antibody therapeutics by design. *Nature reviews. Immunology*, 6(5), pp.343–57.

Chi, E.Y. Krishnan, S., Randolph, T. W., & Carpenter, J. F. , 2003. Physical stability of proteins in aqueous solution: mechanism and driving forces in nonnative protein aggregation. *Pharmaceutical research*, 20(9), pp.1325–36.

Cho, H.-S. Mason, K., Ramyar, K. X., Stanley, A. M., Gabelli, S. B., Denney, D. W., & Leahy, D. J., 2003. Structure of the extracellular region of HER2 alone and in complex with the Herceptin Fab PDB 1n8z. *Nature*, 421(6924), pp.756–60.

Collins, D.M. O'Donovan, N., McGowan, P. M., O'Sullivan, F., Duffy, M. J., & Crown, J.., 2012. Trastuzumab induces antibody-dependent cell-mediated cytotoxicity (ADCC) in HER-2-non-amplified breast cancer cell lines. *Annals of oncology : official journal of the European Society for Medical Oncology / ESMO*, 23(7), pp.1788–95.

Colombo, M., Corsi, F., Foschi, D., Mazzantini, E., Mazzucchelli, S., Morasso, C., Verderio, P., 2010. HER2 targeting as a two-sided strategy for breast cancer diagnosis and treatment: Outlook and recent implications in nanomedical

approaches. *Pharmacological research : the official journal of the Italian Pharmacological Society*, 62(2), pp.150–65.

Cornes, P., 2012. The economic pressures for biosimilar drug use in cancer medicine. *Targeted oncology*, 7 Suppl 1, pp.S57–67.

Couston, R.G., Skoda, M. W., Uddin, S., & van der Walle, C. F., 2012. Adsorption behavior of a human monoclonal antibody at hydrophilic and hydrophobic surfaces. *mAbs*, 5(1), pp.126–39.

Creed, D., 1984a. THE PHOTOPHYSICS AND PHOTOCHEMISTRY OF THE NEAR-UV ABSORBING AMINO ACIDS-I. TRYPTOPHAN AND ITS SIMPLE DERIVATIVES. *Photochemistry and Photobiology*, 39(4), pp.537–562.

Creed, D., 1984b. THE PHOTOPHYSICS AND PHOTOCHEMISTRY OF THE NEAR-UV ABSORBING AMINO ACIDS-II. TYROSINE AND ITS SIMPLE DERIVATIVES. *Photochemistry and Photobiology*, 39(4), pp.563–575.

Creed, D., 1984c. THE PHOTOPHYSICS AND PHOTOCHEMISTRY OF THE NEAR-UV ABSORBING AMINO ACIDS-III. CYSTINE AND ITS SIMPLE DERIVATIVES. *Photochemistry and Photobiology*, 39(4), pp.577–583.

Cromwell, M.E.M., Hilario, E. & Jacobson, F., 2006. Protein aggregation and bioprocessing. *The AAPS journal*, 8(3), pp.E572–9.

Crowther, J.R., 2000. The ELISA guidebook. *Methods in molecular biology (Clifton, N.J.)*, 149, pp.III–IV, 1–413.

Cumming, G., Fidler, F. & Vaux, D.L., 2007. Error bars in experimental biology. *The Journal of cell biology*, 177(1), pp.7–11.

Das, T.K., 2012. Protein particulate detection issues in biotherapeutics development--current status. *AAPS PharmSciTech*, 13(2), pp.732–46.

Daugherty, A.L. & Mrsny, R.J., 2006. Formulation and delivery issues for monoclonal antibody therapeutics. *Advanced drug delivery reviews*, 58(5-6), pp.686–706.

Davies, M.J., 2003. Singlet oxygen-mediated damage to proteins and its consequences. *Biochemical and Biophysical Research Communications*, 305(3), pp.761–770.

Davies, M.J. & Truscott, R.J.W., 2001. Photo-oxidation of proteins and its role in cataractogenesis. *Journal of Photochemistry and Photobiology B: Biology*, 63(1-3), pp.114–125.

Dharati, R., 2007. Forced Degradation Study. authorSTREAM. Available at: http://www.authorstream.com/Presentation/Amitsss15-1453059-forced-degradation-study-dharati/ [Accessed October 5, 2016].

Dill, K.A., Alonso, D.O. V. & Hutchinson, K., 1989. Thermal stabilities of globular proteins. *Biochemistry*, 28(13), pp.5439–5449.

Dong, A. Prestrelski, S. J., Dean Allison, S., & Carpenter, J. F., 1995. Infrared Spectroscopic Studies of Lyophilization- and Temperature-Induced Protein Aggregation. *Journal of Pharmaceutical Sciences*, 84(4), pp.415–424.

Donyai, P. & Sewell, G.J., 2006. Physical and chemical stability of paclitaxel infusions in different container types. *Journal of oncology pharmacy practice : official publication of the International Society of Oncology Pharmacy Practitioners*, 12(4), pp.211–22.

Drug Bank, 2016. Trastuzumab. Available at: http://www.drugbank.ca/drugs/DB00072 [Accessed May 16, 2016].

Egan, W.M., 2009. Analytical Techniques for Characterizing Follow-on Protein Products NDA and BLA Pathways for Biologics. Pharmanet Boston.

Eichhorn, P.J. Gili, M., Scaltriti, M., Serra, V., Guzman, M., Nijkamp, W., Baselga, J., 2008. Phosphatidylinositol 3-kinase hyperactivation results in lapatinib resistance that is reversed by the mTOR/phosphatidylinositol 3-kinase inhibitor NVP-BEZ235. *Cancer research*, 68(22), pp.9221–30.

Elgert, K.D., 2009. Antibody structure and function. In *Immunology: understanding the immune system*. John Wiley and Sons, pp. 58–78.

European Agency for the Evaluation of Medicinal Products (EMEA), 2010. Annex 1 Summary of Product Characteristics Herceptin. Available at: http://www.ema.europa.eu/docs/en_GB/document_library/EPAR_-_Product_Information/human/000278/WC500074922.pdf [Accessed November 2, 2012].

European Agency for the Evaluation of Medicinal Products (EMEA), 2005a. Scientific Discussion Bevacizumab. Available at: http://www.ema.europa.eu/docs/en_GB/document_library/EPAR_-_Scientific_Discussion/human/000582/WC500029262.pdf [Accessed July 5, 2016].

European Agency for the Evaluation of Medicinal Products (EMEA), 2005b. Scientific Discussion Herceptin. Available at: http://www.ema.europa.eu/docs/en_GB/document_library/EPAR_-_Scientific_Discussion/human/000278/WC500049816.pdf [Accessed November 2, 2012].

European Medicines Agency, 2014. Guideline on similar biological medicinal products containing biotechnology-derived proteins as active substance : non-

clinical and clinical issues. Available at: http://www.ema.europa.eu/docs/en_GB/document_library/Scientific_guideline/2015/01/WC500180219.pdf [Accessed July 24, 2015].

European Medicines Agency, 1995. ICH Q5C Stability testing of biotechnological/biological products. *Current*, (November). Available at: http://www.ich.org/fileadmin/Public_Web_Site/ICH_Products/Guidelines/Quality/Q5C/Step4/Q5C_Guideline.pdf [Accessed October 27, 2011].

European Medicines Agency, 1999. ICH Q6B SPECIFICATIONS : TEST PROCEDURES AND A CCEPTANCE CRITERIA FOR BIOTECHNOLOGICAL / BIOLOGICAL P RODUCTS. , (March). Available at: http://www.ich.org/fileadmin/Public_Web_Site/ICH_Products/Guidelines/Quality/Q6B/Step4/Q6B_Guideline.pdf [Accessed October 2, 2012].

European Medicines Agency, 2003. ICH Stability Testing of New Drug Substances and Products Q1A(R2). *International Conference on Harmonisation of Technical Requirements for Registration of Pharmaceuticals for Human Use*, (February). Available at: http://www.ich.org/fileadmin/Public_Web_Site/ICH_Products/Guidelines/Quality/Q1A_R2/Step4/Q1A_R2__Guideline.pdf [Accessed October 12, 2012].

European Medicines Agency, 1998. ICH Topic Q1B Photostability Testing of New Active Substances and Medicinal Products. , (June 1996). Available at: http://www.ema.europa.eu/docs/en_GB/document_library/Scientific_guideline/2009/09/WC500002647.pdf [Accessed May 5, 2016].

European Medicines Agency, 2006. ICH Topic Q5C Quality of Biotechnological Products: Stability Testing of Biotechnological/Biological Products. , (December 1995). Available at: http://www.ema.europa.eu/docs/en_GB/document_library/Scientific_guideline/2009/09/WC500002803.pdf [Accessed October 12, 2012].

Franken, N.A.P. Rodermond, H. M., Stap, J., Haveman, J., & van Bree, C., 2006. Clonogenic assay of cells in vitro. *Nature protocols*, 1(5), pp.2315–9.

Freund, M., Carol, B. & York, N., 1964. FACTORS AFFECTING HAEMOCYTOMETER COUNTS OF SPERM CONCENTRATION IN HUMAN SEMEN. *Journal of the Society of Reproduction and Fertility*, 8, pp.149–155.

Garidel, P., Hoffmann, C. & Blume, A., 2009. A thermodynamic analysis of the binding interaction between polysorbate 20 and 80 with human serum albumins and immunoglobulins: a contribution to understand colloidal protein stabilisation. *Biophysical chemistry*, 143(1-2), pp.70–8.

Genentech, 2015. HER2 HER3 Dimerization | BioOncology. Available at: http://www.biooncology.com/research-education/her/dimer [Accessed January 9, 2015].

Ghetie, M. A., Podar, E. M., Ilgen, a, Gordon, B. E., Uhr, J. W., & Vitetta, E. S., 1997. Homodimerization of tumor-reactive monoclonal antibodies markedly increases their ability to induce growth arrest or apoptosis of tumor cells. *Proceedings of the National Academy of Sciences of the United States of America*, 94(14), pp.7509–14.

Gijsen, M. M., King, P., Perera, T., Parker, P. J., Harris, A. L., Larijani, B., & Kong, A., 2010. HER2 phosphorylation is maintained by a PKB negative feedback loop in response to anti-HER2 herceptin in breast cancer. *PLoS biology*, 8(12), pp.1–16.

Glennie, M.J., French, R. R., Cragg, M. S., & Taylor, R. P.., 2007. Mechanisms of killing by anti-CD20 monoclonal antibodies. *Molecular Immunology*, 44(16), pp.3823–3837.

Goldberg, M.E. & Chaffotte, A.F., 2005. Undistorted structural analysis of soluble proteins by attenuated total reflectance infrared spectroscopy. *Protein science*, 14, pp.2781–2792.

Goldenberg, M.M., 1999. Trastuzumab, a recombinant DNA-derived humanized monoclonal antibody, a novel agent for the treatment of metastatic breast cancer. *Clinical therapeutics*, 21(2), pp.309–18.

Goswami, S. Wang, W., Arakawa, T., & Ohtake, S., 2013. Developments and Challenges for mAb-Based Therapeutics. *Antibodies*, 2(3), pp.452–500.

Grabski, A.C. & Burgess, R.R., 2001. Preparation of protein samples for SDS-polyacrylamide gel electrophoresis: procedures and tips. *inNovations*, 13, pp.10–12.

Gracanin, M., Hawkins, C. L., Pattison, D. I., & Davies, M. J., 2009. Singlet-oxygen-mediated amino acid and protein oxidation: formation of tryptophan peroxides and decomposition products. *Free radical biology & medicine*, 47(1), pp.92–102.

Grdadolnik, J., 2002. A ftir investigation of protein conformation. *Bulletin of the Chemists and Technologists of Macedonia*, 21(1), pp.23–34.

Harris, D.C., 2003. *Quantitative Chemical Analysis* 6th ed., New York: W.H.Freeman.

Hawe, A., Kasper, J. C., Friess, W., & Jiskoot, W., 2009. Structural properties of monoclonal antibody aggregates induced by freeze-thawing and thermal stress. *European journal of pharmaceutical sciences : official journal of the European Federation for Pharmaceutical Sciences*, 38(2), pp.79–87.

Held, P., 2009. An Absorbance-based Cytotoxicity Assay using High Absorptivity, Water-Soluble Tetrazolium Salts. Available at: http://www.biotek.com/assets/tech_resources/An_Absorbance-based-Cytotoxicity_App Note.pdf [Accessed August 14, 2014].

Hermanto, U., Zong, C.S. & Wang, L.H., 2001. ErbB2-overexpressing human mammary carcinoma cells display an increased requirement for the phosphatidylinositol 3-kinase signaling pathway in anchorage-independent growth. *Oncogene*, 20(51), pp.7551–62.

Hernández-Jiménez, J., Salmerón-García, A., Cabeza, J., Vélez, C., Capitán-Vallvey, L. F., & Navas, N., 2016. The Effects of Light-Accelerated Degradation on the Aggregation of Marketed Therapeutic Monoclonal Antibodies Evaluated by Size-Exclusion Chromatography With Diode Array Detection. *Journal of Pharmaceutical Sciences*, 105(4), pp.1405–1418.

Holliday, D.L. & Speirs, V., 2011. Choosing the right cell line for breast cancer research. *Breast cancer research : BCR*, 13(4), p.215.

Hsu, C.P.S., 1997. Infrared Spectroscopy. *Handbook of Instrumental Techniques for Analytical Chemistry*, pp.247–284.

Huber, W. & Mueller, F., 2006. Biomolecular interaction analysis in drug discovery using surface plasmon resonance technology. *Current pharmaceutical design*, 12(31), pp.3999–4021.

Hynes, N.E. & MacDonald, G., 2009. ErbB receptors and signaling pathways in cancer. *Current opinion in cell biology*, 21(2), pp.177–84.

ICH, 2005. ICH H ARMONISED T RIPARTITE G UIDELINE V ALIDATION OF A NALYTICAL P ROCEDURES : *System*, 1994(November 1996). Available at: http://www.ich.org/fileadmin/Public_Web_Site/ICH_Products/Guidelines/Quality/Q2_R1/Step4/Q2_R1__Guideline.pdf [Accessed October 11, 2011].

ICH, 2012. ICH Quality guidelines. Available at: http://www.ich.org/home.html [Accessed October 2, 2012].

IMB, 2014. IMB Jena Image Library: Determination of secondary structure in proteins by FTIR spectroscopy. Available at: http://jenalib.fli-leibniz.de/ImgLibDoc/ftir/IMAGE_FTIR.html.html#Band assignments [Accessed August 28, 2014].

Infostab, 2014. Stabilis 4.0. *Stabilis*. Available at: http://www.stabilis.org/ [Accessed September 5, 2014].

Jackson, M. & Mantsch, H.H., 1995. The Use and Misuse of FTIR Spectroscopy in the Determination of Protein Structure The Use and Misuse of FTIR Spectroscopy in the Determination of Protein Structure. *Critical Reviews in Biochemistry and Molecular Biology*, 30(2), pp.95–120.

Jaspe, J. & Hagen, S.J., 2006. Do protein molecules unfold in a simple shear flow? *Biophysical journal*, 91(9), pp.3415–24.

Jefferis, R., 2009. Chapter 13 Glycosylation of Antibody Therapeutics : Optimisation for Purpose. In *Methods in molecular biology (Clifton, N.J.)*. New York, pp. 223–238.

Junttila, T.T. Akita, R. W., Parsons, K., Fields, C., Lewis Phillips, G. D., Friedman, L. S., Sliwkowski, M. X., 2009. Ligand-independent HER2/HER3/PI3K complex is disrupted by trastuzumab and is effectively inhibited by the PI3K inhibitor GDC-0941. *Cancer cell*, 15(5), pp.429–40.

Kaiser, J. & Kramer, I., 2011. Physiochemical Stability of Diluted Trastuzumab Infusion Solutions In Polypropylene Infusion Bags. *International Journal of Pharmaceutical Compounding*, 15(6), pp.515–520.

Kapp, S.J. Larsson, I., Van De Weert, M., Cárdenas, M., & Jorgensen, L., 2015. Competitive adsorption of monoclonal antibodies and nonionic surfactants at solid hydrophobic surfaces. *Journal of pharmaceutical sciences*, 104(2), pp.593–601.

Kawa, S. Matsushita, H., Ohbayashi, H., Semba, K., & Yamamoto, T., 2009. A novel mouse monoclonal antibody targeting ErbB2 suppresses breast cancer growth. *Biochemical and biophysical research communications*, 384(3), pp.329–33.

Kerwin, B.A. & Remmele, R.L., 2007. Protect from light: photodegradation and protein biologics. *Journal of pharmaceutical sciences*, 96(6), pp.1468–79.

Khalili, H., Sharma, G., Froome, a, Khaw, P. T., & Brocchini, S., 2015. Storage stability of bevacizumab in polycarbonate and polypropylene syringes. *Eye*, 29(January), pp.1–8.

Kiese, S. & Papppenberger, A., 2008. Shaken, not stirred: mechanical stress testing of an IgG1 antibody. *Journal of pharmaceutical sciences*, 97(10), pp.4347–4366.

Kong, J. & Yu, S., 2007. Fourier Transform Infrared Spectroscopic Analysis of Protein Secondary Structures Protein FTIR Data Analysis and Band Assign-ment. *Biochemistry*, 39(8), pp.549–559.

Kruser, T.J. & Wheeler, D.L., 2010. Mechanisms of resistance to HER family targeting antibodies. *Experimental cell research*, 316(7), pp.1083–100.

Kumar, V. & Banker, G.S., 1998. *Maillard Reactions in Chemistry, Food and Health* T. Labuza V. Monnier, J. Baynes, & J. O'Brien, eds., Elsevier.

Laustriat, G. & Hasselmann, C., 1975. PHOTOCHEMISTRY OF PROTEINS. *Photochemistry and Photobiology*, 22(6), pp.295–298.

Lin, J. Luo, R., Li, A., Zhang, J., Lü, C., & Yan, X., 2005. Killing effect of 131I-Herceptin on breast cancer cell lines in vitro. *Di 1 jun yi da xue xue bao Academic journal of the first medical college of PLA*, 25(6), pp.663–666.

Liu, L., Ammar, D. a., Ross, L. a., Mandava, N., Kahook, M. Y., & Carpenter, J. F., 2011. Silicone oil microdroplets and protein aggregates in repackaged bevacizumab and ranibizumab: Effects of long-term storage and product mishandling. *Investigative Ophthalmology and Visual Science*, 52(2), pp.1023–1034.

Liu, X., Pop, L.M. & Vitetta, E.S., 2008. Engineering therapeutic monoclonal antibodies. *Immunological reviews*, 222, pp.9–27.

Lord, M., 2003. Gel Electrophoresis of Proteins. In *Essential Cell Biology*.

De Lorenzo, C., Tedesco, a, Terrazzano, G., Cozzolino, R., Laccetti, P., Piccoli, R., & D'Alessio, G., 2004. A human, compact, fully functional anti-ErbB2 antibody as a novel antitumour agent. *British journal of cancer*, 91(6), pp.1200–4.

Lundholt, B.K., Scudder, K.M. & Pagliaro, L., 2003. A simple technique for reducing edge effect in cell-based assays. *Journal of biomolecular screening*, 8(5), pp.566–70.

Madsen, R.E., Cherris, R. T., Shabushnig, J. G., & Hunt, D. G., 2009. Visible particulates in injections - A history and a proposal to revise USP general chapter injections [1]. *Pharmacopeial Forum*, 35(5), pp.1383–1387.

Madsen, R.E., 2010. Visual Inspection of Parenterals Advisory Panel Meeting Purpose of Visual Inspection AP.

Magdelaine-Beuzelin, C. Kaas, Q., Wehbi, V., Ohresser, M., Jefferis, R., Lefranc, M.-P., & Watier, H., 2007. Structure-function relationships of the variable domains of monoclonal antibodies approved for cancer treatment. *Critical reviews in oncology/hematology*, 64(3), pp.210–25.

Malencik, D.A. & Anderson, S.R., 2003. Dityrosine as a product of oxidative stress and fluorescent probe. *Amino acids*, 25(3-4), pp.233–47.

Manning, M.C., Chou, D. K., Murphy, B. M., Payne, R. W., & Katayama, D. S. , 2010. Stability of protein pharmaceuticals: an update. *Pharmaceutical research*, 27(4), pp.544–75.

Manning, M.C., Patel, K. & Borchardt, R.T., 1989. Stability of Protein Pharmaceuticals. *Pharmaceutical research*, 6(11), p.903 818.

Maple, L., Lathrop, R., Bozich, S., Harman, W., Tacey, R., Kelley, M., &, 2004. Development and validation of ELISA for herceptin detection in human serum. *Journal of immunological methods*, 295(1-2), pp.169–82.

Matheus, S., Friess, W. & Mahler, H.-C., 2006. FTIR and nDSC as analytical tools for high-concentration protein formulations. *Pharmaceutical research*, 23(6), pp.1350–63.

Matheus, S., Mahler, H.-C. & Friess, W., 2006. A critical evaluation of Tm(FTIR) measurements of high-concentration IgG1 antibody formulations as a formulation development tool. *Pharmaceutical research*, 23(7), pp.1617–27.

Mellstedt, H., Niederwieser, D. & Ludwig, H., 2008. The challenge of biosimilars. *Annals of oncology : official journal of the European Society for Medical Oncology / ESMO*, 19(3), pp.411–9.

Molina, M.A., Codony-Servat, J., Albanell, J., Rojo, F., Arribas, J., & Baselga, J., 2001. Trastuzumab (Herceptin), a Humanized Anti-HER2 Receptor Monoclonal Antibody, Inhibits Basal and Activated HER2 Ectodomain Cleavage in Breast Cancer Cells. *Cancer Res.*, 61(12), pp.4744–4749.

Mukhopadhyay, R., 2011. Cast from the same nould. *Chemistry World*.

Nahta, R., 2012. Molecular Mechanisms of Trastuzumab-Based Treatment in HER2-Overexpressing Breast Cancer. *International Scholarly Research Network ISRN oncology*, 2012, pp.1–17.

Nahta, R., Hung, M. & Esteva, F., 2004. The HER-2-Targeting Antibodies Trastuzumab and Pertuzumab Synergistically Inhibit the Survival of Breast Cancer Cells. *Cancer Research*, 64(7), pp.2343–2346.

Nebija, D., Noe, C. R., Urban, E., & Lachmann, B., 2014. Quality control and stability studies with the monoclonal antibody, trastuzumab: application of 1D- vs. 2D-gel electrophoresis. *International journal of molecular sciences*, 15(4), pp.6399–411.

Neve, R.M., Chin, K., Fridlyand, J., Yeh, J., Baehner, F. L., Fevr, T., … Gray, J. W., 2006. A collection of breast cancer cell lines for the study of functionally distinct cancer subtypes. *Cancer cell*, 10(6), pp.515–27.

Nobbmann, U., Connah, M., Fish, B., Varley, P., Gee, C., Mulot, S., … Harding, S. E., 2007. Dynamic light scattering as a relative tool for assessing the molecular integrity and stability of monoclonal antibodies. *Biotechnology & genetic engineering reviews*, 24, pp.117–28.

Nowak, C., Ponniah, G., Cheng, G., Kita, A., Neill, A., Kori, Y., & Liu, H., 2016. Liquid chromatography-fluorescence and liquid chromatography-mass spectrometry detection of tryptophan degradation products of a recombinant monoclonal antibody. *Analytical biochemistry*, 496, pp.4–8.

Ozbay, T., Durden, D. L., Liu, T., O'Regan, R. M., & Nahta, R. , 2010. In vitro evaluation of pan-PI3-kinase inhibitor SF1126 in trastuzumab-sensitive and trastuzumab-resistant HER2-over-expressing breast cancer cells. *Cancer chemotherapy and pharmacology*, 65(4), pp.697–706.

Pabari, R., Ryan, B., Ahmad, W., & Ramtoola, Z.2013. Physical and structural stability of the monoclonal antibody, Trastuzumab (Herceptin®), intravenous solutions. *Current Pharmaceutical Biotechnology*, 14(2), pp.220–225(6).

Pabari, R.M., Ryan, B., McCarthy, C., & Ramtoola, Z., 2011. Effect of microencapsulation shear stress on the structural integrity and biological activity of a model monoclonal antibody, trastuzumab. *Pharmaceutics*, 3(3), pp.510–24.

Pabari, R.M., Ryan, B., Ahmad, W., & Ramtoola, Z., 2013. Physical and Structural Stability of the Monoclonal Antibody, Trastuzumab (Herceptin®), Intravenous Solutions. *Current Pharmaceutical Biotechnology*, 14(2), pp.220–225.

Parekh, B.S., Berger, E., Sibley, S., Cahya, S., Xiao, L., LaCerte, M. A., Gately, M, 2012. Development and validation of an antibody-dependent cell-mediated cytotoxicity-reporter gene assay. *mAbs*, 4(3), pp.310–8.

Parry, R. V., Chapman, T., Khan, M. A., Connolly, M., & Watts, A. G., 2014. Monoclonal Antibodies Functional Improvements at SPC Shelf-Life Limits. Available at: http://mabstalk.com/2014/06/26/do-mabs-improve-maybe-like-a-good-wine-with-age/ [Accessed August 14, 2014].

Pattison, D.I., Rahmanto, A.S. & Davies, M.J., 2012. Photo-oxidation of proteins. *Photochem. Photobiol. Sci.*, 11(1), pp.38–53.

Paul, M., Vieillard, V., Da, R., Lemos, S., Escalup, L., & Astier, A. , 2013. Long-term physico-chemical stability of diluted trastuzumab. *International Journal of Pharmaceutics*, 448(1), pp.101–104.

(a) Paul, M., Vieillard, V., Roumi, E., Cauvin, A., Despiau, M. C., Laurent, M., & Astier, , 2012. Long-term stability of bevacizumab repackaged in 1 mL polypropylene syringes for intravitreal. *Annales Pharmaceutiques Francaises*, 70, pp.139–154.

(b) Paul, M., Vieillard, V., Jaccoulet, E., & Astier, A., 2012. Long-term stability of diluted solutions of the monoclonal antibody rituximab. *International Journal of Pharmaceutics*, 436(1-2), pp.282–290.

Perkin Elmer Life and Analytical Sciences, 2004. FT- IR SPECTROSCOPY Spectrum One FT-IR Spectrometer. Available at: https://shop.perkinelmer.co.uk/Content/relatedmaterials/specificationsheets/spc_spectrumoneftir.pdf [Accessed October 27, 2011].

Ph. Eur, 2000. 2.9.20. Particulate contamination : visible particles. In *European pharmacopoeia 5.0*. Strasbourg: Pharmacopoeia Europaea, pp. 255–256.

Philo, J. & Arakawa, T., 2009. Mechanisms of protein aggregation. *Current pharmaceutical biotechnology*, 10(4), pp.348–351.

Philo, J.S., 2006. Is any measurement method optimal for all aggregate sizes and types? *The AAPS journal*, 8(3), pp.E564–71.

Pinholt, C., Hartvig, R. A., Medlicott, N. J., & Jorgensen, L., 2011. The importance of interfaces in protein drug delivery - why is protein adsorption of interest in pharmaceutical formulations? *Expert opinion on drug delivery*, 8(7), pp.949–64.

Promega, 2014. *ADCC Reporter Bioassays - V and F Variants : Novel , Bioluminescent Cell-Based Assays for Quantifying*,

Qi, P., Volkin, D. B., Zhao, H., Nedved, M. L., Hughes, R., Bass, R., Bond, M. D., 2009. Characterization of the photodegradation of a human IgG1 monoclonal antibody formulated as a high-concentration liquid dosage form. *Journal of pharmaceutical sciences*, 98(9), pp.3117–30.

Raj, A. & van Oudenaarden, A., 2008. Stochastic gene expression and its consequences. *Cell*, 135(2), pp.216–226.

Reichert, J.M., 2012. Marketed therapeutic antibodies compendium. *mAbs*, 4(3), pp.413–5.

Riss, T.L., Niles, A.L. & Minor, L., 2004. Cell Viability Assays Assay Guidance Manual. In *Assay Guidance Manual*. pp. 1–23. Available at: http://www.ncbi.nlm.nih.gov/books/NBK144065/ [Accessed Febuary 29, 2016].

Robinson, N.E. & Robinson, A.B., 2004. *Molecular Clocks – Deamidation of asparaginyl and glutaminyl residues in peptides and proteins*, Cave Junction OR: Althouse Press.

Roche, 2006. *Trastuzumab*, Basel.

Rosenberg, A.S., 2006. Effects of protein aggregates: an immunologic perspective. *The AAPS journal*, 8(3), pp.E501–7.

Rowe, J., 2001. Probing hydration and the stability of protein solutions--a colloid science approach. *Biophysical chemistry*, 93(2-3), pp.93–101.

Roy, S., Mason, B. D., Schöneich, C. S., Carpenter, J. F., Boone, T. C., & Kerwin, B. A., 2009. Light-induced aggregation of type I soluble tumor necrosis factor receptor. *Journal of pharmaceutical sciences*, 98(9), pp.3182–99.

Scaltriti, M., Verma, C., Guzman, M., Jimenez, J., Parra, J. L., Pedersen, K., Baselga, J. , 2009. Lapatinib , a HER2 tyrosine kinase inhibitor , induces stabilization and accumulation of HER2 and potentiates trastuzumab-dependent cell cytotoxicity. *Oncogene*, 28(November 2008), pp.803–814.

Schmid, F., 2001. Biological Macromolecules : UV-visable Spectrophotometry. *Encyclopedia of Life Sciences*, pp.1–4.

Scholl, S., Beuzeboc, P. & Pouillart, P., 2001. Symposium article Targeting HER2 in other tumor types. *Annals of oncology : official journal of the European Society for Medical Oncology / ESMO*, 12, pp.44–50.

Serra, V., Markman, B., Scaltriti, M., Eichhorn, P. J. a, Valero, V., Guzman, M., …, 2008. NVP-BEZ235, a dual PI3K/mTOR inhibitor, prevents PI3K signaling and inhibits the growth of cancer cells with activating PI3K mutations. *Cancer research*, 68(19), pp.8022–30.

Sethuraman, A. & Belfort, G., 2005. Protein structural perturbation and aggregation on homogeneous surfaces. *Biophysical journal*, 88(2), pp.1322–33.

Sewell, G.J., Rigby-Jones, a. E. & Priston, M.J., 2003. Stability of intravesical epirubicin infusion: A sequential temperature study. *Journal of Clinical Pharmacy and Therapeutics*, 28(5), pp.349–353.

Shire, S.J., Shahrokh, Z. & Liu, J.U.N., 2004. Challenges in the Development of High Protein Concentration Formulations. *Journal of pharmaceutical sciences*, 93(6), pp.1390–1402.

Strome, S.E., Sausville, E.A. & Mann, D., 2007. A mechanistic perspective of monoclonal antibodies in cancer therapy beyond target-related effects. *The oncologist*, 12(9), pp.1084–95.

Stryer, L., 1995. Biochemistry. In *Biochemistry*. New York: W H Freeman, pp. 17–41.

Subik, K., Lee, J.-F., Baxter, L., Strzepek, T., Costello, D., Crowley, P., Tang, P., 2010. The Expression Patterns of ER, PR, HER2, CK5/6, EGFR, Ki-67 and AR by Immunohistochemical Analysis in Breast Cancer Cell Lines. *Breast cancer : basic and clinical research*, 4, pp.35–41.

Sundaresan, S., Penuel, E. & Sliwkowski, M.X., 1999. The biology of human epidermal growth factor receptor 2. *Current oncology reports*, 1(1), pp.16–22.

Timonen, T., 1981. Characteristics of human large granular lymphocytes and relationship to natural killer and K cells. *Journal of Experimental Medicine*, 153(3), pp.569–582.

US Food and Drug Administration, 2001. Safety assessment of Di-(2-ethylhexyl) phthalate (DEHP) released from PVC medical devices. *Center for Devices and Radiological Health*, p.119. Available at: http://www.fda.gov/downloads/MedicalDevices/.../UCM080457.pdf [Accessed May 2, 2016].

USP, 2006. <788> PARTICULATE MATTER IN INJECTIONS. *US Pharmacopeia*, 1, pp.1, 8. Available at: http://www.usp.org/sites/default/files/usp_pdf/EN/USPNF/revisions/788_particulate_matter_in_injections.pdf [Accessed June 4, 2014].

USP, 2013. Trastuzumab Summary Validation Report. Available at: http://www.usp.org/global/medicines-compendium [Accessed August 12, 2014].

USP, 2009. USP 31 ⟨ 1 ⟩ injections. , (4). Available at: http://www.usp.org/sites/default/files/usp_pdf/EN/USPNF/generalChapterInjections.pdf [Accessed June 4, 2014].

Valabrega, G., Montemurro, F. & Aglietta, M., 2007. Trastuzumab: mechanism of action, resistance and future perspectives in HER2-overexpressing breast cancer.

Annals of oncology : official journal of the European Society for Medical Oncology / ESMO, 18(6), pp.977–84.

Vermeer, A., Giacomelli, C. & Norde, W., 2001. Adsorption of IgG onto hydrophobic teflon. Differences between the Fab and Fc domains. *Biochimica et Biophysica Acta (BBA) - General Subjects*, 1526(1), pp.61–69.

Vermeer, A.W.P., Bremer, M.G.E.G. & Norde, W., 1998. Structural changes of IgG induced by heat treatment and by adsorption onto a hydrophobic Teflon surface studied by circular dichroism spectroscopy. *Biochimica et Biophysica Acta (BBA) - General Subjects*, 1425(1), pp.1–12.

Vermeer, P.W. & Norde, W., 2000. The thermal stability of immunoglobulin: unfolding and aggregation of a multi-domain protein. *Biophysical journal*, 78(1), pp.394–404.

Vigneron, J., Astier, A., Trittler, R. N. R., Hecq, J. D., Daouphars, M., Larsson, I. Pinguet, F., 2014. SFPO and ESOP recommendations for the practical stability of anticancer drugs: An update. *European Journal of Oncology Pharmacy*, 8(2), pp.3–13.

Vlasak, J. & Ionescu, R., 2011. Fragmentation of monoclonal antibodies. *mAbs*, 3(3), pp.253–63.

Vonhoff, S., Condliffe, J. & Schiffter, H., 2010. Implementation of an FTIR calibration curve for fast and objective determination of changes in protein secondary structure during formulation development. *Journal of pharmaceutical and biomedical analysis*, 51(1), pp.39–45.

Wang, W., 1999. Instability, stabilization, and formulation of liquid protein pharmaceuticals. *International journal of pharmaceutics*, 185(2), pp.129–88.

Wang, W., Nema, S. & Teagarden, D., 2010. Protein aggregation--pathways and influencing factors. *International Journal of Pharmaceutics*, 390(2), pp.89–99.

Wang, X., Li, Q. & Davies, M., 2013. Development of antibody arrays for monoclonal antibody Higher Order Structure analysis. *Frontiers in pharmacology*, 4(August), p.103.

Watts, A., 2012. Article Review – Long-term stability of diluted solutions of the monoclonal antibody rituximab – mAbstalk.com. Available at: http://mabstalk.com/2012/11/10/review-of-long-term-stability-of-diluted-solutions-of-the-monoclonal-antibody-rituximab/ [Accessed October 9, 2013].

Webb, S.D., Cleland, J. L., Carpenter, J. F., & Randolph, T. W., 2002. A new mechanism for decreasing aggregation of recombinant human interferon-γ by a surfactant: Slowed dissolution of lyophilized formulations in a solution containing 0.03% polysorbate 20. *Journal of Pharmaceutical Sciences*, 91(2), pp.543–558.

Weinberg, W.C., Frazier-Jessen, M. R., Wu, W. J., Weir, A., Hartsough, M., Keegan,., 2005. Development and regulation of monoclonal antibody products: challenges and opportunities. *Cancer metastasis reviews*, 24(4), pp.569–84.

Weise, M., Bielsky, M.-C., De Smet, K., Ehmann, F., Ekman, N., Giezen, T. J , & Schneider, C. K, 2014. Biosimilars: the science of extrapolation. *Blood*, 124(22), pp.3191–6.

Weise, M., Kurki, P., Wolff-Holz, E., Bielsky, M.-C., & Schneider, C. K, 2012. Biosimilars: what clinicians should know. *Blood*, 120(26), pp.5111–7.

Wolff, E., Schreiber, G. J., Cosand, W. L., & Raff, H. V., 1993. Monoclonal Antibody Homodimers : Enhanced Antitumor Activity in Nude Mice Monoclonal Antibody Homodimers : Enhanced Antitumor Activity in Nude Mice. , pp.2560–2565.

Wu, K., Wang, C., Amico, M. D., Lee, R. J., Albanese, C., Pestell, R. G., & Mani, S., 2002a. Flavopiridol and Trastuzumab Synergistically Inhibit Proliferation of Breast Cancer Cells : Association with Selective Cooperative Inhibition of Cyclin D1-dependent Kinase and Akt Signaling Pathways 1 This work was supported in part by NIH RO1CA86071 and. *Cancer Research*.

Wu, K., Wang, C., Amico, M. D., Lee, R. J., Albanese, C., Pestell, R. G., & Mani, S.., 2002b. Flavopiridol and trastuzumab synergistically inhibit proliferation of breast cancer cells: association with selective cooperative inhibition of cyclin D1-dependent kinase and Akt signaling pathways. *Molecular cancer therapeutics*, 1(9), pp.695–706.

Xenopoulos, A., 2013. Stress-Induced Antibody Aggregates. *BioProcess International*, 11(3), pp.44–51.

Zabrecky, J., J., Lam, T., McKenzie, S., & Carney, W., 1991. The extracellular domain of p185/neu is released from the surface of human breast carcinoma cells, SK-BR-3. *J. Biol. Chem.*, 266(3), pp.1716–1720.

APPENDIX: INFRA-RED SPECTRA

CHAPTER 2

ATR-FT-IR conditions unless stated otherwise in figure.

Scan range of 4,000 cm^{-1} to 450 cm^{-1} wave numbers 256 continuous scans at a resolution of 4 cm^{-1} and with an accuracy of +/- 0.1 cm^{-1} at 1,600 cm^{-1}. Spectrum normalised to wavenumber 1,850 cm^{-1} and background, water vapour and ATR corrected.

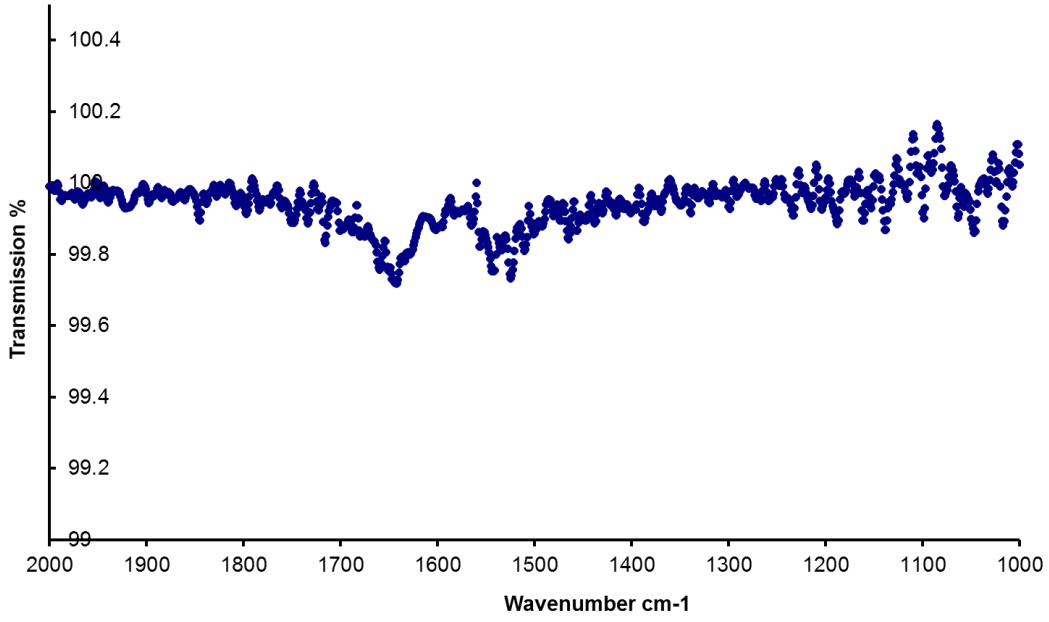

Figure 1 ATR-FT-IR spectrum from 2,000 cm^{-1} to 1,000 cm^{-1} of germanium crystal ATR in air i.e. no sample.

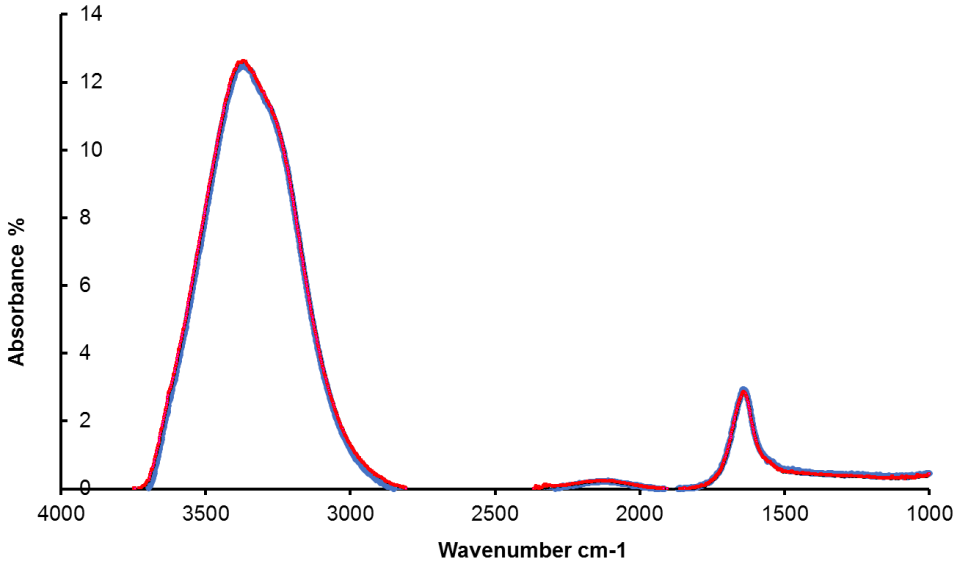

Figure 2 ATR-FT-IR spectrum of reconstituted Trastuzumab 21 mg/mL from two vials (red and blue plots).

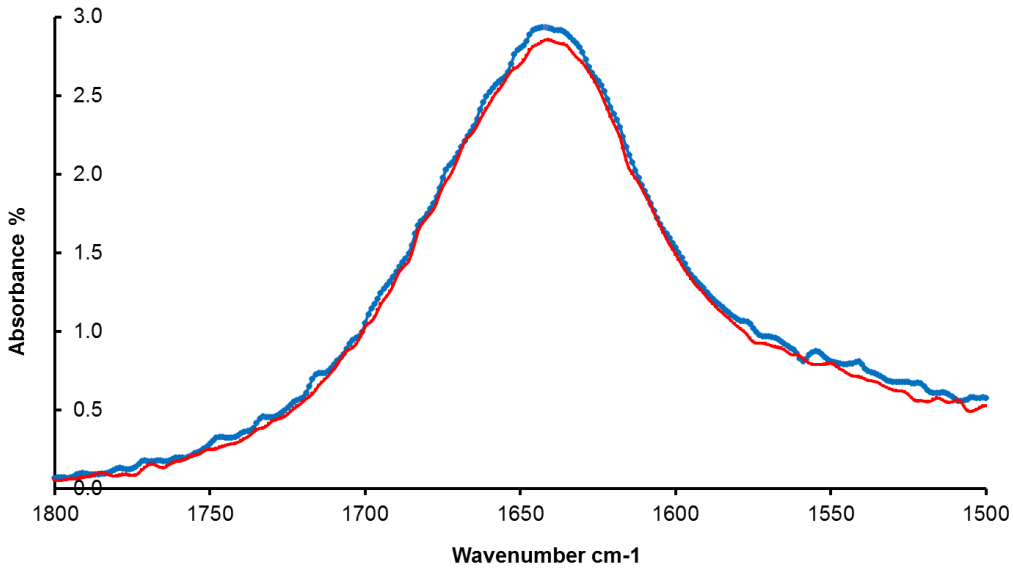

Figure 3 ATR-FT-IR representative spectra of reconstituted Trastuzumab 21 mg/mL from two vials (red and blue plots) showing Amide I region (1,800 cm^{-1} to 1,500 cm^{-1} wave numbers).

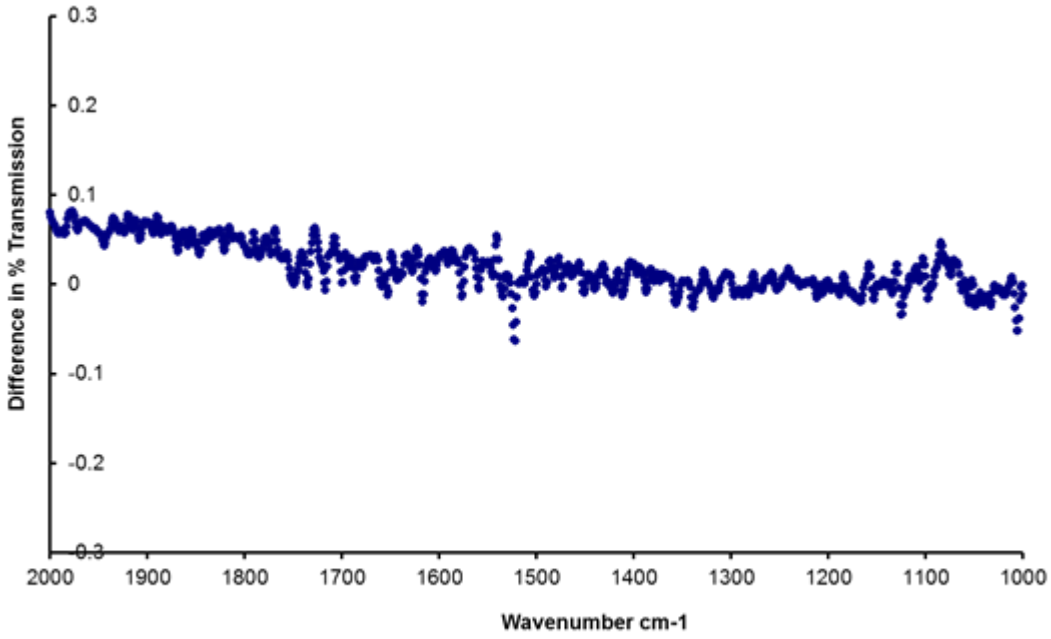

Figure 4 ATR-FT-IR difference spectrum of reconstituted Trastuzumab (heat-stressed and not heat-stressed) at 0.1 mg/mL concentration. Showing region 2,000 cm^{-1} to 1,000 cm^{-1} wave numbers.

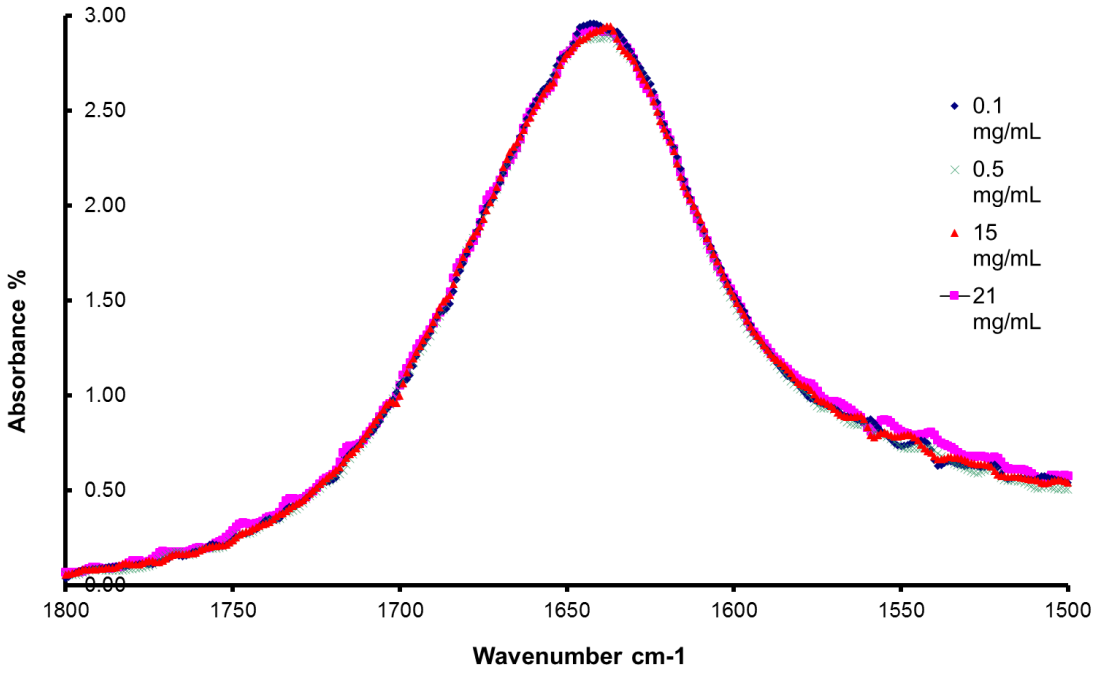

Figure 5 ATR-FT-IR spectra of reconstituted Trastuzumab at 0.1 mg/mL, 0.5 mg/mL, 15 mg/mL and 21 mg/mL showing Amide I region (1,800 cm^{-1} to 1,500 cm^{-1} wave numbers).

CHAPTER 3

Difference Spectra

0.1 mg/mL Infusion bags

Spectrum from time point 0 was subtracted from the spectrum acquired at different time points for day 7 (black), 42 (red) and 119 (green).

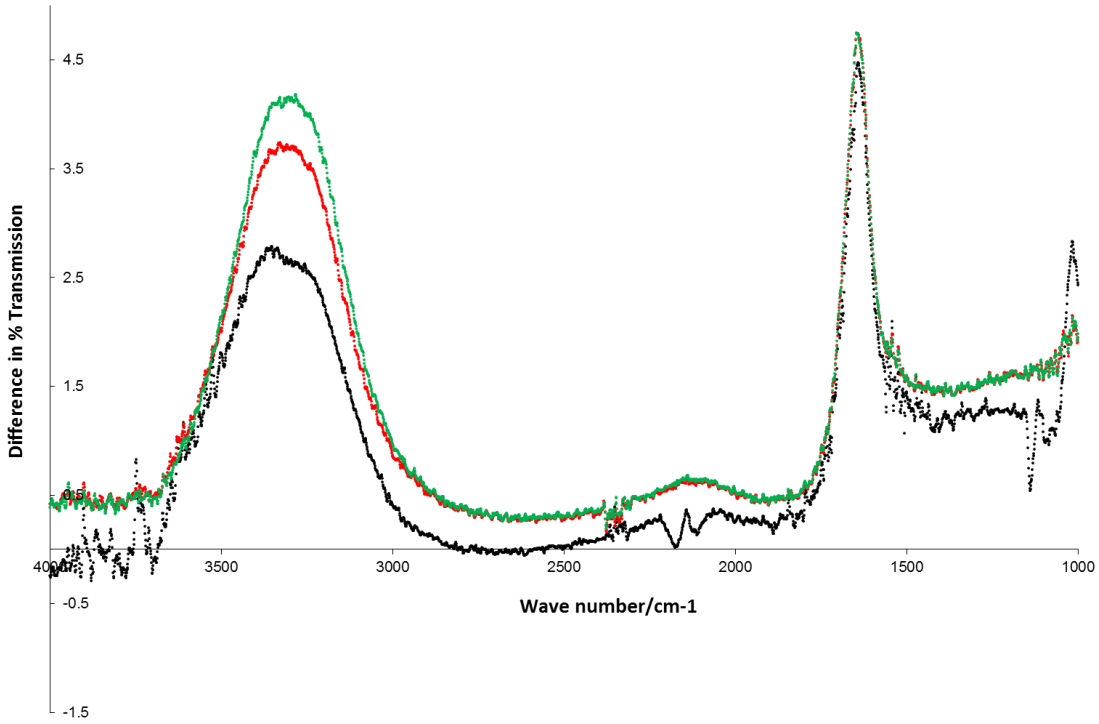

Figure 6 Infusion bag 1

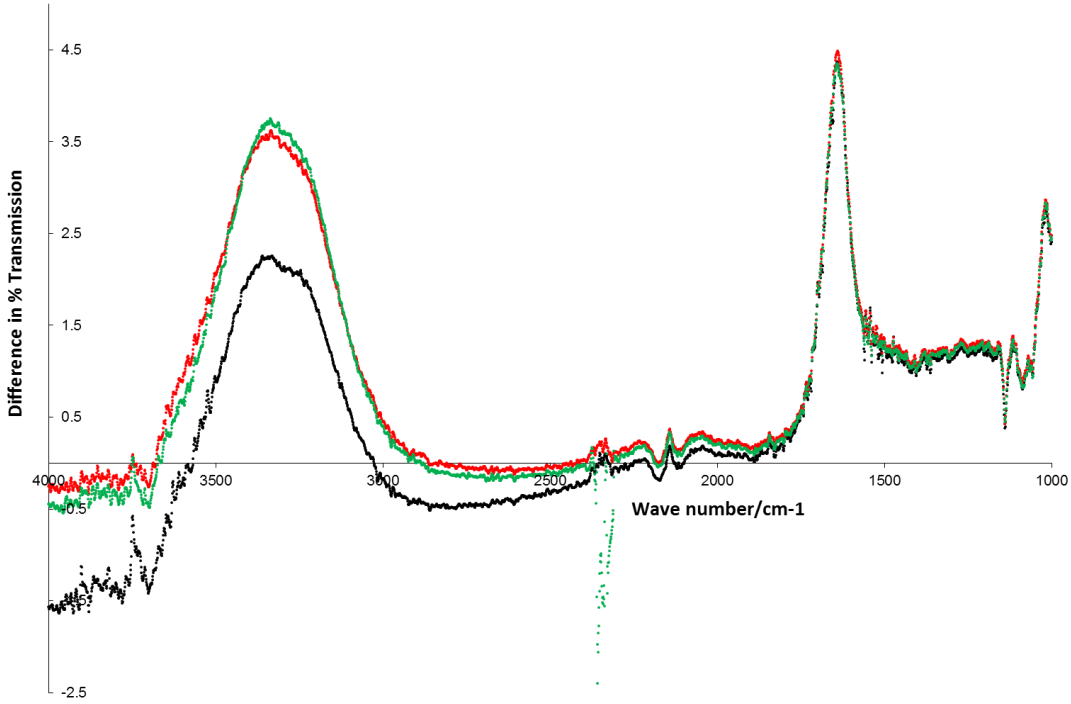

Figure 7 Infusion bag 2

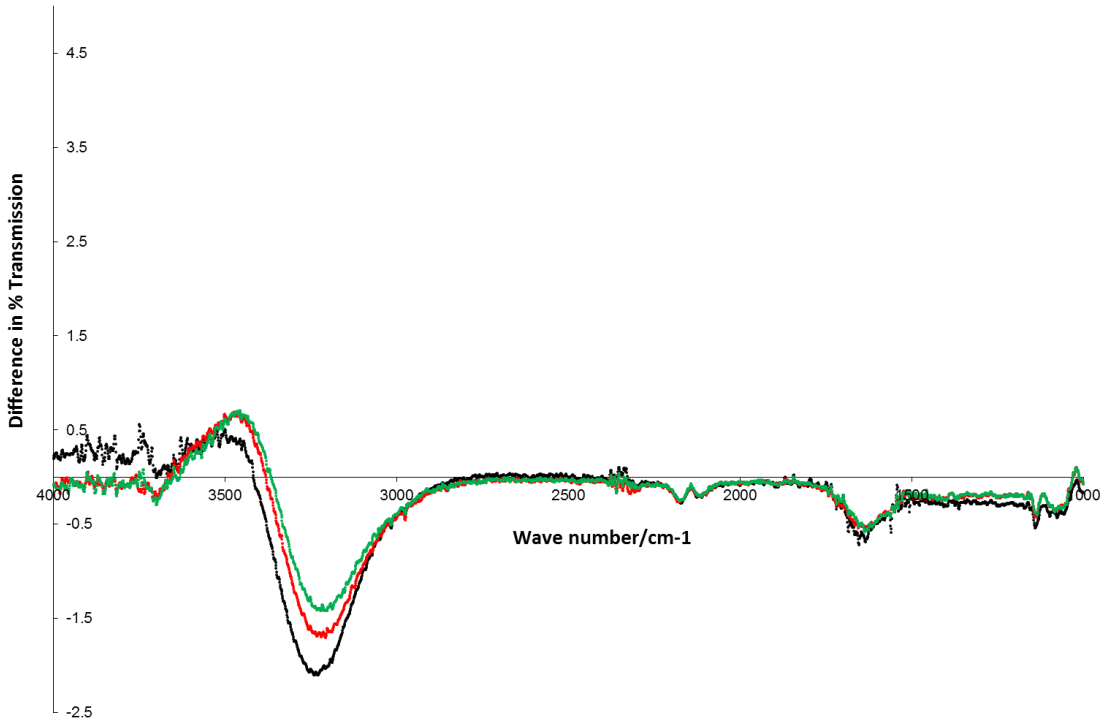

Figure 8 Infusion bag 3

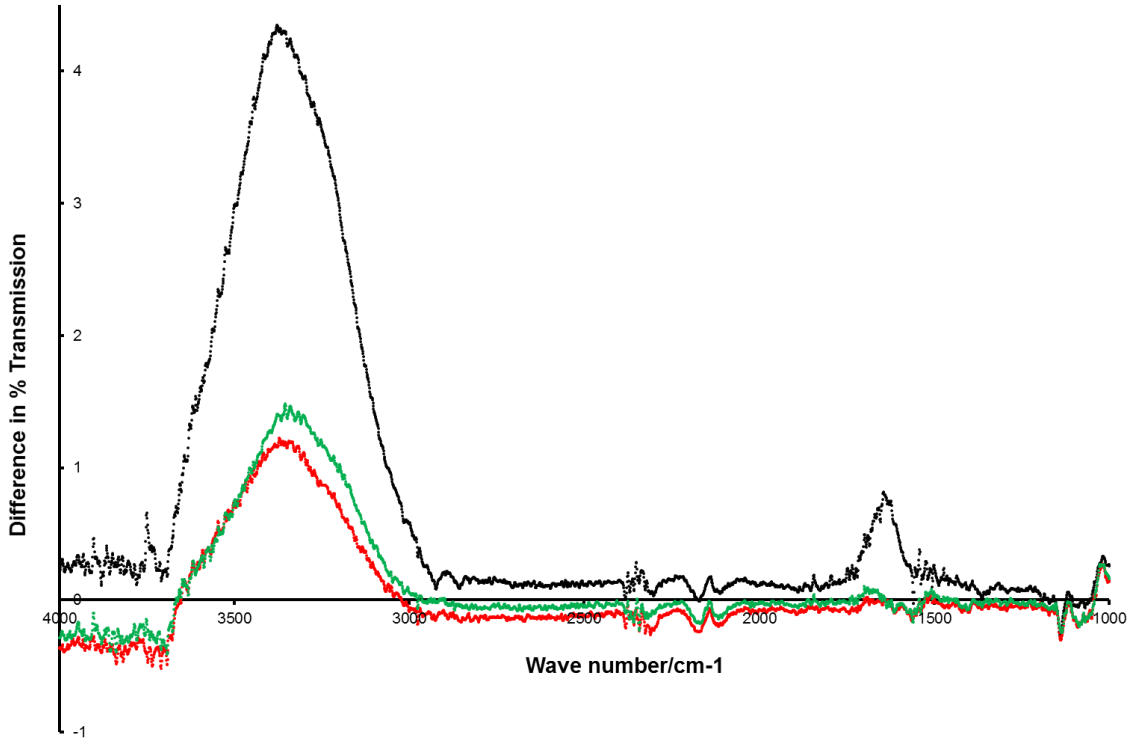

Figure 9 Infusion bag 4

0.5 mg/mL infusion bags

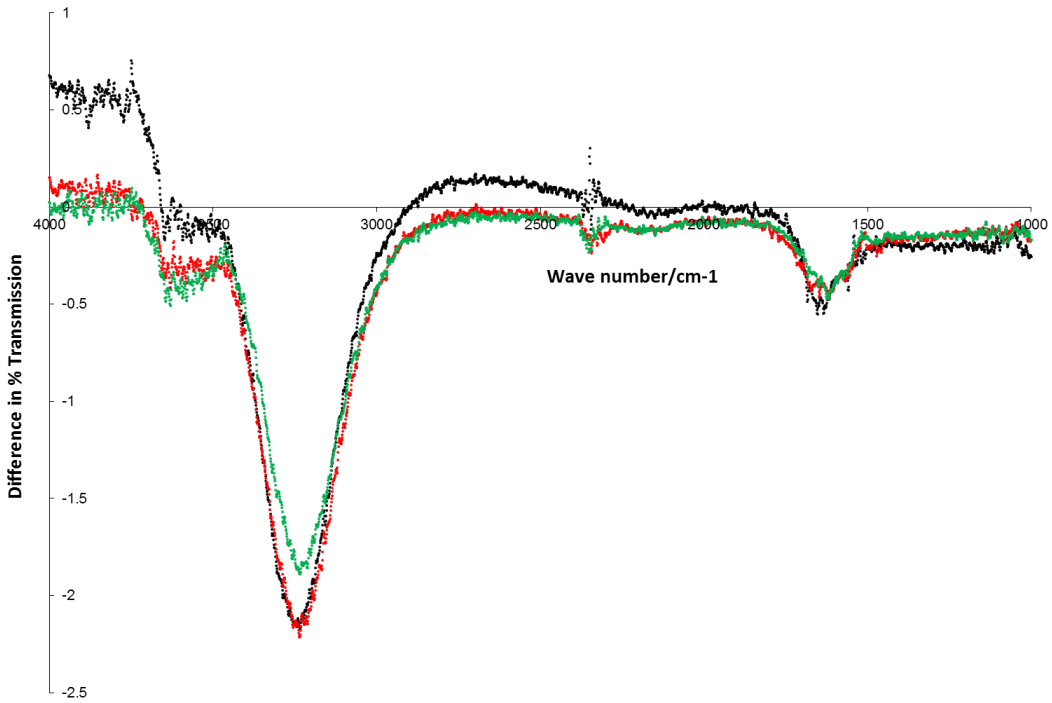

Figure 10 Infusion bag 1

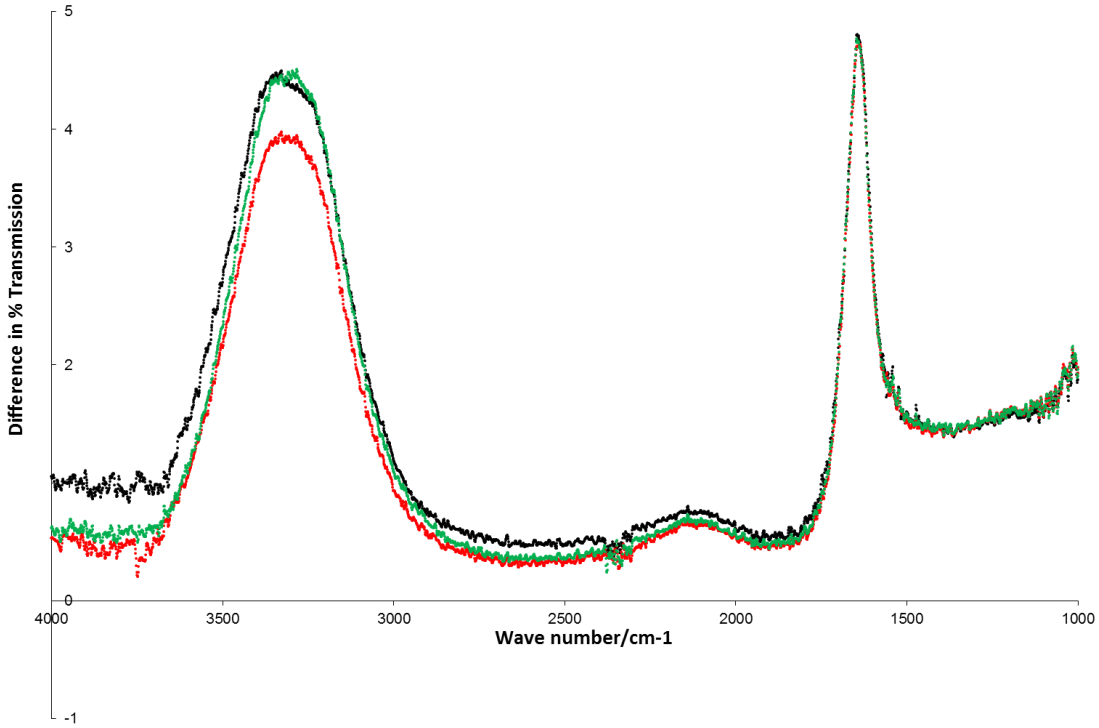

Figure 11 Infusion bag 2

6 mg/mL infusion bags

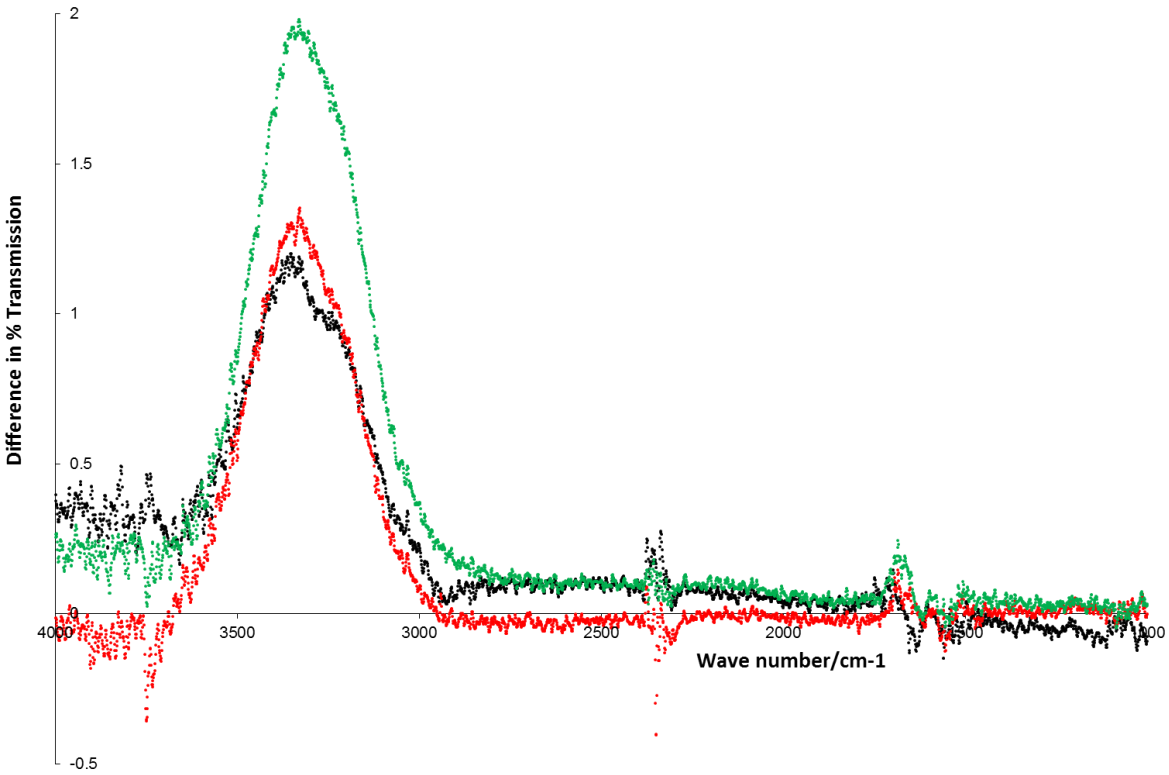

Figure 12 Infusion bag 1

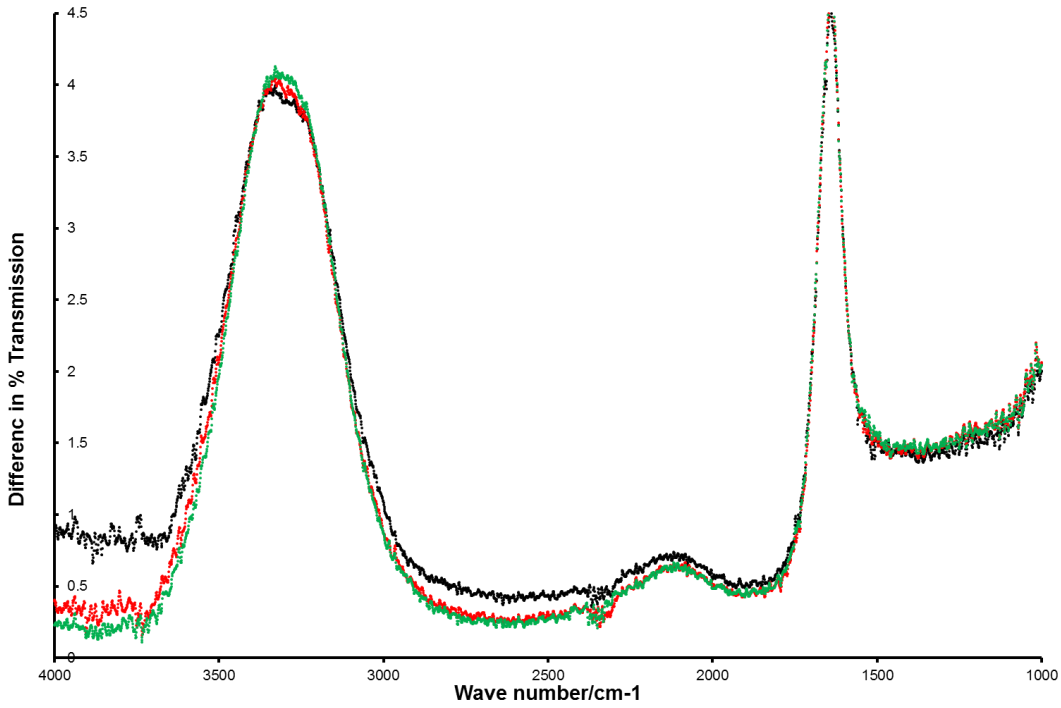

Figure 13 Infusion bag 2

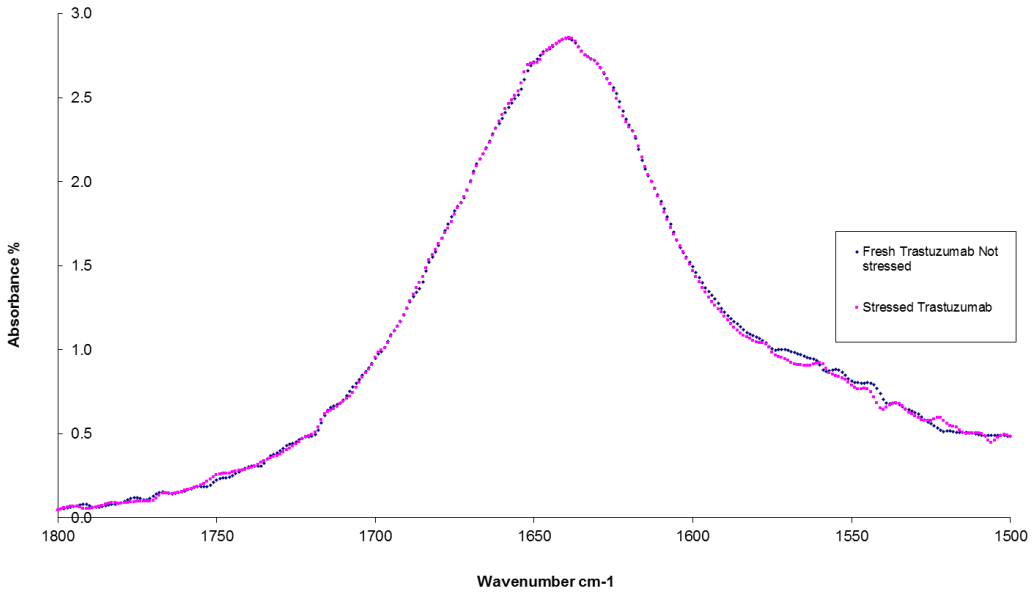

Figure 14 Fresh standard of Trastuzumab at 0.1mg/ml and Trastuzumab at 0.1 mg/ml concentration stressed 75 ^{o}C for 20 minutes.

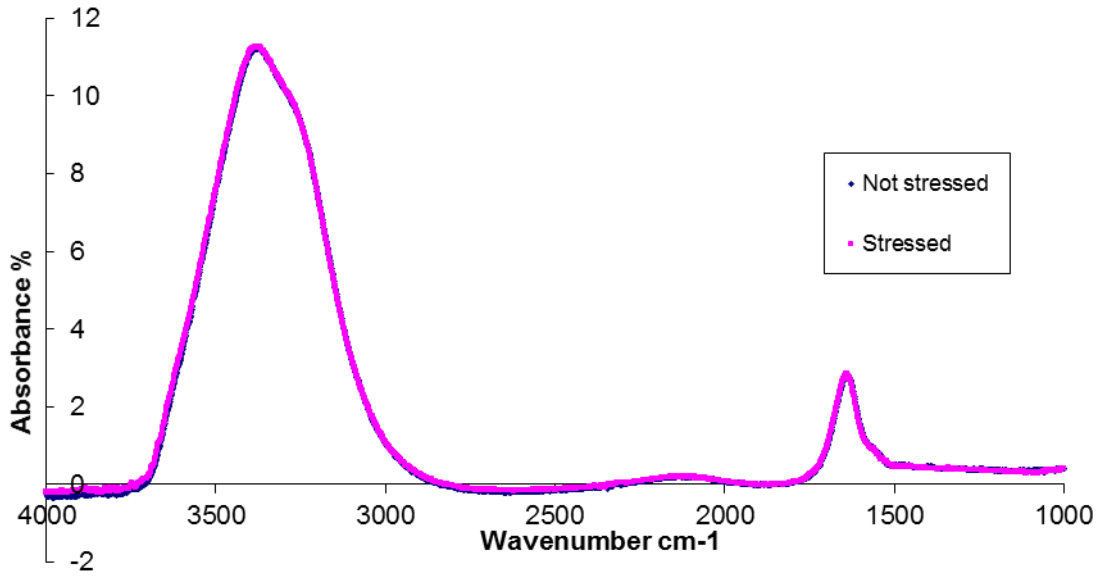

Figure 15 Fresh standard of Trastuzumab at 0.1mg/ml and Trastuzumab at 0.1 mg/ml concentration stressed 75 ^{o}C for 20 minutes. Amide I region (1,800 cm^{-1} to 1,500 cm^{-1} wave numbers) shown.